STUDIES IN Mn–Cr–Cu WEAR RESISTANT WHITE CAST IRONS

A THESIS

Submitted in fulfilment of the
requirements for the award of the degree
of
DOCTOR OF PHILOSOPHY
in
METALLURGICAL ENGINEERING

By

SHARDA SHARAN SINGH

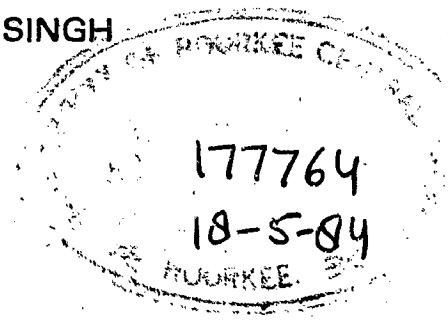

DEPARTMENT OF METALLURGICAL ENGINEERING
UNIVERSITY OF ROORKEE
ROORKEE-247667 (INDIA)

November, 1982

TO

MY WIFE

CANDIDATE'S DECLARATION

I hereby certify that the work which is being presented in the thesis entitled STUDIES IN Mn-Cr-Cu WEAR RESISTANT WHITE CAST IRONS in fulfilment of the requirement for the award of the Degree of Doctor of Philosophy, submitted in the Department of Metallurgical Engineering of the University is an authentic record of my own work carried out during a period from July 1979 to October 1982 under the supervision of Dr.A.K.Patwardhan and Dr.M.L.Mehta.

The matter embodied in this thesis has not been submitted by me for the award of any other degree.

Sharda Sharan Singh

November 28, 1982 (Sharda Sharan Singh)

This is to certify that the above statement made by the candidate is correct to the best of my knowledge.

A.K.Patwardhan

(A.K.Patwardhan)
Reader,
Department of Metallurgical Engineering,
University of Roorkee,
Roorkee.

M.L.Mehta

(M.L. Mehta)
Professor,
Department of Metallurgical Engineering,
University of Roorkee,
Roorkee.

A C K N O W L E D G E M E N T

The author wishes to record his indebtedness with sincere and heartfelt gratitude to Dr.A.K.Patwardhan, Reader, Department of Metallurgical Engineering, University of Roorkee for suggesting the problem, inspiration and expert guidance, active supervision, thought provoking discussions, illuminating criticism and suggestions given by him during the entire period and in all phases of this investigation. Without his timely and untiring help it would not have been possible to present the thesis in its present form.

The undersigned also expresses his deep sense of gratitude and sincere thanks to Dr.M.L. Mehta, Professor, Department of Metallurgical Engineering, University of Roorkee for his valuable guidance, supervision, constructive criticism and help throughout the entire period of this investigation. His efforts in arranging help from outside agencies/organizations proved immensely helpful.

I am extremely thankful to:

— Prof.M.L. Mehta, Ex-Head and Prof.M.L.Kapoor, present Head, Department of Metallurgical Engineering for providing the laboratory facilities.

— Dr.V.S.Arunachalam, Ex-Director, Dr.N.C.Birla and Mr.Kailasam of the Defence Metallurgical Research Laboratory, Hyderabad for providing facilities for melting and EPM analyses.

— Dr.P.Rodriquez, Head, Metallurgy Programme of the Reactor Research Centre, Kalpakkam for providing facilities for EPM analysis.

— Prof.K.P.Gupta of the Indian Institute of Technology, Kanpur, for providing X-ray diffractometry facilities.

— Professors S.Bhan, Head and P.Ramchandra Rao, Department of Metallurgical Engineering, Institute of Technology, Banaras Hindu University, Varanasi for providing laboratory facilities.

— Prof.V.K.Gaur, Dean of Research, University of Roorkee for financial support.

— Mr. T.C.Phatak, Central Building Research Institute, Roorkee and Mr.A.K.Singh, Assistant Executive Engineer, University of Roorkee for the help rendered.

The author also wishes to record his grateful appreciation and thanks to his colleagues Mr.N.C.Jain and Mr.Sahab Prasad for their help.

He wishes to record his sincerest thanks to Dr.P.S.Misra, Dr.V.K.Tewari and Dr.R.P.Ram for their suggestions. Encouragement from Prof.M.N.Saxena, Metallurgical Engineering Department is greatly appreciated.

The help rendered by Sarvasri Harichand, S.P.Kush, S.P.Anand, M.C.Vaish, S.K.Seth and Net Ram is gratefully acknowledged. Thanks are also due to Sri R.C.Sharma for meticulously typing manuscript.

Sharda Sharan Singh

S Y N O P S I S

A comprehensive review of the literature revealed that abrasion resistant white irons can be classified as (i) plain carbon and (ii) alloyed. The plain carbon white irons comprise of a microstructure consisting of pearlite + carbide (P+C) whose attainment in a desired section size is controlled by the C/Si balance and/or by chilling. They have applications only under service conditions involving light to moderate wear because of (i) a restriction on the maximum attainable hardness and (ii) the practical limitation(s) involved in manufacturing them (in relation to chilling). Cr-white irons represent an improvement over the plain carbon variety with regard to (i) the ease of formation of the (P+C) microstructure and (ii) the possibility of attaining a higher level of hardness (and therefore of resistance to wear) through a combination of alloying and heat treatment.

The development of alloyed white cast irons followed two distinct paths. In the U.S.A., the International Nickel Co. initially developed the low alloy versions Ni-hard 1 and 2 which exhibited better wear resistance and shock resistance compared with plain carbon/Cr-C varieties. They were followed by the higher alloy version Ni-hard 4. The main object of developing it was to bring about some increase in toughness through achieving a better eutectic carbide distribution. The other group of alloys more popular in Western Europe

consists of 27 Cr type, 15 Cr-3 Mo type (developed by Climax-Molybdenum Co.) and the more recent 13 Cr variety alloyed with Mn, Mo and/or Ni. Features common to the development of Ni-hard and Cr based white irons are (i) increasing the hardness of the matrix phase by increasing hardenability through alloying with a view to attaining metastable phase(s) in place of pearlite, (ii) increasing the overall hardness further by converting cementite into an alloy carbide and (ii) enhancing the shock resistance/ toughness through improved carbide distribution (applicable mostly to Ni-hard 4 iron).

A critical reappraisal of the physical metallurgy of white cast irons as also their wear characteristics revealed that there was a definite need to reassess (i) the most suitable microstructure from the point of view of abrasive wear and (ii) possible alternative paths of attaining such a microstructure, other than those listed above.

The present investigation was undertaken in response to (ii) above and essentially comprised of conceiving/ designing a series of low cost Fe-Cr-Mn-Cu alloys based on fundamental considerations, assessing their heat treatment response and characterising them for wear. The alloys which were air induction melted and sand cast (25 mm around cylinders), were investigated by employing hardness and microhardness measurements, optical and scanning electron

microscopy, X-ray diffractometry and EPMA techniques and their wear characteristics determined in terms of weight loss as a function of time in a limited number of instances.

The experimental work comprised of subjecting eight alloys, containing approximately 3,4,5 and 6% Mn and 1% Cu at two different Cr contents (6-6.5% and 9-9.5% respectively), in the form of 25 mm round X 18 mm long specimens, to heat treatments comprising of air cooling from 750, 800, 850 and 900°C after holding them at each of these temperatures for periods ranging from 2 to 10 hours. Microstructural examination was carried out predominantly by optical metallography to assess how alloy content and heat-treating schedule influenced the final microstructure. Hardness and microhardness measurements provided a quick yet reliable indication of the nature of the microstructure/microconstituents formed. Detailed structural examination by X-ray diffractometry proved helpful in deciding upon the nature of the matrix phase, the type of alloy carbide formed and whether or not austenite was retained. It was possible to establish a correlation between the data thus obtained and the data generated with the help of EPMA studies, involving the effect of heat treatment schedule on the distribution of alloying elements into different phases/microconstituents. The EPMA data is of fundamental interest and also very useful in the optimal design of alloys. Finally, the alloys were characterized for wear by utilizing two different methods/rigs-

(i) in which a single specimen abrades under a known weight against a rotating abrasive wheel and (ii) in which 9 specimens, mounted on a ring coupled to the shaft of a vertically driven motor, abrade against a sand water slurry. An attempt has been made to establish a correlation between the wear characteristics and the microstructure. Crack propagation studies were carried out to a limited extent to assess the nature of the crack propagation path. Results obtained revealed that the crack propagation was not preferential.

Based on these findings, inferences have been drawn with regard to (i) the optimum Mn/Cr combination and the optimum heat-treating schedule for obtaining the stipulated end properties (hardness/wear), (ii) mechanism of hardening, (iii) interrelation between microstructure, hardness and wear and (iv) the most suitable microstructure from the point of view of wear.

P R E F A C E

The first chapter deals with different grades of plain carbon and alloyed white cast irons currently in use. Since white irons are most extensively used under conditions involving wear in some form, a part of the Chapter I has been devoted to a discussion on the complex phenomenon of wear and its characterization.

The second chapter critically examines the role of microstructures in controlling wear. As a result of this analysis it emerges that a microstructure comprising of martensite + carbide perhaps with some austenite, may prove most beneficial from the point of view of abrasive wear. Accordingly Chapter II also includes a discussion on the effect of alloying elements on the transformation behaviour of alloy white irons with a view to arriving at different alloy combinations, especially the low cost ones, which were likely to prove useful in attaining the 'desired' microstructure. These considerations led to the design of experimental alloys. This aspect along with a phase-wise planning of experiments has been included in Chapter III.

Chapter IV deals with the experimental techniques and procedures employed.

Results summarized in Chapter V include the effect of heat-treatment schedule(s) on hardness and microhardness, study of microstructures by optical and scanning electron metallography, structural investigations by X-ray diffractometry, EPM analysis to assess the partitioning of Mn, Cr, Si and Cu into the matrix and carbide phases in the as-cast state and the effect of heat-treatment on partitioning and finally, crack propagation studies carried out to a limited extent. They have been critically analysed and interpreted in Chapter VI.

Based on the above findings, conclusions have been drawn with regard to (i) the optimum Mn content, heat treating temperature and time for inducing maximum hardening, (ii) identification of microstructure with the help of optical, scanning microscopy and X-ray diffractometry, (iii) partitioning of alloying elements into different phases, (iv) mechanism of hardening and (v) inter-relation between microstructure, hardness and wear. These are enumerated in Chapter VII.

ABBREVIATIONS

Wt.%.	Weight percent
HV_{50}	Vickers hardness at 50 Kg load
VPN	Vickers pyramid number
BHN	Brinell hardness number
L.C.	Low carbon
H.C.	High carbon
P	Pearlite
C_b	Carbide
B	Bainite
M	Martensite
A	Austenite
AC	Air cooled
WQ	Water quenched
h	Soaking/austenitizing period in hours
M_3, M_5, M_7	M_3C, M_5C_2, M_7C_3 — Types of carbides (M represents metallic ions eg Fe,Cr,Mn etc.)
α	Ferrite
α'	Martensite/shear transformation
γ	Austenite product
C	Concentration
Al_0	As-cast alloy Al
Al_{-1}, Al_{-2}, Al_{-3}, Al_{-4} and Al_{-5}	Alloy Al heat-treated at 750°C at equal intervals of 2,4,6,8 and 10 hours respectively.

Al_{-6}, Al_{-7}, Al_{-8}, Al_{-9} and Al_{-10}	Alloy Al heat-treated at 800°C at equal intervals of 2,4,6,8 and 10 hours respectively
Al_{-11}, Al_{-12}, Al_{-13}, Al_{-14} and Al_{-15}	Alloy Al heat-treated at 850°C at equal intervals of 2,4,6,8 and 10 hours respectively
Al_{-16}, Al_{-17}, Al_{-18} Al_{-19} and Al_{-20}	Alloy Al heat-treated at 900°C at equal intervals of 2,4,6,8 and 10 hours respectively
Al_{-23}	Alloy Al heat-treated at 950°C for 6 hours
Soaking period	Holding period at heat-treating/ austenitizing temperature

C O N T E N T S

Page

CHAPTER II FUNDAMENTAL CONSILERATIONS IN THE DESIGN OF HEAVY DUTY ABRASION RESISTANT CAST IRONS

Page

Page

CHAPTER - I

ABRASION RESISTANT WHITE CAST IRONS

1.1 INTRODUCTION

Cast irons are essentially Fe-C-Si alloys containing sulphur and phosphorus as impurities. Depending upon whether 'C' is present in 'free form' or in the 'combined form', there are two broad categorizations namely 'gray' and 'white'. Whereas the domain of the former variety, which includes different grades of gray irons, S.G. irons and malleable irons, is ever encompassing, irons of the latter variety are hard and brittle and are best utilized under conditions where resistance to wear/abrasion is the main requirement. In most instances they are characterized on the basis of hardness in the as-cast/heat treated condition.(1-3)

Wear resistant white irons can be further classified as 'plain carbon' and 'alloyed'. For a given application, whether a given composition should be 'plain carbon' or the 'alloyed' type would essentially be governed by cost considerations and the end-properties desired e.g. for small sized components such as cylindrical grinding media (cylpebs) a plain carbon composition may 'suffice' but not for heavy duty applications.(1-3)

The design of 'plain carbon' and the 'alloyed' white irons is essentially based on rational considerations involving

attainment of 'wear resistant' microstructures. The following sections are devoted to an understanding of these considerations with reference to the important varieties of plain carbon and alloyed cast irons currently in use. A section on wear and its measurement has also been included since besides hardness, it is considered as an important basis for characterizing white irons.

1.2 CLASSIFICATION OF WHITE CAST IRONS

1.2.1 Plain Carbon White Irons

White irons are most extensively used in applications where resistance to wear is the main requirement. This is because of a high hardness (410-470 HV) associated with them.[1,2,4] In plain carbon white irons, hardness increases with an increase in the carbon content. However, difficulty in the attainment of adequate shock/impact resistance precludes the use of hypereutectic white cast irons under service conditions involving even moderate wear. Hypoeutectic white irons are by far the most extensively used materials. Their microstructure consists of pearlite+carbide, the microhardness of the constituents being 200-300 HV and 800-1000 HV respectively. The desired level of hardness can be attained by controlling the proportions of these constituents and would be governed by the carbon content/carbon equivalent.[1,2,4] For most applications a carbon content ~3% is considered as optimum.

The most important single parameter in ensuring that a given composition casts 'white' is the C/Si balance, not withstanding the other variables namely the solidification process and the cooling rate. The combined effect of these three parameters has been summarized into a single diagram called the Maurer diagram[5]. It infact serves as the basis for designing plain carbon white iron compositions. The favourable effect of a high C/Si ratio in ensuring the formation of a 'white' iron structure can be further accentuated by employing chilling. This may lead to an increase in the hardness (and hence the wear resistance) expected from a composition. It should however be remembered that employing chilling has practical limitations. Representative compositions, properties and applications of plain carbon white irons are summarized in Table 1.1.[2,6-8]

1.2.2 Chromium White Irons

The practical limitations in ensuring that a given plain carbon composition is cast 'white' over a range of section sizes have been overcome by developing chromium white irons.[1-3,6] Controlled additions of Cr can most effectively and economically ensure that a composition is cast white(independent of the cooling rate and section size).This is attributed to its carbide forming/stabilizing tendency.[9,10] The effect of Cr on the microstructure of a white iron would depend upon the amount added. This is because in addition to being a carbide

stabilizer a small proportion of Cr also partitions to austenite[9]. The former is effective in counteracting either partly or fully the tendency of the carbide phase to decompose during cooling whereas the latter would prove useful in improving hardenability[10]. Chromium partitioned to the carbide phase will also increase its hardness, the absolute value being a function of the amount added and the nature of the carbide formed[11]. Thus Cr additions bring about an overall increase in the hardness.

The beneficial effect of Cr in improving hardenability can be further accentuated through controlled additions of strong carbide stabilizing elements such as Mo and V. They (particularly Mo)are known to enhance hardenability of steels markedly[10] and would prove equally effective in promoting the formation of hard 'metastable' phases in cast irons. Additional hardening would accrue as majority of Mo and V partition to the carbide phase thereby increasing its hardness[10].

Based on the above considerations, Cr containing white irons can be classified as (i) straight Fe-Cr type and (ii) Fe-Cr-X type and its variants such as Fe-Cr-X-Y, where X,Y denote elements such as Mo, V etc.

1.2.2.1 Straight Cr White Irons

Cr is the main alloying element in this variety of cast irons. Its amount to be added is based on considerations

outlined in Section 1.2. The beneficial effect of Cr additions can be further accentuated by selecting a proper 'C/Si' balance based on the Maurer diagram, although doing so may not be absolutely essential in the presence of 'Cr'. In view of this, it may be possible to incorporate a relatively higher proportion of Si for the beneficial effect(s) it imparts such as improvement in casting characteristics.[12] Typical compositions, properties and applications of Cr white irons are summarized in Table 1.2.[2,6-8]

1.2.2.2 Cr-X and Cr-X-Y Varieties

The Cr-X and Cr-X-Y varieties were developed towards late forties to early fifties and have been finding extensive applications particularly the 27% Cr variety.[13] Around early sixties , the Climax-Molybdenum Co. developed 15 Cr-3 Mo alloy which exhibited extremely high resistance to abrasion.[13] The publication of a comprehensive atlas on the transformation behaviour and hardness values of a series of Cr-Mo white irons (Cr ranging from 12-25% and Mo from 1-3%.) was a further indication of the interest in the Cr-Mo varieites.[14]

Subsequent to this development, interest was shown in the use of 13% Cr white irons in Western Europe. These compositions were alloyed with Mn,Mo and in some instances also Ni to improve their hardenability.[13] Some recent publications indicate that interest in the 12/13% Cr variety

has not yet dwindled.[15] Compositions of some representative Cr-X and Cr-X-Y type of white irons along with their hardness, microstructure and applications have been summarized in the Tables 1.3[2,6-8] and 1.4[2,6-8] respectively.

1.2.3 Ni-Cr White Irons

These alloys were developed by the International Nickel Co. (INCO) and are available in four different grades- the lower alloy versions designated as Ni-hard 1, 2 and 3 and their higher alloy counterpart Ni-hard 4.[16,17]

Ni-hard cast irons are essentially Ni-Cr cast irons possessing outstanding resistance to wear. Their use in the mining, power, cement, ceramic, paint, dredging, coal, coke, steel and foundry industry is now well established as an outcome of the experience gained over nearly fifty years. Cr additions to Ni-hard irons affect structural changes similar to the ones observed in the straight Cr or the Cr-X or Cr-X-Y series. The presence of nickel ensures that hardenability is improved thereby facilitating the formation of metastable phases such as martensite.[16,17]

Ni-hard cast irons possess a matrix microstructure akin to heat treated steel. In addition they contain a multitude of refined carbides which make an important contribution to their wear resistance.[16,17]

Ni-hard types 1 and 2 which contain relatively lower

amounts of Ni and Cr were primarily developed as high hardness wear resisting materials, their fundamental property being high hardness. Microstructurally they comprise of bainite/tempered martensite + carbide[13,16,17]. An important observation concerning Ni-hard 1 and 2 is that their shock resistance in general is low. However, the shock resistance of Ni-hard irons particularly of the low carbon and heat treated varities is substantially better than unalloyed white cast irons.[16] Their important properties and applications are summarized in Table 1.5.

A modified version of Ni-hard 1 and 2 containing higher proportions of Ni and Cr and designated as Ni-hard 4 was developed by INCO around the mid-fifties.[13] The main objective in doing so was to improve the resistance to fracture under repeated impact. In view of a higher alloy content, the Ni-hard type 4 variety is harder and has a greater resistance to corrosion. In fact Ni-hard type 4 possesses the highest strength and greatest resistance to impact of all the Ni-hard varieties. The better resistance to fracture in Ni-hard 4 as compared with Ni-hard 1 and 2 is due to the presence of carbides in a discontinuous and less massive form.[17] The dispersed finer carbide has primarily been achieved by modifying the composition principally in relation to Cr so that the carbide is in the form of a discontinuous trigonal carbide $(Cr,Fe)_7C_3$. As per a more recent appraisal, the attainment of a discontinuous and hard $(Cr,Fe)_7C_3$ carbide

results from a high Cr content and eutectic composition of the type 4. This together with the advantage of a lower carbon content and a somewhat tough high nickel matrix makes Ni-hard type 4 a very useful abrasion resistant material.[17] The chemical composition and properties of Ni-hard type 4 are summarized in Table 1.5.[17] Important changes brought about in the composition of the type 4 namely Ni = 5 to 7% in place of 5.5-6.5% , Cr = 7-11% as against 7-9% and Mn = 1.3% maximum in place of 0.4-0.7%, as per the recent literature published by INCO are note-worthy.[17]

Besides the standard compositions described as Ni-hard, a number of other Ni-Cr white iron compositions are in use. Their representative compositions, properties and applications are summarised in Table 1.6.[2,6-8]

1.3 WEAR

1.3.1 General

The American Society of Lubrication Engineers(ASLE) and others have accepted the definition of wear as 'removal of material by mechanical action',[18] while the Organization for Economic Cooperation and Development (OECD) research group on wear of engineering materials defines wear as the 'progressive loss of substance from the operating surface of a body occurring as a result of relative motion at the surface'.[19] These definitions are not sufficient since

they have not incorporated the concept of material removal due to corrosive, chemical or fluid action.[20] On overcoming this deficiency, wear may be alternately defined as the 'unwanted removal of material by chemical and/or mechanical action.' It manifests itself whenever there are load and motion either in the presence or in the absence of an environment.[20]

Modern research has established that there are four main forms of wear besides a few marginal processes which are often classified as forms of wear and which could be appropriately considered under one or more of the following forms[21],

(1) Adhesive wear,
(2) Abrasive wear,
(3) Corrosive wear and
(4) Surface fatigue wear.

1.3.2 Adhesive Wear[19-22]

Adhesive wear is also called galling, scuffing, scoring or seizing[22]. It is defined as 'wear by transference of material from one surface to another during relative motion, due to a process of solid phase welding'.[19]

It arises whenever there is an intensive interaction between two rubbing surfaces in intimate contact from mutual adhesion. When the adhesive forces between the two rubbing surfaces are greater than the body forces (i.e. internal bond forces between ions) of either of the material/specimen,

adhesive wear occurs.[20,21] Such adhesion results in a heavy tearing of the rubbing surfaces, whenever this contact is broken. The break may not occur at the original interface but within one of the weaker materials. The removed material may remain attached at the adhesive junction, or may become dislodged and remain between the two surfaces as wear debris, causing further damage as an agent for abrasive wear.[20,22]

1.3.3 Abrasive Wear[2,6,7,20-24]

Abrasive or cutting type of wear takes place whenever hard particles (such as metal grit, metallic oxides) are present between the rubbing surfaces. Conditions leading to abrasive wear also exist when (a) two surfaces, one of which is harder and rougher than the other are in sliding contact and (b) hard abrasive particles are embedded in one of the surfaces (softer matrix). Material removal occurs by scratching or ploughing of the softer surface and generally is in the form of loose wear particles.[20-22]

Abrasive wear occurs in a wide variety of operations such as earth-moving, mining, cement, mineral dressing, agriculture, chemical processing, brick and ceramic manufacturing and power production.

Although the conditions leading to abrasive wear vary widely, they may be classified into three distinct types.[6,7,22-24]

(i) Gouging abrasion,
(ii) High stress or grinding abrasion and
(iii) Low stress or scratching abrasion or erosion.

Gouging abrasion involves removal of relatively coarse particles from the wearing surface and is similar to the removal of metal by grinding or machining with a coarse grit grinding wheel. In service, this occurs on impact pulverizer hammers, and some chute liners.(7)

High stress grinding abrasion involves removal of relatively fine particles from the wearing surface. The pinching action of two metal surfaces causes the abrasive to break into fine pieces. Unit compressive or shear stresses are very high. Consequently the hard abrasives such as quartz,are capable of indenting or scratching steel with a hardness of 65-70 HRC. Metal may be removed from the wearing surface by microscopic gouging or by a combination of local plastic flow and microcracking.(7)

Erosion and/or low stress scratching abrasion occur by very light rubbing contact from sharp abrasive particles. The stresses are due mainly to velocity and are normally insufficient to cause much fragmentation of the abrasive.(7,21)

1.3.4 Corrosive Wear (2,6,20-22,25-27)

Corrosive wear or frettage/frettage corrosion occurs as a result of the combined action of corrosive environment and mechanical forces. In the absence of a sliding motion

the products of corrosion would form a 'natural' protective surface (oxide film) which may slow down or even arrest corrosion.[21] During service, the protective surface film may peel off because of the rubbing action between surfaces leading to material loss of small magnitude. The freshly formed surfaces thus exposed may temporarily adhere and small portions of the adhered areas may break off due to further rubbing action resulting in heavy material loss. Eventually the debris may then be converted into a loose agglomerate of an abrasive oxide which will lead to severe damage.[22] The damaged surface may either reveal the presence of a considerable volume of corroded material or may be heavily galled with little oxide.

Sometimes material loss/damage may also occur due to the formation and activation of galvanic cells. This is known as galvanic corrosion or bi-metallic corrosion. It involves damage to a surface caused by a flow of current in a liquid, between two dissimilar metallic surfaces.[22] In relation to wear, galvanic cells may operate either at the surface of a metal containing structural inhomogenities (including differential stresses) or between dissimilar metals in electrical contact.[22,25]

Other types of cells leading to material loss are differential concentration cells, differential aeration cells, and differential temperature cells.[25]

Differential concentration cell or simply concentration cell consists of two identical electrodes in contact with a solution of differing concentration. The electrode in contact with the dilute solution (anode) dissolves and plates out on the other electrode (cathode). The reactions seize when the solutions attain the same concentration.[25]

Differential aeration cell consists of two identical electrodes in the same electrolyte, the electrolyte around one electrode being thoroughly aerated (cathode) and around the other de-aerated (anode). The difference in oxygen concentration produces a potential difference and causes current to flow.[25]

Differential temperature cells comprise of electrodes of the same metal, each of which is at a different temperature, immersed in an electrolyte of the same initial composition.[25]

1.3.5 Surface Fatigue Wear[2,6,20,22]

Pitting, pitting corrosion, spalling and case crushing are similar phenomenon and may be grouped under 'surface fatigue wear'.[22] Its occurrence is attributed to the cyclic repetition of contact stresses between two mating surfaces e.g. pair of gears or ball and a race, under load.[21,22] The resultant cyclic stresses may exceed the fatigue strength of the material causing fatigue cracks below the surface at a depth of ~0.2-0.3 mm.[21,28] Initially small sub-surface cracks propagate parallel to the surface causing characteristic

spalling and flaking of material from the surface. The cavity thus formed is a pit from which material frequently spalls out.[21]

The destructive character of pitting involves a number of factors such as high contact stresses, sliding action accompanying rolling action, possible formation of an elastic wave ahead of the instantaneous area of contact, surface flow and sub-surface fatigue.[22]

Another phenomenon akin to surface fatigue in which cyclic stresses leading to pitting are generated through a mechanism involving a liquid is called cavitation erosion. It is a wear of a solid body moving relative to a liquid in a region of collapsing vapor bubbles which cause local high impact pressures or temperatures resulting in work hardening, fatigue and formation of cavitation pits due to the removal of a particle.[21,22]

1.4 CHARACTERIZATION OF WEAR

1.4.1 Principle

A critical analysis of the section 1.3 reveals wear to be a complex phenomenon. Irrespective of its nature, however, it is evident that it leads to loss of material in some form. Therefore, any method evolved to characterize wear would essentially depend upon the assessment of material loss. The simplest and the most widely used way to summarize wear data is to note changes in length, volume or mass. Wear resistance

is sometimes given as the inverse of one of these quantities.[7]

Different methods that can be employed would depend upon whether they utilize physical, mechanical or optical principles as their basis. Another important aspect related with wear testing is that it would be difficult to simulate actual service conditions in a laboratory test. Therefore, it is difficult to prescribe any particular test as a 'standard' wear test*. As such any test that is employed can at best help in evaluating (i) the relative performance of different materials and, (ii) a newly developed material with reference to a standard material (i.e. one which has been in extensive use). Bearing these difficulties in mind, hardness has been generally considered as a good approximation for representing resistance to wear. Although characterization of wear by a simulated test is gaining in acceptability, it is still a common practice to represent wear resistance on the basis of hardness. Most international standards follow this practice.[17]

1.4.2 Parameters

The simplest method of characterizing wear is by abrading a specimen surface against a hard surface (e.g. abrasive wheel) followed by assessing the weight loss or percent weight loss over a predetermined period at fixed intervals, the pressure being kept constant. The data thus

---

* Although the 'disc and pin method' and its variations are popular.

generated is also helpful in evaluating the wear rate, W_r, which is given by the expression,

$$W_r = \frac{(W_1 - W_2)}{t}$$

where,

W_1 = weight of specimen before wear,

W_2 = weight of specimen after wear,

t = time of wear in hrs or minutes.

Other parameters of interest are termed as specific wear ratio and grinding ratio.

The specific abrasive wear ratio, w, is defined as,[28]

$$w = \frac{\text{weight of material removed due to wear}}{\text{wheel wear}}$$

$$= \frac{\Delta W}{\frac{\pi}{4}(d_1^2 - d_2^2)t.\rho}$$

where,

ΔW = weight of specimen material removed due to wear = $W_1 - W_2$,

W_1 = weight of the specimen before wear,

W_2 = weight of the spcimen after wear,

d_1 = diameter of grinding wheel before wear,

d_2 = diameter of grinding wheel after wear,

t = thickness of the grinding wheel,

ρ = density of wheel material.

The reciprocal value, w^{-1} is a measure of the wear resistance.

1.4.3 Methods

1.4.3.1 Weighing Method[21]

In this method weight loss is measured. This method is very popular and generally employed for characterization of wear resistant materials.

1.4.3.2 Mechanical Gaging Method[21]

Micrometer screw gages are used to measure the loss of material due to wear in terms of reduced thickness of specimen.

1.4.3.3 Optical Method[21]

There are number of methods of measuring wear using an optical technique. One way is to make a small microhardness indentation in a surface, and to study how its size is reduced during sliding/rubbing.

1.4.3.4 Radio-tracer Technique[21]

The advent in the late 1940's of radioactive isotopes of the common engineering metals has had a profound effect on the study of wear. Consequently, it has become possible to measure wear while it is occurring, rather than by before and after types of measurements.

1.5 CONCLUSION

Different types of abrasion resistant white irons currently in use have been classified and their compositions,

properties and applications considered. Whereas plain carbon white irons are most usefully employed for manufacturing small components undergoing moderate wear, heavy duty applications warrant the use of alloy white irons.

Although hardness is most commonly employed for characterizing white irons, there is a growing awareness that wear data in some form is equally pertinent. Accordingly sections 1.3 and 1.4 have been devoted to an understanding of wear as also to the principles involved and methods of characterizing it.

Analysis of the preceding sections reveals a general lack of understanding as to the most suitable microstructure for attaining the optimum in terms of resistance to wear. The next chapter therefore deals with the fundamental considerations in the design of wear resistant cast irons.

CHAPTER - II

FUNDAMENTAL CONSIDERATIONS IN THE DESIGN OF HEAVY DUTY ABRASION RESISTANT CAST IRONS

2.1 INTRODUCTION

Some useful data on the development of plain carbon, Cr base and Ni-Cr white irons along with a brief account of wear and its characterization have been discussed in the previous chapter. It emerged that a definite need existed to examine afresh the most suitable microstructure from the point of view of wear. Equally pertinent would be to evolve all possible alloy combinations which may prove useful in obtaining the 'desired' microstructure. This would necessitate a discussion on how different alloying elements influenced the transformation behaviour of white irons.

Accordingly, the present chapter deals with : (i) a comparison between different microstructures vis-a-vis their resistance to wear, (ii) effect of alloying elements on the transformation behaviour of Fe-C alloys to help attain the 'desired' microstructure and eventually lead to (iii) the basic considerations involved in the economical attainment of alternative wear resistant compositions.

2.2 WEAR IN WHITE IRONS

2.2.1 General

The following sections are devoted to a discussion on the relative wear characteristics of the prominent microstructures encountered in white cast irons. Such an analysis would primarily involve two components : (i) matrix microstructure and, (ii) second phases. The former essentially consists of pearlite, bainite, martensite and tempered martensite. Ferrite has not been considered as it is too soft and would therefore wear out fast. Carbides, inclusions, precipitates, dispersions or soft microstructural constituents such as residual austenite in a matrix are examples of 2nd phase.[31]

Additionally other parameters needing consideration will be (i) matrix- second phase interaction and (ii) properties of the abrasives.

Lastly a separate section is devoted to the characterization of 'wear' based on bulk parameters (such as hardness etc.) including fracture toughness. Especially noteworthy is the introduction of wear strength[31], a recently introduced parameter to characterize wear.

2.2.2 Matrix-Microstructures

2.2.2.1 Pearlitic Matrix

A wear resistant microstructure is one entailing a minimum of material loss commensurate with service requirements

and cost considerations. In plain carbon white irons, the microstructure could be broadly classified as pearlite + carbide (P+C) with an overall hardness of 400-600 VPN[2-4] and microhardness of 200-300and 800-1000 VPN respectively.[2-4] Some of the under-alloyed white irons also attain this microstructure. Although not ideally suited to withstanding heavy duty wear (because of a restriction on the maximum attainable hardness), a discussion on plain carbon white irons as wear resistant materials is imperative since they and the lower alloyed versions are extensively employed (Table 1.1).

Little effort appears to have gone into understanding the wear-mode of pearlite based microstructures in white irons although some data on their behaviour is available.[2,6-8,32] However, the findings of a recent study on plain carbon steels (C varying from 0.1 to 1.2%), in which spheroidized/lamellar pearlite microstructures were tested at identical carbon contents, provide useful insight into the underlying mechanism(s).[33]

Structural variables in the study were interlamellar and interparticle spacing. The former was varied by isothermally transforming steels at different temperatures, whereas the latter was varied by tempering to different temperatures. Wear resistance was measured as weight loss after subjecting specimens to abrasion with fine silica powder. It was observed that in spheroidized structures ferrite phase was heavily grooved (i.e. fractured) whereas the dispersed carbides

prevented or reduced the penetration of the abrasive particles into the softer matrix. The depth of penetration (by the abrasive particles) reduced with an increase in the carbon content. Thus dispersed carbides not only prevented indentation by reinforcing the matrix but also prevented free movement into the softer ferrite matrix. In lamellar pearlite, the grooves were narrower and shallower than in ferrite. Thus pearlite wore less than ferrite. Comparing the spheroidized and lamellar microstructures, the latter occupies a larger area than the rounded carbides in the spheroidized structure. Hence the amount of free ferrite exposed to the abrasive was less in a lamellar microstructure than in the spheroidized microstructure. This suggested that the lamellar structure should exhibit better wear resistance than the spheroidized structure.[33] However, the two microstructures in actuality exhibited comparable wear resistance thereby suggesting that morphology alone did not control wear and that the state of a material associated with a particular microstructure (i.e. whether brittle or tough) was equally important. Usefulness of the spheroidized microstructures is evident in this regard. Thus hardness, toughness and the morphology of the second phase together gave a better indication of wear than any one of the parameters individually.[33]

The above discussion also suggests that the resistance to wear in general would improve if the amount of free ferrite is reduced to a minimum and/or

free carbide introduced into the microstructure. This is possible if the 'C' content is ~0.8 % or higher. Thus it is the carbide phase which appeared to govern the resistance to wear[33]. This inference is of interest since the presence of free carbides is an essential feature of the white iron microstructure. Furthermore, its presence should be considered as desirable for improving resistance to wear.

2.2.2.2 Bainite/Tempered Martensite and Martensite Matrix

If a white iron is to perform satisfactorily under conditions involving 'heavy' wear, the overall hardness of the material should be increased and the disparity between the hardness levels of the matrix and the carbide phase reduced to as low a level as is structurally feasible. Some indications of how such changes are affected have been given in Chapter I (Section 1.2). The nature of the matrix phase could be either bainite/martensite or their combination (with or without austenite) depending upon the nature and the amount of alloying elements added. Since one of the methods of enhancing the overall hardness of a white iron is by increasing the hardness of the free Fe_3C (by converting it into an alloy carbide), attempts to reduce the disparity between the matrix and the carbide phase may not prove successful. However, if the matrix phase were to attain a 'certain minimum' hardness, it is then expected that the overall resistance to wear would 'substantially' improve. The magnitude of

matrix microstructures could be had by maintaining the hardness the same. From fundamental considerations, it would appear that lower bainite (akin to a tempered microstructure) should prove much better than quenched martensites/tempered martensite.[34]. There is some evidence in the literature supporting this contention especially when 'wear strength' is considered.[31]

2.2.3 Effect of Second Phase

2.2.3.1 Retained Austenite

Besides the conventional microstructures M+carbide or bainite+carbide, other microstructures to receive some attention are (i) M+carbide+γ, (ii) M+free carbide+dispersed carbide, (iii) austenite+carbide and (iv) an unconventional microstructure consisting of microconstituents normally present in white irons plus graphite.

A critical analysis of the section 2.2.2 would reveal that there is at least an indirect evidence of the usefulness of austenite in controlling abrasive wear. Some recent findings reinforce this view further. Whereas it has been deduced that 'most' wear resistant irons were those with either a martensitic or a martensitic-austenite structure,[41] in another study[41] which has identified the basic steps in a wear process, it was suggested that although the wear resistance of a martensitic matrix is greater than that of an austenitic matrix, under 'certain' conditions alloys with

austenitic matrices can exhibit better wear resistance than similar alloys with a martensitic matrix. Data contrary to this finding has been reported[42], wherein it was stated that the decrease in the abrasive wear resistance of a 28 % Cr white iron, as consequence of Mn additions, was due to the stability of the austenite matrix and hence to a consequent retardation of hardenability.

Fracture toughness studies on wear resistant brittle materials are gaining in popularity since such an investigation provides a useful insight into the crack propagation behaviour of materials. Wear resistant materials exhibit intrinsically poor resistance to crack propagation. Evidently, if they have to perform satisfactorily, their resistance to shock/repeated impact has to be improved. The simplest method suggested to achieve this is by rendering continuous carbide net work discontinuous.[43] Another possibility could be to introduce a phase/microconstituent which is intrinsically resistant to crack propagation. Austenite may proveuseful in this regard. In its presence, the parameters that would control fracture toughness/ wear resistance would be the relative percentages of carbide, martensite and austenite. During one such study[44], it was revealed that above a 'critical' volume fraction of carbide, the resistance to wear decreased. Whether or not this was due to brittleness of the carbide phase, as suggested in a study,[42] has not been clearly established. Martensitic irons gave consistently better abrasion resistance than

austenitic ones. However, as regards toughness, consistently better values were obtained with austenitic matrices compared with martensitic ones.[44] The observation that the best combination of abrasion resistance and toughness was obtained with 'heat treated cast irons' is a significant one and needs careful analysis.

The findings of the above study[44] are further substantiated by the data obtained on the low stress and 'gouging wear' behaviour of specimens of Ni-hard 4 cast irons. The samples were processed to contain 5-85%. retained austenite and the wear behaviour was measured with loose SiO_2 and Al_2O_3 abrasives in a rubber wheel test system. Gouging abrasion behaviour was determined using a 'bonded Al_2O_3 wheel' test system. Carbides controlled wear behaviour in the low stress tests against SiO_2 and their (carbides) attrition occurred by uniform scratching, preferential chipping at the leading edges and cracking and spalling. In low stress and gouging tests against Al_2O_3, both the carbides and the matrix underwent attrition by uniform micromachining. The inference that retained austenite could be used to optimise wear resistance in a variety of abrasion situations is significant.[45]

The probable mechanismsby which presence of austenite may prove beneficial are (i) transformation of retained austenite to martensite and, (ii) large work hardening induced (as in Hadfield steel) as a result of high local

deformation encountered in abrasive wear loading using a hard abrasive.[31] The advantage with the latter situation is that although a thin layer attains a hardness as high as the surrounding matrix, good ductility, which is an inherent attribute of austenite, is maintained in the inner layers. The probable reason why presence of austenite is not beneficial in certain cases is that the test conditions involve low stress abrasion with an abrasive softer than the carbide.[46] Thus a 'transformable' content of retained austenite would prove favourable for wear resistance when abraded by an abrasive harder than the carbides be it high speed tool steel or an alloy white iron.[31]

Whether or not austenite may be desirable depends upon the matrix microstructure. It has been suggested that residual austenite is desirable in a bainite structure because there is less difference between the hardness than there is between martensite and austenite. After work hardening or transformation of retained austenite, matrix hardness can be higher than that of completely bainitic structure.[31]

2.2.3.2 Dispersed Carbides

Another type of microstructure, which although in principle is similar to those discussed in section 2.2.2, is one in which the martensitic matrix contains dispersed carbides.

Such a microstructure may prove more useful than the conventional M+ carbide microstructure as the matrix would now be further reinforced by the presence of dispersed carbides provided the average particle size, volume fraction and dispersion is optimum. Adhesion of the dispersed carbides with the martensite matrix shall be an important parameter in determining the response of such a composite to wear.

High wear resistance is obtained in the microstructures with fine, well dispersed semicoherent particles[47]. This is because wear depends upon hardness after high local deformation and neither shearable (coherent) particles (having low hardness) nor cold working before wear testing contribute to wear resistance. Non-shearable particles increase wear resistance in proportion to the hardness increment. The ratio of the indentation hardness of noncoherent and coherent particles is approximately five to one. Thus non-coherent/ semicoherent particles are by themselves hard and are not sheared (i.e. no localized work softening is produced) and hence are most useful in improving wear resistance.[31,34]

A more clear picture on the role of dispersed carbides - matrix microstructure interrelation in controlling wear is now available.[48,49] It has been demonstrated that low stress abrasion resistance is principally controlled by hard dispersed-carbide phase and that the

hardness of the matrix is of secondary importance. Strength of the matrix was important in providing mechanical support to the carbide particles. The matrix however played a critical role in determining the fracture toughness of white irons through its ability to prevent brittle crack propagation from one carbide particle to another. Both abrasion resistance/fracture toughness were found to be the greatest for austenitic matrices.[48,49]

2.2.3.3 Graphite

There is some evidence that a microstructure consisting of constituents normally present in white irons along with graphite (preferably in spheroidal form) may prove useful in improving resistance to wear.[13,38,50-52] A possible reason for this is that graphite in nodular form is also likely to improve resistance to crack propagation, wear and spalling.[34] Although the mechanism by which resistance to spalling is improved is not yet established, the observation that indefinite chill rolls have excellent resistance to spalling[53] supports the above contention.

Flake and spherical graphite affect resistance to wear, their effect being akin to micro-cracks, pores, large carbides or inclusions as they act as internal notches.[31] A comparison of wear rates between cast irons with flake and graphite nodules (matrix hardness being same in both the cases) revealed that at low or medium loading (testing with 220 mesh alumina) both graphite

forms produced about equal wear rates. However, at higher loadings, the wear rate of irons with flake graphite increased much faster. This has been attributed to the high notch intensity of the flake morphology which is about one to two orders of magnitude higher than that for spherical morphology. Crack propagation along flakes will occur at relatively low applied loads leading to an increased wear rate.[31,52]

2.2.3.4 Morphology and Distribution of Free Carbides

Wear resistance is directly related to the percentage of 'free' carbide (section 2.2.1). There is a critical amount above which wear resistance is adversely affected[44] due to the brittleness induced.[42] For a given volume fraction of the carbide and under constant abrasive conditions (carbides softer than abrasive particles), resistance to abrasion is improved by increasing its hardness.[31,54] This is achieved by adding carbide forming elements in general, the stronger the carbide forming tendency the greater the increase in hardness.[10] Vanadium additions have led to the attainment of a hardness as high as 2200-2600 VPN.[55]

The importance of a discontinuous carbide net work in improving resistance to crack propagation/ shock resistance has already been brought out.[17,43] The morphology and the dispersion of free carbides are expected to play a prominent role in governing the overall properties.

There are conflicting claims on the effect of morphology. Presence of plate like cementite has been shown to improve the wear resistance of cast irons containing steadite.[56] Presence of plate like carbide of the type M_7C_3 has also been found to be similarly beneficial.[57] This observation perhaps points to crystal structure as an important parameter in controlling wear. Coarser carbides tend to reduce resistance to wear.[58]

It is however opined that for optimum wear resistance and resistance to crack propagation, free carbides should be equiaxed, evenly distributed and adherent with the matrix. In what way the crystal structure will influence the attainment of carbides in this form is not established although it (the crystal structure) is expected to play an important role in governing their morphology and perhaps dispersion.[59]

2.2.4 'Bulk Property' - 'Wear Resistance' Interrelation

2.2.4.1 Hardness, Surface Hardness and 'State' Properties

A very pertinent point to consider while discussing characterization of wear is which of the bulk parameters represent it most effectively. There are conflicting claims regarding such a correlation. An interrelation has been found between bulk properties, in particular elasticity and hardness, by many workers.[60-66] They showed that wear resistance was directly proportional to the hardness of the metal. The effect of physical properties of the abrasive on 'abrasive wear' has also been considered by defining the hardness

ratio H/H_a, where, H = hardness of the material and Ha = hardness of the abrasive.

It was found that for $H/H_a < 0.5$, wear was almost independent of the hardness of the metal matrix.[67-69] In another study involving the determination of the wear resistance of cast irons and steels, no general relationship was found between the bulk hardness of the alloys prior to testing and the amount of abrasive wear that had occurred.[13] However, when strain hardening of the abraded surface was taken into consideration, the results fell very close to a straight line.[13] This observation is of fundamental importance in the understanding of the wear process. During abrasion, hard particles have to penetrate the abraded surface and quite logically therefore it is the hardness of the surface during abrasion that should be a measure of its resistance to penetration and not its hardness prior to abrasion. This may explain why attempts at relating bulk hardness with abrasion resistance have not always been successful. An important parameter that would determine the surface hardness is the extent of surface hardening. The importance of surface hardening by deformation is now well understood.[70-73]

In a recent study on the wear resistance of plain carbon steels (C ~0.1-1.2%), in which both lamellar and dispersed carbide microstructures were investigated, the authors have demonstrated that hardness is not the only

measure of abrasive wear (resistance). A combination of high hardness coupled with toughness is a better indication of the resistance to wear. Thus morphology and amount of the second phase are of importance.[33] Therefore, the parameter 'log t' rather than the interparticle spacing λ appeared to be a more appropriate basis for representing wear resistance. The authors have gone on to further suggest that a kinetic parameter such as T(C+log t) containing both the tempering temperature and time which will govern the type of phases present, their morphology and distribution (and therefore the physical state of the material) may turn out to be a more suitable parameter than hardness alone which does not necessarily depict the type of phases that are present.[33]

2.2.4.2 Wear Strength

Fracture toughness measurements are gaining in prominence for characterizing wear resistant brittle materials. Important data obtained on the crack propagation behaviour as influenced by microstructure has already been discussed in the appropriate preceding sections. An important parameter needing introduction is termed 'wear strength'. High wear resistance in a structural member is not always sufficient for many practical problems. The product of $\sigma_{0.2}$(0.2%proof) and fracture toughness (K_{IC}) represents useful combination of properties if both high resistance to deformation and

the resistance to spalling.

Wear resistance is most appropriately represented by hardness not withstanding the usefulness of parameters which reflect upon the state of a material (e.g. brittle or tough). This contention is especially valid when the microstructure of interest comprises of M+C (martensite + carbide).

Since the desired microstructure can be obtained through alloying, a critical reappraisal of the effect of alloying elements on the transformation behaviour of white irons is essential. The following sections are accordingly devoted to such a discussion.

2.3 ATTAINMENT OF THE DESIRED MICROSTRUCTURE THROUGH ALLOYING

2.3.1 General

Alloying is the key to the attainment of any desired change in the microstructure and hence properties. It is most effectively utilized through appropriately designed heat treatment cycle(s). Alloying elements that are present/ added to cast irons may be broadly classified as:

(i) Carbide-stabilizers[1,2,10] - Cr, Mo, V, W, Mn, Sn, B, Bi, Te.

(ii) Carbide destabilizers/graphitizers[1,2,10] - Si, Ni, Cu, Al, C.

(iii) Promoters of metastable phases[2,10] (e.g. martensite) - Ni, Mn and small amounts of strong carbide formers e.g. Mo.

(iv) Impurity elements[2,10] - S, P, etc.

The following sections deal with the distribution of the above elements into different microconstituents, their effect on the transformation behaviour and any special effects they produce when present in/out of solution.

2.3.2 Effect of Alloying Elements

2.3.2.1 Carbon

It dissolves interstitially in γ and α irons and has a variable solubility in them. An increase in the carbon content (i) decreases depth of chill and (ii) raises the hardness of the chilled zone from 375 BHN (at C~2.5%) to 600 BHN (C~3.5%). Thus in unalloyed white irons, high total carbon is desirable for attaining high hardness and wear resistance. Carbon decreases transverse breaking strength thus promoting brittleness.[7]

The higher the carbon content the greater the tendency towards graphitization during solidification especially when the silicon level is also high. Thus,it is necessary to keep silicon level low in high carbon white cast irons. Normally the carbon content in unalloyed or low alloy white irons is kept between 2.2 to 3.6%. In high Cr white irons the range is from about 2.2% to as high as the eutectic

composition, which is about 3.15% C for a 15% Cr iron and about 2.5% C for a 27% Cr iron.(7)

2.3.2.2 Silicon

It is present in all cast irons and being a strong graphitizer, tends to destabilize cementite. Silicon is the main element that determines the carbon content of the eutectic in all types of cast irons. Increasing it lowers the carbon content of the eutectic and also promotes the formation of graphite on solidification. Thus a careful control is desirable for producing chilled and white iron castings.(7)

Its presence is beneficial as it increases the fluidity of the molten iron and therefore improves casting properties.(12) Silicon reduces hardenability and tends to promote pearlite formation in martensitic irons. But when sufficient quantities of pearlite suppressing elements such as Mn, Ni, Mo and Cr are present, increasing the silicon content raises the Ms temperature of the alloy marginally, thus permitting a near complete transformation to martensite and consequently leading to the attainment of a higher hardness.(7)

Silicon in amounts of 4.5-8% improveshigh temperature properties by elevating the eutectoid transformation temperature and by decreasing the scaling rate and grain growth.(7)

The silicon content of cementite/carbide phase in all irons is very small. Its partitioning is not greatly influenced by the presence of other alloying elements.(9)

2.3.2.3 Phosphorus

Phosphorus acts as a mild graphitizer in unalloyed irons.(7) At a given carbon and silicon contents, an increase in phosphorus by 0.1% decreases the depth of chill by about 0.1 inch (2.5 mm). It has been shown to reduce the toughness of martensitic white irons by forming a brittle phosphide eutectic, whose embrittling effect is pronounced when phosphorus content exceeds 0.3%. (7)

Phosphorus content/level is usually maintained below 0.4% in chilled and white irons and below about 0.3% in alloy cast irons.(1) Sometimes specifications call for even less than 0.1% .(7)

2.3.2.4 Sulphur

It is an impurity element like phosphorus and is known to cause hot shortness. Its adverse effect is counteracted by adding Mn. Sulphur exists as either manganese sulphide (MnS) [when Mn is added or present] or as ferrous sulphide (FeS) in iron and steel.(1) The latter is brittle and low melting yellowish-brown compound. The higher melting dove gray manganese sulphide is only slightly soluble in iron and coalesces into large globules irregularly distributed throughout the matrix.(1) It is plastic at high temperatures

and is soft. Manganese should be about five times that theoretically required to combine with the sulphur present for ensuring its effective elimination.

Sulphur increases the depth of chill.[7] A low sulphur content is preferred as it lowers shock resistance and makes castings weaker. Therefore, in abrasion resistant cast irons it should be as low as is commercially feasible, especially so since sulphides degrade abrasion resistance.[7]

2.3.2.5 Nickel

Solubility of Ni in iron is extensive in both the liquid and solid states (both γ and α forms).[75-77] Consequently the temperature/composition ranges over which austenite is stable are enlarged. It lowers the γ to α transformation temperature ($\sim 22^{\circ}$ for each %. of Ni) and in an iron containing 30% Ni, the transformation of γ to α is suppressed to about room temperature.[75]

Nickel lowers the melting point of cast irons by about 5°C for each 1%. addition and improves the fluidity slightly.[78]

Solubility of C in molten cast iron is lowered as the Ni content is increased. This leads to a decrease in the carbon content of the iron-carbon eutectic which is of the order of 0.06% for each 1%. addition of Ni.[79] The decrease in carbon content of the eutectic becomes significant only at high Ni contents.[2] Ni reduces the C

content of the eutectoid by about 0.04% for each 1% addition. The rate of austenite decomposition is retarded because of a lower rate of carbon diffusion in the iron.[75]

Ni is a mild graphitizer, its effectiveness being 0.3 that of Si.[2] Hence it is useful in preventing low carbon compositions from being cast white.[1,10] It reduces the chill depth and its influence is about one fourth that of Si. Ni additions thus help in (i) lowering the total carbon and silicon contents without incurring chill or hard castings and, (ii) simultaneously raising tensile strength. It is more beneficially employed when used in combination with Cr and Mo since it offsets the chilling tendency of the latter two elements. This way maximum strength can be obtained without unduly affecting machinability in varying sections. Tensile strength in normal sections increases by 8-10% for each 1% addition.[2]

There is a general increase in hardness on raising Ni content upto 4 to 5% and accordingly it is added to general purpose cast irons only in small quantities (from 0.25-4.0%). Quantitatively, hardness increases by about 10-20 BHN for each 1% addition by (i) solid solution hardening, (ii) keeping the iron pearlitic and, (iii) refining it (pearlite).[2]

However, in amounts $\sim$4-5% Ni imparts extreme hardness to the alloy because the pearlitic matrix is transformed to martensitic.[2] Certain authors have, however, reported

that Ni content required to form martensitic matrix is~6% or more.[75] The amount of Ni needed for maximum hardness depends upon the section size of the casting and properties required. If higher amounts (i.e. >5-6%) of Ni are added, the matrix structure retains greater amounts of austenite leading to a decrease in hardness.[75]

Ni prevents the formation of massive carbides. Since it does not form free carbide, its influence on resistance to wear in general purpose castings is not significant apart from its effect in suppressing the formation of free ferrite.[7].

Ni alloyed cast irons have good resistance to corrosion in fresh water, salt water, many acids, salts and alkalies.[2,80]

There is ample evidence that a small proportion of Ni also partitions to cementite. This decreases its (cementite) stability to some extent and may accelerate graphitization. In white irons, Ni partitions preferentially to the matrix rather than to the cementite/ carbide, but the ratio varies with the cooling rate and heat treatment. It has been further reported that the partitioning of Ni is not influenced by the presence of other alloying elements and therefore no significant change in partition ratio was observed.[9]

2.3.2.6 Chromium

It is a carbide stabilizer[10,77] and raises the solidification temperature of cast irons by about 1-1.5°C for

each 1%. addition.[2] The carbon content of the iron-carbon eutectic is raised by about 0.06%. for each 1%. addition upto about 9%. Cr.[2] It raises the eutectoid transformation temperature and improves the hardenability by decreasing the critical cooling rate.[1,10]

Chromium additions also increase the tensile strength by about 3-4%. and hardness by about 5-7 BHN for each 0.1%. addition in the absence of mottle. It also improves the strength of cast irons by reducing the graphite flake size.

When added in small amounts upto 0.5%. , it prevents the formation of free ferrite in critical sections.[2] It also markedly increases the pearlite stability at elevated temperatures.[2,7]

In general, machinability of Cr alloyed cast irons is poorer because of the presence of free carbides and also because of an increase in the hardness of Fe_3C. Cr prevents segregation, thus producing a more uniform structure. This is helpful in general in improving resistance to corrosion.[7,10] Cast irons with a high Cr content have a high resistance to abrasion because of its ability to stabilize carbide and improve hardenability.[2,7,10]

Thus summarising:-

(1) Small amounts of Cr stabilize pearlite in gray irons, control chill depth in chilled irons and ensure a graphite free structure in white irons containing less than 1%. silicon.

It refines and strengthens pearlite and also tends to increase the amount and hardness of the eutectic carbide.

(ii) In amounts ~1 to 4%. it is effective in improving the hardness and abrasion resistance of white irons. Minimum Cr content to render a 'balanced' composition white is ~ 3-4%. .(75)

(iii) At low concentrations, Cr has little or no effect on hardenability, chiefly because most of the Cr partitions to carbide.

(iv) Cr in amounts ranging from 12-35%. is used to confer resistance to corrosion and oxidation at elevated temperatures as well as resistance to abrasion.(2,7,10)

Partitioning of Cr is not restricted to Fe_3C alone. Its amount in the cementite and austenite phases is directly proportional to the amount of Cr added.(9)

2.3.2.7 Molybdenum(2,77)

Molybdenum additions mildly increase the chill depth and are about one third as effective as Cr. When added in concentrations (0.25-0.75%.) to chilled irons, it improves the resistance of the chilled face to pitting, spalling and chipping.(7) Mo reduces grain growth and refines and toughens pearlite.(7)

It is most effective in promoting the formation of martensite as it reduces the γ to α transformation rates

(suppressing pearlite formation) when used singly or in combination with Cr and/or Ni in a white iron. The addition of 1-4%. Mo is effective in suppressing pearlite formation even when castings with large section size are slowly cooled. Thus Mo can replace some of the Ni and/or Cr in the Ni-Cr or Cr-base martensitic white irons.(7)

It is a useful single element which increases tensile strength of low phosphorus irons (0.15%. P max.). In general the rate of increase is ~3.5-4%. for each 0.1%. addition upto ~ 0.8%. .(77) Above 0.6 to 0.8%. Mo, acicular microstructures may be formed, associated with very high tensile strengths and hardness.(77) It confers resistance to growth and creep in the temperature range 350-650°C.(77)

The partitioning behaviour of Mo is similar to that of Cr.(9)

2.3.2.8 Vanadium

It is a potent carbide stabilizer,(2,10,77) but is less prone than Cr to producing massive carbides. It increases the depth of chill.(7) The outstanding chilling effect of V in thinner castings may be balanced by additions of Cu or Ni or by a large increase in the carbon and or silicon contents.(7) Besides its carbide stabilizing influence, V in small amounts (0.1-0.5%.) refines the structure of the chill and minimizes coarse columnar grain structure in castings.(7)

Effect of V on the carbon content of the iron carbon eutectic is negligible i.e. carbon content increases by about 0.1%. for each 1%. addition.[2,77]

Usually it is employed in small amounts from 0.15-0.35%. and is particularly useful in imparting resistance to wear.[2] From 0.37 upto 0.61%., it elevates the pearlite/austenite transformation temperature by about 9°C on heating, but does not effect the temperature on cooling.[2,81]

It increases the tensile strength particularly of low P irons (P $<$ 0.1%.) by about 3 to 8%. for each 0.1%. addition, the corresponding increase in hardness (by refining pearlite) being about 8-10 BHN.[2] Vanadium also increases pearlite stability. But its effect on pearlite stability at high temperatures is less than Cr and Mo.[2]

It was shown by Sandoz[9] that vanadium partitions mainly to the cementite phase, in the ratio 14:1 (Fe_3C/γ) regardless of the average vanadium content.[9]

2.3.2.9 Copper

Generally the effect of copper in cast irons is similar to that of Ni with the exception that Cu has a limited solid solubility in cast irons (upto about 3-3.5%.)[1] and beyond these concentrations it can be detected microscopically as a separate microconstituent containing 96%. Cu

and 4%. Fe.[77,80,82] If Cu is added to cast irons in combination with Ni, its solubility goes up by about 0.4%. for each 1%. Ni addition.[83]

Copper decreases the eutectic carbon of cast irons by about 0.075%. for each 1%. addition.[83] It lowers the eutectoid transformation temperature by about 6-10°C for each 1%. addition and refines pearlite.[1,2,83] It lowers the solidification temperature of cast irons by about 2°C for each 1%. addition.[2,78] Copper, in concentrations $<$ 3.5-4%., diminishes the depth of chill, but in excess of 4%. it increases chill depth and hardness.[2, 7,84]

Copper is a mild graphitizer, refines graphite and increases fluidity during casting. Its graphitizing power is about 0.2 to 0.35 that of silicon.[2,80] It does not form free carbide. As an anti-ferritizer, copper is more effective than Ni.

It acts as pearlite promotor and ferrite hardener and increases tensile strength by 8-10%. for each 1%. addition.[2] Hardness in general goes up at the rate of 10-20 BHN for each 1%. addition[2] by (i) solid solution hardening, (ii) keeping iron pearlitic and, (iii) refining it (pearlite).[2,80] When added in cast irons along with Cr and Mo, tensile strength is generally improved without unduly affecting the machinability as it offsets the chilling tendency of the latter two elements.

Unlike other austenite stabilizers, Cu has a variable solubility in γ and α irons. Further, its solubility in α-ferrite also decreases sharply with temperature.[80,84] Therefore the effectiveness of copper would be determined by the extent to which it is retained in solution. Cooling rate shall be an important parameter in this regard. If retained in solution, copper enhances hardenability. On tempering Cu bearing steels and cast irons[85] beyond 500°C Cu if retained in solution, precipitates in an elemental form. This observation has been utilized in developing special high strength structural steels[85] and high strength malleable cast irons.[86]

Its direct influence on wear resistance of cast irons is not of much significance but indirectly it helps in improving it by suppressing the formation of free ferrite.[2,80,84]

Addition of 0.5 to 1%. Cu to cast irons considerably improves their resistance to corrosion by dilute H_2SO_4, HCl, sea water etc.[1,2,80]

In general most of the copper partitions to austenite.[9,87] Copper in excess of the amount which can be retained in solution is precipitated during cooling in ferrite and contributes little to the overall hardness and hardenability.[88,89] Sandoz[9] has however reported

to become air hardening.[1]

Although Mn as an alloy addition appears versatile, it is surprising that it has been mostly employed as an element of 'secondary' importance in cast irons.

2.3.2.11 Tellurium

Tellurium acts as an extremely powerful carbide stabilizer. Its effect is so strong that even very small amounts will convert an iron normally gray to one that is totally white. Hence, tellurium is used as a potent chill producer.[2]

It is used as a core or mould wash in local spots to promote soundness. Addition of 0.0004% of Te will result in an appreciable increase in chill. When used as a mould additive in excess of 0.0007% , it produces Widmanstatten or mesh graphite leading to a considerable decrease in tensile strength.[90]

2.3.2.12 Titanium

It is present in many phosphoric pig irons in small quantities upto 0.2% . Titanium in small amounts (0.015-0.025%) is useful in eliminating fissuring (produced due to nitrogen) in sand castings.[91] It is a potent carbide stabilizer.[2]

2.3.2.13 Boron

It is a powerful carbide stabilizer. Normally it is not added to gray irons, but enters accidentally from vitreous enamel scrap or from borax bonded refractories and may interfere with chill control methods.[2,92] Boron additions above 0.1% promote chilling and carbide stabilization.

2.3.2.14 Antimony

In certain pig irons it is present in small amounts (upto about 0.2%) as impurity. Sometimes it enters castings in large amounts (upto 0.3-0.5%) through vitreous enamelled scrap.[2] It tends to stabilize pearlite, raises hardness and lowerstensile strength, transverse strength, impact strength and deflection. Even small amounts of antimony (0.1%) lower the impact strength by about 30-50% and increase the tendency of light castings to cracking.[2,92]

2.3.2.15 Bismuth

Bismuth is a carbide former and acts as a carbide-inducing inoculant in cast irons. It promotes the formation of Widmanstatten graphite, causing a marked reduction in tensile strength.[2]

Bismuth acts as a subversive element (like lead, titanium and antimony) to magnesium in the production of nodular iron.[2,93] In amounts 0.002% it is useful in controlling chill and annealability of malleable irons.[2] Bismuth,

about 7%., the hardness by 30 BHN and modulus of elasticity by 4-5% .[2] There is no significant loss of impact strength when tin is present in amounts below 0.15% .[95] It does not promote the formation of free cementite and due to this reason is preferred over Cr in preventing ferrite formation under conditions of lubricated and sliding wear.[2]

2.3.2.18 Aluminium

Aluminium improves oxidation resistance [10] of gray irons if added in amounts ~ 1-5.5% .[2,96] It is used in small amounts (0.01-0.03%.) to control chill and annealability in malleable irons.[2]

Aluminium raises the pearlite transformation temperature by about 16°C for a 2% addition and 96°C for a 6.2% addition. It also raises the freezing point by about 16°C for each 1% addition upto 5.75% .[2]

2.3.3 Summary

The effect of alloying elements on the microstructure, mechanical properties, machinability, casting characteristics and embrittlement likely to be caused when added to cast irons, has been discussed. Their effect relevant to the design of wear resistant compositions, has been summarized in table 2.1.

2.4 ECONOMICAL ATTAINMENT OF THE DESIRED MICROSTRUCTURE

Efforts aimed at developing low cost white iron compositions have proceeded on the following lines:

(i) those aimed at investigating whether the proportion of high cost elements could be reduced and/or eliminated and

(ii) those aimed at investigating whether the proportions of other element(s) incorporated in the composition(s) currently in use, could be further reduced.

As an outcome of the discussion in the preceding section, the following are some of the alloy systems based on low priced alloying elements-[97]

Fe-Cr-Cu

Fe-Cr-Mn

Fe-Cr-Mn-Cu

In one of the recent efforts in this direction, it was concluded that the type of microstructures observed in the Ni-Cr white irons could be attained with the alloy combination Mn-Cr-Cu.[98] However, the carbides formed were massive and were rendered discontinuous on heat-treating from high temperatures ($> 850^{\circ}C$).

Encouraged by the results obtained, further studies were planned to optimize Cu and Mn contents while maintaining Cr ~7% and Si ~1.5-2% .

Studies to optimize Cu revealed that in Cu bearing white irons, hardness greater than 650 VPN could be obtained only on quenching. Cu was however extremely effective in rendering the carbide net-work discontinuous. Taking an overall view, the optimum Cu content appeared to be $\sim$ 1%. .[99]

Studies to optimize Mn revealed that while Mn was extremely useful in attaining a high hardness ($>$ 650 VPN) without quenching, it was not effective in rendering carbide network discontinuous.[100] The optimum Mn content appeared to be $\sim$ 4%. .[100]

Results from these three studies were helpful in designing a white iron composition, based on Mn, Cr and Cu as the main alloying elements, which resembled heavy duty Ni-Cr white iron with regard to its transformation behaviour. Accordingly, a preliminary investigation was carried out involving a comparison between the transformation behaviour of the newly conceived composition containing Mn,Cu and Cr (namely 3.5-4 Mn, $\sim$ 1%. Cu and $\sim$7%. Cr) and Ni-hard 4. Such a study revealed that the new composition resembled its existing counterpart.[101-102]

2.5 CONCLUSION

Starting with a comparison between different micro-structures vis-a-vis their resistance to wear to be followed by an identification of the desired microstructure, it has

been possible to highlight its 'conventional' and 'economical' attainment through alloying. How this has proved useful in the design of new low cost wear resistant compositions has been critically discussed in the next chapter.

CHAPTER-III

FORMULATION OF THE PROBLEM

3.1 THE APPROACH

The present investigation was primarily undertaken to assess the possibility of economically attaining the microstructure(s) commonly encountered in heavy duty alloy white irons. It was felt appropriate to undertake such an exercise as the back up information (section 2.4) had revealed that such possibilities indeed existed. It was planned to design alloys consistent with the philosophy that (i) the microstructure of interest was martensite + carbide with some austenite, (ii) the alloy combination(s) chosen should contain element(s) which enhances hardenability, stabilizes carbide, provides for the attainment of discontinuous carbide net-work in the heat treated condition and facilitates attainment of austenite and, (iii) the desired microstructure should be attained by adding a minimum/ optimum amounts of low cost alloying elements.

Hardness was decided upon as the criterion to ascertain whether the stipulated mechanical properties/wear resistance had been attained (section 2.2). Its choice can be appropriately justified by a perusal of the specifications on

alloy white irons.[17]

It was decided to assess the heat treatment response of the alloys designed, elucidating the operative strengthening mechanism(s) and establishing a correlation between the microstructure and wear.

The following sections are devoted to an understanding of the alloy design and phase wise planning of experiments.

3.2 ALLOY DESIGN

The Fe-Cr-Mn-Cu system was chosen for study in view of the encouraging results obtained[101-102] and also because neither the Fe-Cr-Cu[99] nor the Fe-Cr-Mn[100] systems in themselves had proved useful (Section 2.3.3). The choice of the alloying elements is justified as follows:

(i) Mn improves hardenability significantly at a low cost, stabilizes carbide, helps in the retention of austenite and does not adversely influence fluidity,

(ii) Cu unlike Mn has useful graphitizing tendency (helpful in attaining discontinuous carbide), solution hardens and is useful in improving corrosion resistance,

(iii) Cr stabilizes carbide (not as powerfully as either Mo, V or W), is helpful in attaining a uniform

microstructure, increases the overall hardness and hence resistance to wear and may also prove useful in the attainment of martensite/austenite.

The first 'stage' in the planning was to decide upon the minimum Cr content to ensure that a base composition containing 3%. C and 1.5-2%. Si is cast white during sand moulding over a range of section sizes.[103] A review of the literature suggested the amount to be 3-4%. .[75] Allowing for safety, it was decided to restrict Cr to ~6-6.5%. . Another set of higher Cr alloys (Cr ~9-9.5%.) was also planned to investigate whether raising the Cr content influenced the transformation behaviour and hardening mechanism(s).

At each of the two Cr contents, four different Mn levels were chosen namely 2.5-3.0; 3.5-4.0; 4.5-5.0; and 5.5-6.0%. to (i) ascertain the lowest Mn content to obtain martensitic matrix on air cooling and (ii) to ensure that martensite forms in thicker sections with ease.[103]

Cu was restricted to 0.75-1.0%. consistent with its solubility in the γ and α irons and the reasons for its inclusion discussed in Section 2.3.2. A silicon content 1.5-2%. ensured that the alloys had good fluidity (Section 2.3.2). Thus in all eight alloys were planned.[103]

	Low Cr(6-6.5%.)		High Cr(9-9.5%.)	
A1-	2.5-3.0%. Mn	A5-	2.5-3.0%. Mn
A2-	3.5-4.0%. Mn	A6-	3.5-4.0%. Mn
A3-	4.5-5.0%. Mn	A7-	4.5-5.0%. Mn
A4-	5.5-6.0%. Mn	A8-	5.5-6.0%. Mn

As indicated earlier, carbon, silicon and copper in both series were 3.0%., 1.5-2.0%. and 1.0%. respectively.

3.3 PLANNING OF EXPERIMENTS

Phase I

Experiments involved subjecting the alloys to different heat treatments, assessing hardness and observing their microstructure to arrive at the tentative hardening mechanism(s).

Phase II

Detailed structural investigations by EPMA, X-ray diffractometry and to a limited extent by scanning electron microscopy to supplement the information obtained in Phase.I.

Phase III

Assessment of wear resistance, to interrelate it qualitatively with the microstructure and to draw inferences concerning the most suitable microstructure from the point of view of wear.

3.4 CONCLUSION

The physical metallurgical parameters that have gone into initiating this investigation, the design of alloys and planning of experiments have been highlighted. The next chapter deals with the experimental strategy.

CHAPTER-IV

EXPERIMENTAL TECHNIQUES AND PROCEDURES

4.1 ALLOY PREPARATION

Raw materials used for preparing different alloys were pig iron, low carbon ferro-alloys (ferro-chromium, ferro-manganese and ferro-silicon), graphite powder, electrolytic copper and mild steel scrap. Compositions of the pig iron and the ferro-alloys are reported in Table 4.1.

The charge consisted of raw materials in the requisite proportions to attain the final compositions as desired. Due consideration was given to the metal content of the ferro-alloys and melt losses while making charge calculations. Alloys were air melted in clay bonded graphite crucibles in a medium frequency induction furnace.

Initially two base alloys each weighing 65 kgs and containing~6-6.5%. Cr (low chromium) and~9-9.5%. Cr (high chromium) respectively were prepared by first melting requisite proportions of pig iron, mild steel scrap and graphite to a superheat followed by deslagging and subsequent addition of ferro-chromium, ferro-silicon and copper. After ensuring complete dissolution of alloy additions, small samples were taken out of the melt for estimation of carbon by the LECO analyser. In the intervening period the

melt temperature was lowered to reduce losses. After ensuring that the carbon content had reached the desired level, the liquid metal temperature was raised to about 1400°C and slag removed. Molten alloy was then cast into four cylindrical blocks of approximately equal weight at each of the two Cr levels. Thus in all eight castings were poured.

Finally, Mn content was adjusted to the desired level (i.e. 2.5-3%, 3.5-4%, 4.5-5% and 5.5-6%) by adding requisite amount of ferro-manganese to each of the eight base alloy castings in the molten condition. Carbon content was rechecked even at this stage to ensure that it was maintained at the desired level. After deslagging, temperature of the molten metal was measured with the help of an optical pyrometer. The alloys were poured at about 1400±25°C into ~ 25 mm diameter X 250 mm long cylindrical ingots and 8x22x120 mm rectangular strips in sand moulds.

Alloys were analysed for C,S,P and Si on a vacuum quantometer. Chemical analysis is reported in Table 4.2.

4.2 SPECIMEN PREPARATION

Alloys were very hard and could not be cut either with power saw or with high speed steel tools. Disc samples (height 14 to 18 mm) were made from the cylindrical ingots by making a 2 to 3 mm deep cut all along the circumference on a silicon carbide cut-off wheel followed by hammering.

Heating of specimens during slitting was kept to a minimum through water cooling. Specimens thus obtained were ground to have parallel faces and paper polished in the usual manner.

4.3 HEAT-TREATMENT

Heat treatments mostly involved air cooling from 750, 800, 850 and 900°C after soaking for 2,4,6,8 and 10 hours. They were carried out in muffle furnaces whose temperature was measured with chromel-alumel thermocouple and controlled to ± 5°C.

4.4 HARDNESS MEASUREMENT

4.4.1 Macro-hardness

Hardness testing was extensively employed because it provides a quick yet reliable indication of the effect of heat-treatment on properties (both strength and wear resistance).

Heat treated specimens were initially ground to a uniform depth of about 1 mm to remove any decarburized layer. Thereafter they were paper polished upto 3/o stage in the usual manner. Hardness measurements were carried out on both faces of a specimen on a Vickers hardness testing machine employing 50 kg load. However, the data reported represents measurements carried out only on one face. A minimum of 10 impressions were taken on each specimen. The permissible scatter in the hardness values was ±17 VPN.[104] In the

event of the variation exceeding this limit, the corresponding hardness value has been represented as a band denoting both the maximum and the minimum values.

As the alloy system under investigation was likely to be heterogeneous in character, both the representative hardness readings as well as the average values have been reported.

4.4.2 Microhardness

Microhardness measurements were carried out on polished and etched specimens using TUKON MICROHARDNESS TESTER at 25 gm load and an objective magnification of X40. Microhardness estimations were carried out with the help of WILSON CALCULATOR provided with the tester. The interconversion of impression diameters into microhardness values is given in Table 4.3.

Microhardness measurements were made at different locations within a region as also in a large number of carbide and matrix regions. As before, all the microhardness readings along with the average values have been reported.

4.5 METALLOGRAPHY

4.5.1 Optical Microscopy

This has been extensively used to comprehend the effect of heat treatment on hardness as well as to study the transformation behaviour of the alloys. Specimens were

paper polished in the usual manner (Section 4.2). The final polishing was carried out on wheels impregnated with 6μ and 1/4 μ diamond paste. After proper cleaning, specimen surfaces were etched in freshly prepared 2%. nital. Metallographic examination was carried out on REICHERT METAVERT-368 microscope.

4.5.2 Scanning Electron Microscopy

Scanning microscopy was used to a limited extent to study the microstructure of some selected as-cast and heat treated samples, especially to ascertain whether or not dispersed carbides were present in the matrix in some of the alloys. Studies were carried out on bulk samples which were polished and over etched to ensure that the matrix structure was appropriately revealed.

To ensure good electrical contact, specimens were glued to the specimen holder using a silver base paint. These were allowed to dry before being examined on a Phillips 501 Scanning Electron Microscope.

4.6 ELECTRON PROBE MICRO-ANALYSIS

4.6.1 General

Electron probe micro-analysis has been extensively used to study the partitioning behaviour of different alloying elements particularly Mn and Cr in the experimental alloys in the as-cast as well as in the heat-treated conditions.

Three different modes of analysis usually employed are:- fixed-probe technique, the line-scan technique and the area-scan technique. All the three methods were employed in the present investigation.

Specimens for electron probe micro-analysis were approximately 7 mm cube in size. These were cut from rectangular strips, heat treated, and after removing approximately 1 mm thick layer from all faces were mounted in bakelite (mount size: 25 mm dia x 7 mm height). The samples prepared in the usual manner, were etched just enough to reveal the microstructure. This way it was ensured that the composition of different phases/ micro-constituents was practically unaltered.

4.6.2 Fixed Probe Technique

In this technique the emitted X-rays, characteristic of the various elements present in the bombarded region, are analysed for wavelength and intensities by suitable X-ray spectrometers for the purpose of identifying elements as well as for determining their concentrations. The method consisted of positioning the electron probe (~1 micron in diameter) with the help of cross wires on the region of interest (i.e. carbide or matrix phase). Intensities of the characteristic X-ray lines (such as Kx, Lx, Mx etc.), corresponding to the element of interest

(i.e. Cr, Mn, Si, Cu and Fe), were measured in terms of counts per second. Under identical conditions, intensity of the characteristic lines from the corresponding pure metal (e.g. 100% of Mn or Cr etc.) was similarly measured. This served as the 'standard-count' for the particular element. To a first approximation the intensity ratio I_A^S/I_A^A is equal to the mass concentration C_A of the element A in the sample provided the intensities referred to are the intensities generated from within the specimen and excited directly by the incident electrons.(105)

Thus,

$$K_A = \frac{I_A^S}{I_A^A} = C_A$$

where,

K_A = relative X-ray intensity,

I_A^S = intensity of the characteristic ray of an element A in a sample,

I_A^A = intensity of the same characteristic ray in the pure element A (i.e. standard) generated under identical electron bombardment conditions,

C_A = mass concentration of the element A in the sample.

Estimation of composition from the X-ray intensity data is made by evaluating the composition dependent correction factors corresponding to atomic number (Z), absorption (A) and fluorescence (F) effects, for which several semi-empirical formulations are available. The estimation of correction factors by the (ZAF) technique

involves long and cumbersome calculations and depends upon the availability of high speed computers. The empirical method of obtaining chemical composition as suggested by Ziebold and Ogilvie for the binary alloys has led to the so-called 'alpha coefficient method'.[111,112] Subsequent improvements in the method employed semi-empirical approach to obtain alpha coefficients for complex multicomponent systems. This method is found to be simple, fast and as effective as the ZAF method. The correction procedure adopted in this method can be further simplified by distinguishing the major and minor constituents of a multicomponent system and by considering the effect of major constituents alone. The modified α-coefficient method was used in the present study.[111-113]

Calculations were facilitated by considering Cr, Mn and Fe as the major constituents. The following expression was employed for computing their concentration:[114]

$$C_A = K_A(1+\alpha_{AB}C_B+\alpha_{ABB}C_B^2+\alpha_{AC}C_C+\alpha_{ACC}C_C^2+\alpha_{ABC}C_BC_C)$$

where,

For Cr estimation

$$C_A = C_{Cr}$$
$$C_B = C_{Mn}$$
$$C_C = C_{Fe}$$

C stands for concentration

$\alpha_{AB} = -0.014857$

$\alpha_{ABB} = -0.016421$

$\alpha_{AC} = -0.065966$
$\alpha_{ACC} = -0.098488$
$\alpha_{ABC} = -0.14181$

For Mn estimation,

$C_A = C_{Mn}$
$C_B = C_{Cr}$
$C_C = C_{Fe}$

$\alpha_{AB} = 0.0074218$
$\alpha_{ABB} = 0.00036017$
$\alpha_{AC} = 0.018233$
$\alpha_{ACC} = -0.019822$
$\alpha_{ABC} = 0.0010083$

For Fe estimation,

$C_A = C_{Fe}$
$C_B = C_{Mn}$
$C_C = C_{Cr}$

$\alpha_{AB} = -0.02763$
$\alpha_{ABB} = 0.00029335$
$\alpha_{AC} = 0.36114$
$\alpha_{ACC} = 0.012791$
$\alpha_{ABC} = -0.0056572$

Since the element concentration is not known, an iterative procedure must be employed considering intensity ratios as the concentration to start with. Usually after the third iteration, concentrations become constant. A program incorporating five iterations (given in the appendix) was made and run on DEC 2050 computer for computing Cr, Mn and Fe concentrations.

Corrected values have been reported for major elements Cr and Mn only. For Cu and Si, however, only the intensity ratios corresponding to the first approximation have been reported as probable concentrations.

4.6.3 Line Scan Technique

This technique enables determination of the distribution of a selected element along a preferred direction or path. To carry out such an analysis, the electron beam was kept stationary while moving the sample along the desired direction. Few specimens were analysed by this technique for evaluating the element distribution/ partitioning into different phases as influenced by heat treatment.

4.6.4 Area Scan Technique

In this mode, selected areas on a sample are scanned and the emitted X-rays containing characteristic radiation of an element present are detected by the X-ray spectrometer. The signal from the X-ray detector, after suitable amplification, is allowed to modulate the brightness of the spot of a cathode ray oscilloscope scanned synchronously with the beam of the electron probe. This will produce a black and white image on the oscilloscope screen which has point to point correspondence with the area scanned on the sample. Such an image, called an X-ray image, shows the distribution of any selected element as bright and dark areas, the bright areas indicating its

presence in large proportions and the dark areas indicating its presence in small concentrations. Although scanning X-ray images are generally qualitative in nature, in many instances they yield very useful information.

Typical X-ray images were recorded showing the distribution of Cr, Fe, Si and Mn in the matrix/carbide regions of different specimens as affected by heat treatment.

4.7 X-RAY DIFFRACTOMETRY

As-cast and the heat-treated bulk specimens of the different alloys were subjected to structural investigations on the following three diffractometers in the present investigation:

1. XRD-6, GE, employing an iron target and manganese filter at a voltage of 40 KV and a current of 7 mA.
2. XRD-5, GE, employing an iron target and manganese filter at a voltage of 40 KV and a current of 7 mA.
3. PW 1140/90, PHILIPS employing an iron target and manganese filter at a voltage of 35 KV and a current of 12 mA.

Specimens, which were polished and lightly etched, were scanned from 35 to 150°. In most instances time constant and scanning speed were kept at 2 seconds and 2° per minute respectively. Diffractograms were analysed/indexed by adopting the following procedure:

(i) 'd' values were obtained for all the discernable reflections/peaks in the usual manner,

(ii) assuming the height of the most prominent reflection as 100(I_o), the relative intensities (I/I_o) of all the peaks/reflections were calculated, and

(iii) indices were assigned to different 'd' spacings based on the standard 'd' and 'I/I_o' values available from the X-ray data/ASTM data cards. While doing so, reflections/peaks with (I/I_o) values less than $\sim$ 3 were not considered.

4.8 WEAR TESTING

4.8.1 General

It was decided to evaluate resistance to wear in both the 'dry' and the 'wet' conditions. Accordingly two types of test rigs were fabricated to evaluate the relative performance of the alloys designed in the present investigation:

(i) Disc and pin type rig for testing under dry condition and,

(ii) Slurry-pot type rig for testing under wet condition.

4.8.2 Disc and Pin Type Rig

In this rig a bonded alumina grinding wheel was horizontally mounted on to a polishing machine (Fig.4.1). Specimens, one at a time, were held against its surface at a predecided distance from the axis of rotation through a specimen holder held vertically in position by passing it through a heavy horizontal beam supported at both ends(Fig.4.1)

Although the load on the specimen being tested could be varied, it was maintained constant at 2.5 kg in the present investigation. The speed of rotation of the abrasive wheel, measured with a tachometer, was adjusted to 1100 r.p.m. During testing a specimen rotated about its own axis in addition to being ground. This way it was ensured that specimen surface abraded evenly. It was further ensured that the surface area undergoing abrasion was the same for all the specimens (20 mm in diameter).

Wear data has been reported as weight loss in gms of the abrading surface at equal intervals of 15 minutes for a total of $1\frac{1}{2}$ hours for each specimen. The advantage with this method is that it is simple and permits the possibility of using bulk samples on which other investigations had been previously completed.

4.8.3 Slurry Pot Rig

An assembly of the rig is shown in Fig 4.2. In this method, cylindrical specimens suitably mounted, are made to abrade against a sand water slurry. As a result, specimen surfaces would undergo abrasion erosion.

Wear test specimens 21 mm in dia x 50.5 mm in length were machined and shaped with carbide tipped tools from the cast cylindrical ingots. A slight taper was provided at one end in the form of frustum of a cone to facilitate mounting. After heat treating, decarburized layer, if any, was machined

out to arrive at the final dimensions of 20 mm diax50 mm length.

As-cast/heat treated specimens were vertically mounted on to a ring coupled through a shaft to the main drive of a vertically mounted motor rotating at a speed of 960 r.p.m. (Fig.4.2). The specimens rotating at the high speed, in turn, vigorously stirred a sand-water slurry contained in a bowl and consisting of equal volumes of water and river sand. Its screen analysis (Table 4.4) prior to starting the test was obtained. Because of vigorous stirring of the slurry by the rotating specimens, the latter underwent wear. Temperature rise during the test was kept to a minimum by water cooling the bowl.

Wear losses in gms were noted at equal intervals of 10 hours. In each test, a specimen of mild steel (normalised) was also used as a reference standard. Fresh sand was used for each run. This ensured that identical test conditions were maintained during each run. The total test run for each set of specimens was 50 hours.

4.9 CRACK PROPAGATION STUDIES

These were carried out to a limited extent on as-cast/heat treated specimens. The procedure involved taking as-cast/heat treated specimens which contained large sized cracks. These were propagated in a controlled manner by making indentation(s) under a load of 250 kg on a Vicker's hardness testing

machine. Crack propagation path was studied mostly with the help of optical metallography. In order to propagate a crack over a sizable distance, it became necessary to repeat the 'indenting' procedure(Section 5.7).

4.10 CONCLUSION

Experimental techniques and procedures adopted have been critically summarized. The next chapter deals with the results obtained.

CHAPTER V

EXPERIMENTAL RESULTS

5.1 GENERAL

As stated earlier, investigations involved assessing (i) the heat-treatment response of the alloys A1 to A8 with the help of hardness measurements, metallography, X-ray diffractometry and EPMA techniques and, (ii) the resistance to wear by the 'dry' and the 'wet' (sand-water slurry) methods. The results obtained have been summarized in the following sections.

5.2 RESULTS

5.2.1 Effect of Heat-treatment on Hardness

Disc specimens (25 mm dia x 18 mm height) of the different alloys were heat-treated by austenitizing them at 750, 800, 850 and 900°C for periods ranging from 2 to 10 hours at intervals of 2 hours followed by air cooling. This was done primarily to determine (i) how the heat-treatment schedule influenced the as-cast hardness, (ii) the maximum attainable hardness in different alloys and, (iii) how it (the maximum attainable hardness) was influenced by composition and/or heat-treatment. The results thus obtained

are summarized in Tables 5.1 to 5.9 and Figures 5.1 to 5.5. A perusal of the tables and figures reveals that:

(1) In the lower Cr alloys, the as-cast hardness increased upto~5%. Mn and thereafter decreased on raising it (Mn) to~6%. . Although the effect of Mn content on the as-cast hardness was small, a definite trend, as mentioned above, was discernable (Fig.5.1a).

(2) In the higher Cr alloys, however, the as-cast hardness continuously increased with an increase in the Mn content (Fig.5.1b).

(3) In alloy A1, heat-treating from 750°C led to a decrease in hardness (with respect to the as-cast hardness) at all the soaking periods. At 800°C, the hardness remained unaltered and was independent of the soaking period. However, a marginal increase in hardness was observed on heat-treating from 850 and 900°C (Fig.5.2a).

(4) A nearly similar situation existed for alloy A5 except that (i) the hardness changes with respect to the as-cast hardness were pronounced even at 800°C and, (ii) on heat-treating from 900°C hardness continuously increased with soaking period (Fig.5.2b).

(5) Raising the Mn content from~3%. (alloy A1 and A5) to~4%. (alloy A2 and A6) substantially altered the transformation behaviour (Figs.5.3a and b). In alloy A2, soaking from 750°C led to a decrease in hardness with respect to the

as-cast hardness, the decrement being maximum within the first 2 hours and negligibly small thereafter. On raising the temperature to 800°C, hardness of the alloy A2 remained unaltered and practically independent of the soaking period (Fig.5.3a). It (hardness) attained a peak after soaking for 2 hours at 850°C and remained practically unaltered thereafter on raising the soaking period further (Fig.5.3a). On heat-treating from 900°C, hardness increased continuously, although its magnitude at each of the soaking periods was lower than the corresponding value at 850°C (Fig.5.3a).

(6) In the higher Cr alloy A6, heat-treating from (i) 750°C led to a continuous decrease and, (ii) 800°C led to a continuous albeit a small increase in hardness with respect to the as-cast hardness. The peak was attained on heat treating from 850 and 900°C after soaking for 2 hours and a further increase in soaking period upto 10 hours had little effect on the final hardness. In general, the absolute hardness values on heat treating from 900°C were marginally lower than those obtained on heat-treating from 850°C (Fig.5.3b).

(7) At a Mn content 5%. (alloys A3 and A7), heat treating temperature of 850°C was most favourable from the point of view of attaining maximum hardness in a minimum of time (Figs.5.4a and b). Whereas the hardness vs time curves showed an increasing trend at 800°C for both the alloys, the nature of the curves on heat-treating from 900°C showed an increase in hardness within the first 2 hours followed by (i) a very gradual increase in it (hardness) in

Although the data summarized in Tables 5.1 to 5.8 and Figs.5.1 to 5.5 gave useful information on the optimum temperature-time and Mn/Cr combinations for obtaining maximum hardness, interest in carrying out this investigation was not confined to standardizing these parameters alone. Since ascertaining the mechanism(s) of hardening was equally pertinent, it was felt appropriate to replot the data summarized in Tables 5.1 to 5.8 in different ways. Four different combinations were thought of as being useful:

(i) Effect of Mn content and soaking period on hardness at different heat treating temperatures.

(ii) Effect of temperature and Mn content on hardness at different soaking periods.

(iii) Effect of temperature and soaking period on the hardness as influenced by Mn content.

(iv) Effect of Mn content and temperature on hardness at different soaking periods.

Accordingly, curves were plotted corresponding to the first possibility and are summarized in Figs.5.6 to 5.9. Although it was difficult to draw meaningful inferences from each of the curves, the plots all the same provided useful insight into the behaviour of the alloys as influenced by Mn content and soaking period at different heat treating temperatures. This would be evident from the important deductions summarized below:

(i) Heat treating temperature of 750°C was insufficient

to promote attainment of high hardness in both the lower Cr and higher Cr alloys in general (Fig.5.6). However, a steep rise in hardness was observed beyond~5% Mn in both the low Cr and high Cr alloys, it being more pronounced in the former (Fig.5.6)

(ii) On raising the temperature to 800°C, maximum hardness was attained at~5% Mn and a soaking period of 10 hrs, its magnitude being marginally higher in the higher Cr alloys (Fig.5.7).

Hardness of the lower Cr alloys increased gradually between~3 to 4% Mn and steeply thereafter, the rate of increase being higher at soaking periods ranging from 6 to 10 hours. Hereafter the alloy behaviour differed.

At soaking periods $\geq$ 6 hours, hardness peaks were attained at 5% Mn. On increasing it (Mn) to~6%, hardness remained unaltered at 6 hrs. soaking period and decreased marginally at periods higher than this. At soaking periods $<$6 hrs., hardness increased continuously with Mn content (Fig.5.7a).

Almost a similar situation existed in the higher Cr alloys except that the increase in hardness was steep even between~3 and~4% Mn (Fig.5.7b).

(iii) At 850°C, the peak hardness was attained at~4%.Mn. It remained practically unaltered between~4 and~5%.Mn (Fig.5.8). Beyond~5%.Mn, however, a general gradual drop in hardness was observed, it (the drop) being marked in the lower Cr alloys specially at 2 and 4 hours soaking periods (Fig.5.8a).

(iv) On raising the temperature to 900°C, the magnitude of the maximum attainable hardness was lower than that attained at 800 and 850°C, the decrease being more pronounced in the lower Cr alloys. Peak hardness was obtained at ~4%. Mn (low Cr alloy) after soaking for 10 hours, whereas for the higher Cr alloy this condition was attained after soaking for only 2 hours.

In lower Cr alloys, a general drop in hardness was observed at Mn content higher than ~5%. for soaking periods upto 8 hours. However this tendency sets in for the 10 hour soaking period at 4%. Mn itself.

In the higher Cr alloys, however, the decrease in hardness began gradually beyond ~4%. Mn and was very steep beyond ~5%. Mn.

Although these deductions were useful, mutual interpenetration of the curves came in the way of arriving at a more meaningful interpretation of the transformation behaviour based on kinetic considerations. To overcome this difficulty and thereby to arrive at a rationalized picture of the 'alloy behaviour', a modified approach was adopted. Assuming the nature of the best fit curves (Figs.5.2-5.5) to be representative of the 'true' behaviour of the alloys under investigation, derived hardness values corresponding to different holding periods, as influenced by temperature, were obtained from these curves (Tables 5.9a and b). They were replotted as a function of different variables cited earlier (Figs.5.10-5.13). A perusal of these figures leads to important

inferences some of which reinforce the deductions arrived at on the basis of the Figs.5.6 to 5.9 whilst others lead to the following additional useful information:

(i) Soaking temperature of 750°C was 'insufficient' in affecting hardening (compared to the as-cast state) in low/high Cr alloys (Fig.5.10).

(ii) The optimum heat-treating temperature was found to be 850°C. At this temperature maximum hardening was obtained between ~4 and ~5% Mn in both the lower and the higher Cr alloys and was independent of the holding periods (Fig.5.10).

(iii) Beyond ~5% Mn, hardness in the lower Cr alloys decreased on heat treating from 850 and 900°C; the higher the holding period the smaller the fall in the peak hardness (Fig.5.10).

(iv) However, the peak hardness in the higher Cr alloys was more or less independent of the heat-treating temperatures (i.e. 850 or 900°C) and time (Fig.5.10).

(v) At 800°C, the hardness vs Mn content curves as influenced by soaking period showed an increasing trend upto 5% Mn in a majority of instances (both in the lower and higher Cr alloys). Beyond that (upto ~6% Mn), the increase in hardness slowed down considerably/remained unaltered in most instances (Figs 5.10b and f) except in the lower Cr alloys where infact a marginal decrease in hardness was observed at longer soaking periods (i.e. 8 and 10 hrs) (Fig.5.10).

(vi) At 850°C, the peak hardness was attained at ~4% Mn

in both the lower and the higher Cr alloys. In higher Cr alloys, increasing the Mn content upto ~6%. led to a gradual (marginal) decrease in hardness which was independent of the soaking period (Fig.5.10g).

In the lower Cr alloys, the peak hardness remained unaltered from ~4 to ~5%. Mn. On increasing Mn from ~5 to ~6%. , the decrease in hardness was a function of the soaking period, it being steep at smaller soaking periods and very gradual at larger soaking periods (Fig.5.10C).

(vii) At 900°C, the transformation behaviour of the lower Cr and higher Cr alloys differed. In the lower Cr alloys, for soaking periods upto 6 hrs, hardness increased upto ~5%. Mn and then decreased as the Mn content was increased to ~6%. . For soaking periods of 8 and 10 hrs, maximum hardness was attained at ~4%. Mn, it remained unaltered upto ~5%. Mn and decreased as Mn was raised to ~6%. (Fig.5.10d).

For the higher Cr alloys, hardness attained peak at 4%. Mn independent of the holding period. It decreased by ~50 VPN on raising the Mn to ~5%. (the magnitude of the decreased hardness being higher than the maximum hardness attained in lower Cr alloys) and further decreased by ~125 VPN on raising the Mn to ~6%. at all the soaking periods (Fig.5.10 h).

(viii) Fig.5.11 further confirms deductions (i)-(vii) and reaffirms that the optimum Mn content and heat-treating temperature at both Cr contents are ~4-5%. and 850°C

respectively, and are independent of the holding period. The maximum attainable hardness was only marginally higher in the higher Cr alloys (Fig.5.11).

Usefulness of 800°C temperature in affecting hardening only at ~5%. Mn and soaking periods $\geq$ 6 hrs is also clearly borne out.

Heat treating temperature of 900°C was not effective in inducing maximum hardening in the lower Cr alloys at any of the soaking periods. However, the difference between the maximum attainable hardness and the hardness values obtained on heat-treating from 900°C reduced with an increase in the soaking period, reaching a minimum at 4%. Mn at a soaking period of 10 hrs.(Fig.5.11 a to e).

In the higher Cr alloys also, the difference between the maximum attainable hardness and that obtained on heat-treating from 900°C reached a minimum at ~4%. Mn (for all the soaking periods) with the former (maximum hardness) now only marginally higher than the latter (Fig.5.11). On increasing the Mn content beyond ~4%.(upto ~6%.), the difference between the maximum attainable hardness and that obtained on heat treating from 900°C increased,its(difference) rate of decrease being nearly constant and independent of holding period(Fig.5.11).

(ix) Fig.5.12 further highlights the usefulness of the combination 4-5%.Mn, 850°C (independent of soaking period) in contributing to maximum hardening provided the temperature is accurately controlled. The higher Cr alloys appeared to be

harder but only marginally.

(x) Increasing the Mn content to ~5%. proved beneficial for both the lower and higher Cr alloys as by doing so substantial hardening could be achieved at a temperature lower than 850°C i.e. at 800°C. At a Mn content ~5%. and 800°C, the higher the soaking period the higher was the magnitude of the hardness obtained. This is clearly brought out by comparing Figs.5.12(a)-(c) and (e)-(g). At this level of Mn, maximum hardening also occurred at 850°C but was independent of soaking period.

(xi) On increasing the Mn content to ~6%. the behaviour of the lower Cr and higher Cr alloys differed. In the lower Cr alloys the magnitude of the maximum hardness at temperatures $\geqslant$ 800°C was lower than the corresponding values at ~5% Mn. Further, at 800°C the effectiveness of increasing the soaking period to induce hardening is reduced. (Figs.5.12b,d,g and h).

At 850°C the hardness of the lower Cr alloys in the heat treated condition was a function of the soaking period which is exactly contrary to what was observed at the same temperature at ~4 and ~5%. Mn (Figs.5.12c and d).

In the high Cr alloys raising the Mn to ~6%., proved beneficial in attaining substantial hardening at 800°C even at lower soaking periods (Figs.5.12g and h). The maximum hardness at 850°C was still independent of the soaking period as had been the case at ~4 and ~5%. Mn (Fig.5.12f,g and h).

A comparison between Figs.5.12(d) and (h) clearly

brings out the usefulness of the higher Cr content (or lower Mn/Cr ratio) in sustaining a higher level of hardness on heat treating from temperatures upto 850°C.

(xii) Heat treating temperature of 900°C was not useful in inducing maximum hardening in the lower Cr alloys because barring a solitary instance, the hardness on heat treating from 900°C was always lower than that obtained on heat treating from 850°C.

In the higher Cr alloys, however, this temperature (900°C) is not counter productive upto ~5%. Mn (Figs.5.12e-g). Raising the Mn to ~6%. led to a steep fall in the hardness in comparison to that obtained at 850°C (Figs.5.12g and h).

(xiii) A comparison between Figs.5.12d and h revealed that beyond 850°C, the overall decrease in hardness in lower Cr alloys was less compared with higher Cr alloys. Further, this decrease was a function of the soaking period in lower Cr alloys and independent of it in the higher Cr alloys (Figs.5.12d and h).

(xiv) Fig.5.13 revealed that the optimum heat treating time (commensurate with the optimum Mn content and the heat treating temperature i.e.~ 4-5%. and 850°C respectively) was 6 hours. Fig.5.13 also indirectly supports the already arrived at deductions concerning the optimum heat treating temperature and the useful Mn content to affect maximum hardening.

(xv) Amongst the lower Cr series, the 5%. Mn alloy appeared most favourable from the point of view of reaction 'kinetics' (Fig.5.13 a-e). This contention is valid for the higher Cr alloys except that at shorter soaking periods the reaction rate was faster in the ~6%. Mn alloy. It may however be noted that the hardness attained at 850°C (the optimum heat treating temperature) was higher in the 5%. Mn alloy and not in the ~6%. Mn alloy even at shorter soaking periods (Figs.5.13 f-j).

5.2.2 Microstructure

Microstructural examination was carried out to assess whether it reflected the changes in the as-cast hardness of different alloys brought about by heat treatment.

A preliminary examination of the as-cast/heat treated specimens revealed a certain degree of repetitiveness in the microstructures. It was however, easy to identify three basic features:

(i) The matrix microstructure comprising of pearlite/tempered martensite or bainite/martensite or a combination of these. Distinguishing between bainite/tempered martensite and martensite proved difficult in most instances except when the heat treating temperatures and Mn content were high (i.e. ~900°C and $\geqslant$ 5%.). Additionally, in many instances, the matrix contained dispersed carbides.

(ii) Free carbide which was either massive, 'plate like' or 'equiaxed' in nature.

(iii) Retained austenite whose presence was more easily detected in alloys with higher Mn(in the lower Cr series) and/or Cr contents.

The repetitiveness was minimized by confining the microstructural examination to (i) the as-cast specimens of all the alloys and (ii) those heat treatments at which distinct changes in the properties (hardness) were observed. Representative microstructures for the different alloys, currently investigated, are summarized in Figures 5.14 to 5.21. As discussed in the earlier paragraph, the three distinct features were discernable.

It was possible to identify pearlitic matrix which was predominantly confined to as-cast microstructures(Figs.5.14b, 5.16b, 5.18b and 5.21c). Similarly martensite could be clearly identified in one of the instances in the as-cast condition(Fig.5.17b) and in a number of instances in the heat treated condition (Figs.5.14f, 5.15f-g, 5.16g-h, 5.17g-h, 5.18e, g-i, 5.19e-f, 5.20h, 5.21i and k). However, the difficulty in identifying the nature of the matrix phase persisted in the remaining instances. Retained austenite could be detected in the alloys A4 and A8 in the as-cast conditions (Figs 5.17a-b and 5.21a-b and d) and in the alloys A3,A4 and A8 in the heat treated condition (Figs.5.16h, 5.17c and 5.21d,e and j).The matrix contained dispersed carbides in most instances (Figs.5.14c-f, 5.15c-g, 5.16e-h, 5.17c-f, 5.18e-i, 5.19c-e, 5.20d-h, 5.21e-k).

Concerning the morphology and dispersion of free carbides,

5.2.4 EPMA Studies

They were confined to the alloys A2,A3,A6 and A7 to ascertain (i) the distribution of Mn,Cr,Si and Cu into the different microconstituents (namely matrix and carbide) in the as-cast condition and, (ii) how it (the distribution) was affected by heat-treatment and/or alloy content. The EPMA data is reported in the Tables 5.18 to 5.36. Additionally concentration profiles for Mn,Cr and Fe (Fig.5.26) along with the corresponding X-ray images for Mn,Cr,Fe and Si (Figs.5.27-5.28) have also been provided. As discussed in Chapter IV, concentrations of Mn and Cr were computed by using α-coefficient correction method (Section 4.6.2) while Si and Cu concentrations correspond to first approximations.

A perusal of the Tables 5.18 to 5.36 and Figs.5.26 to 5.28 revealed that :

(1) (a) Concentration level of Cr and Mn distributing into the matrix and carbide phases was influenced by an increase in the alloy content. This is effectively demonstrated with the help of the data (derived from Tables 5.18 to 5.36) summarized below:-

Table A

Alloy	Concentration*			
	Matrix		Carbide	
	Mn	Cr	Mn	Cr
(1) A2 (~4% Mn and ~6% Cr)	3.00	3.61	4.44	14.16
(2) A3 (~5% Mn and ~6% Cr)	4.31	3.96	6.71	14.21
(3) A6 (~4% Mn and ~9% Cr)	3.28	5.58	4.81	28.87
(4) A7 (~5% Mn and ~9% Cr)	4.20	5.99	6.24	27.35

* Average value considering as-cast and heat-treated specimens.

lower Cr alloys (A2 and A3).

(c) Similarly when Cr was increased from ~6 to ~9%. keeping the Mn content the same, the concentration ratios of Mn and Cr in the microconstituents altered as shown in the table C.

Table C

	Concentration ratio of element	Matrix	Carbide
Low Mn alloys (A2,A6)	$C_{Cr\ A6}/C_{Cr\ A2}$	1.55	2.04
	$C_{Mn\ A6}/C_{Mn\ A2}$	1.09	1.08
High Mn alloys (A3,A7)	$C_{Cr\ A7}/C_{Cr\ A3}$	1.40	1.90
	$C_{Mn\ A7}/C_{Mn\ A3}$	1.00	0.90

As is evident, although the concentration of Mn in the matrix and carbide phases varied little both in the lower and in the higher Mn alloys, the increase in the concentration level of Cr was more pronounced in the lower Mn alloys (A2,A6).

(2) After correcting for the volume fractions of the carbide and matrix phases most likely present (e.g. 30:70 in lower Cr alloys), the distribution of Mn into the matrix and carbide phases worked out to be approximately in the ratio of 1.5:1. Similarly Cr distribution in the matrix/carbide phases was approximately in the ratio of 1:2.

(3) Heterogenity in the Mn distribution was substantially reduced in the higher Cr alloys even in the as-cast condition (Tables 5.28-5.32).

(4) Heat-treatment at best had a marginal or little effect on the element distribution into the carbide and matrix phases. Whatever little effect was observed can perhaps be accounted for on the basis of the changes in the volume fractions of the matrix and the carbide phases.

(5) Amount of Mn distributing into the carbide phase in both the lower and higher Cr alloys appeared a little higher than can be expected from an austenite stabilizing element. This is effectively highlighted in the table D below:

Table D

Alloy	$\frac{C_{Cr \text{ in carbide}}}{C_{Cr \text{ in matrix}}}$	$\frac{C_{Mn \text{ in carbide}}}{C_{Mn \text{ in matrix}}}$
A2	3.93	1.48
A3	3.60	1.56
A4	5.18	1.47
A5	4.88	1.49

(6) The amount of Cr and Mn in the matrix and the carbide phases corresponding to maximum hardening in alloy A2 (2h 850°C and 10h 850°C) was approximately 3.7 and 3% and 14-15% and 4.5% respectively (Tables 5.21-5.22). The

corresponding figures for the alloy A3 (4h 800°C, 10h 800°C and 2h 850°C) were approximately 3.7-4% and 4.0-4.6% and 13.3-14.6% and 6.3-6.9% respectively (Tables 5.25-5.27).

(8) The corresponding figures for the higher Cr alloy A6 (2h 850°C) were approximately 5.3 and 3.3% and 30.0& 4.8% respectively (Table 5.31). The figures for alloy A7(10h 800°C and 2h 850°C) were approximately 5.1-6.4% & 4.2-4.3% and 26.0-30.0% & 6.1-6.5% respectively (Tables 5.35 and 5.36).

(9) Representative x-ray images on the as-cast and heat treated specimens (Figs.5.27 and 5.28) along with the concentration profiles (Fig.5.26) agreed well with the quantitative observations summarized in the Tables 5.18-5.36.

(10) Distribution of Si and Cu, although not commented upon because their concentrations (i) have been reported as first approximations and, (ii) in the two phases appeared less than anticipated (based on chemical analysis), was none the less consistent with their general behaviour. This is duly substantiated as a major proportion of both of them (especially Cu) partitioned to the matrix phase (Tables 5.18-5.36).

5.2.5 Structural Analysis by X-Ray Diffractometry

Microhardness measurements did prove useful in partly resolving the unanswered questions arising out of microstructural interpretations. The nature of the carbide formed in different alloys as also whether its/their formation was influenced by heat-treatment and or alloying could not, however, be

ascertained. Similarly an additional confirmation as to the nature of the matrix microconstituent was equally welcome. Structural investigations by X-ray diffractometry proved useful in overcoming these deficiencies to a major extent.

As before, the as-cast specimens and certain selected heat-treated specimens were subjected to structural examination. The diffractograms fully indexed are summarized in Tables 5.37 to 5.64.

In the event of a doubt or difficulty in identifying a reflection, a question mark has been put. With the help of diffraction data it was possible to interpret the structures more or less completely as would be evident from the following deductions (Tables 5.37 to 5.64):

(i) Ambiguity concerning the identity of the matrix microstructure was satisfactorily resolved in most instances.

(ii) In the event of 'marginal' cases, deductions concerning the nature of the matrix microstructure were arrived at only after considering the corresponding microhardness values.

(iii) M_3C was the predominant carbide identified in most alloys. Additionally, the presence of M_7C_3 and M_5C_2 type of carbides was also detected, occasionally only in traces. In one of the instances $M_{23}C_6$ (Table 5.45) type carbide appeared to form in the lower Cr alloys.

(iv) A comparison between Tables 5.37 to 5.64 and 5.10

to 5.17 revealed that the formation of M_7C_3 and/or M_5C_2 type of carbides was generally accompanied by an increase in hardness of the carbide phase.

(v) Maximum hardness was not necessarily associated with the formation of martensitic matrix (Tables 5.39). This led to the possible deduction that alternative hardening mechanism(s) were also operative in some of the alloys.

(vi) This analysis proved effective in detecting the presence of retained austenite especially in specimens in whom it was difficult to ascertain its presence by optical metallography.

To ascertain whether a rationalised picture emerged concerning the effect of Mn/Cr ratio and heat-treatment on the nature of the matrix phase and the type of carbide(s) formed, the data in Tables 5.37 to 5.64 was summarized into a master Table 5.65. A perusal of this table revealed as follows:

(i) Martensite formed relatively easily on heat treating in alloys with Mn content around 4.5-5.0% or higher. Heat-treating temperatures higher than 800°C proved most useful. At a Mn content lower than ~4.5-5% (alloys A2 and A6), martensite formed on heat treating from higher temperatures generally after prolonged soaking.

(ii) Austenite was retained in the heat-treated microstructures again at Mn concentrations around 4.5-5.0% or higher.

(iii) In most instances M_7C_3 type carbide formed along with M_3C type.

(iv) Conditions favouring the formation of M_5C_2 type of carbide could not be clearly established. However, it appeared as though the possibility of its formation diminished as the Mn content and/or heat treating temperatures were raised.

5.2.6 Crack Propagation Behaviour

In the present study crack propagation path was determined only in the alloy A6. This alloy when heat-treated to high hardness had a tendency to develop macro-cracks starting from the periphery and leading towards the centre. Amongst the methods tried to bring about controlled propagation of an existing crack, indenting on the advancing crack front proved most useful. Only when indentation was made at 250 Kg load (on a Vickers hardness tester) did the crack propagate over a small distance. Further propagation was brought about by making another indentation as before. The process of making indentations had to be repeated several times to make a crack traverse a reasonable distance. After each indentation, microphotographs of the advancing crack were taken. Composite photograph(s) revealing how crack propagation was influenced by microstructure were prepared from individual micrographs and are shown in Figs. 5.29 and 5.30.

Cracks appeared to originate in the matrix and its propagation in general occurred within the matrix phase (Fig. 5.29a). Preference for the matrix phase was further demonstrated as the crack path was altered at least during

the initial stages when it encountered a carbide region with the crack now propagating interfacially (Figs.5.29a and b and 5.30a). On further propagation, the path no longer remained preferential and was through the matrix as well as across the carbide plates (Figs.5.29-5.30). An advancing crack 'climbed on' before cutting across a carbide plate (Figs.5.29a and b). Presence of discontinuous carbides changed the direction of crack propagation locally from the matrix to the interface (Fig.5.30a) before a carbide plate was cut across (Figs.5.30 a and b). Dispersed spherical carbides were easily sheared by an advancing crack and thus contributed little to resisting its propagation (Fig.5.30b).

Secondary cracking was also observed (Figs.5.30a and c). Only in one region it appeared as though the crack propagation path was preferential along a direction in which most of the carbide plates were aligned (Fig.5.30a).

Summarizing the observations, it is evident that the carbide path is not preferential.

5.2.7 Wear Test Results

5.2.7.1 General

Both the disc and pin and slurry-pot methods were employed. Mild steel served as the reference standard for evaluating the relative wear characteristics of the alloys under investigation. Wear rates were found (Tables 5.67A-B and 5.69) from the slopes of the cumulative weight loss vs time curves (Figs.5.31-5.37). Where such curves did not represent linear behaviour,

wear rates corresponding to changed slopes were also found. In such instances two different wear rates are reported.

5.2.7.2 Gouging Wear

Weight loss in the disc and pin test at the end of each of the six runs was measured. From it the cumulative weight loss was obtained (Tables 5.66A and B) and the cumulative weight loss vs time curves plotted (Fig.5.31-5.34). They formed the basis for calculating the gouging wear rates which have been summarized in Tables 5.67A and B.

A perusal of these tables revealed that:

(i) Amongst the lower Cr alloys the least wear rate was observed in the alloy A2 on heat-treating from 900°C and in the alloy A4 in the as-cast and 10h 800°C heat treated condition (Figs.5.31-5.34 and Table 5.67A).

(2) Although the alloy A3 showed the highest gouging wear rate initially, the final values were perhaps the least amongst all the alloys belonging to the lower Cr series (Figs.5.31-5.34 and Table 5.67A).

(3) Amongst the alloys belonging to the higher Cr series, the least overall wear rates were observed in alloy A5 (Figs.5.31-5.34 and Table 5.67B).

(4) Increasing the Mn content of the higher Cr alloys in general resulted in an increase in the wear rate except in the alloy A8 in which the wear rate decreased with time in at least three instances. Excluding these, only a single wear rate was observed (Table 5.67B).

(5) On comparing the lower and higher Cr alloys (hardness values $\geq$ 800 VPN) it became evident that although the lower Cr alloys wore more initially, their overall performance was substantially better than their higher Cr counterparts.

(6) However, at hardness values $\leq$725 VPN the performance of the higher Cr alloys in general was better than the lower Cr counterparts.

(7) Under high stress wear conditions, a microstructure having a high hardness did not necessarily guarantee a high resistance to gouging wear (Tables 5.67A and B).

A perusal of the Figs.5.31-5.34 clearly brought out the superiority of the alloys A5 (Fig.5.31) and A3(Fig.5.33) (deductions 2 and 3 above) as demonstrated by low/decreasing slopes of the cumulative weight loss vs time curves. A trend similar to that observed in alloy A3 was also exhibited by alloy A8 when it was heat treated from high temperatures (Fig.5.34).

5.2.7.3 Erosion Wear

Weight loss in slurry-pot test at the end of each of the 5 runs was measured. From it cumulative weight loss was obtained and is summarized in Table 5.68. From this data cumulative weight loss vs time curves were plotted (Figs.5.35-5.37), which formed the basis for calculating the erosion wear rates summarized in Table 5.69.

This table revealed that:

(1) Erosion wear was the least when hardness of the alloys was greater than 800 VPN. In this condition although the erosion

rate for all the alloys was low to start with, it increased in most instances. The least erosion wear was observed in alloys A3 and A7 under identically heat treated (2h 850°C AC) condition (Table 5.69 and Fig.5.36).

(2) The overall resistance to erosion was the least when the alloys were heat-treated to a hardness around 700-750 VPN. It may be mentioned that the heat-treating temperatures for this set of specimens in all instances was either 900 or 950°C i.e. maximum (Table 5.69 and Fig.5.37).

(3) Amongst specimens with hardness in the range of 700-750 VPN, it is noteworthy that for specimens A1(6h 850°C AC), A3(4h 900°C AC) and A7(6h 900°C AC), the initial rate of erosion was very low (even better than the corresponding values when alloys were heat treated to hardness $\geq$ 800 VPN). However, this was not sustained throughout the duration of the test (Table 5.69 and Fig.5.37).

(4) The erosion behaviour of the as-cast specimens was a little superior than those with medium hardness (heat treated from 900°C or more) but a little inferior than those with the maximum hardness (Table 5.69 and Fig.5.35).

5.3 SUMMARY

Results obtained in the present investigation have been summarized in Section 5.2. They have been discussed in the next chapter. This is followed by a 'critical reappraisal' consisting of an analysis providing a comprehensive review of the investigation from its initiation to the conclusion stage.

CHAPTER-VI

DISCUSSION OF RESULTS

6.1 THEORETICAL CONSIDERATIONS

The present investigation had been aimed at establishing (i) the transformation behaviour of the newly designed Fe-Mn-Cr-Cu white irons especially with regard to their ability to form the 'desired' microstructure, (ii) the hardening mechanism(s) and (iii) a correlation between microstructure and wear. The last aspect, pursued to a limited extent, was likely to provide useful information on the most suitable microstructure from the point of view of gouging and erosion wear. Except this aspect, bulk of the interpretation of the data shall be governed by the distribution/partitioning of Mn and Cr into different microconstituents and how their distribution/partitioning is influenced by heat-treatment (both qualitatively and quantitatively).

As a first approximation, the transformation behaviour of the alloys would be mainly governed by the influence of Mn on the (i) Ar_1/M_s temperatures and (ii) tendency/ability of austenite to transform to non-equilibrium microstructures on cooling from the heat treating temperature. Whereas, the former depends upon the amount of Mn added, the latter is governed mainly by the heat-treating temperature, alloy content

and cooling rate. Additionally, (i) the quantitative data on the effect of Cr, Si and Cu on the A_1 temperature and their effect on hardenability (Section 2.3.2), (ii) the experimental observation that ~2% Mn is required to render an eutectoid steel air hardening[1,10,115,116] and (iii) the possibility of retaining austenite at 'high' Mn contents would help in arriving at a reasonable estimate of the transformation behaviour of the alloys even in the absence of their critical temperatures and TTT/CCT curves.

In order to understand how hardness in the heat treated condition is a function of Mn content (at the two different Cr contents) and the heat-treating schedule, an appreciation of the structural changes that are likely to occur, is necessary. Three types of changes are possible: (i) involving redistribution of alloying elements into different microconstituents, (ii) changes in the high temperature microstructure consequent upon holding at the heat treating temperature and (iii) changes occurring during cooling from the heat-treating temperature to room temperature, firstly, till the stage when the microstructure is austenitic and subsequently when it transforms to α or its variant α' (martensite). The EPMA data summarized in Tables 5.18-5.36 clearly reveals that heat-treatment has had no major effect on the element distribution. Thus, the alloy/Mn content of austenite in the heat-treated and in the as-cast conditions is not expected to be much different

in the experimental alloys.

A change that may occur on soaking and is likely to influence the alloy content of austenite involves a reduction in the volume fraction of the carbide phase because of the presence of graphitizing elements Si and Cu. This will lead to (i) a larger availability of both the interstitial and substitutional elements and (ii) the attainment of discontinuous carbide.[98-100] However, a larger availability of the alloying elements is accompanied by a corresponding increase in the volume fraction of the matrix phase. Thus the overall element balance in austenite remains unaltered, however, with the matrix now retaining a higher proportion of the alloy content. Another change that may occur in the high temperature microstructure during soaking involves precipitation of carbides (cf-precipitation in austenitic stainless steels).[117] This carbide is likely to be different from M_3C, would be one needing a larger activation for its formation and one involving a participation of relatively larger amounts of substitutional elements in its formation.[118] Carbide precipitation will also occur during cooling from the heat-treating temperature, mainly because of a decrease in solid solubility of carbon in austenite with a decrease in temperature. The carbide formed will be of the type $(FeMnCr)_xC_y$ (e.g. $(FeCrMn)_7C_3$ or simply M_7C_3 type) as both Mn and Cr are carbide formers.[1,10,77] The other likely changes namely rendering of free carbides

possibility of forming non-equilibrium microstructure(s)). With an increase in the alloy content a stage may be reached when austenite is retained either partly or fully. The extent of austenite stabilization will be a function of the (i) amount(s) of γ-stabilizer(s) and (ii) the ratio of γ/α stabilizers.

The above mentioned considerations proved extremely useful in interpreting the data summarized in the tables 5.1-5.65 and the Figures 5.1 to 5.27 as will be evident from the following sections.

6.2 INTERRELATION BETWEEN ALLOY CONDITION AND HARDNESS

6.2.1 As-Cast Hardness

Considering the as-cast hardness, an increase in it upto ~5% Mn (Fig.5.1a) in the lower Cr alloys is due to solid-solution hardening effect of Mn and Cr with some possibility that there may be a change in the matrix microstructure even at the slow cooling rates attained during sand moulding. It has not been possible to detect these changes in the as-cast microstructures of alloys A_2 and A_3 (Figures 5.15b and 5.16b), the matrix microstructure of the as-cast alloy A1 being pearlitic (Figs.5.14a and b). However, the attainment of martensite at higher Mn contents i.e. at ~6% Mn in the as-cast condition (Fig.5.17b, Table 5.47) supports the above contention. The decrease in hardness on raising Mn from ~5 to~6% is attributed to the retention of a sizable

proportion of austenite at room temperature(Figs.5.17a and b).

In the higher Cr alloys, the trend of the hardness variation with Mn content is similar to that observed in the lower Cr alloys upto ~5%. Mn (Fig.5.1b). However, the overall hardness in the higher Cr alloys is lower than that observed in the lower Cr alloys due to a low Mn/Cr ratio in the former. This makes retention of γ and formation of acicular microstructure(s) difficult at least at the lower Mn contents(Figs.5.18a and b, 5.19a and b). Contrary to the behaviour of the lower Cr alloys, hardness in the higher Cr alloys increased even beyond ~5%. Mn (Fig.5.1a and b). This must have been brought about by a change in the matrix microstructure which has not been clearly detected (Figs.5.20a-c, 5.21a,b,d and e). It is likely that had the Mn content been increased beyond ~6%. say to ~7%. , the hardness vs Mn content curve would have shown a decreasing trend as observed in the lower Cr alloys.

6.2.2 Heat-treated Hardness

Assuming that (i) the trend of Mn distribution in the alloys A2,A3,A6 and A7 to be a representative one for all the alloys and (ii) the quantitative relationships concerning the effect of relevant alloying elements (Section 2.3.2), cited earlier, as valid, it appears that the heat-treating temperatures of 750 and 800°C at least for the lower Mn alloys are insufficient to promote hardening. This is reflected by the hardness values summarized in Tables 5.2-5.9.

Presence of spheroidal carbides in the microstructure in most alloys (akin to **spheroidized** structure in high C steels) on heat-treating from 750°C and the experimental observations that hardness decreases with (i) Mn content at a given Cr level (alloy content) and (ii) an increase in the soaking period at a given alloy content, point to the possibility that the heat-**treating** temperature of 750°C is higher (slightly) than the effective A_1 temperature in most instances.

In the alloy A1, decrease in hardness on heat treating from 750°C is due to the formation of a spheroidized **microstructure** which will be less harder than the matrix microstructure attained in the as-cast condition. This is also true for the alloys A2 and A3 (Figs. 5.2a, 5.3a, 5.4a and 5.5a). Hardness decrement on heat-treating from 750°C (with respect to the as-cast condition) increases with Mn content upto ~5%. (Figs. 5.2-5.5) due to particle coarsening. This also signifies that the heat treating temperature of 750°C is insufficient to bring about any change in the as-cast microstructure other than producing a spheroidized-structure. The slight decrease in hardness with an increase in soaking period is also due to particle coarsening. This trend is reversed only in the heat-treatment response of alloy A4 (Fig. 5.5a) in which the starting microstructure is martensite+austenite (Figs. 5.17a and b) and the slight increase in hardness is because of the following reactions

out of which reaction (i) predominates:

(i) $\gamma \xrightarrow{\text{on soaking}}$ carbides + γ (with less alloy content) | leading hardness increase

γ (with less alloy content) $\xrightarrow{\text{on cooling}}$ P/B/M) | leading hardness increase

(ii) Martensite $\xrightarrow{\text{on heating}}$ α + carbides] Leading to Hardness decrease

The absence of hardening in alloy A8 (Fig.5.5b) on heat treating from 750°C clearly reveals that the basis of explaining an increase in hardness in the alloy A4, when identically heat-treated, is valid. This is because the as-cast matrix micro-structure in alloy A8, unlike in alloy A4, is mostly P/B + some martensite(?) + some austenite (Fig.5.21a-e) and on being heat treated from 750°C such a microstructure will lead to a decrease in hardness because the reaction of the type (ii) as mentioned above, predominates.

This argument also leads to the conclusion that the remaining higher Cr alloys A5 to A7, on being heat-treated from 750°C, will respond in a manner similar to alloy A8. That is what has been observed (Figs.5.2b to 5.5b).

The hardness of the alloy A1 in the heat treated condition increases as the temperature is raised from 800 to 900°C, albeit marginally (it being maximum at 900°C), consistent with the (i) laws governing diffusion controlled processes and (ii) the effect of temperature and cooling rate on the possible formation of shear transformation product (Fig.5.2a).

The increase in hardness on heat-treating from 900°C

A further increase in the soaking period leads to a solute enrichment of γ (due to some decrease in the volume fraction of the carbide and/or by redissolution of the microconstituents present at lower temperatures) to an extent that formation of martensite on air cooling is rendered feasible in preference to bainite (Fig.5.18e).

On raising the Mn content to ~3.5-4% (alloys A2 and A6) (Figs.5.3a and b), the ineffectiveness of 800°C in inducing hardening can be explained as before. Attainment of a slightly higher hardness in alloy A6 compared with A2 is because of a higher alloy content in the former (i.e. A6). The peak hardness in alloy A2 is associated with a microstructure containing an optimum combination of mostly martensite and some dispersed carbides (Figs.5.15 c and d). Increasing the soaking period to 10 hrs has considerably increased the volume fraction of martensite (leading to hardness increase) but at the same time coarsened dispersed carbides (leading to a hardness decrease) resulting in an overall hardness which is approximately similar to that observed on heat-treating for 2 hours. A nearly similar situation exists in the alloy A6 in which formation of light etching areas has begun at 800°C (Fig.5.19c) and is comparable with that observed in alloy A2 both at lower and higher soaking periods (Fig.5.19d).

On raising the heat-treating temperature to 900°C, the hardness values in alloy A2 are appreciably low at the lower

soaking periods (compared to corresponding values at 850°C) because the matrix microstructure has undergone coarsening and the percentage of lighter etching areas is smaller than before (Fig.5.15e). With an increase in time, although the extent of coarsening will be more (leading to a decrease in hardness), the simultaneous enrichment of austenite will aid the formation of a relatively larger volume fraction of martensite whose amount would further increase with soaking period. Additionally, some fine carbides will also precipitate during cooling. The last two factors lead to an increase in hardness. Thus, the overall hardness is expected to increase with an increase in soaking period at 900°C. This is what has been observed in alloy A2 (Fig.5.3a) and is duly supported by microstructural observations (Figs.5.15e to to f). Unlike A2, the alloy A6 responded identically when heat treated from 850 and 900°C, the hardness on heat-treating from 900°C being only marginally lower (Figs.5.3a and b). This difference in behaviour between A2 and A6 is attributed to a higher overall alloy content (Mn+Cr) and hence to an improved ease of martensite formation in the latter (Figs.5.19d-f, Table 5.15).

On raising the Mn content to ~4.5-5%. (alloys A3 and A7), the transformation behaviour has significantly altered. In view of the Mn content approaching ~4.5-5%., the heat treating temperatures in general are well above the operative

A_1 temperature(s). This has enabled hardening of the alloys A3 and A7 even on being heat-treated from 800°C (at higher soaking periods) [Figs.5.4a-b, 5.16d and e and 5.20 f and g] and this can be explained by stating that the different microstructural changes which could not be initiated earlier at 800°C (i.e. at Mn ~3.5-4%.) are now at least partly feasible at lower soaking periods and to a larger extent at soaking periods $\geq$ 6 hrs (Figs.5.4a and b). As before, the maximum hardening has been attained in a minimum of time on heat-treating from 850°C and that the maximum hardness is sustained independent of the soaking period. This further reveals that at this high Mn content (~4.5-5%.), heat-treating from 850°C has as yet not initiated structural changes that may lead to a decrease in hardness i.e. retention of austenite is occurring at best to an extent that there is no countermanding effect on the overall hardness. Structural observations (Figs. 5.16e and f, Tables 5.12, 5.16, 5.44 and 5.45) confirm this reasoning.

On heat treating from 900°C, although the microstructure in alloy A3 is martensitic in character (Figs.5.16g and h), the lower hardness is due to retention of austenite whose amount reduces at best only marginally with soaking period. This has led to a very small increase in hardness at soaking periods $\geq$ 6 hrs, by mechanism (s) stated earlier (Fig.5.4a and Table 5.12). Alternatively, this observation can also be explained by stating that the amount of austenite is unaltered but precipitation occurs which attains a

reasonable volume fraction to induce marginal hardening only at soaking periods $\geq$ 6 hours.

The heat treatment behaviour of the alloy A7 is similar to A3 except that the difference between the hardness values attained on heat-treating from 850 and 900°C is much smaller than observed in A3 (Figs.5.4a and b). This is attributed to a low Mn/Cr ratio and hence to a reduced tendency towards γ stabilization (Figs.5.19c to f).

On raising the Mn content to ~5.5-6%. (alloys A4 and A8), the retarding effect of retained austenite has prevented the alloy A4 from attaining hardness as high as the alloy A3 on heat treating from all temperatures at soaking periods $\leq$ 6 hrs. Contrary to the transformation behaviour of alloy A3, the fastest reaction rates have been attained at 800°C followed by 850 and 900°C (Fig.5.5a). This has come about because at Mn ~5.5 to 6%., the operative A_1 temperature has been substantially lowered so that even on heat treating from 750°C an increase in hardness is observed (Fig. 5.5a). Accordingly the attainment of high hardness on heat-treating from 800°C is understandable. A comparison between Figs 5.4a and 5.5a reveals that the heat-treating temperature of 800°C, which was ineffective in inducing hardening in the lower Mn alloys (Figs.5.2a and 5.3a) and slowly gained ascendency over other temperatures as the Mn content was raised from ~2.5-3%. to ~5.5-6%.,

is the most favoured temperature for inducing hardening in alloy A4 because at temperatures higher than 800°C the γ-stabilizing effect predominates due to a high Mn/Cr ratio. A similar situation had existed in the alloy A3 on soaking at 900°C (Fig.5.4a). As in the earlier alloys, an increase in hardness in the alloy A4, on increasing the soaking period, is associated with the decomposition of 'γ' into non-equilibrium microstructure as explained earlier (Figs.5.7c to e) with the maximum hardness associated with the formation of a martensitic matrix (Fig.5.17f). At temperatures higher than 800°C, the decrease in hardness is due to the attainment of a coarse martensitic matrix and to a simultaneous retention of some austenite (Figs.5.17g and h). The latter is not clearly evident from the micrographs (Figs.5.17g and h) but its presence has been detected with the help of scanning microscopy (Fig.5.24) and X-ray diffractometry (Table 5.50). It may be noted that the martensite shown in Figs.5.17g and h (i.e. in the form of obtuse plates) (Fig.5.24) is formed in high 'C' steels/Fe-Ni-C alloy steels (119,120) and is therefore invariably associated with retained austenite.

A nearly similar situation exists in the alloy A8(Fig.5.21) except that till about 6 hours holding period, the rate of reaction is faster at 850°C compared with 800°C. However, beyond this soaking period, the rate of reaction (transformation) became faster at 800°C. Thus there is only a marginal difference in behaviour between the alloys A4 and A8 and this is

essentially attributed to a lesser 'γ' stabilizing tendency in the latter because of a lower Mn/Cr ratio. However, on heat treating from 900°C, the extent of γ stabilization is more in the alloy A8(Fig.5.21j) as compared with alloy A4 (Fig.5.17h) because of a higher overall alloy content in the former. It may be mentioned here that the tendency towards γ stabilization would basically be a function of the amount γ stabilizing element present, heat treating temperature and time. Once the threshold condition for γ stabilization is established, the γ-stabilizing tendency will now be a function of the overall alloy content. This is so because any element in solution in general will retard the decomposition of γ and Cr is no exception to this[1,10].

Coming now to the data summarized in Figures 5.6 to 5.9, these figures were constructed based on the data in Tables 5.1-5.8 mainly to draw more meaningful inferences from the hardness data. The results summarized in these figures can be largely explained on the basis of the arguments put forward earlier while interpreting the Figures 5.2 to 5.5.

The difficulties encountered in arriving at a more complete interpretation of Figs.5.6 to 5.9 have already been discussed in Section 5.2.1. Further, how these were overcome by constructing the Figures 5.10 to 5.13, by utilizing the derived hardness values obtained from figures 5.2 to 5.5,has also been elaborated upon. Additionally it may be stated here that the alloys deviated from their 'true' transformation behaviour because the system under consideration is multi-component in nature and therefore likely to respond to heat-

treatment as a heterogeneous system.

Inferences drawn from the Figs.5.10-5.13 (page 85) part of which reinforce the deductions arrived at from the Figs.5.2-5.9, can also be interpreted on the basis of which the data in Figs.5.2 to 5.5 was explained. However, those inferences derived from Figs.5.10-5.13, which provide direct answers to queries, both fundamental and applied in nature, are enumerated and interpreted afresh below.

(1) The optimum range of Mn content and heat-treating temperature to induce maximum hardening for both the lower and higher Cr alloys is 4-5%. and 850°C respectively (Fig.5.10-5.13). This is because at 4%. Mn, austenite has the required necessary Mn content to form fully martensitic matrix on air cooling from 850°C. On raising the Mn content to ~5%., although the effective concentration of Mn in austenite is larger than before, it is still insufficient to bring about retention of austenite (because of the presence of a sizeable proportion of Cr) to an extent that hardness is adversely affected. The hardness in the heat-treated condition would be independent of the soaking period from that stage onwards at which the austenite at the heat-treating temperature contains a minimum of ~3%. Mn (consistent with the Mn content of the matrix in A2 on heat treating from 850°C to induce maximum hardening).

The volume fraction of free carbides is likely to diminish with soaking period. However, the larger amount

of alloy content thus made available is accounted for by an increase in the volume fraction of the matrix. This justifies hardness in the heat-treated condition to be independent of the soaking period.

(2) The optimum heat-treating time to induce maximum hardening commensurate with the optimum Mn content and heat-treating temperature is ~6 hrs (Figs. 5.11 and 5.13). This is justified by stating that corresponding to this soaking period even if there is an error in controlling the heat-treating temperature, the final hardness would remain relatively uneffected. In fact, the lower limit of Mn content for attaining maximum hardening is ~4%. However, if for some reason the Mn level drops below this level, there is a steep fall in hardness for reasons already explained earlier. For this reason the optimum Mn content has been specified as between 4 and 5%.

(3) The 5% Mn alloy is the most favourable one from the point of view of responding to the hardening treatment in both the lower and higher Cr series because the slope of the hardness vs temperature curves, as influenced by soaking period, is the maximum for this alloy (Fig. 5.13). Reasons for this have already been elaborated upon.

(3) Higher Cr alloys in general exhibited a slightly higher level of hardness compared with the lower Cr alloys because of a higher alloy content. Further, a low Mn/Cr ratio in the higher Cr alloys has proved useful in their

sustaining a higher level of hardness even on being heat treated from 900°C. This reasoning is valid upto 5%. Mn.

6.3 MICROSTRUCTURE

6.3.1 Dispersed Carbides

Although the effect of heat-treating temperature and time on hardness in different alloys has been satisfactorily explained, some aspects related with the microstructure and strengthening/hardening mechanism(s) need commenting upon. An important observation relates to the presence of dispersed carbide in the microstructure. In steels, when γ transforms to martensite, although carbides do form, they are present on such a fine scale that their identity is revealed only by thin foils and/or replica electron microscopy[121,122]. In the present investigation the situation is slightly different from that observed in steels in that γ, during cooling from the heat-treating temperature to the Ar_1/Ms temperature contains a larger amount of interstitial solute. As a consequence of this, it will contain dispersed carbides formed during cooling from the heat treating temperature to the temperature at which it begins transforming to martensite for reasons already mentioned. However, if this was the only likely mechanism by which carbides are formed, they should have been observed even in the alloy cast irons such as Ni-hard 4 as also in the as-cast microstructures of the alloys presently

under investigation. Their absence in heat treated Ni-hard 4 may be due to two reasons (1) firstly, the heat treating temperature employed in low i.e. only 750°C and/or (ii) the mechanism(s) by which they form in the alloys presently under investigation are different from what has been indicated earlier. The first postulate is self explainatory. Considering the second possibility, another mechanism by which carbides may be formed is as a consequence of holding at the heat-treating temperature (as in precipitation hardening) provided no other structural change is preferred. This mechanism has already been explained earlier(section 6.1).

The presence of dispersed carbides contributes additionally to hardening as is evident from the microhardness data summarized in Tables 5.10-5.17. In instances where the matrix microstructure is martensite (matrix hardness $\geq$ 750-800 VPN), the additional hardness of the matrix over and above this value can be attributed to the presence of dispersed carbides.

6.3.2 Morphology and Nature of Free Carbides

Nature of the carbides formed in the alloys presently under investigation will be of the type (FeCrMn)xCy as both Cr and Mn are carbide formers. Based on the diffractometric studies it is inferred that M_3C is the main carbide constituent present in the experimental alloys (Table 5.37 to 5.65). Additionally, presence of M_7C_3 and M_5C_2(only in

some instances) carbides has also been detected (Table 5.65). Study of the relevant ternary sections of the Fe-Cr-C and Fe-Mn-C phase diagrams reveals that the predominant carbide to form in the alloys under investigation should be M_3C. Further, there is a definite possibility of the M_7C_3 type of carbide forming in addition to M_3C in the experimental alloys in the heat-treated condition.(11) Thus a major part of the findings on the formation of carbides (Table 5.65) is consistent with the information obtained from isothermal sections of the relevant phase diagrams.

The formation of M_5C_2 type of carbide now needs explaining. This carbide has been detected both in the lower as well as in the higher chromium alloys mostly in traces. An examination of the Fe-Mn-C ternary reveals that the M_5C_2 carbide is stable at high temperatures and generally formed at relatively high Mn and carbon concentrations.(11) Recalling the suggestion given earlier that the type of carbide formed during soaking may involve participation of a larger proportion of substitutional elements, the possible formation of M_5C_2 carbide in the heat-treated condition does not appear improbable.

The formation of $M_{23}C_6$ carbide in one of the instances in the lower Cr alloys can be similarly explained and also on the basis of the experimental observation that '$M_{23}C_6$ type of carbide may appear in alloys containing less than 10% Cr.(11)

(equiaxed/polyhedral/hexagonal) in the higher Cr alloys (Figs. 5.18-5.21). Free carbides, in a discontinuous and dispersed form, were similarly present in most of the higher Cr alloys in the as-cast condition and more readily identified in the alloys A5 (Fig. 5.18b) and A8 (Fig. 5.21b). A similar tendency is observed in the lower Cr alloy A4 (Figs. 5.17a and b). Thus, in general, the morphology and dispersion of free carbides are better in the higher Cr alloys. Certain pertinent queries arise at this stage related with the above observation:

(i) Why free-carbide morphology should at all alter on heat-treating and is more favourable in a certain set of alloys even in the as-cast condition?

(ii) What factors should bring forth the desired changes in the free-carbide morphology and dispersion?

The two questions are infact inter-related and can be suitably answered based on the fundamental considerations explained below:

Free-carbides increase the overall energy of the matrix microstructure by acting as discontinuities and such a microstructure, when heat-treated, would try to attain a lower energy configuration. This would be made possible only if the microconstituent, acting as a discontinuity,

attains a minimum energy configuration by reducing its surface energy. This would automatically entail a change in the morphology of free-carbides. For a given volume, a sphere has the least surface area and accordingly the ideal morphological configuration for the free-carbides to attain is a sphere. This configuration would be attained only after a prolonged soaking at a high austenitizing temperature. In actuality, however, free-carbides would acquire a minimum energy configuration consistent with their crystal structure) within the constraints of heat-treating temperature and time employed in the present investigation (a higher temperature and a longer soaking time bringing about a more pronounced change), e.g. an equiaxial or polyhedral free carbides in a hexagonal form consistent with the hcp crystal structure of one of the carbidesnamely, M_7C_3 (Figs. 5.18f, 5.20b and g, 5.21g).

Free-carbides which contain a higher proportion of Cr would be more amenable to a change in morphology as they are not likely to undergo any other change on heat-treating except being rendered discontinuous. In the present context this implies a more favourable free-carbide morphology in the higher Cr alloys. This is what has been observed. Thus, the reasons (i) leading to a change in the free-carbide morphology and (ii) why higher Cr alloys should exhibit a more favourable free-carbide morphology and dispersion on heat-treating are satisfactorily explained.

Free carbides are discontinuous and equiaxed/ polyhedral in most of the as-cast higher Cr alloys but not in the as-cast lower Cr alloys because the freezing characteristics of the two sets of alloys differ. Whereas the former compositions are perhaps closer to the eutectic, those of the lower Cr alloys atleast at lower Mn contents are perhaps not[17]. Whether this alone is a sufficient reason in explaining the observation is not clear especially because the cooling curves for the experimental alloys have not been established.

Perhaps a more generalized explaination in support of using relatively higher Cr contents may in some way be related with the case with which Cr atoms are able to migrate. A perusal of the data on the diffusivities of Cr and Mn atoms in α and γ irons reveals that they are governed by an expression of the type:[127]

$$D = A \, Exp(- \frac{Q}{RT})$$

where,

D = diffusivity,

Q = activation energy

A = frequency factor,

R = universal gas constant, and

T = absolute temperature

In Iron

	A	Q	Temp.°C
C	6.2×10^{-3}	19.2	350-850(α)
	0.1	32.4	900-1060(γ)
Cr	$8.52^{+3.2}_{-2.33}$	59.9±1.6	800-880(α)
	$10.80^{+3.35}_{-2.56}$	69.7±1.7	950-1400(γ)
Mn	$1.49^{+1.0}_{-0.60}$	55.8±2.5	700-760 (Ferrom.α)
	$0.35^{+0.31}_{-0.17}$	52.5±2.3	800-900 (Param.α)
	$0.16^{+0.06}_{-0.05}$	62.5±1.0	920-1280(γ)
	0.78	60.1	809-901

By substituting the relevant values for the diffusion of Cr and Mn atoms in austenite at a temperature of 900°C,

$$D_{Cr} = 1.3504\times10^{-12} \text{ cm}^2/\text{sec.}$$

and $$D_{Mn} = 4.3056\times10^{-13} \text{ cm}^2/\text{sec.}$$

This leads to the inference that at 900°C Cr atoms diffuse about three times as fast as the Mn atoms. Its direct effect will be that at a given temperature the overall rate of diffusion will be faster in the higher Cr alloys and accordingly microstructural changes involving a modification in the (i) matrix microstructure and (ii) carbide morphology will be more rapid in the higher Cr alloys than in the lower Cr alloys. This is a more convincing argument to explain how higher Cr alloys would respond more favourably to a change

instances, has been separately commented upon (Section 6.3.1).

The formation of pearlite (Figs.5.14b, 5.16b, 5.18b, and 5.21c) and martensite (Figs.5.14f, 5.15f-g, 5.16g-h, 5.17b,g-h,5.18e and g-i, 5.19e-f, 5.20h, 5.21 i and k) in the experimental alloys, in the as-cast/heat treated conditions, is consistent with the physical metallurgical thinking. This has been critically discussed in some of the preceding sections (6.1 and 6.2). Difficulties in interpreting the matrix microstructure arose while distinguishing (i) pearlite from bainite and (ii) bainite/tempered martensite from martensite based on optical metallography alone especially at critical juncture when the latter (in both the cases) just about begins to form in preference to the former (directly from austenite). Presence of dispersed carbides additionally contributed to the existing difficulties especially when the matrix microstructure was fine. X-ray diffractometry, microhardness measurement and scanning microscopy proved extremely useful in overcoming the difficulties. Infact the first two techniques proved most valuable in deciding marginal cases (e.g. possible formation of martensite in preference to bainite/tempered martensite in the alloys A2 and A6 and other similar cases) [Table 5.65].

The microhardness values for the matrix phase have been in the range of ~380 to 1000 VPN (Tables 5.10-5.17). Recalling that the matrix microstructure has varied from pearlite through bainite to martensite, microhardness is

expected to vary from ~200 to ~800 VPN. That the lower limit of microhardness in the present investigation has been found to be slightly higher may be explained by stating that a microhardness of ~200 VPN is associated with pearlite in plain carbon compositions and accordingly alloyed pearlite is expected to have a higher hardness. The hardness of the matrix phase has approached ~1000 VPN because in most instances martensite matrix has contained dispersed carbides. Evidently the hardness over and above that exhibited by martensite can be attributed to the presence of dispersed carbides. Matrix microstructure was identified as (i) bainite in the microhardness range ~500 to ~750 VPN and (ii) martensite at hardness ~750-800 VPN.

Scanning electron metallography proved useful in confirming the matrix to be martensitic in the alloys A2 and A3 (Fig. 5.23b). At higher alloy (Mn) contents, a change in the morphology of martensitic matrix from its usual appearance (Fig. 5.23b) to the obtuse plate-like morphology (Fig. 5.24c) is noteworthy and consistent with the effect of (1) carbon and (ii) alloy content on martensite morphology.[119,120]

Dispersed carbides are an integral feature of the matrix microstructure (Figs. 5.14c-f, 5.15c-g, 5.16e-h, 5.17c-f, 5.18e-i, 5.19c-e, 5.20d-h and 5.21e-k). It would be pertinent to consider how well they are entrenched within the matrix as this is likely to affect the wear behaviour. In the

present instance scanning microscopy was employed to ascertain this. Their presence is clearly revealed in the Figures 5.22b, 5.23, 5.24a and b and 5.25b. High magnification observation reveals that at least in the alloy A3, dispersed carbides were easily dug out (Fig.5.23b). Thus on the basis of limited evidence, their adherency with the matrix appears unsatisfactory.

Presence of austenite has been readily detected only in instance when it was (i) present in sizable amounts within the matrix (Figs.5.16h, 5.17c and 5.21e,j), (ii) retained along with martensite (Figs.5.17a and b) and (iii) present around free-carbides (Figs.5.17b and 5.21b and d). Its formation in the experimental alloys in the as-cast/heat-treated conditions is consistent with the physical metallurgical thinking based on which the hardness data has been explained in the section 6.2. Diffractometric studies (Table 5.65) and to some extent scanning microscopy (Fig.5.24) proved very useful in establishing its presence in instances when optical metallography proved inadequate (e.g. alloy A3 and A7). Microhardness of retained austenite (500 to 700 VPN) appears a little higher than expected and is perhaps an indication that its stability is a little less as compared with that of austenite formed at high alloy and/or carbon contents.

6.3.4 Hardening Mechanism(s)

Based on the discussion above, it clearly emerges that the hardening in the alloys has been mainly due to the formation of the martensite matrix. Additional strengthening/hardening has occurred from the presence of dispersed carbides. There are a few instances when the overall hardness of the alloy is higher than 800 HV_{50} although the matrix microstructure is not fully martensitic (Table 5.39). Strengthening/hardening under these conditions has mainly arisen from the presence of an optimum dispersion of dispersed carbides and can be explained on the basis of the equation[128] valid for strengthening from the presence of incoherent hard particles

$$\tau_y = \tau_s + \frac{Gb \cdot 2\phi}{4(d-2r)} \ln\frac{(d-2r)}{2b}$$

where,

$$\phi = \frac{1}{2}\left(1 + \frac{1}{1-\mu}\right)$$

τ_y = shear stress at yielding

τ_s = yield stress of the matrix

G = shear modulus

b = Burger's vector

d = particle spacing

γ = particle radius

μ = Poisson's ratio

which highlights the importance of reducing the interparticle

spacing in inducing strengthening. The interrelation between (i) the volume fraction of the second phase particles (i.e. carbides), (ii) particle diameter and (iii) interparticle spacing (mean free path), which together will control the particle dispersion and hence hardening, is given by [31],

$$f^{1/2} = C(\frac{D}{\lambda})$$

where,

f = volume fraction of carbide,

D = particle diameter

λ = mean free path

C = statistical constant

De Sy[129] and others have also pointed to the possibility that a dense dispersion of fine spherical carbides in a ferrite matrix may in some cases induce strengthening in alloy white irons as has been observed in one of the alloys (i.e. A2) in the present investigation although the basic premise of alloy design has been to induce hardening only through forming martensitic matrix (Chapter 3).

6.4 PARTITIONING OF ALLOYING ELEMENTS

The microprobe data reveals that heat-treatment has had at best a marginal effect on the element distribution (vis-a-vis the as-cast condition) in the alloys presently under investigation. This observation is of design interest

and its usefulness lies in that the heat treating temperature and especially the time can be decided upon solely on the basis that (i) the high temperature microstructure (HTM) of the required configuration is just attained and (ii) it (the HTM) on cooling transforms by a mechanism such that the final microstructure formed conforms to the properties desired.

It is significant to note that the heterogeneity in the Mn distribution is observed to be less in the higher Cr alloys as compared with the lower Cr alloys (Tables 5.18-5.36). This experimental finding can be explained on the basis of the beneficial effect of a higher diffusivity associated with Cr atoms in comparison to Mn atoms (Section 6.3.2). It is noteworthy that the utilization of a higher Cr content has proved useful in overcoming the natural tendency of the Mn atoms towards segregation[130] and is of special relevance to the present investigation which aims at exploring the possibility of utilizing a higher Mn content for developing alloy white irons. The above experimental finding should be regarded as yet another advantage in utilizing Cr contents higher than normally required [over and above what has already been concluded on this theme in the Section 6.3.2].

With the help of the EPMA data, it has been possible to ascertain the alloy content of the different micro-constituents corresponding to heat-treatments inducing

larger concentration of it to migrate to the carbide phase. This observation is also of interest from the point of view of alloy design as Mn has been primarily chosen for enhancing hardenability and it was believed that even after allowing for its carbide forming tendency at least a major part of it will partition to austenite. This assumption has been proved to be incorrect.

As regards the partitioning of Cr, it has been found to be consistent with its general behaviour. Although partitioning data for Si and Cu has also been included in the tables, it has not been commented upon because (i) the overall concentration levels of these two elements were found to be lower than expected and (ii) their concentrations have been reported only as first approximations. However, their partitioning is consistent with their general behaviour- i.e. a major proportion of each of thesepartitions to the matrix phase (Tables 5.18-5.36 and Section 5.2.4).

6.5 WEAR BEHAVIOUR

Wear data summarized in Tables 5.66 to 5.69 and Figures Figures 5.31-5.37 has proved useful in arriving at some useful deductions concerning how micro-structure controls gouging and erosion wear. Instead of following the more conventional method of evaluating wear, slopes of the cumulative weight loss vs time curves were calculated as this was likely to provide information on whether more than

one wear mechanism was operative.

Considering the gouging wear data, alloys A1 and A5 have shown high wear rates when the matrix microstructure is either coarse pearlite or spheroidized consistent with their low hardness (Table 5.67A and B). The resistance to wear improved in general in both these alloys when martensite is introduced into the microstructure by heat-treating them from 900°C (Tables 5.67A and B), the higher its volume fraction the better the resistance to wear as is evident from the data on the alloy A5 (Table 5.67B). It is significant to note that the microstructure corresponding to the best in terms of gouging wear is not fully martensitic but a combination of martensite + pearlite/bainite (containing fine dispersed carbides). Another factor contributing to a high wear resistance of the alloy A5 is the very favourable 'free' carbide morphology and dispersion (Fig. 5.18 f and i). On raising the Mn content to ~5% wear resistance of the lower and higher Cr alloys in general deteriorated and subsequently improved as the Mn content was further increased from ~5 to ~6% (Tables 5.67A and B). Similarly, except alloy A5, wear resistance exhibited by lower Cr alloys is in general better than the higher Cr alloys (Tables 5.67A and B). This has been appropriately discussed in the following sections.

It is significant to note that the wear resistance exhibited by A2, on being heat treated from 900°C

(microstructure not fully martensitic) [Table 5.67A], is exhibiting the trend observed in alloy A5 (Table 5.67B), thereby once again confirming that fully martensitic structures do not necessarily lead to high resistance to wear.

In the alloys A6 and A7, as the tendency towards forming fully martensitic structure increases, the resistance to wear decreases. This observation does not contradict the earlier contention that presence of martensite is useful in improving resistance to wear. Infact the conditions prevailing in the alloys A1, A2 and A5 are different from those in A6 and A7 as martensite in the former group of alloys does not contain dispersed carbides whereas that in A6 and A7 contains dispersed carbides. These are easily dug out because of their low adherency with the matrix and hence contribute little to improving the resistance to gouging wear. Their adverse effect is further reflected in the wear performance of alloy A3 in the heat treated condition during the initial stages (Table 5.67A, Fig.5.23b). However, the retention of some 'transformable' (Section 2.2.3.1) low-stability austenite in A3 has perhaps ensured that the resistance to wear improves with time (Table 5.67A) because of an increase in the hardness of the retained austenite either by work hardening or by its transformation[31,46]. The relatively inferior wear characteristics of A7 in comparison to A3 (Tables 5.67A and B) are perhaps due to a reduced possibility towards

austenite retention resulting from a low Mn/Cr ratio in the former.

In the alloy A4, although the amount of retained austenite (γ) is large and its stability high (unfavourable from the point of view of improving resistance to wear, being less transformable), its favourable location around carbides (Fig.5.17b) has contributed to a high resistance to wear even in the as-cast condition. The observation that the resistance to wear of the alloy A4 in the as-cast condition and heat-treated (containing less stable γ) conditions is similar (Table 5.67A) further tends support to the above inference. Of the two types of austenites mentioned above, controlled quantities of a less stable austenite may perhaps prove more useful in improving resistance to gouging wear, as the former is less stable. This becomes evident by comparing the wear data on alloys A3 and A4 (Table 5.67A).

Some improvement in the wear performance of A8 in comparison to A6 and A7 points to the possibility that the favourable conditions prevailing in alloys A3 and A4 in the heat-treated condition perhaps exist in the alloy A8 (Tables 5.67A and B). Wear data on alloy A8 further reflects that a microstructure consisting of dispersed carbides in an austenitic matrix may also prove useful in imparting high resistance to gouging wear (Fig.5.34 and Table 5.67B). Such a microstructure represents a useful combination of high

hardness and high toughness and hence the contention[130].

Summarising, the following important points emerge:

(i) A fully martensitic matrix does not necessarily impart high resistance to gouging wear.

(ii) Presence of relatively softer phases in combination with martensite can prove useful when the second phase is:

(a) Preferably bainite and containing fine dispersed carbides,

(b) 'transformable' austenite present in controlled quantities, and,

(c) stable austenite present in relatively larger amounts around free carbides.

(iii) A fully martensitic matrix would either prove most useful all by itself or when dispersed carbides, with poor adherency with the matrix, are absent.

(iv) High hardness is not a prerequisite to attaining a high resistance to wear.

Considering the erosion wear data (Table 5.69 and Figs.5.35-5.37), the best overall values have been observed in different alloys when they were heat-treated to attain maximum hardness i.e. in the range of 800-850 HV_{50} (Fig.5.36). This appears logical since best overall erosion resistance

will be associated with (i) high/maximum hardness and (ii) freedom from softer microconstituents. Consistent with this thinking, specimens of different alloys when heat treated to attain a hardness of 700-750 HV_{50} have shown the least overall wear resistance (Fig.5.37) because in most instances the specimens contained a softer phase i.e. austenite(γ). The wear behaviour of the as-cast microstructure falls in between the two situations stated earlier (i.e. one with maximum hardness and the one with intermediate hardness) with the alloys A3, A7 and A8 (i.e. alloys with some shear transformation product in the as-cast microstructures) exhibiting lower wear rates than the rest. An analysis of the data in Table 5.69 reveals that in most instances the resistance to erosion is high during the initial stages. This is perhaps due to work hardening of the samples during machining.

Summarising, thus, the presence of a softer microconstituent is found to be harmful from the point of view of erosion wear.

6.6 CRACK PROPAGATION

In the present study it has not been possible to pinpoint where the crack originated. However, it would not be incorrect to presume that it infact originates within the matrix at the interface between the matrix and carbide. Thereafter, it has not shown preference for the matrix.

as it has sheared dispersed carbides and cut across carbide plates lying in its path (Figs.5.29 and 5.30). Therefore, the belief that a 'discontinuous carbide' phase net work was likely to improve resistance to crack propagation by altering the fracture path is perhaps not valid.

Before drawing any firm conclusions on this and related aspects, it would be of interest to carry out crack propagation studies in the higher Cr alloys especially alloys A5 and A7 which exhibit very favourable 'free carbide' morphology and dispersion.

It has not been possible to explain the formation of secondary cracks. Absence of plastic deformation in the vicinity of an indentor impression (Fig.5.29a) has made it difficult to clarify the occurrence of secondary cracking.

6.7 CRITICAL REAPPRAISAL

Through this investigation, it has been possible to demonstrate that alloy combinations other than Ni-Cr and Cr-Mo can be usefully employed in attaining microstructures (M+discontinuous carbide with or without austenite) which are generally considered useful in imparting high resistance to wear. Different heat-treatments and alloy combinations to attain the desired level of hardness have been established. Similarly, optimum (i) Mn content at the two Cr levels, (ii) heat-treating temperature and (iii) heat-treating time to induce maximum hardening have been arrived at. Microstructural changes in the experimental alloys follow a logical

trend, are consistent with the changes in hardness/microhardness and can be satisfactorily explained on the basis of fundamental considerations.

A fuller interpretation of the microstructures was possible only with the help of microhardness measurements, scanning microscopy and X-ray diffractometry. Although the last mentioned technique proved extremely useful in deciding upon the nature of the matrix microconstituent (to assess whether martensite had formed), in detecting the presence of retained austenite particularly in cases where it was difficult to do so, and also in identifying the nature of the carbides formed to a major extent, it is opined that a more rigorous analyses would have helped in affirmatively concluding whether certain carbides (e.g. M_5C_2) were infact present or not. The problem arises since certain prominent reflections are common to more than one carbide. The difficulty arising thus can be resolved by selecting a carbide reflection corresponding to which a peak has perhaps occurred/expected to occur in the diffractogram and which is absent in other carbides, fixing a series of 2θ values close to the anticipated one, counting the number of impulses for a given length of time at each of the predecided 2θ values and finally plotting these impulses against the corresponding 2θ values to ascertain whether the peak existed.

Another method which could have proved useful is the selective etching technique.

The importance of microhardness measurements in helping to interpret microstructures cannot be overlooked as has been demonstrated in the present study. A possible source of error is that only a limited number of observations are recorded. This has been appropriately overcome in the present investigation.

THE EPM studies have provided an interesting insight into the 'ineffectivenss' of heat-treatment schedules in general in bringing about a change in the element distribution vis-a-vis the as-cast condition. Implications of this data in relation to alloy-design have been critically analysed. The importance of a higher Cr content in reducing the heterogeneity in Mn distribution is clearly brought out and is of special significance to the present study. The EPMA data has proved very helpful in predicting the alloy content within the matrix and the carbide phases in different alloys corresponding to heat-treatments inducing maximum hardening. The fundamental and practical implications of the EPMA data have been analysed.

Although wear studies have not been extensively carried out, the data obtained reveals a definite logical trend and provides useful information on the wear behaviour of different microstructures. The possible deduction that besides a fully martensitic matrix (minus dispersed carbides with poor adherency), a mixed microstructure (consisting of martensite +P/B) may prove useful in imparting good resistance

to gouging wear needs to be reinforced through further experimentation. The investigation reaffirms the beneficial effect of retained austenite in enhancing resistance to gouging wear. It is shown that whereas stable γ is beneficial only when favourably located, controlled quantities of less stable (transformable) austenite in general may prove more beneficial. Presence of softer microconstituents such as austenite, however, proved harmful from the point of view of erosion wear.

A study of the wear tracks would have proved useful in elucidating the role of matrix and free carbides in controlling gouging wear.

Finally, the 'crack propagation' studies have questioned the usefulness of 'discontinuous' free carbides in resisting crack propagation in brittle materials. Further experimentation is also needed in ascertaining the role of free 'dispersed' carbides (of the type attained in alloy A5) and 'discontinuous' carbides (of the type present in most of the experimental alloys and in Ni-hard irons) in controlling wear/crack propagation.

CHAPTER VII

CONCLUSIONS AND SUGGESTIONS FOR FUTURE WORK

7.1 CONCLUSIONS

Under the existing experimental conditions the following important conclusions emerged:

(1) Low cost elements Mn and Cu along with Cr can be advantageously employed in developing wear resistant alloy cast irons. An important feature of this study has been that Mn has been employed as a major alloying element and utilized in proportions much larger than hitherto employed.

(2) The above mentioned elements can be employed to produce a microstructure consisting of martensite+discontinuous carbide in the heat treated condition and martensite+retained austenite+discontinuous carbide in the as-cast condition.

(3) For attaining maximum hardening (800-850 HV_{50}) the optimum Mn content required is between 4 and 5%. . This range is independent of the Cr contents (~6-6.5% and ~9-9.5%.) of the experimental alloys. The higher Cr alloys are only marginally harder than the lower Cr alloys.

(4) The optimum heat-treating temperature and time to induce maximum hardening are 850°C and 6 hrs respectively.

(5) At the optimum heat-treating temperature of 850°C, ~5%. Mn alloy responded to hardening heat-treatment most

favourably at both the Cr levels.

(6) For obtaining maximum hardening at temperatures lower than 850°C a higher proportion of Mn and a larger soaking period are required at both the Cr levels e.g. at 800°C, the Mn content required is ~5% and a soaking period of (i) 8-10 hrs for lower Cr alloys and (ii) 6-8 hrs for higher Cr alloys.

(7) Presence of a higher Cr content was useful in sustaining a higher level of hardness at a heat-treating temperature of 850°C as the Mn content was raised from ~4 to ~6% and soaking period raised from 2 to 10 hrs. In the lower Cr alloys, high hardness was sustained only upto ~5% Mn independent of the soaking period.

(8) Heat treating temperature of 750°C proved ineffective in contributing to hardening.

(9) Hardness values obtained on heat treating from 900°C were in general lower than those obtained on heat-treating from 850°C. Further, the 900°C temperature was effective in inducing hardening only in a limited number of instances that too mostly in the higher Cr alloys, e.g. those containing ~4 and ~5% Mn.

(10) The effect of temperature and time on hardness in the lower and higher Cr alloys, as influenced by Mn content, followed a definite logical pattern. The data thus obtained can be explained on the basis of the partitioning of Mn and Cr into different phases at the heat treating temperature

and the transformation behaviour of austenite on air cooling from the heat-treating temperature to room temperature.

(11) Hardening in the alloys is attributed to the presence of a martensitic matrix. In most instances the martensitic matrix contained dispersed carbides.

(12) Martensite formed with relative ease at Mn contents around 4.5 to 5% or more at both Cr levels. Heat-treating temperatures higher than 800°C proved most useful in forming martensite at this Mn level.

(13) Austenite was retained in the heat treated microstructures at Mn concentrations 4.5-5% or higher.

(14) Free carbide is the hardest microconstituent in the experimental alloys (Microhardness 1000-2150 VPN). In addition to M_3C, the other carbides most frequently observed were M_7C_3 and M_5C_2.

(15) The presence of the two latter carbides contributed to an increase in the hardness of the carbide phase.

(16) EPMA studies revealed that heat treatment did not appreciably alter the distribution of Mn and Cr into the matrix and carbide phases vis-a-vis the as-cast condition. A higher Cr content proved useful in reducing the heterogeneity in Mn distribution in the as-cast state.

(17) Although the overall partition ratio $\frac{\text{Cr in carbide}}{\text{Cr in matrix}}$ for the lower Cr alloys was 3.6-3.9:1 and for the higher Cr alloys ~5.0:1 (i.e. more or less consistent with earlier

observations), a much larger proportion of Mn partitioned to the carbide phase than can be expected from an austenite-stabilizer i.e. the ratio $\frac{\text{Mn in carbide}}{\text{Mn in matrix}}$ was 1.5:1 in the experimental alloys.

(18) The amount of Cr and Mn in the matrix and the carbide phases corresponding to maximum hardening in A2(2h 850°C and 10h 850°C) was approximately 3.7 and 3% and 14-15% and 4.5% respectively. The corresponding figures for the alloy A3 (4h 800°C, 10h 800°C and 2h 850°C) were approximately 3.7-4% and 4-4.6% and 13.3-14.6% and 6.3-6.9% respectively.

Figures for the higher Cr alloy A6(2h 850°C) were approximately 5.3 and 3.3% and 30.0 and 4.8% respectively and that for alloy A7 (10h 800°C and 2h 850°C) approximately 5.1-6.4% and 4.2-4.3% and 26.0-30.0% and 6.1-6.5% respectively.

(19) From the point of view of gouging wear, in addition to the martensitic matrix, a matrix consisting of mixed microstructure i.e. a combination of martensite and another phase which is less harder than martensite (e.g. P/B), may prove very useful. This implied that maximum hardness was not a necessary precondition for obtaining the best in terms of gouging wear.

(20) From the point of view of erosion wear, presence of softer microconstituents was found to be harmful e.g.

a fully pearlitic matrix may prove better than a matrix containing martensite and austenite.

(21) Crack propagation path in the experimental alloys in the hardened condition is not preferential - cracking is likely to occur within the matrix, along the interface between the matrix and the carbide plates or within/across the carbide plates.

7.2 SUGGESTIONS FOR FUTURE WORK

Further work may be carried out on the following lines:

(a) construction of TTT/CCT curves for the experimental alloys,

(b) a detailed evaluation of the wear resistance of the experimental alloys as influenced by heat treatment and

(c) a detailed structural investigation by X-ray diffractometry.

REFERENCES

1. E.C. ROLLASON; 'Metallurgy for Engineers', Edward Arnold, London, 1961, pp.200-211.

2. H.T.ANGUS; 'Cast Iron-Physical and Engineering Properties', Butterworths, London, 1976, pp.161-253 and 286-310.

3. 'The Metallurgy of Cast Irons', Proc. of the 2nd Int.Symp., Geneva, Switzerland, May 29-31, 1974, Edit.B.lux Battelle, I.Minkoff and F.Mollard.

4. R.W.HEINE, C.R.LOPER and P.C.ROSENTHAL; 'Principles of Metal Casting', McGraw Hill, New York, 1967.

5. E.C.ROLLASON; 'Metallurgy for Engineers', Edward Arnold, London, 1961, p.258.

6. ASM Metals Hand Book, Vol.1, 8th Edition, ASM, Metals Park, Ohio, 1961.

7. ASM Metals Handbook, Vol.1, 9th Edition, ASM, Metals Park, Ohio, 1978,p.599.

8. Materials Handbook, ASM, Metals Park, Ohio, 1981,p.134. (also consulted Ref.7,pp.82, 86 and 87).

9. G.SANDOZ; 'The partitioning of alloying elements in malleable irons', NRL Report 5268, U.S.Naval Research Laboratory, Washington,D.C., Feb.1959, pp.1-25.

10. E.C.BAIN and H.W.PAXTON; 'Alloying Elements in Steels', ASM, Metals Park, Ohio,1962.

11. Metals Handbook; 'Metallography, Structures and Phase Diagrams', Vol.8, 1973, p.402-403 and 407-408.

12. R.A. HIGGIN; 'Engineering Metallurgy, Part 1,' The English University Press Ltd., London, pp.246-262.

13. J.W.BOYES; 'Development and use of an abrasion test for cast ironsand steels,' Iron and Steel, 42(1), Feb.1968,pp.57-63.

14. F.MARATRAY and R.USSEGLIONANOT; 'Atlas of Transformation Characteristics of Cr and Cr-Mo White Irons, Climax Molybdenum, S.A. Paris, 1970.

15. A.BASAK, J.PENNING and J.DILEWIJNS; 'Effect of Mn on wear resistance and impact strength of 12%. Cr white cast irons,' AFS International Cast Metals Journal, 6(3), 1981,pp.12-17.

16. 'Engineering Properties and Applications of Ni-Hard Cast Irons', International Nickel Co.INC, New York(old).

17. 'Engineering Properties and Applications of Ni-Hard Cast Irons', International Nickel Co.INC, New York,1978.

18. 'Standard Handbook of Lubrication Engineering', Ed. J.J.O'Connar, McGraw Hill, New York, 1968.

19. 'Friction, Wear and Lubrication Glossary', Organisation for Economic Co-operation and Development, Paris, France, 1969.

20. R.G.BAYER; 'Selection and use of wear tests for metals', ASTM Special Technical Publication 615, Jan 1977, pp.1-29.

21. E.RABINOWICZ; 'Friction and Wear of Materials', John Wiley and Sons, Inc., New York, London, Sydney, 1965,p.113.

22. 'Handbook of Mechanical Wear - Wear, Frettage, Pitting, Cavitation; Corrosion', Ed. by C.Lipson and L.V.Colwell, Ann Arbor, The University of Michigan Press, 1961.

23. H.S.AVERY; 'Surface protection against wear and Corrosion', Amer.Soc. for Metals, Cleveland, 1954, Chapter 3.

24. H.S.AVERY; Wear, 4, Nov.1961, pp.427-449.

25. H.H.UHLIG; 'Corrosion and Corrosion Control', John Wiley and Sons Inc., New York, London, 1971,p.10-13.

26. M.E.SIKORSKI; Wear, 7, 1964, pp.144-162.

27. E.RABINOWICZ; 'Friction and Wear of Materials', John Wiley and Sons, Inc., New York, London, Sydney,1965, pp.165-167.

28. V.J.COLANGELO and F.A.HEISER; 'Analysis of Metallurgical Failures', John Wiley and Sons, New York, 1973, pp.206-223.

29. A.KASAK, G.STEVEN and T.A.NEUMEYER; 'High Speed Tool Steels by P/M', Crucible Metal Research Centre, Colt Industry, Canada.

30. W.D.JONES; 'Fundamental Principle of Powder Metallurgy', Adward Arnold, London, 1960.

31. K.H.ZUMGAHR; 'How microstructure affects abrasive wear resistance,' Metal Progress, 116, Sep.1979, pp.46-52.

32. A.D.LAMB; 'Wear resistance of cast irons', BCIRA, CIBF Conf.paper, 1976 (10 pages).

33. N.PRASAD and S.D.KULKARNI; 'Relation between microstructure and abrasive wear of plain carbon steels', Wear, 63, 1980, pp.329-338.

34. A.K. PATWARDHAN; Personal Communication.

35. MEEHNITE METAL CPN and W.H.MOORE; U.S.Patent No.3042512, Filing Date July 3, 1962.

36. 'The Uses of Mo in Nodular Irons', Publ.Climax Molybdenum Co., New York, 1964, p.112.

37. Foundry, 73, Nov.1945, p.151. (Cross ref.of ref.13).

38. Meehanite Metal Cpn., British Patent No.832579, Filing Date Nov.19, 1957.

39. A.N. VOLKOV, V.B.LYADSKII and S.T.TESHAEY; Russian Castings Production, 1, Jan 1966, pp.8-10.

40. A.M.MAYURNIKOV, I.A.FOMICHEV and V.V.MAYURNIKOV; 'Influence of composition on abrasion wear resistance of Mn cast iron', Russian Castings Production, 3, March 1976, pp.103-104.

41. I.KATAVIC; 'Investigations into the influence of the structure of white cast irons on abrasive wear', Wear, 48, 1978, pp.35-53.

42. R.NIWA; 'Influence of Mn content on the mechanical properties, microstructure, and abrasion resistance in 28% Cr cast iron', Journal of the Japan's Foundrymen Society, 52(3), 1980, pp.135-140.

43. G.SANDOZ; 'Recent research in cast iron', Ed.H. Merchant, Gordon and Breach, New York, 1968, p.509.

44. K.H.ZUMGAHR and D.V.DOANE; 'Optimizing fracture toughness and abrasion resistance in white cast irons', Met. Trans., 11A(4),1980,pp.613-620.

45. N.F.FIORE, J.P.COYLE, S.P.UDVARDY, T.H.KOSEL and W.A.KONNEL; 'Abrasive wear microstructure interactions in a Ni-Cr white iron', Wear, 62,1980,pp.387-404.

46. K.ROHRIG; 'Gefuge und Bestanligkeit gogen Mineralverschluss cor.carbide schem gusseisen', Gisserei, 58,1971, pp.697-705(Cross ref.18 of ref.31).

47. K.H.ZUMGAHR; 'Friction and wear of a precipitation hardenable, austenitic steel under abrasive conditions', Z.Metallkunde, 68,1977,pp.381-389.

48. I.R.SARE; 'Abrasion resistance and fracture toughness of white cast irons', Metals Technology, 6(11), 1979, pp.412-419.

49. J.D.WATSON, P.J.MUTTON and I.R.SARE; 'Abrasive wear of white cast iron', Met ls Forum, 3(1), 1980,pp.74-78.

50. P.SINGH; 'Effect of heat treatment on the microstructure and wear characteristics of a white cast iron', P.G. Thesis, University of Roorkee,1981.

51. 'Successful application of 'Acicular', by Qualter, Hall and Company Ltd.,' Foundry Trade Journal,112,June 1962, p.703.

52. H.NOCKER and K.H.ZUMGAHR; 'Abrasive wear of cast iron with flake and nodular graphite', Arch.Eisenh, 49,1978, pp.155-160.

53. J.C.RICHARDSON; 'Selection and use of rolls in mini mills', SFAISI Quarterly, Jan 1981,pp.40-48, (also consulted-'Roll types and their usage' from Light Bar and Section Mill Technology-16').

54. D.N.STEFANESCU and S.CRACUM; 'Abrasion resistant cast irons alloyed with Cr and V', 42nd International Foundry Congress, Lisbon,1975, Paper No.18(11 pages).

55. S.PARENT SIMOUIN and J.M.SCHISSLER; 'Fe-C-Cr-V alloys. Present data on their abrasion', Proc. of the 4th Inter.Abrasion Colloquim, Grenoble, May 1979,pp.12.1-12.16.

56. O.YANAGESAWA and M.MARUYAMA; 'Formation of plate like cementite in steadite', Journal of the Japan Foundrymen's Society, 50, July 1978, pp.409-413.

57. R.S.JACKSON; JISI, 204, 1970,p.163.

58. R.NIWA; 'Effect of silicon on the mechanical properties microstructure and abrasion resistance of 28%. Cr cast iron', Journal of the Japan Foundrymen's Society, 50, 1978, pp.78-84.

59. A.K.Patwardhan; Personal Communication.

60. T.L.OBERLE; Journal of Metals, 3,1951,pp.438-439.

61. R.T.SPURR and T.P.NEWCOMBE; Proc. of Conf.on Lubrication and Wear, Instt.of Mech.Engrs., London,1957,pp.269-275.

62. M.M.KHRUSHOV and M.A.BABICHEV; Frict.Wear Mach.(U.S.S.R.), 17,1962, pp.1-8.

63. M.M.KHRUSHOV and M.A.BABICHEV; Ibid, 17,1972,pp.9-18.

64. M.M.KHRUSHOV and M.A.BABICHEV'; Ibid, 11,1956,pp.5-18.

65. M.M.KHRUSHOV; 'Resistance of metals to wear by abrasion, as related to hardness', Proc.of Conf.on Lubrication and Wear, Inst.of Mech.Engg., London, 1957,pp.655-659.

66. M.M.KHRUSHOV and M.A.BABICHEV; 'Research on wear of metals', NEL Trnl.No.893,1960,Chap.8.

67. R.C.D.RICHARDSON; WEAR,11,1968,p.265.

68. K.WELLINGER, H.HETZ and M.GURLEYIK; Wear,11,1968,p.173.

69. M.M.KHRUSHOV and M.A.BABICHEV; Friction and Wear Mach. (U.S.S.R.), 11,1956,pp.19-30.

70. M.M.KHRUSHOV and M.A. BABICHEV; 'Research on wear of metals', Izdat Akad.Nauk, Moscow, NEL Tranl., pp.889-893.

71. R.C.D.RICHARDSON; Journal of Agr.Engg.Research,12(1), 1967,pp.22-37.

72. R.C.D.RICHARDSON; 'The maximum hardness of strained surfaces and the abrasive wear of metals and alloys', Wear,10,(July-Aug.) 1967, pp.291-309 and 353-382.

73. R.C.D.RICHARDSON; 'The wear of metals by relatively soft abrasives', Wear,11,(April) 1968,pp.245-275.

74. E.HORNBOGEN; Z.Metallkunde, 68,1977, pp.455-469.

75. 'Nickel as an Alloy in Cast Iron', A.F.S.Current Information Report,1977,pp.1-16.

76. I.FUKUMOTO and SHIBATA; 'Ni and Cr present in primary crystal of alloy white iron', Jr. Japan Inst.of Metals, 22, 1959,p.538.

77. R.BARTON; BCIRA.J., 8, July 1960, pp.567-585.

78. E.R.EVANS; BCIRA.J., Research and Development, 4,Oct.1951, pp.86-139.

79. J.S.MARSH; 'Alloy of Iron and Nickel', I-Special-Purpose Alloys, McGraw Hill, London,1938,p.593.

80. J.G.PEARCE and K.BROMAGE; 'Copper in Cast Iron', Copper Development Association, London,1964,p.127.

81. J.W.GRANT; BCIRA.J., Research and Development, 1,Oct. 1946, pp.217-232, also Dec.1946,pp.245-258.

82. J.A.DILEWIJNS and A.L.deSY;'Influence of copper upon structure and mechanical properties of gray cast iron', Foundry Trade J., 123, July 13,1967, pp.37-44, also Aug.3, 1967,pp.153-161.

83. Founderie, 97, Feb.1954,pp.3825-2827.

TABLE 1.1 COMPOSITION AND PROPERTIES OF SOME REPRESENTATIVE PLAIN CARBON WHITE IRONS (2,6–8)

Sl No.	Type / Class / Designation	Composition					Hardness BHN	Micro-structure	Wear Rate* (relative)	Application
		TC	Si	Mn	S	P				
1	Pearlitic Iron	2.80	0.3	0.4	0.15	0.1–0.12	415–477	C + P	179.0	Grinding Balls
2	Unalloyed, low hardness Iron	3.0	0.75	0.25	0.4	0.12	320–440	C + P	–	Iron Rolls
3	Unalloyed high hardness Iron	3.5	0.5	0.25	0.4	0.12	440–520	C + P	–	Iron Rolls
4	Unalloyed chill Cast Iron	2.78	0.53	0.42	–	–	444 as-cast	Carbide in C.P.	174.0	—
5	Unalloyed Iron (Sand Cast)	3.05	0.4	0.5	—	—	444	C + P	122.0	Grinding Balls
6	Chill Cast unalloyed Iron	3.59	0.7	0.8	—	—	495	C + P	100.0	Grinding Balls
7	Pearlitic Iron	2.9	0.5	0.5	0.12	0.1	415–460	C + P	–	—
8	Cupola White Iron	3.2–3.6	0.4–1.0	0.5–0.7	0.15 max.	0.3 max.	400	C + P	–	—
9	Unalloyed high hardness alloys	3.2–3.8	0.4–0.8	0.3–0.7	0.1	0.2	380–600	C + P	–	—
		3.0–3.4	0.9–1.3	0.6–1.0	0.1	0.2	380–520	C + P	–	—

* Wear rates are relative to an assigned rate of 100 for Chill Cast Unalloyed Iron

PHYSICAL AND MECHANICAL PROPERTIES

1. Hardness (DPN)	410–520 (Sand Cast) 435–550 (Chill Cast) (abrasion resistant) 400 (L.C., 2.5 – 2.8 % C) 650 (H.C., 3.75 – 4.0 % C)
2. Tensile strength (ton / in^2)	15 –30 (Sand Cast) 18 –30 (Chill Cast) 16 – 18 (H.C., 3.0 – 3.5 % C) (Pearlitic, Hard) 18 – 30 (L.C., 2.75 – 2.9 % C) (Pearlitic, Tough)
3. Modulus of elasticity ($lb / in^2 \times 10^6$)	30 (Sand Cast, Chill Cast)
4. Transverse rupture stress 1.2 in bar, 12 in span (ton / in^2)	24 – 40 (Sand Cast) 33 – 47 (Chill Cast)
5. Transverse deflection	0.05 – 0.1 (H.C., 3.0 – 3.5 % C) 0.07 – 0.11 (L.C., 2.75 – 2.9 % C)
6. Specific gravity	7.6 – 7.8
7. Electrical resistivity (microhm / cm^3 at 78°F)	53 – 72
8. Impact strength (0.798 in dia machined from 0.875 in as-cast dia.) lft. lb.	6 – 11 (impact strength of white cast iron is about one third that of gray iron)
9. Thermal conductivity (Cal / cm^3 / s / °C)	0.035 – 0.076
10. Thermal expansion coefficient	
0 – 276 °C	$10 - 11 \times 10^{-6}$
276 – 684 °C	$15.9 - 16.4 \times 10^{-6}$
11. Yield strength	Usually not determined because of low ductility of white irons. The yield strength is considered to be close to the tensile strength.

70. M.M.KHRUSHOV and M.A. BABICHEV; 'Research on wear of metals', Izdat Akad.Nauk, Moscow, NEL Tranl., pp.889-893.

71. R.C.D.RICHARDSON; Journal of Agr.Engg.Research,12(1), 1967,pp.22-37.

72. R.C.D.RICHARDSON; 'The maximum hardness of strained surfaces and the abrasive wear of metals and alloys', Wear,10,(July-Aug.) 1967, pp.291-309 and 353-382.

73. R.C.D.RICHARDSON; 'The wear of metals by relatively soft abrasives', Wear,11,(April) 1968,pp.245-275.

74. E.HORNBOGEN; Z.Metallkunde, 68,1977, pp.455-469.

75. 'Nickel as an Alloy in Cast Iron', A.F.S.Current Information Report,1977,pp.1-16.

76. I.FUKUMOTO and SHIBATA; 'Ni and Cr present in primary crystal of alloy white iron', Jr. Japan Inst.of Metals, 22, 1959,p.538.

77. R.BARTON; BCIRA.J., 8, July 1960, pp.567-585.

78. E.R.EVANS; BCIRA.J., Research and Development, 4,Oct.1951, pp.86-139.

79. J.S.MARSH; 'Alloy of Iron and Nickel', I-Special-Purpose Alloys, McGraw Hill, London,1938,p.593.

80. J.G.PEARCE and K.BROMAGE; 'Copper in Cast Iron', Copper Development Association, London,1964,p.127.

81. J.W.GRANT; BCIRA.J., Research and Development, 1,Oct. 1946, pp.217-232, also Dec.1946,pp.245-258.

82. J.A.DILEWIJNS and A.L.deSY;'Influence of copper upon structure and mechanical properties of gray cast iron', Foundry Trade J., 123, July 13,1967, pp.37-44, also Aug.3, 1967,pp.153-161.

83. Founderie, 97, Feb.1954,pp.3825-2827.

70. M.M.KHRUSHOV and M.A. BABICHEV; 'Research on wear of metals', Izdat Akad.Nauk, Moscow, NEL Tranl., pp.889-893.

71. R.C.D.RICHARDSON; Journal of Agr.Engg.Research,12(1), 1967,pp.22-37.

72. R.C.D.RICHARDSON; 'The maximum hardness of strained surfaces and the abrasive wear of metals and alloys', Wear,10,(July-Aug.) 1967, pp.291-309 and 353-382.

73. R.C.D.RICHARDSON; 'The wear of metals by relatively soft abrasives', Wear,11,(April) 1968,pp.245-275.

74. E.HORNBOGEN; Z.Metallkunde, 68,1977, pp.455-469.

75. 'Nickel as an Alloy in Cast Iron', A.F.S.Current Information Report,1977,pp.1-16.

76. I.FUKUMOTO and SHIBATA; 'Ni and Cr present in primary crystal of alloy white iron', Jr. Japan Inst.of Metals, 22, 1959,p.538.

77. R.BARTON; BCIRA.J., 8, July 1960, pp.567-585.

78. E.R.EVANS; BCIRA.J., Research and Development, 4,Oct.1951, pp.86-139.

79. J.S.MARSH; 'Alloy of Iron and Nickel', I-Special-Purpose Alloys, McGraw Hill, London,1938,p.593.

80. J.G.PEARCE and K.BROMAGE; 'Copper in Cast Iron', Copper Development Association, London,1964,p.127.

81. J.W.GRANT; BCIRA.J., Research and Development, 1,Oct. 1946, pp.217-232, also Dec.1946,pp.245-258.

82. J.A.DILEWIJNS and A.L.deSY;'Influence of copper upon structure and mechanical properties of gray cast iron', Foundry Trade J., 123, July 13,1967, pp.37-44, also Aug.3, 1967,pp.153-161.

83. Founderie, 97, Feb.1954,pp.3825-2827.

84. J.G.PEARCE and K.BROMAGE; 'Copper in cast iron', Copper Development Association, London,1964,pp.41-43.

85. M.R.KRISHANDEV and I.LeMAY; 'Microstructure and Mechanical properties of a commercial low carbon Cu-bearing steel', JISI,208,1970,p.458.

86. S.K.GOEL; Ph.D.Thesis, Ent. 'Graphitization Characteristics and Mechanical Properties of Malleable Irons Alloyed with Cu', University of Roorkee, 1977.

87. W.E.DAY; 'Copper as an alloy in iron castings', Modern Castings, 42, Nov.1962, pp.87-98.

88. M.REISS, P.C.ROSENTHAL, C.R.LOPER and R.W.HEINE; 'Sn and Cu in malleable iron', AFS Transactions, 79,1971,p.565.

89. P.B. BURGESS; AFS Transactions, 71,1963,p.477.

90. G.E.MORTON; BCIRA. J., Research and Development, 6, Dec.1956, pp.436-443.

91. F.A. MOUNTFORD; 'The influence of nitrogen on the strength, soundness, and structure of gray cast iron', Brit Foundryman,59,April 1966, p.141-151.

92. E.R.EVANS; BCIRA.J., Research and Developments,5,Feb.1954, pp.145-159.

93. H.MORROGH; BCIRA.J., Research and Development,6, June 1957, pp.638-659.

94. E.R.EVANS; BCIRA.J., 8, May 1960,pp.340-342.

95. J.A.DAVIS,D.E.KRAUSE and H.W.LOWNIE; Modern Castings, 31, May 1957, pp.96-98.

96. J.W.BAMPFYLDE; BCIRA.J., Research and Development, 4, June 1952,pp.340-359.

97. A.K. PATWARDHAN; Personal Communication.

98. T.SRINIVASAN,A.K.PATWARDHAN and M.L.MEHTA; 'Effect of Mn and Cu additions on microstructure of Cr white cast iron', AFS Int.Cast Metals Journal, 2(1), 1977,pp.57-60.

99. A.S.SUDAN, M.L. MEHTA and A.K.PATWARDHAN; 'Evaluation of the role of Cu as an additive to a Cu-white iron for producing a wear resistant microstructure', Ibid, 5(1), 1980, pp.42-46.

100. A.K.PATWARDHAN, M.L. MEHTA and C.P.SHARMA; 'Mn as an additive to Cr white iron for producing wear resistant microstructure', Ibid, 6(1), 1981,pp.3-9.

101. B.K.JHA and P.K. SHARMA; 'Structural studies in Ni-hard4 and Cu-Mn-Cr white irons', B.E.Project Report, University of Roorkee, May 1978.

102. J.C.NAITHANI and S.K.NATH; 'Structural studies in Mn-Cu-Cr white irons', B.E. Project Report, University of Roorkee, June 1977.

103. A.K. PATWARDHAN; Personal Communication.

104. H.T.ANGUS; 'Cast Iron', Butterworths, London,1976, p.53.

105. R. CASTAING and A.GUINIER; Proc. of Inst.Int.Conf.on Electron Microscopy, Delft, 1949.

106. J.PHILIBERT and R.TIXIER; Brit.J., App.Phys., 19,1968, pp.685-694.

107. P.DUNCUMB and S.J.B.REED; 'Quantitative Electron Probe Microanalysis', NBS Special Publ., 298, Ed.by K.F.J. HEINRICH,1968, pp.133-154.

108. J.PHILIBERT; 'X-ray Optics and X-ray Microanalysis', Academic Press, New York, 1963,pp.379-392.

109. K.F.J.HEINRICH; 'Advan.X-ray Anal.', Plenum Press, New York,11,1968,p.40.

110. S.J.B.REED; Brit.J, Appl.Phys., 16, 1965,p.913.

111. T.O.ZIEBOLD and R.E.OGILVIE; Anal.Chem., 36,1964,p.322.

112. T.O.ZIEBOLD; 'Precision and sensitivity in electron microprobe analysis', Anal.Chem., 39,1967,p.858.

113. D.LAGUTTON, R.ROUSSEAU and F.CLAISSE; 'Computed alpha coefficients for electron microprobe analysis', Anal. Chem., 47, 1975,pp.2174-2178.

114. V.S.RAGHUNATHAN; Personal Communication.

115. J.D.BOLTEN, E.R.PETTY and G.B.ALLEN; 'The mechanical properties of α-phase low-carbon Fe-Mn alloy', Met.Trans., 2(10), 1971,p.2915.

116. C.H.WHITE and R.W.K.Honycombe; 'Structural changes during the deformation of high purity Fe-Mn-C alloys', JISI, 200, 1962,p.457.

117. R.BLOWER and G.MAYER; 'Precipitation hardenable stainless steels', I.S.I. Special Report.86, 1964,p.184.

118. E.C.BAIN and H.W.PAXTON; 'Alloying Elements in Steels', ASM, Metals Park, Ohio, 1962, p.183.

119. R.BROOK and A.R.ENTWISLE; JISI, 203, 1965,p.905.

120. A.R.MARDER and G.KRASS'; 'The morphology of martensite in iron carbon alloys', Trans.ASM Quart.60, 1967,p.651.

121. R.H.ABORN; Trans.ASM, 48, 1959,p.51.

122. K.J.IRVINE, F.B.PICKERING and J.GARSTONE; JISI, 196, 1960,p.60.

123. H.T.ANGUS; 'Cast Iron-Physical and Engineering Properties', Butterworths, London,1976, p.50.

124. M.S.KOVALCHENKO and YU.E.ROGOVOI; Poroshovaya, Metallurgia, 2, 1971,p.93.

125. H.J.GOLDSCHIMIDT; 'Interstitial Alloys', Butterworths, London,1967, p.94.

126. T.Ya.KOSOLAPOVA; 'Carbides-properties, production and applications', Plenum Press, New York, London,1971, pp.1-50.

127. Metals Reference Book, Ed.by C.J.SMITHELLS and E.A.BRANDES; Butterworths, London, and Boston,1976, p.865, and 874.

128. E.OROWAN; Symp.on Internal Stresses in Metals and Alloys, 1948, p.451.

129. A.De Sy; 'Alloyed grey cast irons for machine components', Modern Castings, 41, June 1962, p.62.

130. A.K.PATWARDHAN; Personal Communication.

131. T.NISHIZAWA; 'Thermodynamic Study of Fe-C-Mn, Fe-C-Cr and Fe-C-Mo Systems', Ph.D.Thesis, Swedish Institute for Metals Research, Stockholm.

TABLE. 1.1 COMPOSITION AND PROPERTIES OF SOME REPRESENTATIVE PLAIN CARBON WHITE IRONS (2,6–8)

Sl No.	Type / Class / Designation	Composition					Hardness BHN	Micro-structure	Wear Rate* (relative)	Application
		TC	Si	Mn	S	P				
1	Pearlitic Iron	2.80	0.3	0.4	0.15	0.1–0.12	415–477	C + P	179.0	Grinding Balls
2	Unalloyed, low hardness Iron	3.0	0.75	0.25	0.4	0.12	320–440	C + P	–	Iron Rolls
3	Unalloyed high hardness Iron	3.5	0.5	0.25	0.4	0.12	440–520	C + P	–	Iron Rolls
4	Unalloyed chill Cast Iron	2.78	0.53	0.42	–	–	444 as-cast	Carbide in C.P.	174.0	–
5	Unalloyed Iron (Sand Cast)	3.05	0.4	0.5	–	–	444	C + P	122.0	Grinding Balls
6	Chill Cast unalloyed Iron	3.59	0.7	0.8	–	–	495	C + P	100.0	Grinding Balls
7	Pearlitic Iron	2.9	0.5	0.5	0.12	0.1	415–460	C + P	–	–
8	Cupola White Iron	3.2–3.6	0.4–1.0	0.5–0.7	0.15 max.	0.3 max.	400	C + P	–	–
9	Unalloyed high hardness alloys	3.2–3.8	0.4–0.8	0.3–0.7	0.1	0.2	380–600	C + P	–	–
		3.0–3.4	0.9–1.3	0.6–1.0	0.1	0.2	380–520	C + P	–	–

* Wear rates are relative to an assigned rate of 100 for Chill Cast Unalloyed Iron

PHYSICAL AND MECHANICAL PROPERTIES

1. Hardness (DPN)	410–520 (Sand Cast) 435–550 (Chill Cast) (abrasion resistant) 400 (L.C., 2.5 – 2.6 % C) 650 (H.C., 3.75 – 4.0 % C)
2. Tensile strength (ton / in^2)	15 –30 (Sand Cast) 18 –30 (Chill Cast) 16–18 (H.C., 3.0 –3.5 % C) (Pearlitic, Hard) 18 –30 (L.C., 2.75 – 2.9 % C) (Pearlitic, Tough)
3. Modulus of elasticity ($lb / in^2 \times 10^6$)	30 (Sand Cast, Chill Cast)
4. Transverse rupture stress 1.2 in bar, 12 in span (ton / in^2)	24 – 40 (Sand Cast) 33 – 47 (Chill Cast)
5. Transverse deflection	0.05 – 0.1 (H.C., 3.0 – 3.5 %C) 0.07 – 0.11 (L.C., 2.75 – 2.9 %C)
6. Specific gravity	7.6 – 7.8
7. Electrical resistivity (microhm / cm^3 at 78°F)	53 – 72
8. Impact strength (0.798 in dia machined from 0.875 in as-cast dia.) (ft. lb.)	6 –11 (impact strength of white cast iron is about one third that of gray iron)
9. Thermal conductivity (Cal / cm^3/s/°C)	0.035 – 0.076
10. Thermal expansion coefficient	
0 – 276 °C	10 – 11 x 10^{-6}
276 – 684 °C	15.9 – 16.4 x 10^{-6}
11. Yield strength	Usually not determined because of low ductility of white irons. The yield strength is considered to be close to the tensile strength.

TABLE 1.2

COMPOSITION AND PROPERTIES OF SOME REPRESENTATIVE CHROMIUM WHITE IRONS[2,6-8]

Sl. No.	Type/class/ Designation	Composition						Hardness BHN
		T.C.	Si	Mn	Cr	P	S	
1.	Cupola white iron(1%.Cr)	3.30-3.60	0.40-1.0	0.5-0.70	0.80- 1.00	0.3(Max)	0.15(Max)	444
2.	High Cr white iron	2.25-2.85	0.25-1.0	0.5-1.25	24.00-30.00	0.4(Max)	0.15(Max)	500
3.	Pearlitic	3.3	0.5	0.5	1.0	0.20	0.12	444
4.	Sand cast** Pearlitic white iron	3.2-3.5	-	-	1.2	-	-	-
5.	Plain Cr white iron	3.50	0.5	0.5	1.0	0.30	0.12	444-477
6.	Plain Cr white iron	3.20	0.6	0.5	2.0	0.15	0.15	477-555
7.	Low Cr Iron (chill cast)	3.20	1.7	0.4	0.9	-	-	477
8.	Low Cr iron (sand cast)	3.00	0.9	0.6	0.8	-	-	477
9.	Sand cast 5%. Cr Iron	3.65	0.6	0.6	5.0	-	-	514
10.	Pearlitic Cr-iron	3.00	0.6	0.5	2.0	0.10	0.15	-
11.	30%. Cr	2.5-2.9	0.33-0.65	0.6-0.8	28.00-33.00	0.10	0.10	340-420

**Transverse strength(kg)	Deflection (mm)	Toughness (kgm)
635-815	2.0-2.3	1.27-1.87

TABLE 1.3

COMPOSITION OF Cr-X TYPE ABRASION RESISTANT ALLOY CAST IRONS[2,6-8]

Sl. No.	Type/Class/ Desgination	Composition								Hardness BHN	Micro-structure
		T.C.	Si	Mn	Cr	Mo	S	P	Other element		
1.	ASTM A-532-750 II Grade 1	3.1-3.6	0.3-0.8	0.4-0.9	14.0-18.0	2.5-4.5	0.06 Max	0.1 Max	0.5 Ni	-	-
2.	II Grade 2	2.4-3.1	0.3-0.8	0.4-0.9	14.0-18.0	2.5-3.5	0.06 Max	0.1 Max	0.5 Ni	-	-
3.	III Grade 2	2.3-3.0	0.2-1.5	1.5 Max	24.0-28.0	0.06 Max	0.06 Max	0.1 Max	0.5 Ni	-	-
4.	Martensitic 15% Cr, H.C.	3.25	0.6	0.7	15.0	3.0	0.03	.06	-	600-750	M.A.
5.	Martensitic 27% Cr	2.75	0.7	0.7	27.0	0.5	0.03	.06	-	653	-
6.	Martensitic 15% Cr, 3% Mo	2.75	0.7	0.7	15.0	3.0	0.03	.06	-	712	-
7.	Sand cast	2.8-3.4	-		12-16	2.4	-	-	-	-	-
8.	Sand cast	3.5-4.1	-	-	12-16	2.5-3.0	-	-	-	-	-
9.	Chill cast martensitic	3.2-3.4	-	-	12-16	1.5-3.0	-	-	-	-	-
10.	Chill cast martensitic	3.5-4.1	-	-	12-16	2.5-3.0	-	-	-	-	-
11.	12-18% Cr, 2-4% Mo	3.0-4.0	0.4-1.0	0.5-0.9	12-18	2-4	0.06	0.1	-	600-950 VPN	-

Continued

Table 1.3 continued

Properties of cast iron from sl. no.5 to 10

Sl. No.	Type/Class/Designation	Wear rate relative to pearlitic iron*			
		Crushing plant chute liners	Ball Mill end liners	Akin classifier wear shoes	Flotation impellers
5.	Martensitic 27% Cr	70	49	48	27
6.	Martensitic 15% Cr,3% Mo	51	44	44	-
		Transverse strength (kg)		Deflection (mm)	Toughness** kgm
7.	Sand cast	1015-1370		3.2-3.6	3.25-4.93
8.	Sand cast	800-1000		2.0-2.8	1.60-2.8
9.	Chill cast Martensitic	1980-2300		5.1-6.5	10.1-15.0
10.	Chill cast martensitic	1270-1570		3.6-3.8	4.57-5.9

* The pearlitic white iron (3.3%.C, 0.5%.Mn, 0.5% Si, 1.0%.Cr, 0.12%.S, 0.2%.P) had a nominally assigned relative wear rate of 100 in each application. The other wear rates are relative to this rate of 100 for the pearlitic white iron

** Data from as cast 30.5 mm dia. test bars broken over a 457 mm span. Relative toughness evaluated as product of transverse strength.

TABLE 1.4

Cr-X-Y-TYPE ABRASION RESISTANT ALLOY CAST IRONS[2,6-8]

	Type/Class/Designation	Composition								
		T.C.	Si	Mn	Cr	Mo	Cu	Ni	S	P
1	A/II/ 12% Cr	2.4-2.8	1.0	0.5-1.5	11.0-14.0	0.5-1.0	1.2	0.5	0.06	0.1
2	B/II/15%.Cr-Mo-L.C.	2.4-2.8	1.0	0.5-1.5	14.0-18.0	1.0-3.0	1.2	0.5	0.06	0.1
3	C/II/15%.Cr-Mo-H.C.	2.8-3.6	1.0	0.5-1.5	14.0-18.0	2.3-3.5	1.2	0.5	0.06	0.1
4	D/II/20%.Cr-Mo-L.C.	2.0-2.6	1.0	0.5-1.5	18.0-23.0	1.5	1.2	1.5	0.06	0.1
5	E/II/20%.Cr-Mo-H.C.	2.6-3.2	1.0	0.5-1.5	18.0-23.0	1.0-2.0	1.2	1.5	0.06	0.1
6	A/III/25%. Cr.	2.3-3.0	1.0	0.5-1.5	23.0-28.0	1.5	1.2	1.5	0.06	0.1
7	Martensitic-Cr-Mo iron*	2.0-3.6	1.0	0.5-1.5	11.0-23.0	0.5-3.5	1.2	1.5	0.06	0.1
8	ASTM** A-532-750 III Grade 1	2.3-3.0	0.2-1.5	1.5 (maxm.)	24.0-28.0	0.6	-	1.2	0.06	0.1

* Structure: Martensite/Austenite

** Hardness : 400 BHN (as-cast)
550 BHN (hardened)

TABLE 1.5 CHEMICAL ANALYSIS AND PROPERTIES OF NI-HARD

	TYPE 1-REGULAR (ASTM A 532 1-A)		TYPE 2-HI-STREN. (ASTM A 532 I-B)		TYPE 3 (ASTM A532 I-C)		TYPE 4 (ASTM A 532 I-D)	
CHEMICAL ANALYSIS, %								
TOTAL CARBON	3.0 – 3.6		2.90 max		2.9 – 3.7		2.5 – 3.6	
SILICON	0.8 max		0.8 max		0.8 max		1.0 – 2.2	
MANGANESE	1.3 max		1.3 max		1.3 max		1.3 max	
SULFUR	0.15 max		0.15 max		0.15 max		0.15 max	
PHOSPHORUS	0.30 max		0.30 max		0.30 max		0.10 max	
NICKEL	3.3 – 5.0		3.3 – 5.0		2.7 – 4.0		5.0 – 7.0	
CHROMIUM	1.4 – 4.0		1.4 – 4.0		1.1 – 1.5		7.0 – 11.0	
ENGINEERING PROPERTIES	SAND CAST	CHILL CAST	SAND CAST	CHILL CAST	SAND CAST	CHILL CAST	SAND CAST	CHILL CAST
BRINELL HARDNESS, MINIMUM	550	600	550	600	550	600	550	550
TRANS. STRENGTH, 1.20" DIA. TEST BARS, 12" SPAN, lb.	4000 to 5000	4500 to 6800	4500 to 5500	5500 to 7000			5000 to 6000	5500 to 7000
TRANS. DEFL., 1.20" DIA. TEST BARS, 12" SPAN, in.	0.080 to 0.110	0.080 to 0.120	0.100 to 0.120	0.100 to 0.120			0.08 to 0.11	0.10 to 0.15
TENSILE STRENGTH, 1.20" DIA. TEST BARS, psi	40 to 50,000	50 to 60,000	45 to 55,000	60 to 75,000			75 to 85,000	80 to 110,000
MODULUS OF ELASTICITY, million psi	24-26	24-26	24-26	24-26			24-26	24-26
IZOD AB IMPACT, ft-lb	20-30	25-40	25-35	35-55			35-45	35-45

TABLE 1.6 - COMPOSITION PROPERTIES AND APPLICATIONS OF VARIOUS Cr-Ni WHITE CAST IRONS (2,6-8)

Sl. No.	Type/Class/ Designation	COMPOSITION T.C.	Si	Mn	Cr	Ni	S	P	Other element	Hardness	
1	Martensitic Ni-Cr	3.2	0.5	0.6	2.0	4.5	0.12	0.2	—	601 BHN	Wear rate relative to Pearlitic White Iron: Ball mill end liner 55; Akin classifier shoe 80
2	Martensitic Ni-Cr	3.2	0.5	0.6	2.0	4.5	0.12	0.2	—	550-650 BHN	Microstructure: MA; Application: Mill liners
3	Martensitic Ni-Cr	3.5	0.5	0.6	2.0	3.0	0.12	0.1	1.0 Mo	600-650 BHN	MA — Mill liners
4	Martensitic Ni-Cr	3.2	0.5	0.3	1.4	3.5	0.15	0.2	—	555-627 BHN	— Grinding balls
5	L.C. White Iron	2.2-2.8	1.0-1.6	0.2-0.6	1.0	1.5	0.15	0.15	0.5 Mo	—	CP (as-cast)
6	H.C.&L.Si, White Iron	2.8-3.6	0.3-1.0	0.3-2.0	3.0	2.5	0.15	0.3	1.0 Mo	—	CP (as-cast)
7	Martensitic Ni-Cr Iron	2.5-3.7	0.8	1.3	1.1-4.0	2.7-5.0	0.15	0.3	1.0 Mo		MA
8	Alloyed hardest type	3.4	0.6	0.3	1.25	4.5	0.1	0.35	0.4 Mo	690-830 VPN	Precise hardness obtained will depend on specific composition & section size
9	Alloyed Intermediate hardness	3.4	0.8	0.3	0.6	2.5	0.1	0.35	0.4 Mo	610-690 VPN	
10	Chill Cast Ni-Cr iron	2.85	0.56	0.48	0.98	1.67	—	—	—	600 BHN	Micro-structure: Carbides in Fine Pearlite; Wear rate (Relative): 134
11	Chill Cast Ni-Cr iron	2.83	0.60	0.50	1.33	2.2	—	—	—	627 BHN	Carbides in very fine Pearlite: 124
12	Chill Cast Ni-Cr iron	2.87	0.60	0.50	1.55	2.54	—	—	—	600 BHN	Carbides in Martensitic matrix: 59
13	Chill Cast Ni-Cr iron	3.79	0.55	0.50	1.49	2.61	—	—	—	744 BHN	Carbides in Martensitic matrix: 54
14	Martensitic Ni-Cr iron	2.8	0.5	0.3	1.4	2.5	0.15	0.1	—	—	Relative wear rate 106 (Where Martensitic forged steel — (0.8 % C, 0.3 % Si, 0.7 % Mn, 0.2 % Cr, 0.2 % Mo, 0.03 % S, 0.01 % P) had a nominally assigned relative wear rate of 100
15	ASTM A-532 -750 I Grade 1	3.0-3.6	0.3-0.8	0.3-0.8	1.4-2.5	3.3 5.0	0.15	0.3	0.75 Mo	500 SC 600 CC	BHN
16	ASTM A-532 -750 I Grade 2	2.5-3.0	0.3-0.8	0.3-0.8	1.4-2.5	3.3-5.0	0.15	0.3	0.75 Mo	450 SC 500 CC	BHN
17	ASTM A-532 -750 I Grade 3	2.9-3.7	0.3-0.6	0.2-0.5	1.1-1.5	2.7-4.0	0.15	0.3	0.75 Mo	525 SC 600 CC	BHN

SC-SAND CAST, CC-CHILL CAST

(a) Where a single value is given rather than a range that value is a maximum limit.
(b) CP-Coarse Pearlite MA-Martensite Austenite

PHYSICAL AND MECHANICAL PROPERTIES

1	Specific gravity	7.6-7.8 (Ni-Cr Martensitic white cast iron)
2	Coefficient of thermal expansion (Micro-in. per in. per °F 0-430 °C	8-9 x 10^{-6} (2.5-4.75 % Ni, H.C. 3-3.5 % C)
	0-95 °C	12.2-14.2 x 10^{-6} (2.5-4.75 % Ni, L.C. 2.75-2.9 % C)
3	Electrical resistivity microhm / cm^3 at 78 °F	80-100
4	Modulus of elasticity lb / in^2 x 10^6	24-26 (2.5-4.75 % Ni, 2.75-3.5 % C)
5	Tensile strength, ton / in^2	16-17 (2.5-4.75 % Ni, H.C. 3-3.5 % C)
		21-36 (2.5-4.75 % Ni, L.C. 2.75-2.9 % C)
6	Hardness (DPN)	590-800 (2.5-4.75 % Ni, H.C. 3-3.5 % C)
		550-650 (2.5-4.75 % Ni, L.C. 2.75-2.9 % C)
7	Transverse rupture stress ton / in^2	31-53 (H.C. 2.5-4.75 % Ni)
		35-55 (L.C. 2.5-4.75 % Ni)
8	Transverse deflection (1.2 in bar, 12 in span) in.	0.08-0.11 (H.C. 2.5-4.75 % Ni)
		0.1-0.12 (L.C. 2.5-4.75 % Ni)

TABLE 2.1 - EFFECT OF ALLOYING ELEMENTS PREFERRED IN WHITE CAST IRONS

Sl. No.	ELEMENT	α-STABILIZER	γ-STABILIZER	GRAPHITIZER	CARBIDE FORMING TENDENCY	CHILL	HARDENABILITY	EUTECTOID TEMP.	PARTITIONS	OTHER EFFECTS / APPLICATION
1	Cr	✓	—	—	STRONG	(Strong) ↑	↑	↑	MOSTLY TO CARBIDE	(1) EUTECTIC C ↓ (2) T.S. ↑ (3) HARDNESS ↑ (4) PREVENTS FREE FERRITE (5) MACHINABILITY ↓ (6) RESISTANT TO CORROSION ↑ (7) REFINES PEARLITE & HARDENS (8) IMPROVES WEAR RESISTANCE (9) RESISTS OXIDATION AT HIGH TEMPERATURES
2	Mn	—	STRONG	—	MILD Cr>Mn >Fe	↑	↑ Markedly at low Cost	↓	NOT ESTABLISHED MORE IN γ	(1) DEOXIDIZER (2) RETARDS $\gamma \rightarrow \alpha$ TRANSFORMATION (3) REFINES PEARLITE AND HARDENS (4) INDUCES AIR HARDENING CHARACTER (IF >1.8 %) (5) EXPECTED TO IMPROVE WEAR RESISTANCE
3	Cu	—	MILD	MILD (0.2 - 0.35 OF Si)	—	↓ (UPTO ~4 %) ↑ (IF > 4 %)	↑ WHEN IN SOLUTION	↓	MOSTLY TO AUSTENITE	(1) SOLUBILITY LIMITED UPTO ~ 3.5 % (PPT IF MORE) (2) EUTECTIC C ↓ (3) REFINES PEARLITE & HARDENS (4) FLUIDITY ↑ (5) FERRITE HARDENER (6) T S ↑ (7) SUPPRESSES FREE FERRITE FORMATION (8) RESISTANT TO CORROSION ↑ (9) PEARLITE FORMER & STABILIZER (10) INDIRECTLY IMPROVES WEAR RESISTANCE
4	Ni	—	STRONG	MILD (0.3 OF Si)	LESS THAN Fe	↓ (1/4 OF Si)	MILD	↓	MAINLY TO AUSTENITE	(1) FLUIDITY ↑ (2) EUTECTIC C ↓ (3) TRANSFORMATION RATE ↓ (4) T S ↑ (5) MACHINABILITY IMPROVES (6) REFINES PEARLITE AND HARDENS (7) FREE FERRITE FORMATION ↓ (8) CORROSION RESISTANCE ↑ (9) HARDNESS ↑ (10) PROMOTES PEARLITE FORMATION (11) IMPROVES WEAR RESISTANCE
5	Mo	✓	—	—	STRONG	↑ (MILD)	↑	↑	MOSTLY TO CARBIDE	(1) REFINES PEARLITE AND HARDENS (2) PROMOTES FORMATION OF MARTENSITE (3) SUPPRESSES PEARLITE FORMATION (4) T S ↑ (5) PEARLITE PROMOTER (POWERFUL) (6) IMPROVES WEAR RESISTANCE
6	V	✓	—	—	VERY strong	↑	↑	↑	MAINLY TO CARBIDE	(1) REFINES PEARLITE AND HARDENS (2) EUTECTIC C ↓ (SLIGHTLY) (3) IMPROVES WEAR RESISTANCE (4) T S ↑ (5) PROMOTES PEARLITE FORMATION
7	Si	✓	—	STRONG	negative	↓ (Restrains Strongly)	↓	↑	MAINLY TO AUSTENITE	(1) EUTECTIC C ↓ (2) FLUIDITY ↑ (3) PROMOTES PEARLITE FORMATION (4) PRODUCES FERRITE AND SOFTENS
8	S	—	—	—	—	↑	—	—	—	(1) INDUCES HOT SHORTNESS (2) LOWERS SHOCK RESISTANCE (3) SHOULD BE LOW IN ABRASION RESISTANT C.I.
9	P	—	—	MILD	NIL	↓	↑	—	—	(1) PHOSPHIDE EUTECTIC INDUCES EMBRITTLING EFFECT (2) TOUGHNESS ↓ (3) KEPT BELOW 0.3 % IN WHITE IRONS

↑ — INCREASES

↓ — DECREASES

TABLE 4.1

CHEMICAL ANALYSIS† OF RAW MATERIALS

Raw material	C	Si	P	S	Mn	Cr
Pig iron	3.55	2.15	0.40	0.050	1.12	-
Ferro-chromium (Low Carbon)	0.10 max.	0.70 max.	0.03 max.	0.010 max.	-	67.00-75.00
Ferro-manganese (Low Carbon)	0.03 max.	-	0.03 max.	0.008	97.00	-
Ferro-silicon (Low Carbon)	0.03 max.	75.00	-	-	-	-

† weight percent

TABLE 4.2

CHEMICAL ANALYSIS† OF ALLOYS

Alloy	C	S	P	Si	Mn††	Cr††	Cu††
A1	3.393	0.0521	0.103	1.90	~3.0	~6.0	~1.0
A2	3.233	0.0340	0.107	1.97	~4.0	~6.0	~1.0
A3	3.140	0.0338	0.112	1.92	~5.0	~6.0	~1.0
A4	3.088	0.0323	0.121	1.85	~6.0	~6.0	~1.0
A5	3.158	0.0296	0.090	2.25	~3.0	~9.0	~1.0
A6	3.189	0.0269	0.086	2.30	~4.0	~9.0	~1.0
A7	3.203	0.0271	0.164	2.16	~5.0	~9.0	~1.0
A8	3.127	0.0274	0.143	2.09	~6.0	~9.0	~1.0

† weight percent

†† Nominal amount

TABLE 4.3

RELATION BETWEEN IMPRESSION DIAMETER* AND MICROHARDNESS

Dia. (micron)	VPN	Dia. (micron)	VPN
55	340	37	755
54	352	36	795
53	367	35	840
52	380	34	890
51	395	33	950
50	412	32	1010
49	428	31	1075
48	447	30	1140
47	466	29	1230
46	486	28	1320
45	508	27	1420
44	532	26	1530
43	557	25	1650
42	585	24	1800
41	612	23	1950
40	645	22	2140
39	680	21	2350
38	715	20	2580

* Objective magnification X40

TABLE 4.4

SIEVE ANALYSIS OF SAND
USED IN SLURRY POT TEST

Sl. No.	Screen aperture (microns)	Wt.%
1.	+600	0.8
2.	-600+425	2.9
3.	-425+300	26.3
4.	-300+212	0.6
5.	-212+180	27.3
6.	-180+150	17.1
7.	-150+120	15.2
8.	-120+106	6.3
9.	-106	3.5

TABLE 5.1

EFFECT OF HEAT-TREATING TEMPERATURE AND TIME ON HARDNESS OF ALLOY A1
As-cast hardness: 603 HV_{50}

Temp. °C	Hardness HV_{50}									
	2 hrs		4 hrs		6 hrs		8 hrs		10 hrs	
750	557 544 552 554 560 568 565	557	554 557 563 546 536 546 563	552	554 557 560 554 549 544 546	552	563 513 531 544 531 526	535	538 541 538 538 531 536	537
800	610 603 610 603 619 591 594	604	600 594 588 597 616 619	602	607 603 619 613 607 613 607	610	607 603 597 603 619 616 623	610	610 607 600 603 610 616 613	608
850	607 596 610 610 616	608	625 616 628 646 625	628	649 616 625 631 625	629	652 631 640 625 631	636	646 616 640 640 631	635
900	631 646 631 634 649	638	649 643 640 646 640	644	637 640 646 652 655	646	655 640 634 634 643	641	643 646 655 655 646	649

TABLE 5.2

EFFECT OF HEAT-TREATING TEMPERATURE AND TIME ON HARDNESS OF ALLOY A2

As-cast hardness: 625 HV_{50}

Temp. °C	Hardness HV_{50}									
	2 hrs		4 hrs		6 hrs		8 hrs		10 hrs	
750	546 552 544 549 541 544 549	546	546 531 538 528 536 549 544	539	518 538 531 513 526 531 536 518	526	546 521 502 513 531 511 526 518	522	526 513 528 523 521 526 526 528	524
800	616 613 631 634 613 631 616	622	607 625 619 625 619 622 625	620	640 607 619 607 610 604 613	614	646 652 649 637 631 628 631	639	659 652 637 659 655 640 662	652
850	849 858 804 800 778 818	818	812 812 826 802 836 821 818 793	815	802 802 766 788 793 797	791	841 793 797 766 797 793	798	844 840 795 826 831 826	827
900	682 682 688 695 702	690	720 682 702 702 709	703	731 717 728 731 739	729	778 754 747 724 747	750	800 795 791 795 800	796

TABLE 5.3

EFFECT OF HEAT-TREATING TEMPERATURE AND TIME ON HARDNESS OF ALLOY A3

As-cast hardness : 637 HV_{50}

Temp. °C	Hardness HV_{50}									
	2 hrs		4 hrs		6 hrs		8 hrs		10 hrs	
750	565 546 544 552 544	550	533 560 546 536 541	543	544 538 536 526 521	533	531 521 531 533 528	529	531 536 513 536 544 528	531
800	724 696 688 700 757 724	715	775 766 775 775 757 696	757	779 775 793 802 812 802	794	821 818 812 851 788 836	821	822 817 831 863 800	827
850	846 826 812 802 812 841	823	851 826 821 821 836 831	831	826 804 822 844 844	828	826 818 807 821 797 821 818	815	831 818 793 841 851 826	827
900	724 747 747 739 735	738	758 754 758 731 728	746	791 747 758 747 731	755	747 750 770 731 739	747	762 758 762 754 762	760

TABLE 5.4

EFFECT OF HEAT-TREATING TEMPERATURE AND TIME ON HARDNESS OF ALLOY A4

As-cast hardness: 593 HV_{50}

Temp. °C	Hardness HV_{50}				
	2 hrs	4 hrs	6 hrs	8 hrs	10 hrs
750	619 625 634 630 631 643	640 652 662 656 659 665	668 678 643 666 665 678	672 662 665 663 655 662	665 643 678 665 662 678
800	747 762 647 747 724 754	770 774 770 777 787 783	800 800 795 799 804 795	802 793 802 797 807 788 788	822 835 791 800 783 770
850	708 704 696 700 700 692	750 758 758 756 754 762	804 770 791 788 787 787	804 791 800 799 800 800	795 795 791 793 795 791
900	711 685 692 695 708 677	695 662 685 684 688 688	682 678 678 681 668 699	717 695 692 696 699 675	728 696 728 727 740 732 736

TABLE 5.5

EFFECT OF HEAT-TREATING TEMPERATURE AND TIME ON HARDNESS OF ALLOY A5

As-cast hardness : 539 HV_{50}

Temp. °C	Hardness HV_{50}				
	2 hrs	4 hrs	6 hrs	8 hrs	10 hrs
750	506 499 493 491 483 479 488	502 490 490 495 493 497 495	479 493 464 481 479 483 490	499 493 490 493 488 495 493	502 483 490 487 479 481 486
800	565 560 571 563 565 554 563	585 591 594 594 585 610 597	580 585 591 586 597 580 582	594 600 588 598 603 591 610	580 585 549 576 591 557 591
850	643 655 688 654 655 631	652 649 646 641 622 637	643 652 655 658 678 662	678 688 672 665 655 634	652 662 616 649 662 652
900	602 599 607 604 596 616	631 640 624 633 643 625	649 643 637 641 634 640	688 665 675 678 672 688	731 731 750 725 695 735

TABLE 5.6

EFFECT OF HEAT-TREATING TEMPERATURE AND TIME ON HARDNESS OF ALLOY A6

As-cast hardness : 570 HV_{50}

Temp. °C	Hardness HV_{50}				
	2 hrs	4 hrs	6 hrs	8 hrs	10 hrs
750	504 506 504 506 509 509	479 502 486 489 488 488	483 466 473 476 479 477	479 473 479 477 486 470	468 464 450 465 479 466
800	666 652 649 658 652 646 685	677 646 666 667 677 666 670	649 666 663 650 626 656 642	700 696 692 691 677 688 692	700 670 677 679 681 670 677
850	867 857 836 846 841 836 841	862 867 857 847 821 836 841	831 835 835 834 831 840	812 841 831 828 841 826 841 807	841 851 821 842 826 862 851
900	836 851 841 836 831 821	818 821 836 823 812 826	791 804 813 804 808 804	826 821 818 824 831 826	821 826 841 822 836 788

TABLE 5.7

EFFECT OF HEAT-TREATING TEMPERATURE AND TIME ON HARDNESS OF ALLOY A7

As-cast hardness: 613 HV_{50}

Temp. °C	Hardness HV_{50}				
	2 hrs	4 hrs	6 hrs	8 hrs	10 hrs
750	499 497 495 497 499 497	462 490 479 483 495 490	464 486 479 475 475 473	475 448 495 473 479 468	502 479 475 485 490 477
800	731 747 695 713 695 699	795 778 774 777 758 778	813 800 808 810 826 804	818 802 818 803 784 793	851 826 831 842 841 862
850	836 812 831 817 793 812	812 807 812 815 826 818	831 835 775 808 788 812	840 822 817 825 844 800	863 858 858 842 804 826
900	787 791 783 792 808 791	791 778 778 787 795 795	787 783 787 788 791 791	804 778 787 784 787 766	818 778 757 785 775 788 793

TABLE 5.8

EFFECT OF HEAT-TREATING TEMPERATURE AND TIME ON HARDNESS OF ALLOY A8

As-cast hardness: 666 HV_{50}

Temp °C	Hardness HV_{50}				
	2 hrs	4 hrs	6 hrs	8 hrs	10 hrs
750	538 541 538 538 533 541 538	536 552 546 542 538 536 544	541 549 541 542 538 546 536	557 554 552 557 563 560 557	557 560 563 557 560 549 552
800	804 804 770 792 778 804	835 795 783 804 800 808	851 812 831 818 775 802 836	851 826 779 827 841 831 836	846 831 836 834 826 836 831
850	821 788 812 804 818 807 779	831 826 831 828 802 841 836	802 807 802 817 826 831 836	836 826 812 824 821 826 821	791 822 800 801 791 800
900	631 610 665 642 655 637 652	619 634 625 625 622 625	672 678 682 675 672 672	646 640 652 647 646 649	652 665 668 660 655 659

TABLE 5.9

DERIVED HARDNESS VALUES (HV_{50}) OF HEAT TREATED ALLOYS

Temp °C ↓ / Duration (hrs) →	2	4	6	8	10
ALLOY-A1					
750	560	550	545	540	537
800	600	602	604	605	607
850	620	630	630	632	635
900	643	645	647	650	652
ALLOY-A2					
750	542	537	532	528	524
800	625	628	630	632	634
850	814	814	814	814	814
900	690	710	732	750	770
ALLOY-A3					
750	545	540	535	530	525
800	713	760	798	820	835
850	820	820	820	820	820
900	739	745	750	755	760
ALLOY-A4					
750	630	657	665	665	665
800	745	780	800	800	800
850	700	755	790	795	800
900	685	695	700	705	710

continued/-

continued/-

Temp °C ↓ / Duration (hrs) →	2	4	6	8	10
ALLOY-A5					
750	490	490	490	490	490
800	568	588	588	588	588
850	650	652	654	656	659
900	605	630	652	675	700
ALLOY-A6					
750	505	494	485	475	467
800	658	664	670	675	680
850	840	840	840	840	840
900	825	825	825	825	825
ALLOY-A7					
750	495	490	485	480	475
800	713	777	810	825	825
850	825	825	825	825	825
900	788	788	788	788	788
ALLOY-A8					
750	537	541	545	550	555
800	790	802	815	827	838
850	815	815	815	815	815
900	650	650	650	650	650

TABLE 5.10

EFFECT OF HEAT TREATMENT ON MICROHARDNESS OF ALLOY A1

Heat treatment	Constituent	Microhardness VPN (25 gm) Variation	Average
As-cast	Carbide	1120, 1280*, 1060, 1020**, 1020, 1060,	1093
	Matrix	570, 590, 630*, 615, 535, 435**, 485, 555, 520	548
2h 800°C AC	Carbide	890, 1075, 795**, 1010, 950, 1075, 1010, 1140*, 1075	1002
	Matrix	508, 486, 380**, 508, 508, 508, 486, 508, 532*, 508	493
10h 800°C AC	Carbide	890, 715**, 1140, 715, 715, 1320, 1420*, 1320, 1230	1052
	Matrix	557, 508, 486, 395**, 466, 532, 447, 412, 466, 532, 645*	495
2h 850°C AC	Carbide	1230, 1420, 1320, 1530*, 1140, 1320, 1320, 1420, 1320, 1010**, 1010	1276
	Matrix	532*, 532, 466**, 466, 486, 508, 486, 466, 508, 532	498
10h 850°C AC	Carbide	1140, 1010, 890**, 950, 950, 1320, 1010, 1320, 1420*, 1320	1133
	Matrix	532*, 466, 447, 532, 428**, 486, 508, 486, 466, 508	486

* Maximum value,
** Minimum value.

TABLE 5.11

EFFECT OF HEAT TREATMENT ON MICROHARDNESS OF ALLOY A2

Heat treatment	Constituent	Microhardness VPN (25 gm)	
		Variation	Average
As-cast	Carbide	1420, 1280, 1280, 760**, 1060, 1160, 1420, 1530*, 1160, 1280, 1420	1252
	Matrix	655*, 570, 535, 520, 485**, 520, 535, 570, 570, 535, 535, 555, 485	544
2h 850°C AC	Carbide	1060**, 1115, 1500*, 1160, 1280, 1140, 1230, 1320, 1230, 1140, 1320	1227
	Matrix	890, 890, 930, 820, 680**, 795, 680, 950*, 840, 890, 755	829
10h 850°C AC	Carbide	1530, 1420, 1650, 1230**, 1320, 1230, 1230, 1420, 1650*, 1320	1400
	Matrix	680, 715, 645, 715, 680, 612** 680, 755*, 715, 612, 705	683
2h 900°C AC	Carbide	895**, 1280, 1065, 1220, 1360, 1320, 1420*, 1420, 1320, 1420	1272
	Matrix	520, 475**, 555, 615, 590, 532, 612, 612, 585, 680, 790*, 645, 755, 645, 680	619
10h 900°C AC	Carbide	1420, 1420, 1320**, 1320, 1420, 1320, 1320, 1650*, 1320	1390
	Matrix	755, 795*, 715, 715, 645**, 715 645, 795, 680, 755	722

* Maximum value,
** Minimum value.

TABLE 5.12

EFFECT OF HEAT TREATMENT ON MICROHARDNESS OF ALLOY A3

Heat treatment	Constituent	Microhardness VPN (25 gm) Variation	Average
As-cast	Carbide	1320, 1420*, 1230**, 1230, 1320, 1320, 1320, 1320, 1420	1322
	Matrix	645*, 585, 508, 612, 508, 557, 486, 532, 508, 428**	537
2h 800°C AC	Carbide	1230**, 1320, 1320, 1230, 1320, 1420* 1320, 1420, 1230, 1320	1313
	Matrix	612, 715*, 508**, 557, 645, 532, 585, 532, 557, 585	583
10h 800°C AC	Carbide	1530*, 1530, 1420, 1530, 1530, 1420, 1530, 1530, 1320**, 1320	1466
	Matrix	1010*, 890, 890, 840, 890, 890, 840**, 950, 890, 950	904
2h 850°C AC	Carbide	1320**, 1420, 1650*, 1530, 1320, 1420, 1650, 1530, 1420, 1420	1468
	Matrix	795, 795, 840, 840, 1010*, 950 840, 795, 795, 755**	842
10h 850°C AC	Carbide	1320, 1420, 1075, 1320, 1420, 1075, 1530, 890**, 1650*, 1530.	1323
	Matrix	755**, 890*, 840, 840, 840, 795 795, 755, 795.	812

* Maximum value,
** Minimum value

TABLE 5.13

EFFECT OF HEAT TREATMENT ON MICROHARDNESS OF ALLOY A4

Heat treatment	Constituent	Microhardness VPN (25 gm) Variation	Average
As-cast	Carbide	1230,1230,1140,1230,1800*,1140, 1010**,1650,1800,1420	1365
	Matrix	612,585,612,680*,645,645 612,612,508,486**,508	591
2h 800°C AC	Carbide	1650*,1530,1420,1650,1530,1420, 1230,1530,1140**,1650	1475
	Matrix	755**,840,890*,840,840,795,840,890	836
	Austenite	585,645*,557,645,557**,585,585,612	596
10h 800°C AC	Carbide	1320**,1420,1650,1530,1800,1650 1950*,1800,1800,1650	1657
	Matrix	890*,795**,840,795,795,840,840	828
	Austenite	645,585,612,508**,557,532,680*	588
2h 850°C AC	Carbide	1420,1320**,1650,1650,1650,1800, 1950*,1800,1650,1800	1669
	Matrix	890,840,1010*,890,890,795,840, 755**	864
	Austenite	532,557*,508**,508,532,508,532, 508	523
10h 850°AC	Carbide	1420,1530,1530,1320,1230,795, 1530,1650*,1320,840,950,715**	1236
	Matrix	795,755,755,755,840*,585**,680	738
	Austenite	532,585,755*,532**	601

* Maximum value,
** Minimum value

TABLE 5.14

EFFECT OF HEAT TREATMENT ON MICROHARDNESS OF ALLOY A5

Heat treatment	Constituent	Microhardness VPN (25 gm)	
		Variation	Average
As-cast	Carbide	1230, 1320, 1420, 890, 840**, 1530*, 1230, 1530, 1140, 1320	1245
	Matrix	412, 508, 395**, 508, 486, 486, 645*, 466, 466, 486	486
10h 800°C AC	Carbide	1420, 1530*, 1530, 1420, 1530, 950**, 1320, 1010, 950, 1420	1308
	Matrix	486, 585*, 532, 557, 508, 486, 508, 486, 466**, 508	512
10h 850°AC	Carbide	1530*, 1420, 1140, 1230, 1140 1075**, 1320, 1230, 1320, 1320	1273
	Matrix	680*, 557, 532, 612, 466**, 508, 486, 557, 532, 585	552
2h 900°C AC	Carbide	1650*, 1420, 1650, 1530, 1230, 1650, 890**, 1010, 950	1331
	Matrix	557, 532, 557, 557, 508, 486**, 532, 557, 508, 585*, 557	540
10h 900°C AC	Carbide	1320, 1320, 1650*, 1530, 1320** 1420, 1320, 1650.	1441
	Matrix	680**, 795, 840*, 840, 680, 755, 795, 680, 755	758

* Maximum value,
** Minimum value

TABLE 5.15

EFFECT OF HEAT TREATMENT ON MICROHARDNESS OF ALLOY A6

Heat treatment	Constituent	Microhardness VPN (25 gm)	
		Variation	Average
As-cast	Carbide	1800, 1950*, 1420, 1650, 1075** 1950, 1650, 1950, 1420, 1800	1667
	Matrix	795*, 680, 612, 612, 680, 612, 585**, 645, 680	656
2h 800°C AC	Carbide	1320, 1230, 1800, 1230, 1320, 1140**, 1230, 1320, 1950, 2140*, 1800, 1320	1483
	Matrix	645, 557, 585, 645*, 612, 585, 557, 532**	590
10h 800°C AC	Carbide	890**, 1530, 1530, 1650*, 1650, 1530, 1650, 1530, 1420	1487
	Matrix	795**, 890, 950, 1010*, 795, 890, 840	881
2h 850°C AC	Carbide	1800, 1650, 1230, 1420, 1530, 1650, 1650, 1950*, 1950, 1140**, 1650	1602
	Matrix	840**, 890, 840, 840, 950*, 890, 890, 840, 950	881
10h 850°C AC	Carbide	1420, 1800*, 1800, 1650, 1650, 1530, 1800, 1650, 1320**, 1420	1604
	Matrix	890, 890, 950, 795**, 950*, 890, 840, 890, 890	887

* Maximum value,
** Minimum value

TABLE 5.16

EFFECT OF HEAT TREATMENT ON MICROHARDNESS OF ALLOY A7

Heat Treatment	Constituent	Microhardness VPN (25 gm) Variation	Average
As-cast	Carbide	1530, 1320**, 1800*, 1530, 1650, 1800, 1800, 1650, 1650, 1530	1626
	Matrix	715, 585, 715, 680, 755*, 680, 612, 532**, 557, 680	651
2h 800°C AC	Carbide	1950*, 1230**, 1530, 1320, 1320, 1230, 1230, 1650, 1800, 1320	1458
	Matrix	715, 612**, 645, 715, 715, 715, 755*, 715	698
10h 800°C AC	Carbide	2140*, 1650, 1650, 1530, 1650, 1950, 1950, 1800, 1075**, 1800	1720
	Matrix	950*, 950, 890, 890, 840, 715**, 755, 755	843
2h 850°C AC	Carbide	1230**, 1650, 1530, 1650, 1800* 1420, 1650, 1800, 1650, 1650	1603
	Matrix	840, 715**, 715, 755, 840, 890*, 890, 795	805
10h 850°C AC	Carbide	1320**, 1950*, 1950, 1950, 1800 1950, 1800, 1650, 1530, 1320	1722
	Matrix	950, 1010*, 890, 890, 1010, 840**	932

* Maximum value,
** Minimum value .

TABLE 5.17

EFFECT OF HEAT TREATMENT ON MICROHARDNESS OF ALLOY A8

Heat Treatment	Constituent	Microhardness VPN (25 gm) Variation	Average
As-cast	Carbide	1320,1650,1530,1420,1320,1075**, 1530,1650*,1420,1530	1445
	Matrix	612,645,645,612,680,645,557**, 715,715*,645	647
2h 800 °C AC	Carbide	1140,1800,1950*,1530,1650, 1650,1530,1530,1140**,1530	1545
	Matrix	645**,755,795*,755,715, 645,715,680,755,795	726
10h 800 °C AC	Carbide	1420**,1950*,1800,1800,1950, 1800,1650,1950,1800,1800	1792
	Matrix	795,950*,755**,890,890,840,890 950,950,890	880
2h 850°C AC	Carbide	1800,1650,1420,1800,1950*,1650, 1530,1230**,1950,1800	1678
	Matrix	840,795,840,840,795,890*,755**, 755	814
6 h 950°C AC	Carbide	1530,1420,1530,1650*,1530, 1420,1320,1075**,1420,1320	1422
	Austenite	585,612*,557,532**,585,585, 585,612,557,585	580

* Maximum value,
** Minimum value

TABLE 5.20

EFFECT OF HEAT-TREATMENT ON ELEMENT DISTRIBUTION IN ALLOY A2

HEAT-TREATMENT - 10 h 800°C AC

Constituent	Weight Percent			
	Cr*	Mn*	Si**	Cu**
Matrix	3.466	2.829	1.810	0.720
	4.527	3.259	1.742	0.772
	3.818	3.029	1.776	0.874
	4.353	3.430	1.673	1.029
	4.240	3.401	1.708	1.003
	3.857	3.430	1.639	1.055
	4.609	3.231	1.639	0.797
	3.735	3.143	1.776	0.849
Average	4.076	3.219	1.720	0.887
Carbide	13.596	4.840	1.160	0.154
	14.184	4.268	1.092	0.129
	15.422	4.355	1.195	0.105
	14.064	4.640	1.160	0.180
	12.572	4.925	1.195	0.231
	14.514	4.209	1.160	0.129
	14.467	4.468	1.126	0.154
	14.697	4.325	1.160	0.154
Average	14.190	4.504	1.156	0.155

* Corrected concentration

** Approximate concentration

TABLE 5.21

EFFECT OF HEAT-TREATMENT ON ELEMENT DISTRIBUTION IN ALLOY A2

HEAT TREATMENT- 2h 850°C AC

Constituent	Weight Percent			
	Cr*	Mn*	Si**	Cu**
Matrix	3.569	3.087	1.400	0.977
	4.776	3.603	1.263	0.694
	3.732	2.857	1.434	1.003
	4.157	3.172	1.400	0.926
	4.342	3.029	1.297	0.720
	3.494	3.115	1.332	0.952
	1.798	3.028	1.434	0.849
Average	3.695	2.984	1.366	0.874
Carbide	15.021	4.354	1.160	0.154
	15.375	4.699	1.092	0.180
	14.243	4.296	1.160	0.105
	14.953	4.727	1.058	0.129
	16.373	4.241	0.990	0.206
	10.160	4.636	1.195	0.180
	9.738	4.637	1.160	0.154
	15.950	4.699	1.058	0.129
Average	13.977	4.536	1.109	0.156

* corrected concentration

** approximate concentration

TABLE 5.22

EFFECT OF HEAT-TREATMENT ON ELEMENT DISTRIBUTION IN ALLOY A2

HEAT TREATMENT- 10h 850°C AC

Constituent	Weight Percent			
	Cr*	Mn*	Si**	Cu**
Matrix	3.606	2.884	1.400	0.746
	3.958	3.028	1.195	0.874
	4.333	3.258	1.229	0.720
	1.691	3.341	1.332	1.003
	4.017	3.085	1.263	0.797
	3.634	2.913	1.366	0.926
	2.748	3.000	1.297	0.874
	5.137	3.659	1.195	0.900
Average	3.641	3.146	1.285	0.855
Carbide	16.183	4.670	1.126	0.180
	13.954	4.783	1.058	0.206
	16.308	4.498	1.058	0.105
	15.097	4.583	1.024	0.129
	11.799	4.782	1.092	0.180
	15.867	4.441	0.990	0.154
	13.442	4.669	1.160	0.129
	13.962	4.442	1.024	0.154
Average	14.952	4.609	1.067	0.154

* corrected concentration

** approximate concentration

TABLE 5.23

EFFECT OF HEAT-TREATMENT ON ELEMENT DISTRIBUTION IN ALLOY A3

HEAT TREATMENT - As-cast

Constituent	Weight Percent			
	Cr*	Mn*	Si**	Cu**
Matrix	3.926	4.255	1.878	1.055
	3.413	4.455	1.639	0.874
	3.637	4.514	1.639	0.952
	4.101	4.028	1.639	0.746
	4.228	4.256	1.708	1.003
	3.789	4.228	1.742	0.797
	4.135	4.400	1.742	0.874
	3.933	4.370	1.878	0.900
Average	3.895	4.313	1.733	0.900
Carbide	14.422	7.079	1.297	0.180
	14.368	7.109	1.195	0.105
	15.844	6.451	1.366	0.154
	14.397	7.081	1.332	0.206
	12.788	6.220	1.400	0.129
	15.059	6.565	1.297	0.105
	13.908	7.740	1.366	0.180
	13.133	7.540	1.400	0.206
Average	14.239	6.973	1.332	0.142

* corrected concentration

** Approximate concentration

TABLE 5.24

EFFECT OF HEAT-TREATMENT ON ELEMENT DISTRIBUTION IN ALLOY A3

HEAT TREATMENT- 2h 800°C AC

Constituent	Weight Percent			
	Cr*	Mn*	Si**	Cu**
Matrix	3.819	3.885	1.263	0.874
	4.276	4.143	1.332	0.926
	4.138	4.142	1.400	0.900
	4.277	4.229	1.332	0.900
	4.084	4.228	1.366	0.694
	4.089	4.114	1.297	0.926
	3.883	4.170	1.263	0.900
	4.201	4.114	1.332	0.926
Average	4.096	4.128	1.323	0.881
Carbide	16.373	6.221	1.058	0.105
	12.819	6.737	1.058	0.180
	15.355	6.537	1.058	0.154
	10.362	6.705	1.126	0.206
	14.967	7.053	0.887	0.231
	16.417	6.825	1.024	0.129
	15.408	6.135	1.058	0.105
	14.619	6.737	1.024	0.180
Average	14.540	6.619	1.037	0.161

* corrected concentration

** approximate concentration

TABLE 5.25

EFFECT OF HEAT-TREATMENT ON ELEMENT DISTRIBUTION IN ALLOY A3

HEAT TREATMENT - 4h 800°C AC

Constituent	Weight Percent			
	Cr*	Mn*	Si**	Cu**
Matrix	3.161	4.601	1.844	0.977
	3.522	4.141	1.742	0.797
	3.809	4.313	1.844	1.003
	3.988	4.342	1.742	1.029
	3.106	4.427	1.708	0.694
	4.058	4.400	1.708	0.874
	3.837	4.828	1.844	0.977
	4.291	4.114	1.878	0.772
Average	3.722	4.395	1.789	0.890
Carbide	13.630	6.707	1.434	0.129
	15.810	6.364	1.400	0.180
	13.645	6.564	1.297	0.105
	14.846	6.364	1.434	0.154
	15.434	6.449	1.297	0.206
	11.256	5.616	1.400	0.180
	14.827	6.621	1.366	0.154
	16.027	6.106	1.400	0.129
	16.057	5.790	1.366	0.129
Average	14.615	6.287	1.377	0.152

* corrected concentration

** approximate concentration

TABLE 5.26

EFFECT OF HEAT TREATMENT ON ELEMENT DISTRIBUTION IN ALLOY A3

HEAT TREATMENT- 10h 800°C AC

Constituent	Weight Percent			
	Cr*	Mn*	Si**	Cu**
	4.161	3.856	1.366	0.823
	3.504	4.142	1.366	0.874
	3.857	4.286	1.366	0.952
	4.164	4.057	1.434	0.772
Matrix	4.708	3.886	1.776	1.131
	4.879	4.029	1.571	1.003
	4.350	4.429	1.605	0.797
	3.732	3.970	1.844	0.952
	4.221	4.286	1.605	0.977
	2.430	3.969	1.913	1.003
Average	4.001	4.091	1.585	0.843
	14.327	7.080	1.195	0.180
	14.477	6.765	1.092	0.154
	16.116	6.594	1.126	0.154
	9.522	7.904	1.126	0.129
	13.041	6.074	1.366	0.154
Carbide	14.727	6.765	1.366	0.180
	13.529	6.821	1.263	0.206
	15.281	6.565	1.366	0.154
	9.127	6.358	1.503	0.105
	13.110	7.021	1.366	0.129
Average	13.325	6.794	1.369	0.155

* corrected concentration
** approximate concentration

TABLE 5.27

EFFECT OF HEAT TREATMENT ON ELEMENT DISTRIBUTION IN ALLOY A3

HEAT TREATMENT- 2h 850°C AC

Constituent	Weight Percent			
	Cr*	Mn*	Si**	Cu**
Matrix	3.770	4.371	1.878	0.874
	3.788	4.113	1.878	1.055
	4.708	4.952	1.913	1.029
	3.980	4.086	1.844	0.772
	3.116	5.171	1.776	0.720
	4.483	4.772	1.742	1.131
	4.105	4.857	1.810	0.823
	4.684	4.800	1.673	0.977
Average	4.079	4.640	1.814	0.923
Carbide	14.847	6.736	1.469	0.129
	14.647	6.736	1.332	0.105
	16.157	6.077	1.503	0.154
	13.441	7.078	1.503	0.180
	13.499	7.509	1.469	0.129
	13.169	7.565	1.332	0.105
	14.162	7.051	1.503	0.180
	14.816	6.478	1.503	0.206
Average	14.342	6.903	1.452	0.149

* corrected concentration
** approximate concentration

TABLE 5.28

EFFECT OF HEAT TREATMENT ON ELEMENT DISTRIBUTION IN ALLOY A6

HEAT TREATMENT - As-cast

Constituent	Weight Percent			
	Cr*+	Mn*	Si**	Cu**
	6.542	3.945	1.503	1.003
	5.763	2.972	1.673	1.029
	4.469	3.543	1.673	0.720
Matrix	5.844	2.830	1.742	0.900
	4.164	3.285	1.639	0.952
	5.262	3.114	1.810	0.874
	4.994	3.315	1.673	0.926
Average	5.291	3.286	1.673	0.915
	32.944	4.483	0.956	0.129
	25.793	5.139	1.092	0.105
	22.895	5.481	1.229	0.154
Carbide	23.308	4.505	1.092	0.180
	29.385	4.624	1.092	0.154
	25.351	4.966	1.160	0.105
	23.453	4.591	1.160	0.129
Average	26.161	4.827	1.112	0.137

* corrected concentration
** approximate concentration

TABLE 5.29

EFFECT OF HEAT-TREATMENT ON ELEMENT DISTRIBUTION IN ALLOY A6

HEAT TREATMENT - 2h 800°C AC

Constituent	Weight Percent			
	Cr*	Mn*	Si**	Cu**
Matrix	5.890	3.087	1.469	0.874
	5.377	2.886	1.708	0.952
	6.836	3.144	1.537	0.823
	6.426	2.772	1.571	1.106
	5.462	3.487	1.503	0.977
	5.699	3.344	1.639	0.720
	4.438	3.086	1.708	0.926
	5.283	3.286	1.673	1.029
Average	5.676	3.136	1.601	0.926
Carbide	28.017	4.337	1.024	0.105
	32.416	4.798	0.990	0.154
	30.855	4.970	1.024	0.129
	30.643	5.056	0.956	0.129
	24.253	5.166	1.092	0.154
	21.299	4.676	1.092	0.105
	29.577	4.940	0.922	0.180
	32.255	4.568	0.990	0.206
Average	28.664	4.813	1.011	0.145

* corrected concentration
** approximate concentration

TABLE 5.30

EFFECT OF HEAT-TREATMENT ON ELEMENT DISTRIBUTION IN ALLOY A6

HEAT TREATMENT - 10h 800°C AC

Constituent	Weight Percent			
	Cr*	Mn*	Si**	Cu**
Matrix	5.530	2.857	1.742	0.823
	5.233	3.228	1.639	1.055
	6.837	3.802	1.571	1.029
	6.630	3.660	1.776	0.977
	6.696	3.803	1.639	0.694
	6.539	3.344	1.742	0.797
	4.576	3.344	1.776	1.003
Average	6.005	3.434	1.698	0.911
Carbide	28.004	5.285	1.024	0.180
	31.317	4.712	1.024	0.105
	29.758	4.682	1.024	0.129
	31.188	4.683	1.092	0.154
	30.627	5.084	1.058	0.154
	32.367	4.655	0.956	0.129
	31.226	4.711	0.922	0.105
Average	30.641	4.830	1.014	0.137

* corrected concentration
** approximate concentration

TABLE 5.31

EFFECT OF HEAT-TREATMENT ON ELEMENT DISTRIBUTION IN ALLOY A6

HEAT TREATMENT- 2h 850°C AC

Constituent	Weight Percent			
	Cr*	Mn*	Si**	Cu**
Matrix	3.420	3.572	1.742	1.029
	6.002	3.144	1.639	0.720
	3.968	3.372	1.605	0.977
	4.361	3.229	1.605	1.003
	6.390	3.086	1.537	0.823
	6.005	3.201	1.605	0.874
	6.486	3.459	1.503	0.926
	3.917	3.486	1.776	1.003
	6.004	3.259	1.639	1.029
	6.176	3.316	1.537	0.797
	5.897	2.944	1.639	0.874
Average	5.329	3.279	1.621	0.914
Carbide	32.671	4.597	1.058	0.105
	31.357	4.883	0.990	0.154
	30.506	4.165	0.990	0.105
	22.276	5.251	1.092	0.129
	28.622	5.227	1.058	0.154
	30.246	4.768	0.922	0.154
	32.873	4.597	0.887	0.180
	31.455	4.712	0.990	0.105
Average	30.000	4.775	0.998	0.136

* corrected concentration
** approximate concentration

TABLE 5.32

EFFECT OF HEAT-TREATMENT ON ELEMENT DISTRIBUTION IN ALLOY A7

HEAT-TREATMENT- As-cast

Constituent	Weight Percent			
	Cr*	Mn*	Si**	Cu**
	6.571	4.259	1.810	0.823
	6.332	4.231	1.708	0.849
	6.199	4.402	1.673	0.720
Matrix	7.063	4.089	1.776	1.055
	6.806	3.916	1.742	1.131
	6.406	3.916	1.673	0.952
	5.720	3.888	1.776	0.926
Average	6.442	4.100	1.737	0.922
	27.958	5.629	1.126	0.105
	20.603	5.164	1.366	0.129
	23.149	6.228	1.297	0.154
Carbide	31.215	6.953	1.092	0.180
	31.241	6.349	1.024	0.154
	33.922	6.006	0.887	0.105
	18.103	7.515	1.332	0.129
	23.671	8.434	1.092	0.154
Average	26.232	6.534	1.152	0.139

* corrected concentration
** approximate concentration

TABLE 5.34

EFFECT OF HEAT-TREATMENT ON ELEMENT DISTRIBUTION IN ALLOY A7

HEAT TREATMENT- 4h 800°C AC

Constituent	Weight Percent			
	Cr*	Mn*	Si**	Cu**
	6.259	4.402	1.537	0.772
	5.753	3.973	1.673	0.823
	4.602	3.884	1.673	0.694
Matrix	5.698	3.916	1.571	1.055
	6.294	4.664	1.400	0.977
	4.889	4.257	1.503	0.823
	5.459	4.058	1.469	0.874
Average	5.564	4.164	1.547	0.860
	28.814	6.233	0.990	0.105
	28.848	6.261	0.887	0.129
	29.792	5.256	0.887	0.154
Carbide	29.096	6.175	1.024	0.180
	29.198	5.572	0.922	0.105
	31.001	5.774	0.922	0.154
	28.118	5.657	0.956	0.129
Average	29.266	5.846	0.941	0.137

* corrected concentration
** approximate concentration

TABLE 5.35

EFFECT OF HEAT TREATMENT ON ELEMENT DISTRIBUTION IN ALLOY A7

HEAT TREATMENT- 10h 800°C AC

Constituent	Weight Percent			
	Cr*	Mn*	Si**	Cu**
Matrix	4.709	4.085	1.639	0.874
	5.646	3.973	1.605	0.849
	6.049	4.088	1.605	1.003
	4.657	3.942	1.673	0.823
	7.589	4.975	1.434	0.797
	2.291	4.739	1.537	0.720
	4.928	4.285	1.639	0.694
Average	5.124	4.298	1.590	0.823
Carbide	23.118	7.089	1.058	0.105
	25.784	5.569	0.887	0.129
	21.540	7.721	1.297	0.154
	25.717	6.712	1.024	0.154
	28.216	5.801	0.956	0.129
	30.062	5.917	0.922	0.105
	26.944	6.806	0.990	0.180
Average	25.91	6.516	1.019	0.137

* corrected concentration
** approximate concentration

TABLE 5.36

EFFECT OF HEAT TREATMENT ON ELEMENT DISTRIBUTION IN ALLOY A7

HEAT TREATMENT- 2h 850°C AC

Constituent	Weight Percent			
	Cr*	Mn*	Si**	Cu**
	5.743	4.202	1.742	0.823
	6.565	3.918	1.708	0.874
	6.522	4.202	1.571	0.746
Matrix	7.981	4.633	1.400	0.797
	5.106	4.259	1.469	1.003
	5.269	3.659	1.434	1.055
	7.453	4.489	1.434	1.080
Average	6.377	4.194	1.537	0.911
	23.627	5.426	1.195	0.105
	28.785	6.865	0.887	0.105
	33.340	6.294	0.990	0.129
Carbide	30.846	6.551	0.820	0.129
	29.799	5.832	0.853	0.180
	29.519	6.119	0.956	0.154
	31.830	5.689	0.787	0.105
Average	29.678	6.110	0.927	0.130

* corrected concentration
** approximate concentration

TABLE 5.37

X-RAY DIFFRACTOGRAM OF ALLOY- A2

HEAT TREATMENT- As-cast*

Sl. No.	2θ	d(Å)	$\frac{I}{I_o}$	(hkl) Matrix	(hkl) Carbide(s)	
1	48.00	2.382	4		$(112,021)M_3$	$(311,20\bar{2})M_5$
2	50.80	2.258	4		$(200)M_3$	$(020)M_5$
3	51.50	2.230	6		unidentified	
4	56.00	2.063	9		$(210)M_3$	$(510,021)M_5$
5	57.28	2.021	100	$(110)_\alpha$	$(022)M_3$ $(103)M_3$	$(31\bar{2},40\bar{2})M_5$
6	58.80	1.973	9		$(211)M_3$	$(51\bar{1},22\bar{1})M_5$
7	62.40	1.870	7		$(113)M_3$	
8	85.10	1.432	5	$(200)_\alpha$		
9	111.90	1.169	31	$(211)_\alpha$		$(62\bar{3},912)M_5$
10	118.00	1.130	7			$(13\bar{3},60\bar{4})M_5$
11	118.90	1.125	5			
12	119.3	1.123	5			$(041)M_5$
13	146.0	1.013	8	$(220)_\alpha$		

Structure: Pearlite/bainite

+ M_3C [isomorphous with Fe_3C(23-1113)]

+ Trace M_5C_2(? ?) [isomorphous with Fe_5C_2(20-508)]

* $A2_{-5}$ similar to this

TABLE 5.38

X-RAY DIFFRACTOGRAM OF ALLOY- A2

HEAT TREATMENT- 2h 850°C AC

Sl. No.	2 θ	d(Å)	$\frac{I}{I_o}$	(hkl)			
				Matrix	Carbide(s)		
1	48.10	2.377	10		$(112,021)M_3$	$(321)M_7$	
2	51.25	2.240	8		$(200)M_3$	$(102)M_7$	$(020)M_5$
3	54.90	2.101	19		$(121)M_3$	$(202,501)M_7$	
4	55.80	2.070	26				$(510,021)M_5$
5	56.10	2.060	28	$(011)_{\alpha'}$	$(210)M_3$		
6	57.10	2.027	100	$(110)_{\alpha}$ $(110)_{\alpha'}$	$(022)M_3$ $(103)M_3$	$(421)M_7$	$(31\bar{2},40\bar{2})M_5$
7	58.85	1.972	12		$(211)M_3$	$(511)M_7$	$(51\bar{1},22\bar{1})M_5$
8	62.40	1.869	10		$(113)M_3$	$(222)M_7$	
9	63.20	1.849	7		$(122)M_3$	$(601)M_7$	
10	65.10	1.800	6			$(431)M_7$	$(312,511)M_5$
11	66.90	1.757	4		$(212)M_3$	$(412)M_7$	$(402)M_5$
12	111.75	1.173	17	$(211)_{\alpha}$ $(211)_{\alpha'}$			$(62\bar{3},912)M_5$
13	114.80	1.150	8				$(423,802)M_5$
14	119.35	1.122	7				$(13\bar{3},60\bar{4})M_5$

Structure: Martensite

+ some bainite

+ M_3C [isomorphous with Fe_3C(23-1113)]

+ trace M_7C_3 [isomorphous with Cr_7C_3(11-550)]

+ trace M_5C_2 [isomorphous with Fe_5C_2(20-508)]

TABLE 5.42

X-RAY DIFFRACTOGRAM OF ALLOY- A3

HEAT TREATMENT- 2h 800°C AC

Sl. No.	2θ	d(Å)	$\frac{I}{I_o}$	(hkl) Matrix	(hkl) Carbide(s)		
1	48.00	2.382	10		$(112,021)M_3$		$(311,20\bar{2})M_5$
2	50.80	2.260	4		$(200)M_3$	$(120)M_7$	$(020)M_5$
3	51.70	2.222	6		$(120)M_3$		
4	55.00	2.098	6		$(121)M_3$	$(012)M_7$	
5	56.20	2.057	15		$(210)M_3$		$(510,021)M_5$
6	57.30	2.020	100	$(110)_\alpha$	$(022)M_3$	$(121)M_7$	$(31\bar{2},40\bar{2})M_5$
7	57.40	2.017	70		$(103)M_3$		
8	58.90	1.970	16		$(211)M_3$	$(300)M_7$	$(51\bar{1},22\bar{1})M_5$
9	62.50	1.867	9		$(113)M_3$		
10	63.35	1.845	4		$(122)M_3$	$(301)M_7$	
11	65.55	1.790	3			$(022)M_7$	$(312,511)M_5$
12	66.95	1.756	6		$(212)M_3$		$(402)M_5$
13	70.40	1.681	5		$(004,023)M_3$		$(51\bar{2})M_5$
14	85.20	1.431	8	$(200)_\alpha$			
15	105.90	1.214	5			$(303,500)M_7$	$(11\bar{4},821)M_5$
16	111.95	1.169	18	$(211)_\alpha$		$(322)M_7$	$(62\bar{3},912)M_5$
17	114.85	1.150	5			$(501)M_7$	$(423,802)M_5$
18	118.50	1.127	5			$(004,142)M_7$	$(13\bar{3},60\bar{4})M_5$
19	119.30	1.123	10			$(133,014)M_7$	$(041)M_5$
20	145.95	1.013	9	$(220)_\alpha$			
21	146.30	1.012	8				

Structure- Bainite/tempered martensite
+ M_3C [isomorphous with Fe_3C(23-1113)]
+ some M_7C_3 [isomorphous with Fe_7C_3(17-333)]
+ trace M_5C_2 [isomorphous with Fe_5C_2(20-508)]

TABLE 5.43

X-RAY DIFFRACTOGRAM OF ALLOY-A3

HEAT TREATMENT - 10h 800°C AC

Sl. No.	2θ	d(Å)	$\frac{I}{I_o}$	(hkl) Matrix	Carbides		
1	47.8	2.391	6		$(112,021)M_3$		$(311,20\bar{2})M_5$
2	50.6	2.267	5		$(200)M_3$	$(120)M_7$	$(020)M_5$
3	51.2	2.242	6	unidentified			
4	52.0	2.210	4		$(120)M_3$		
5	54.8	2.105	8		$(121)M_3$	$(012)M_7$	
6	56.0	2.063	46	$(011)_\alpha, (111)_\gamma$	$(210)M_3$		$(510,021)M_5$
7	57.2	2.024	100	$(110)_\alpha (110)_\alpha$,	$(022)M_3$ $(103)M_3$	$(121)M_7$	$(31\bar{2},40\bar{2})M_5$
8	58.8	1.973	23		$(211)M_3$	$(300)M_7$	$(51\bar{1},22\bar{1})M_5$
9	62.5	1.867	19		$(113)M_3$		
10	63.1	1.851	8		$(122)M_3$		
11	65.3	1.795	10	$(200)_\gamma$		$(022)M_7$	$(312,511)M_5$
12	66.8	1.760	12		$(212)M_3$		$(402)M_5$
13	70.5	1.678	8		$(004,023)M_3$		$(51\bar{2})M_5$
14	75.3	1.586	7		$(130)M_3$		$(11\bar{3})M_5$
15	79.8	1.510	7	$(002)_\alpha$,			$(42\bar{2})M_5$
16	85.0	1.433	7	$(200)_\alpha (200)_\alpha$,			
17	105.8	1.215	10				$(11\bar{4},821)M_5$
18	109.0	1.190	8	$(112)_\alpha$,		$(303,500)M_7$	
19	112.0	1.168	17	$(211)_\alpha (211)_\alpha$,		$(322)M_7$	$(62\bar{3},912)M_5$
20	114.5	1.152	9			$(501)M_7$	
21	119.5	1.121	10				$(13\bar{3},60\bar{4})M_5$
22	124.3	1.096	7				$(041)M_5$
23	126.6	1.084	19	$(311)_\gamma$			

Structure:- Martensite
+ trace austenite
+ M_3C [isomorphous with Fe_3C(23-1113)]
+ some M_7C_3 [isomorphous with Fe_7C_3(17-333)]
+ some M_5C_2 [isomorphous with Fe_5C_2(20-508)]

TABLE 5.44

X-RAY DIFFRACTOGRAM OF ALLOY- A3

HEAT TREATMENT - 2h 850°C AC

Sl. No.	2θ	d(Å)	$\frac{I}{I_o}$	(hkl) Matrix	(hkl) Carbide(s)		
1	48.18	2.373	14		$(112,021)M_3$		
2	51.45	2.232	11	Unidentified			
3	55.00	2.098	16		$(121)M_3$	$(051,202)M_7$	
4	56.10	2.060	63	$(011)_\alpha, (111)_\gamma$	$(210)M_3$	$(600,122)M_7$	$(510,021)M_5$
5	57.20	2.024	89	$(110)_\alpha$	$(022)M_3$		$(31\bar{2},40\bar{2})M_5$
6	57.65	2.009	100	$(110)_{\alpha'}$	$(103)M_3$		
7	58.95	1.969	30		$(211)M_3$		$(51\bar{1},22\bar{1})M_5$
8	62.60	1.865	18		$(113)M_3$		
9	63.30	1.846	9		$(122)M_3$		
10	65.00	1.803	32	$(200)_\gamma$		$(431,402)M_7$	$(312,511)M_5$
11	66.90	1.757	11		$(212)M_3$	$(530,322)M_7$	$(402)M_5$
12	70.50	1.678	13		$(004,023)M_3$		$(51\bar{2})M_5$
13	75.40	1.580	8		$(130)M_3$		$(11\bar{3})M_5$
14	99.60	1.268	11	$(200)_\gamma$			$(53\bar{1})M_5$
15	103.30	1.235	6				$(712)M_5$
16	106.00	1.213	14	$(112)_{\alpha'}$		$(603)M_7$	$(11\bar{4},821)M_5$
17	111.60	1.171	11	$(211)_\alpha (211)_{\alpha'}$			$(62\bar{3},912)M_5$
18	113.40	1.159	14			$(750)M_7$	$(423,802)M_5$
19	119.40	1.122	24				$(13\bar{3},60\bar{4})M_5$
20	120.90	1.114	9				$(041)M_5$
21	126.95	1.083	11	$(311)_\gamma$			
22	127.50	1.080	9				$(404)M_5$

Structure: Martensite
+ Austenite
+ M_3C [isomorphous with Fe_3C(23-1113)]
+ some M_7C_3 [isomorphous with $(CrFe)_7C_3$(5-072)]
+ some M_5C_2 [isomorphous with Fe_5C_2(20-508)]

TABLE 5.45

X-RAY DIFFRACTOGRAM OF ALLOY- A3
HEAT TREATMENT- 10h 850°C AC

Sl. No.	2θ	d(Å)	$\frac{I}{I_o}$	(hkl) Matrix	Carbide(s)		
1	48.00	2.382	13		$(112,021)M_3$		$(420)M_{23}$
2	50.55	2.269	8		$(200)M_3$	$(002)M_7$	
3	50.80	2.258	8			$(120)M_7$	
4	51.80	2.218	7		$(120)M_3$		
5	54.80	2.105	8		$(121)M_3$	$(012)M_7$	
6	55.95	2.065	52	$(011)_\alpha, (111)_\gamma$	$(210)M_3$		$(333,511)M_{23}$
7	57.60	2.011	100	$(110)_\alpha (110)_{\alpha'}$	$(103)M_3$	$(121)M_7$	
8	58.80	1.973	29		$(211)M_3$	$(300)M_7$	
9	62.44	1.869	21		$(113)M_3$		$(440)M_{23}$
10	63.10	1.851	17		$(122)M_3$		
11	65.10	1.800	12	$(200)_\gamma$		$(022)M_7$	$(531)M_{23}$
12	66.85	1.759	12		$(212)M_3$		$(442,600)M_{23}$
13	70.28	1.683	10		$(004,023)$		$(620)M_{23}$
14	93.70	1.328	13			$(023)M_7$	$(800)M_{23}$
15	99.32	1.271	7	$(220)_\gamma$			
16	104.95	1.221	10				$(555,751)M_{23}$
17	105.80	1.215	14	$(112)_{\alpha'}$			
18	108.80	1.191	6			$(303,500)M_7$	$(840)M_{23}$
19	111.50	1.172	13	$(211)_\alpha (211)_{\alpha'}$			
20	112.10	1.168	14			$(322)M_7$	$(753,911)M_{23}$
21	113.60	1.158	7			$(501)M_7$	
22	115.10	1.148	7			$(330)M_7$	
23	118.20	1.129	12			$(004,142)M_7$	
24	119.30	1.123	14				
25	126.80	1.083	13	$(311)_\gamma$			$(844)M_{23}$
26	127.40	1.081	8				

Structure: Martensite
+ some austenite
+ M_3C [isomorphous with Fe_3C(23-1113)]
+ some M_7C_3 [isomorphous with Fe_7C_3(17-333)]
+ trace $M_{23}C_6$(11-0545)

TABLE 5.46

X-RAY DIFFRACTOGRAM OF ALLOY- A3

HEAT TREATMENT- 10h 900°C AC

Sl. No.	2θ	d(Å)	$\frac{I}{I_o}$	(hkl) Matrix	(hkl) Carbide(s)	
1	48.20	2.372	12		$(112,021)M_3$	
2	52.00	2.210	10		$(120)M_3$	
3	55.00	2.098	33		$(121)M_3$	
4	55.80	2.070	74	$(011)_{\alpha'}, (111)_{\gamma}$	$(210)M_3$	$(510,02\bar{1})M_5$
5	57.15	2.025	100	$(110)_{\alpha}(110)_{\alpha'}$	$(022)M_3$ $(103)M_3$	$(31\bar{2},40\bar{2})M_5$
6	58.60	1.979	22		$(211)M_3$	$(51\bar{1},22\bar{1})M_5$
7	63.28	1.847	21		$(122)M_3$	
8	65.20	1.798	47	$(200)_{\gamma}$		$(312,511)M_5$
9	73.80	1.613	12		$(221)M_3$	$(60\bar{2})M_5$
10	75.40	1.584	13		$(130)M_3$	$(11\bar{3})M_5$
11	85.00	1.433	12	$(200)_{\alpha}(200)_{\alpha'}$		
12	99.20	1.272	7	$(220)_{\gamma}$		$(53\bar{1})M_5$
13	104.80	1.223	7	unidentified		
14	105.40	1.218	9	$(112)_{\alpha'}$		$(11\bar{4},821)M_5$
15	111.80	1.170	14	$(211)_{\alpha}(211)_{\alpha'}$		$(62\bar{3},912)M_5$
16	126.30	1.086	19	$(311)_{\gamma}$		$(404)M_5$

Structure: Martensite
+ austenite
+ M_3C [isomorphous with Fe_3C(23-1113)]
+ some M_5C_2 [isomorphous with Fe_5C_2(20-508)]

TABLE 5.47

X-RAY DIFFRACTOGRAM OF ALLOY: A4
HEAT TREATMENT- As-cast

Sl. No.	2θ	d(Å)	$\frac{I}{I_o}$	(hkl) Matrix	(hkl) Carbide (s)
1	48.10	2.377	3		$(112,021)M_3$
2	50.10	2.288	4		unidentified
3	50.80	2.258	4		$(200)M_3$
4	54.50	2.116	3		$(121)M_3$
5	55.62	2.076	100	$(011)_\alpha, (111)_\gamma$	$(210)M_3$
6	57.30	2.02	29	$(110)_\alpha (110)_\alpha$,	$(022)M_3$ $(103)M_3$
7	58.82	1.973	5		$(211)M_3$
8	62.30	1.873	3		$(113)M_3$
9	63.30	1.846	3		$(122)M_3$
10	65.00	1.803	15	+ $(200)_\gamma$	
11	99.00	1.274	3	$(220)_\gamma$	
12	99.60	1.268	3		
13	111.50	1.172	3	$(211)_\alpha$,	
14	112.00	1.168	3	$(211)_\alpha$	
15	126.00	1.087	5	$(311)_\gamma$	
16	137.30	1.040	6	$(220)_\alpha, (222)_\gamma$	

Structure: Austenite
+ martensite
+ M_3C [isomorphous with Fe_3C(23-1113)]

TABLE 5.51

X-RAY DIFFRACTOGRAM OF ALLOY- A6
HEAT TREATMENT- As-cast

Sl. No.	2θ	d(Å)	$\frac{I}{I_o}$	(hkl) Matrix	(hkl) Carbide(s)	
1	48.20	2.372	3		$(112,021)M_3$	
2	50.60	2.267	8		$(200)M_3$	$(411)M_7$
3	51.45	2.232	6	unidentified		
4	54.90	2.101	4		$(121)M_3$	$(202,501)M_7$
5	57.15	2.025	100	$(110)_\alpha$	$(022)M_3$ $(103)M_3$	$(421)M_7$
6	59.75	1.945	3		$(211)M_3$	
7	59.90	1.940	3			$(511)M_7$
8	68.10	1.730	3			$(412)M_7$
9	84.90	1.435	9	$(200)_\alpha$		$(801)M_7$
10	111.80	1.170	24	$(211)_\alpha$		
11	113.40	1.159	4	unidentified		
12	145.75	1.014	8	$(220)_\alpha$		
13	146.55	1.011	7			

Structure: Pearlite
+ M_3C [isomorphous with Fe_3C(23-1113)]
+ trace M_7C_3 [isomorphous with Cr_7C_3(11-550)]

TABLE 5.52

X-RAY DIFFRACTOGRAM OF ALLOY- A6

HEAT TREATMENT- 2h 750°C AC

Sl. No.	2θ	d(Å)	$\frac{I}{I_o}$	(hkl) Matrix	(hkl) Carbide(s)
1	50.60	2.267	5		$(200)M_3$
2	51.50	2.234	6		Unidentified
3	54.80	2.105	3		$(121)M_3$
4	56.10	2.060	3		$(210)M_3$
5	57.15	2.025	100	$(110)_\alpha$	$(022)M_3$, $(103)M_3$
6	85.00	1.434	5	$(200)_\alpha$	
7	111.85	1.169	10	$(211)_\alpha$	
8.	146.00	1.013	11	$(220)_\alpha$	

Structure: Pearlite

+ M_3C [isomorphous with Fe_3C(23-1113)]

TABLE 5.53

X-RAY DIFFRACTOGRAM OF ALLOY- A6

HEAT TREATMENT- 2h 800°C AC

Sl. No.	2θ	d(Å)	$\frac{I}{I_o}$	(hkl) Matrix	(hkl) Carbide (s)		
						(303,500)M_7	
1	47.85	2.389	3		(112,021)M_3		(311,202)M_5
2	50.85	2.256	7		(200)M_3	(120)M_7	(020)M_5
3	51.40	2.234	7		unidentified		
4	52.00	2.210	9		(120)M_3		
5	52.70	2.182	4				$(11\bar{2},202)M_5$
6	54.75	2.107	25		(121)M_3	(012)M_7	
7	56.00	2.063	9		(210)M_3		(510,021)M_5
8	57.10	2.027	100	$(110)_\alpha$	(022)M_3 (103)M_3	(121)M_7	$(31\bar{2},40\bar{2})M_5$
9	58.65	1.978	7		(211)M_3	(300)M_7	$(51\bar{1},22\bar{1})M_5$
10	61.90	1.884	4		(113)M_3	(112)M_7	(221)M_5
11	62.80	1.859	4		(122)M_3		
12	65.20	1.798	7			(022)M_7	(312,511)M_5
13	85.00	1.434	9	$(200)_\alpha$			
14	92.40	1.342	5			(023)M_7	(331)M_5
15	107.70	1.200	4			(303,500)M_7	$(11\bar{4},821)M_5$
16	111.75	1.170	34	$(211)_\alpha$		(322)M_7	$(62\bar{3},912)M_5$
17	145.20	1.015	9		unidentified		
18	145.50	1.014	11				
19	145.85	1.013	11	$(220)_\alpha$			(404)M_5
20	146.10	1.013	10				

Structure: Pearlite/bainite
+ M_3C [isomorphous with Fe_3C(23-1113)]
+ some M_7C_3 [isomorphous with Fe_7C_3(17-333)]
+ some M_5C_2 [isomorphous with Fe_5C_2(20-508)]

TABLE 5.54

X-RAY DIFFRACTOGRAM OF ALLOY- A6

HEAT TREATMENT- 10 h 800°C AC

Sl. No.	2θ	d(Å)	$\frac{I}{I_o}$	(hkl) Matrix	(hkl) Carbide (s)		
1	48.05	2.379	2		$(112,021)M_3$		$(311,20\bar{2})M_5$
2	50.60	2.267	9		$(200)M_3$	$(002)M_7$	$(020)M_5$
3	51.45	2.232	5		$(120)M_3$	$(120)M_7$	
4	54.80	2.105	4		$(121)M_3$	$(012)M_7$	
5	55.75	2.072	11	$(011)_{\alpha'}$	$(210)M_3$		$(510,021)M_5$
6	57.10	2.027	100	$(110)_{\alpha}(110)_{\alpha'}$	$(022)M_3$ $(103)M_3$	$(121)M_7$	$(31\bar{2},40\bar{2})M_5$
7	65.10	1.800	3			$(022)M_7$	$(312,511)M_5$
8	68.05	1.731	4			$(220)M_7$	$(42\bar{1})M_5$
9	84.85	1.436	5	$(200)_{\alpha}(200)_{\alpha'}$			
10	111.75	1.170	11	$(211)_{\alpha}(200)_{\alpha'}$		$(322)M_7$	
11	113.25	1.160	4			$(501)M_7$	
12	113.45	1.159	4			$(330)M_7$	$(11\bar{3})M_5$
13	145.90	1.013	5	$(220)_{\alpha}(220)_{\alpha'}$			$(404)M_5$

Structure: Bainite/martensite
+ M_3C [isomorphous with Fe_3C(23-1113)]
+ some M_7C_3 [isomorphous with Fe_7C_3(17-333)]
+ trace M_5C_2 [isomorphous with Fe_5C_2(20-508)]

TABLE 5.55

X-RAY DIFFRACTOGRAM OF ALLOY- A6

HEAT TREATMENT- 10h 850°C AC

Sl. No.	2θ	d(Å)	$\frac{I}{I_o}$	(hkl) Matrix	(hkl) Carbide(s)		
1	48.06	2.379	4		$(112,021)M_3$		
2	50.60	2.267	20		$(200)M_3$	$(002)M_7$	$(020)M_5$
3	51.30	2.238	12		unidentified		
4	51.55	2.228	10		$(120)M_3$		
5	53.10	2.167	6				$(11\bar{2},202)M_5$
6	54.60	2.112	10			$(012)M_7$	
7	54.80	2.105	11		$(121)M_3$		
8	55.70	2.074	32	$(011)_{\alpha'}$, $(100)_\gamma$	$(210)M_3$		$(510,021)M_5$
9	57.15	2.025	100	$(110)_\alpha$ $(110)_{\alpha'}$	$(022)M_3$, $(103)M_3$	$(121)M_7$	$(31\bar{2},40\bar{2})M_5$
10	58.40	1.986	14			$(300)M_7$	$(51\bar{1},22\bar{1})M_5$
11	58.60	1.979	11		$(211)M_3$		
12	59.34	1.957	6		unidentified		
13	62.96	1.855	5		$(122)M_3$		
14	63.30	1.846	5		unidentified		
15	64.20	1.823	7			$(301)M_7$	
16	65.10	1.800	14	$(200)_\gamma$		$(022)M_7$	$(312,511)M_5$
17	68.02	1.732	7			$(220)M_7$	$(42\bar{1})M_5$
18	75.20	1.588	5		$(130)M_3$		$(11\bar{3})M_5$
19	80.65	1.497	5	$(002)_{\alpha'}$			
20	85,15	1.432	9	$(200)_\alpha$ $(200)_{\alpha'}$		$(401)M_7$	
21	99.30	1.271	6	$(220)_\gamma$			
22	111.60	1.171	21	$(211)_\alpha$ $(211)_{\alpha'}$		$(322)M_7$	
23	113.03	1.161	12		unidentified		
24	113.60	1.158	10			$(501)M_7$	
25	114.23	1.154	9			$(330)M_7$	
26	126.60	1.084	9	$(311)_\gamma$			
27	145.90	1.013	10	$(220)_\alpha$			
28	147.70	1.008	7	$(220)_{\alpha'}$			

Structure: Martensite + some austenite + M_3C [isomorphous with Fe_3C (23-1113)] + some M_7C_3 [isomorphous with Fe_7C_3(17-333)] + trace M_5C_2 [isomorphous with Fe_5C_2(20-508)]

TABLE 5.56

X-RAY DIFFRACTOGRAM OF ALLOY- A6
HEAT TREATMENT- 10h 900°C A.C.

Sl. No.	2θ	d(Å)	$\frac{I}{I_o}$	(hkl) Matrix	(hkl) Carbide(s)		
1	48.10	2.377	3		$(112,021)M_3$		
2	50.60	2.267	15		$(200)M_3$	$(002)M_7$	$(020)M_5$
3	51.20	2.242	8			$(120)M_7$	
4	51.40	2.234	7	unidentified			
5	51.80	2.218	4	unidentified			
6	52.30	2.198	3		$(120)M_3$		$(11\bar{2},202)M_5$
7	54.85	2.103	8		$(121)M_3$	$(012)M_7$	
8	55.65	2.077	43	$(011)_\alpha, (111)_\gamma$	$(210)M_3$		$(510,021)M_5$
9	57.15	2.025	100	$(110)_\alpha (110)_{\alpha'}$	$(022)M_3$ $(103)M_3$	$(121)M_7$	$(31\bar{2},40\bar{2})M_5$
10	59.50	1.952	4		$(211)M_3$	$(300)M_7$	
11	61.40	1.897	4		$(113)M_3$	$(112)M_7$	
12	64.95	1.804	11	$(200)_\gamma$		$(022)M_7$	$(312,511)M_5$
13	68.10	1.730	8			$(220)M_7$	
14	84.70	1.438	7			$(401)M_7$	
15	85.20	1.431	8	$(200)_\alpha (200)_{\alpha'}$			
16	99.50	1.269	5	$(220)_\gamma$			
17	111.05	1.175	12	$(211)_\alpha (211)_{\alpha'}$			$(62\bar{3},912)M_5$
18	112.70	1.164	13			$(322)M_7$	
19	113.70	1.157	7			$(501)M_7$	$(423,802)M_5$
20	126.05	1.087	5	$(311)_\gamma$			$(404)M_5$
21	138.08	1.037	5	$(022)_\alpha, (222)_\gamma$			
22	144.05	1.018	6	unidentified			
23	144.60	1.017	7				
24	145.70	1.014	8	$(220)_\alpha (220)_{\alpha'}$			
25	146.40	1.012	7				

Structure: Martensite
+ some austenite
+ M_3C [isomorphous with Fe_3C(23-1113)]
+ some M_7C_3 [isomorphous with Fe_7C_3(17-333)]
+ trace M_5C_2 [isomorphous with Fe_5C_2(20-508)]

TABLE 5.57

X-RAY DIFFRACTOGRAM OF ALLOY- A7

HEAT TREATMENT- As-cast

Sl. No.	2θ	d(Å)	$\frac{I}{I_o}$	(hkl) Matrix	(hkl) Carbide (s)		
1	48.04	2.380	2		$(112,021)M_3$		
2	50.67	2.264	8		$(200)M_3$	$(120)M_7$	$(020)M_5$
3	51.36	2.235	6		unidentified		$(11\bar{2})M_5$
4	54.90	2.101	3		$(121)M_3$	$(012)M_7$	$(112)M_5$
5	56.10	2.06	4		$(210)M_3$		$(021)M_5$ $(510)M_5$
6	57.10	2.027	100	$(110)_\alpha$	$(022)M_3$ $(103)M_3$	$(121)M_7$	$(40\bar{2})M_5$ $(31\bar{2})M_5$
7	59.00	1.967	3		$(211)M_3$	$(300)M_7$	$(600)M_5$
8	68.10	1.730	4		$(212)M_3$	$(220)M_7$	$(42\bar{1})M_5$
9	69.80	1.693	4				$(51\bar{2})M_5$
10	70.40	1.680	4		$(004,023)$		$(022)M_5$
11	84.95	1.435	8	$(200)_\alpha$			
12	111.90	1.169	18	$(211)_\alpha$		$(322)M_7$	
13	113.95	1.155	4				
14	114.15	1.154	4			$(501)M_7$	
15	146.10	1.013	9	$(220)_\alpha$			

Structure: Pearlite/bainite
+ M_3C [isomorphous with Fe_3C(23-1113)]
+ trace M_7C_3 [isomorphous with Fe_7C_3(17-333)]
+ trace M_5C_2 [isomorphous with Mn_5C_2(16-38)]

TABLE 5.59

X-RAY DIFFRACTOGRAM OF ALLOY- A7

HEAT TREATMENT- 4h 800°C AC

Sl. No.	2θ	d(Å)	$\frac{I}{I_o}$	(hkl)	
				Matrix	Carbide(s)
1	50.70	2.262	9		$(200)M_3$ $(120)M_7$
2	51.48	2.230	6		unidentified
3	54.95	2.100	4		$(121)M_3$ $(012)M_7$
4	55.86	2.068	8	$(011)_{\alpha'}$	$(210)M_3$
5	57.16	2.025	100	$(110)_{\alpha}(110)_{\alpha'}$	$(022)M_3$ $(103)M_3$ $(121)M_7$
6	59.00	1.967	3		$(211)M_3$ $(300)M_7$
7	68.20	1.728	3		$(220)M_7$
8	85.30	1.430	4	$(200)_{\alpha}(200)_{\alpha'}$	
9	111.60	1.171	10	$(211)_{\alpha}(211)_{\alpha'}$	$(322)M_7$
10	112.75	1.163	6		unidentified
11	114.00	1.155	4		$(501)M_7$
12	145.80	1.014	8	$(220)_{\alpha}(220)_{\alpha'}$	

Structure: Bainite
+ some martensite
+ M_3C [isomorphous with Fe_3C(23-1113)]
+ trace M_7C_3 [isomorphous with Fe_7C_3(17-333)]

TABLE 5.60

X-RAY DIFFRACTOGRAM OF ALLOY- A7
HEAT TREATMENT- 10h 800°C AC

Sl. No.	2θ	d(Å)	$\frac{I}{I_o}$	(hkl) Matrix	(hkl) Carbide(s)		
1	48.00	2.382	4		$(112,021)M_3$	$(311,20\bar{2})M_5$	
2	50.60	2.267	15		$(200)M_3$	$(020)M_5$	
3	51.20	2.242	6	unidentified			
4	54.85	2.103	7		$(121)M_3$		$(012)M_7$
5	55.80	2.070	36	$(011)_{\alpha'}, (111)_{\gamma}$	$(210)M_3$	$(510,021)M_5$	
6	57.17	2.025	100	$(110)_{\alpha}(110)_{\alpha'}$	$(022)M_3$ $(103)M_3$	$(31\bar{2},40\bar{2})M_5$	$(121)M_7$
7	58.70	1.976	6		$(211)M_3$	$(51\bar{1},22\bar{1})M_5$	$(300)M_7$
8	59.15	1.963	4	unidentified			
9	59.60	1.9491	4				
10	59.90	1.940	4			$(221)M_5$	
11	64.80	1.808	5			$(312,511)M_5$	$(301)M_7$
12	65.10	1.800	6		$(200)_{\gamma}$		$(022)M_7$
13	65.45	1.792	5				
14	68.10	1.730	5				$(220)M_7$
15	76.00	1.573	4			$(11\bar{3})M_5$	
16	85.30	1.430	7	$(200)_{\alpha}(200)_{\alpha'}$			
17	99.46	1.270	4		$(220)_{\gamma}$	$(53\bar{1})M_5$	
18	107.30	1.203	3	$(112)_{\alpha'}$			
19	110.50	1.179	5			$(62\bar{3},912)M_5$	
20	111.40	1.173	10	$(211)_{\alpha}(211)_{\alpha'}$		$(423,802)M_5$	$(322)M_7$
21	112.00	1.168	11				
22	113.45	1.159	8				$(501)M_7$
23	114.20	1.154	7				
24	127.95	1.078	4		$(311)_{\gamma}$		
25	138.15	1.037	6	$(022)_{\alpha'}, (222)_{\gamma}$			
26	145.55	1.014	8	$(220)_{\alpha}(022)_{\alpha'}$			
27	146.70	1.011	7				

Structure: Martensite
+ trace austenite
+ M_3C [isomorphous with Fe_3C(23-1113)]
+ some M_5C_2 [isomorphous with Fe_5C_2(20-508)]
+ some M_7C_3 [isomorphous with Fe_7C_3(17-333)]

TABLE 5.61

X-RAY DIFFRACTOGRAM OF ALLOY- A8
HEAT TREATMENT - As-cast

Sl. No.	2θ	d(Å)	$\frac{I}{I_o}$	(hkl) Matrix	(hkl) Carbide(s)		
1	47.95	2.384	4		$(112,021)M_3$		
2	50.67	2.264	4		$(200)M_3$	$(120)M_7$	$(020)M_5$
3	51.50	2.230	5		unidentified		
4	54.80	2.105	4		$(121)M_3$	$(021)M_7$	
5	55.88	2.067	7		$(210)M_3$		$(510,021)M_5$
6	57.20	2.024	100	$(110)_\alpha$	$(022)M_3$, $(103)M_3$	$(121)M_7$	$(31\bar{2},40\bar{2})M_5$
7	58.80	1.973	8		$(211)M_3$	$(300)M_7$	$(51\bar{1},22\bar{1})M_5$
8	62.28	1.873	4		$(113)M_3$	$(112)M_7$	
9	63.20	1.849	3		$(122)M_3$		
10	66.60	1.764	3		$(212)M_3$		$(402)M_5$
11	85.00	1.434	9	$(200)_\alpha$			
12	111.85	1.169	15	$(211)_\alpha$		$(322)M_7$	$(62\bar{3},912)M_5$
13	113.20	1.160	3				$(423.802)M_5$
14	114.30	1.153	3			$(501)M_7$	
15	145.80	1.014	8	$(220)_\alpha$			
16	146.50	1.012	6				

Structure: Pearlite/bainite (austenite not detected)
+ M_3C [isomorphous with Fe_3C(23-1113)]
+ trace M_7C_3 [isomorphous with Fe_7C_3(17-333)]
+ trace M_5C_2 [isomorphous with Fe_5C_2(20-508)]

TABLE 5.64

X-RAY DIFFRACTOGRAM OF ALLOY- A8

HEAT TREATMENT- 6h 950°C AC

Sl No	2θ*	d(Å)	$\frac{I}{I_o}$	(hkl) Matrix	(hkl) Carbide(s)	
1	60.60	2.270	17		$(200)M_3$	$(240,241)M_7$
2	65.64	2.113	5		$(121)M_3$	$(051,202)M_7$
3	66.80	2.081	100	$(111)_\gamma$	$(210)M_3$	
4	68.80	2.028	27		$(022)M_3$ $(103)M_3$	$(600,122)M_7$
5	69.70	2.005	6	Unidentified		
6	78.62	1.808	58	$(200)_\gamma$		$(431,402)M_7$
7	82.60	1.736	3			$(530,322)M_7$
8	127.6	1.277	13	$(220)_\gamma$		
9	128.8	1.270	13			

Structure: Austenite
+ M_3C [isomorphous with Fe_3C(23-1113)]
+ some M_7C_3 [isomorphous with $(FeCr)_7C_3$(5-072)]

* Target- Cr

TABLE 5.66A

CUMULATIVE WEIGHT LOSS IN DISC-PIN TEST

Alloy	Heat Treatment	Weight loss in gms					
		15	30	45	60	75	90
		(minutes)					
A1	As-cast	0.885	2.680	4.870	7.060	9.195	10.590
A1	750°C 10h AC	1.305	3.565	6.115	8.797	10.985	12.405
A1	900°C 10h AC	0.945	2.460	4.580	6.185	7.723	9.704
A2	As-cast	2.928	5.230	7.450	9.422	11.214	14.819
A2	850°C 4h AC	2.227	3.970	5.442	7.118	10.314	11.774
A2	900°C 2h AC	1.060	2.352	3.567	6.795	8.036	9.085
A2	900°C 6h AC	1.667	2.864	3.833	6.565	7.786	8.968
A2	900°C 10h AC	1.735	2.815	4.292	6.374	7.668	8.724
A3	As-cast	1.376	3.532	6.276	8.079	9.040	9.624
A3	800°C 2h AC	1.383	5.738	8.397	10.445	11.631	12.467
A3	800°C 4h AC	1.665	6.059	9.458	10.391	11.494	12.267
A3	800°C 8h AC	1.382	4.969	7.727	9.235	10.683	11.765
A4	As-cast	2.991	4.837	6.249	7.057	8.370	10.616
A4	800°C 10h AC	4.110	5.401	7.159	8.441	10.028	11.541

TABLE 5.66B

CUMULATIVE WEIGHT LOSS IN DISC-PIN TEST

Alloy	Heat-treatment	Weight loss in gms					
		15	30	45	60	75	90
		(minutes)					
A5	As-cast	3.114	4.689	6.079	6.804	7.996	9.716
A5	850°C 10h AC	2.582	3.782	5.093	5.781	6.907	7.678
A5	900°C 2h AC	2.351	3.617	4.704	5.987	6.958	8.907
A5	900°C 4h AC	2.309	3.364	4.292	5.067	6.011	7.159
A_5	900°C 6h AC	2.354	3.590	4.566	5.238	5.967	7.037
A_5	900°C 10h AC	2.901	3.830	4.560	5.246	6.063	6.956
A_6	As-cast	1.415	2.419	3.847	5.813	7.693	9.586
A_6	800°C 2h AC	2.012	3.530	5.345	7.152	9.094	10.936
A_6	850°C 2h AC	2.274	4.085	6.051	7.584	9.501	11.108
A_6	850°C 4h AC	2.627	4.757	6.972	8.792	10.690	11.965
A_7	As-cast	2.955	5.040	6.928	9.927	11.964	13.423
A_7	800°C 2h AC	2.424	4.456	6.698	9.063	11.340	12.830
A_7	800°C 4h AC	2.636	4.525	6.502	9.125	11.359	12.736
A_7	800°C 8h AC	3.231	5.186	7.505	10.168	12.445	13.753
A_8	As-cast	2.162	5.034	6.489	8.357	10.346	11.369
A_8	800°C 8h AC	2.648	5.267	6.008	8.059	10.130	11.399
A_8	800°C 10h AC	3.742	5.950	9.320	11.923	14.364	16.103
A_8	850°C 10h AC	2.619	5.152	7.233	10.439	12.804	14.383
A_8	900°C 10h AC	2.584	4.656	6.789	9.092	10.767	11.779

TABLE 5.67A

EFFECT OF HEAT TREATMENT ON GOUGING WEAR

Alloy	Heat-treatment	Hardness (HV_{50})	Gouging Wear (gms/min)
A1	As-cast	603	0.145
A1	750°C 10h AC	537	0.159
A_1	900°C 10h AC	649	0.121
A2	As-cast	625	0.150
A2	850°C 4h AC	815	0.132
A2	900°C 2h AC	690	0.100
A_2	900°C 6h AC	729	0.095
A_2	900°C 10h AC	796	0.088
A3	As-cast	637	0.172-0.053
A3	800°C 2h AC	715	0.255-0.076
A3	800°C 4h AC	757	0.258-0.066
A_3	800°C 8h AC	821	0.238-0.089
A4	As-cast	593	0.100
A4	800°C 10h AC	800	0.100

TABLE 5.67B

EFFECT OF HEAT TREATMENT ON GOUGING WEAR

Alloy	Heat-treatment	Hardness (HV_{50})	Gouging Wear (gms/min)
A5	As-cast	539	0.090
A5	750°C 10h AC	487	0.073
A5	900°C 2h AC	604	0.084
A5	900°C 4h AC	633	0.068
A5	900°C 6h AC	641	0.077
A5	900°C 10h AC	725	0.060
A6	As-cast	570	0.101
A6	800°C 2h AC	658	0.121
A6	850°C 2h AC	846	0.120
A6	850°C 4h AC	847	0.133
A7	As-cast	613	0.142
A7	800°C 2h AC	713	0.144
A7	800°C 4h AC	777	0.144
A7	800°C 8h AC	803	0.153
A7	800°C 10h AC	842	0.136-0.095
A7	900°C 10h AC	785	0.144
A8	As-cast	666	0.159-0.093
A8	800°C 8h AC	827	0.159-0.093
A8	850°C 10h AC	801	0.170
A8	900°C 10h AC	660	0.157-0.093

TABLE 5.68

CUMULATIVE WEIGHT LOSS IN SLURRY POT TEST

Alloy	Heat treatment	Weight loss in gms				
		10 h	20 h	30 h	40 h	50 h
A1	As-cast	0.312	0.753	1.257	1.749	2.246
A2	As-cast	0.308	0.789	1.351	1.754	2.283
A3	As-cast	0.538	1.075	1.489	1.992	2.495
A5	As-cast	0.565	1.097	1.637	2.233	2.846
A6	As-cast	0.441	0.896	1.538	2.087	2.805
A7	As-cast	0.379	0.941	1.558	1.941	2.425
A8	As-cast	0.336	0.861	1.387	1.776	2.226
A1	900°C 8h AC	0.735	1.088	1.544	1.981	2.466
A2	850°C 2h AC	0.531	0.859	1.308	1.876	2.288
A3	850°C 2h AC	0.309	0.529	0.839	1.131	1.477
A5	900°C 8h AC	0.326	0.686	1.069	1.568	2.014
A6	850°C 2h AC	0.274	0.741	1.106	1.692	2.111
A7	850°C 2h AC	0.213	0.472	0.826	1.228	1.594
A8	850°C 2h AC	0.290	0.603	1.092	1.623	2.104
A1	950°C 6h AC	0.305	0.568	0.769	1.271	1.704
A2	900°C 4h AC	0.444	1.021	1.409	2.119	2.722
A3	900°C 4h AC	0.318	0.533	0.805	1.217	1.643
A5	950°C 6h AC	0.380	0.833	1.225	1.717	2.277
A6	900°C 4h AC	0.537	1.082	1.559	2.176	2.936
A7	900°C 4h AC	0.427	0.729	0.962	1.473	2.071
A8	900°C 4h AC	0.700	1.085	1.438	2.260	2.967

TABLE 5.69

EFFECT OF HEAT TREATMENT ON EROSION WEAR

Alloy	Heat Treatment	Erosion Wear
A1	As-cast	0.048
A2	As-cast	0.049
A3	As-cast	0.059
A5	As-cast	0.070
A6	As-cast	0.056
A7	As-cast	0.054
A8	As-cast	0.054-0.043
A1	900°C 8h AC	0.034-0.048
A2	850°C 2h AC	0.036-0.050
A3	850°C 2h AC	0.028-0.033
A5	900°C 8h AC	0.037-0.047
A6	850°C 2h AC	0.047-0.046
A7	850°C 2h AC	0.029-0.037
A8	850°C 2h AC	0.038-0.051
A1	950°C 6h AC	0.026-0.044
A2	900°C 4h AC	0.049-0.062
A3	900°C 4h AC	0.024-0.045
A5	950°C 6h AC	0.040-0.055
A6	900°C 6h AC	0.051-0.074
A7	900°C 6h AC	0.019-0.059
A8	900°C 6h AC	0.046-0.070

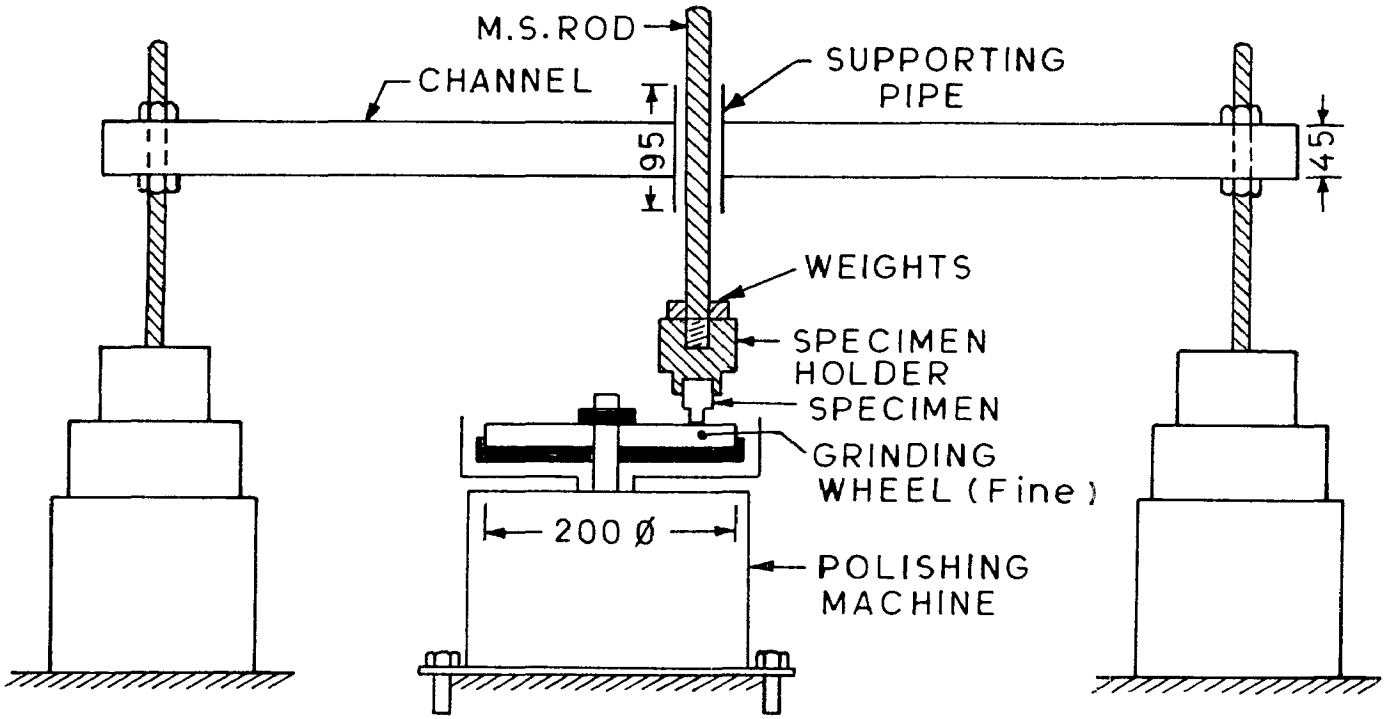

Dimensions in mm

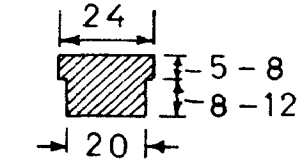

TEST SPECIMEN

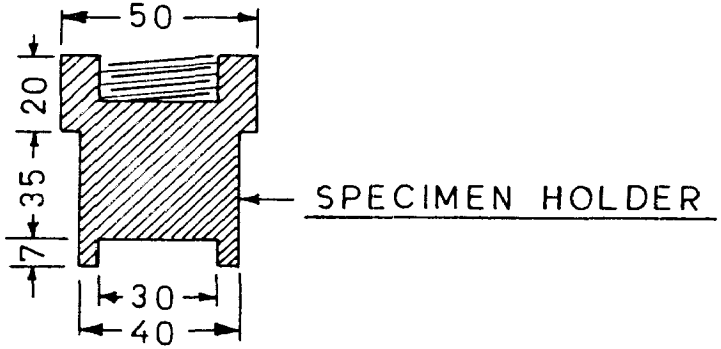

SPECIMEN HOLDER

FIG. 4.1 DISC - PIN RIG FOR GOUGING WEAR TEST

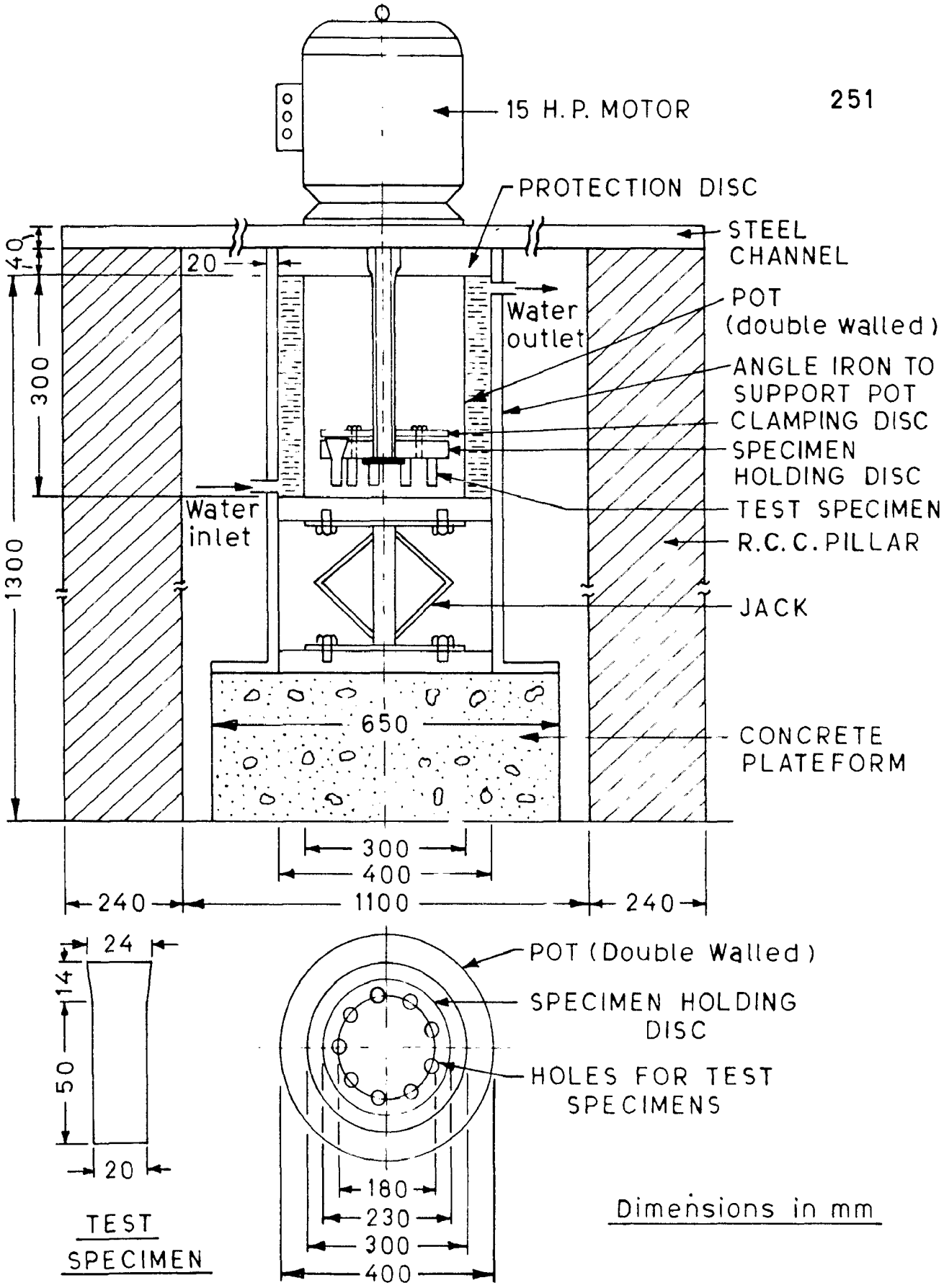

FIG. 4.2 SLURRY-POT RIG FOR EROSION WEAR TEST

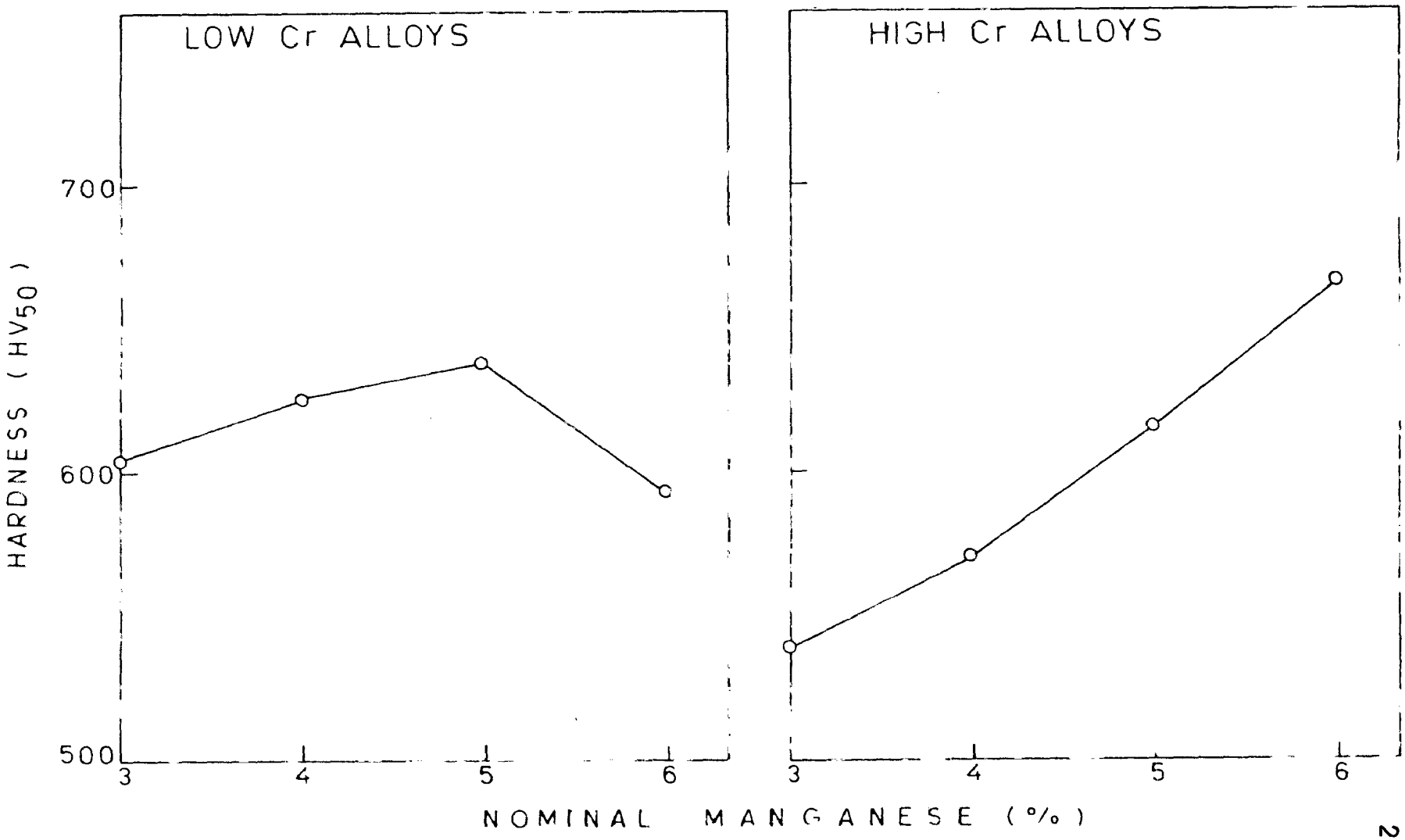

FIG. 5.1 EFFECT OF Mn CONTENT ON AS CAST HARDNESS.

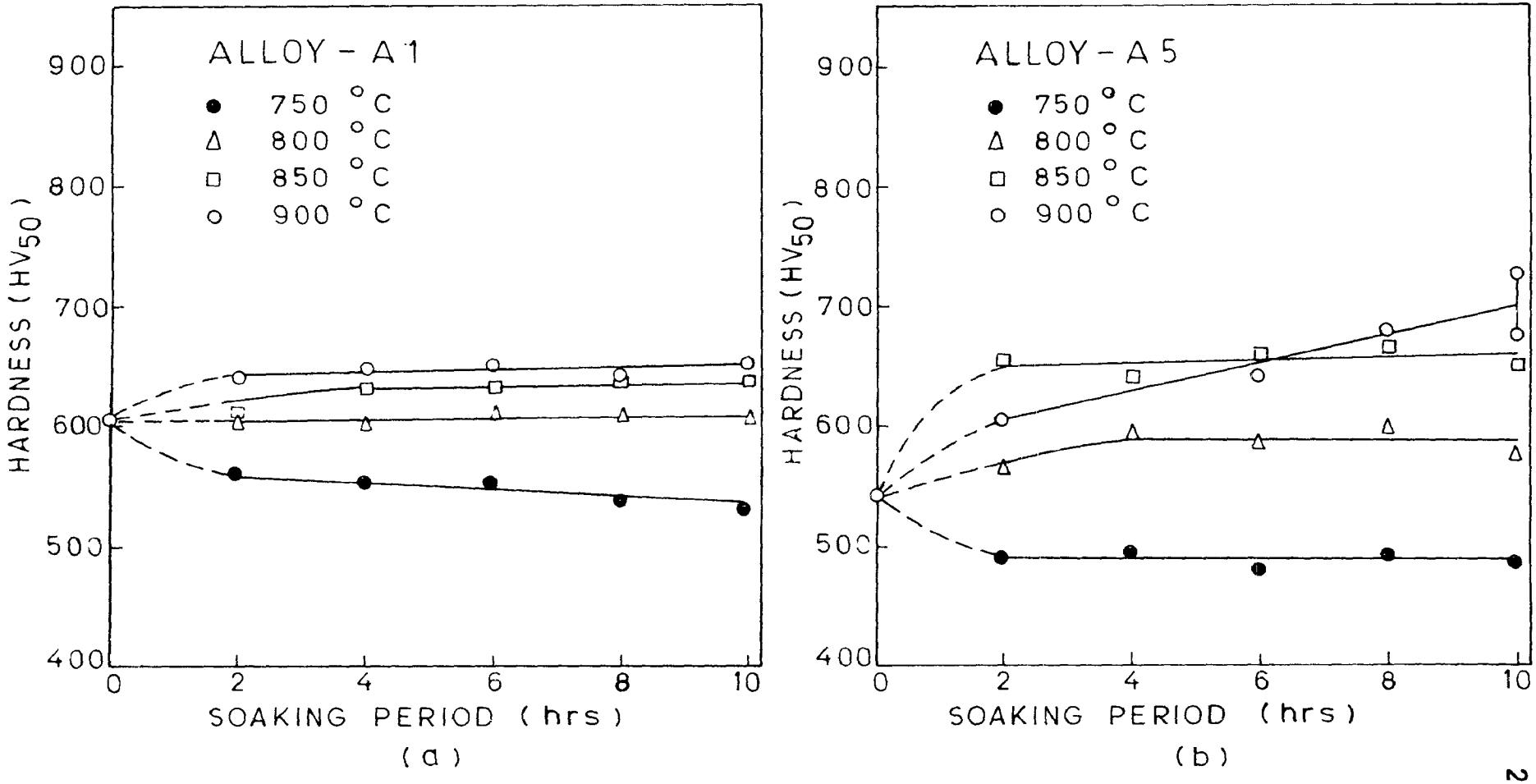

FIG. 5.2 EFFECT OF SOAKING PERIOD ON HARDNESS AT DIFFERENT TEMPERATURES.

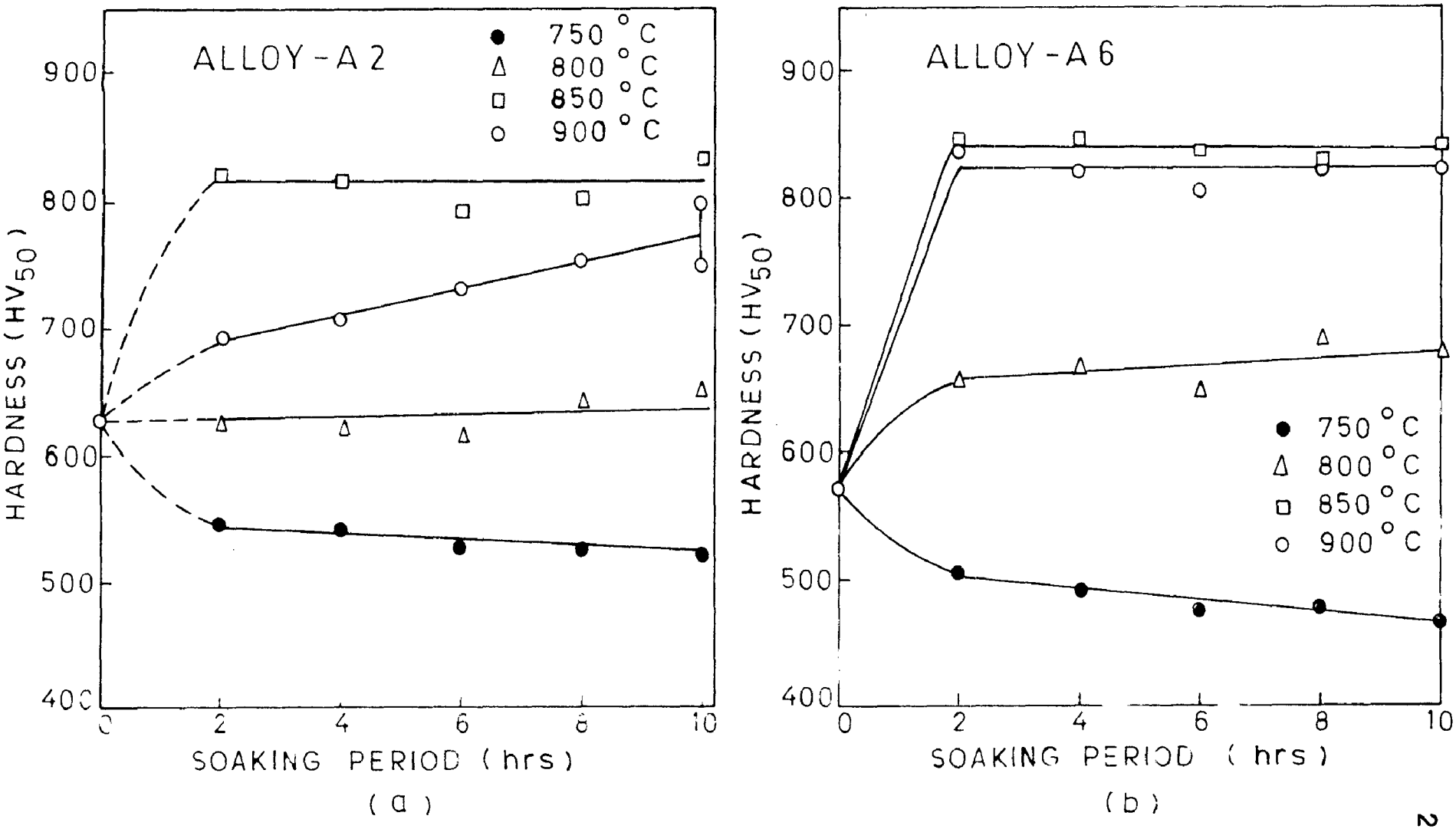

FIG.5.3 EFFECT OF SOAKING PERIOD ON HARDNESS AT DIFFERENT TEMPERATURES.

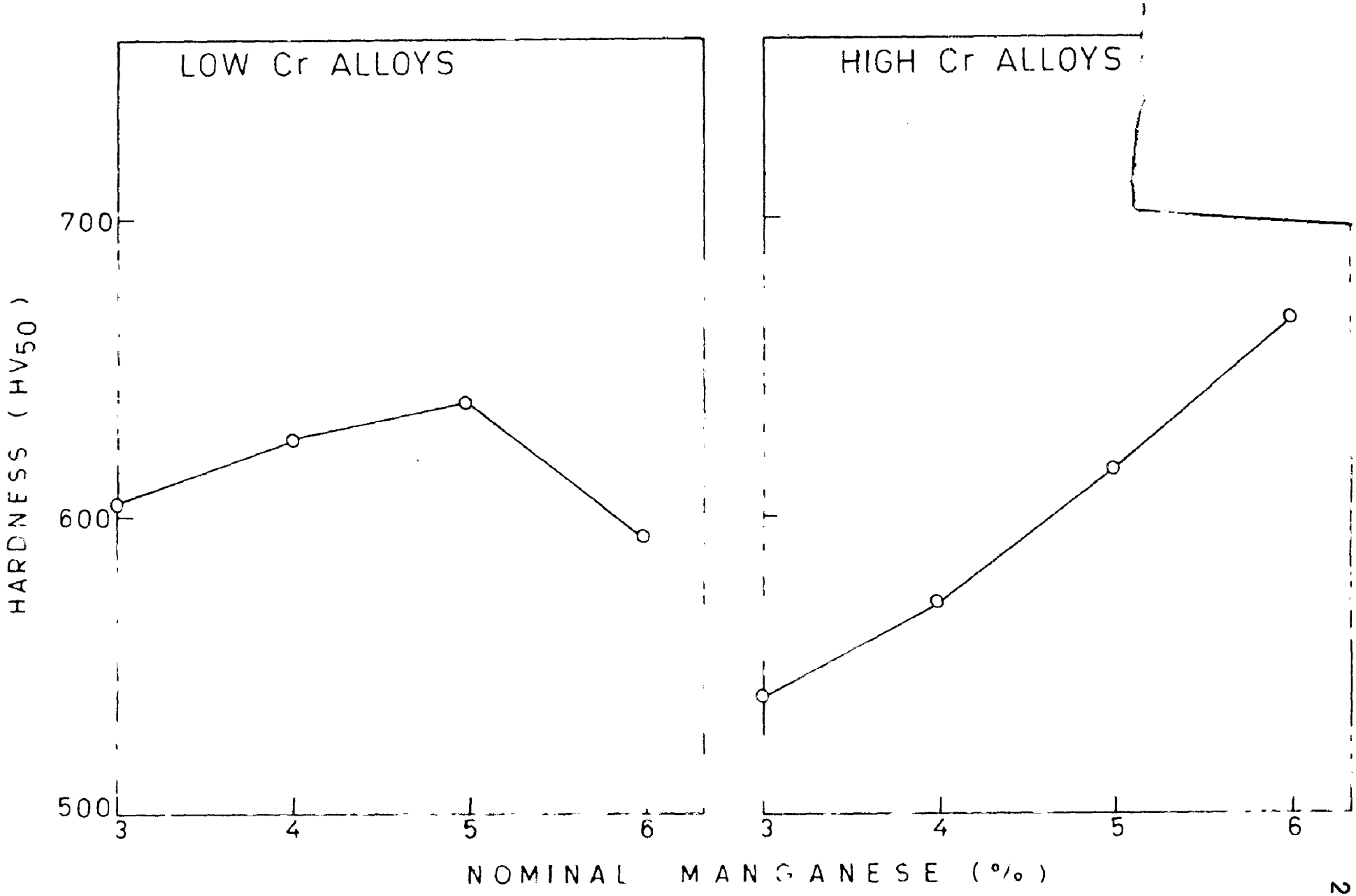

FIG. 5.1 EFFECT OF Mn CONTENT ON AS CAST HARDNESS.

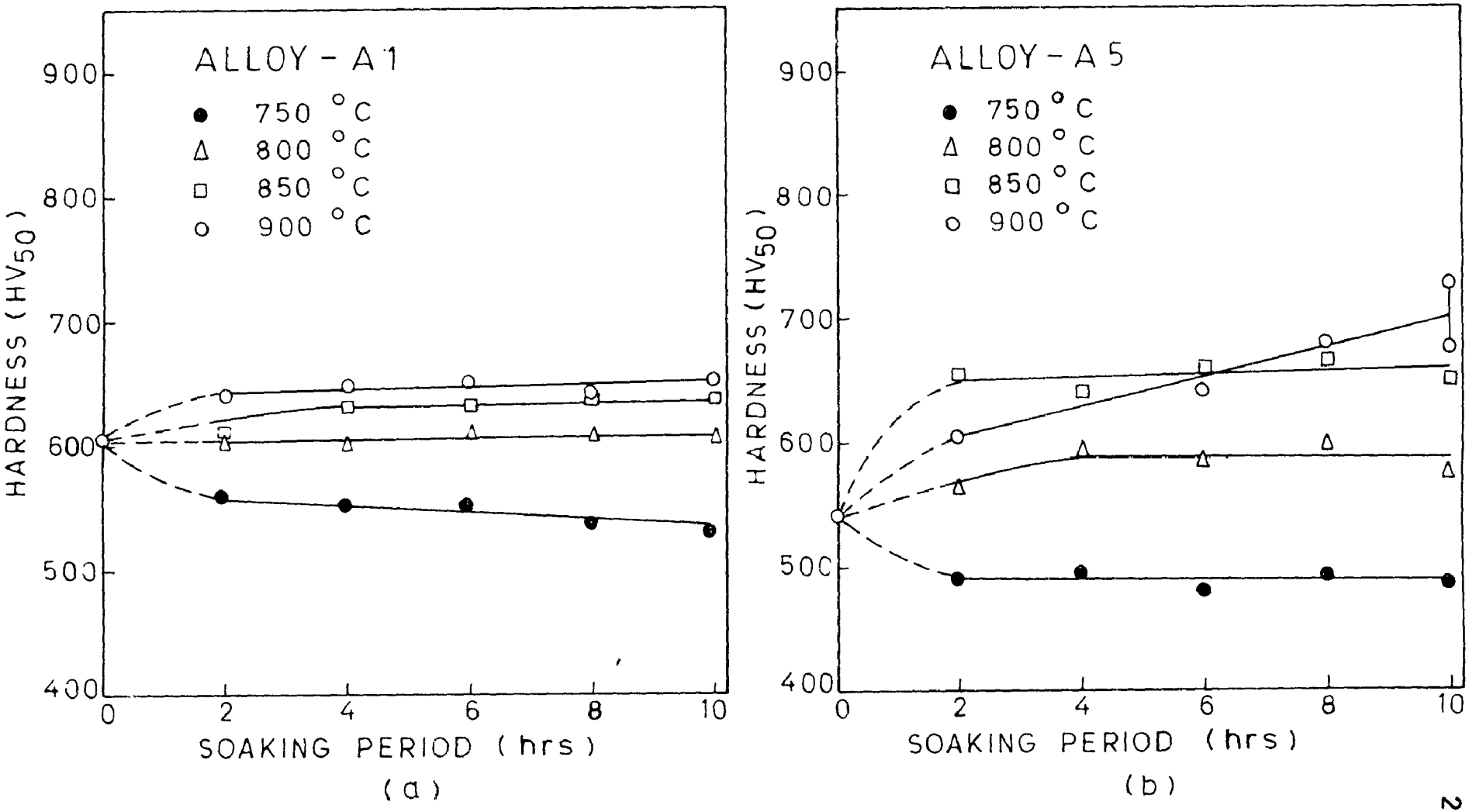

FIG. 5.2 EFFECT OF SOAKING PERIOD ON HARDNESS AT DIFFERENT TEMPERATURES.

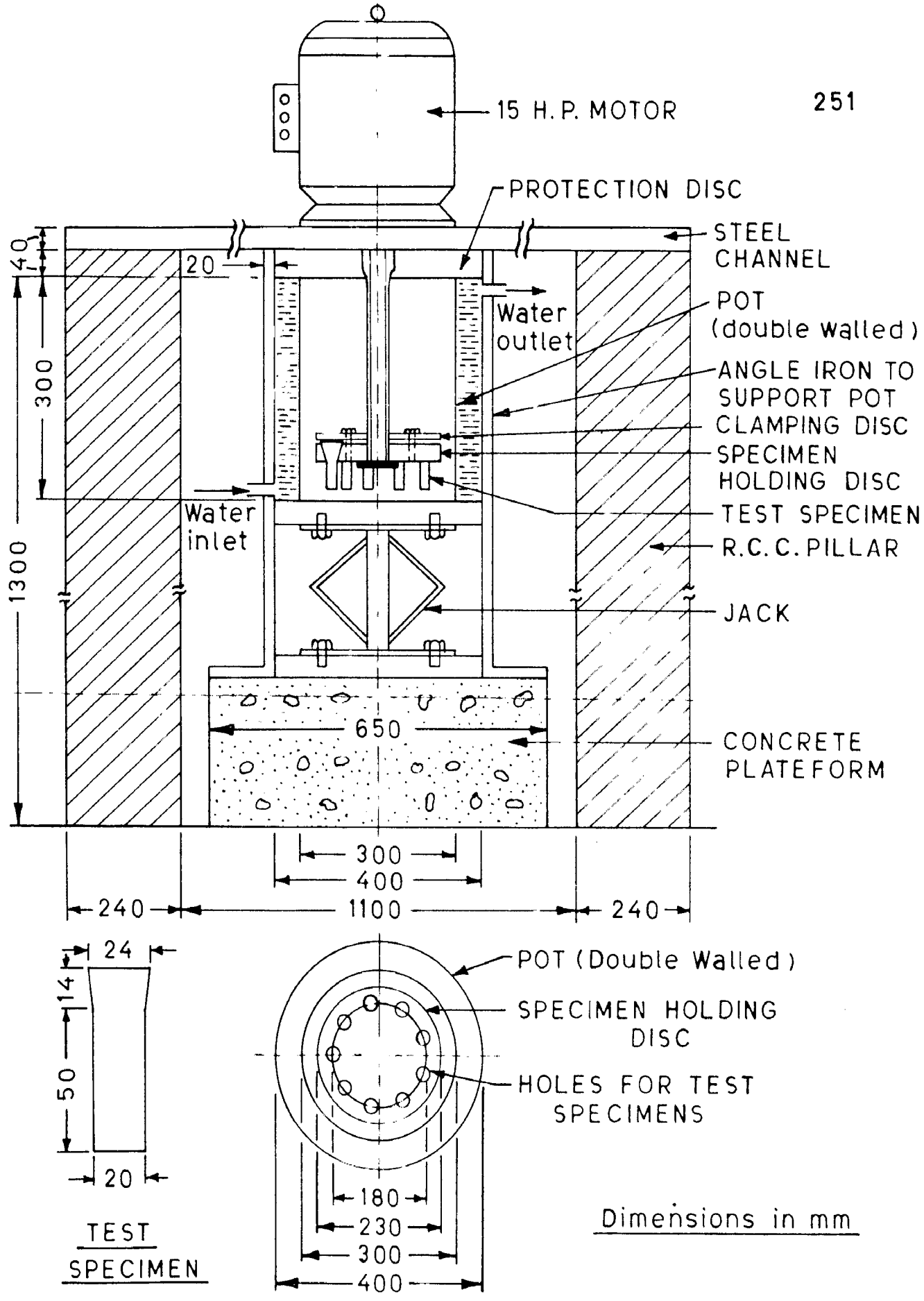

FIG. 4.2 SLURRY-POT RIG FOR EROSION WEAR TEST

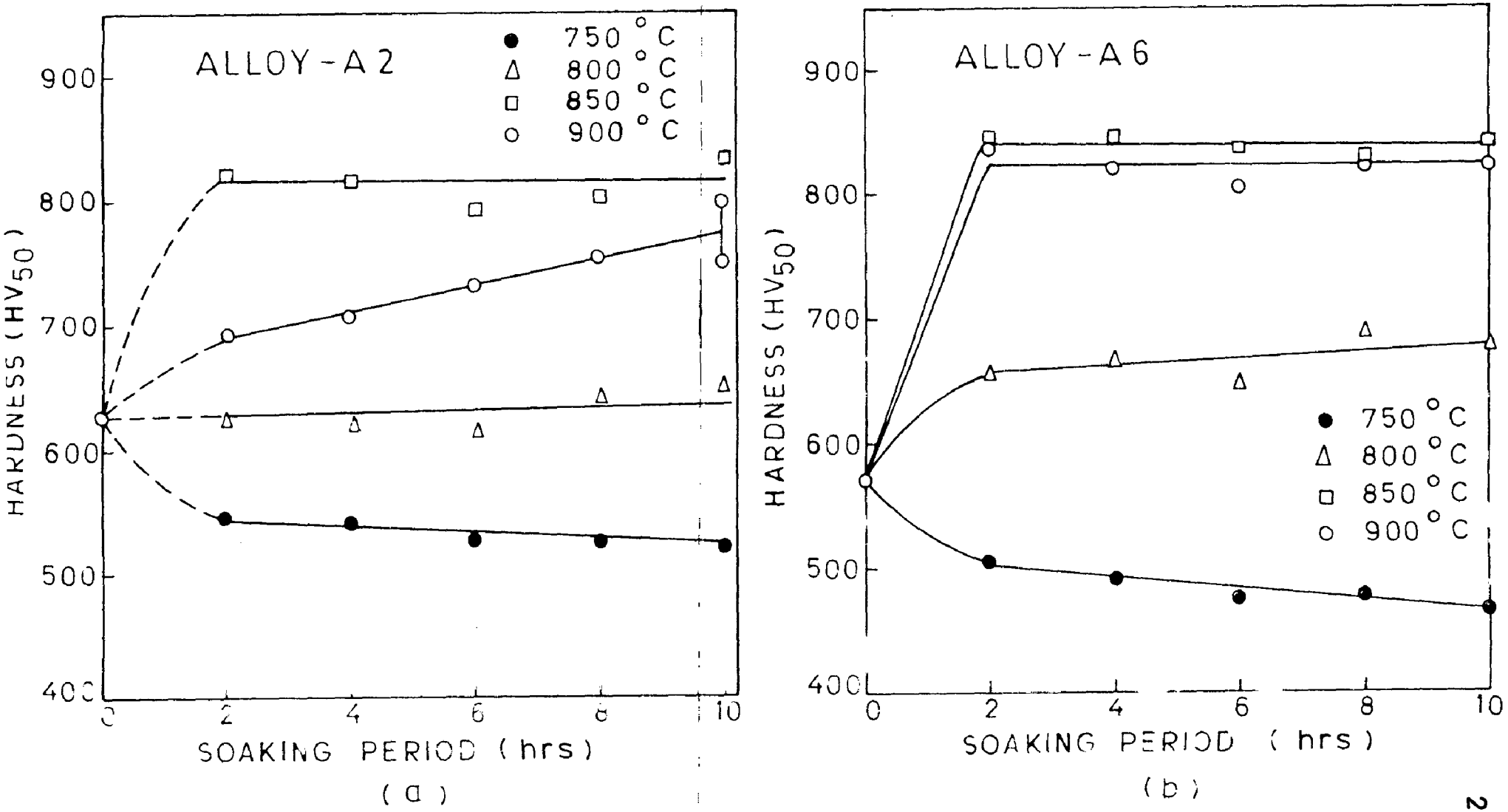

FIG.5.3 EFFECT OF SOAKING PERIOD ON HARDNESS AT DIFFERENT TEMPERATURES.

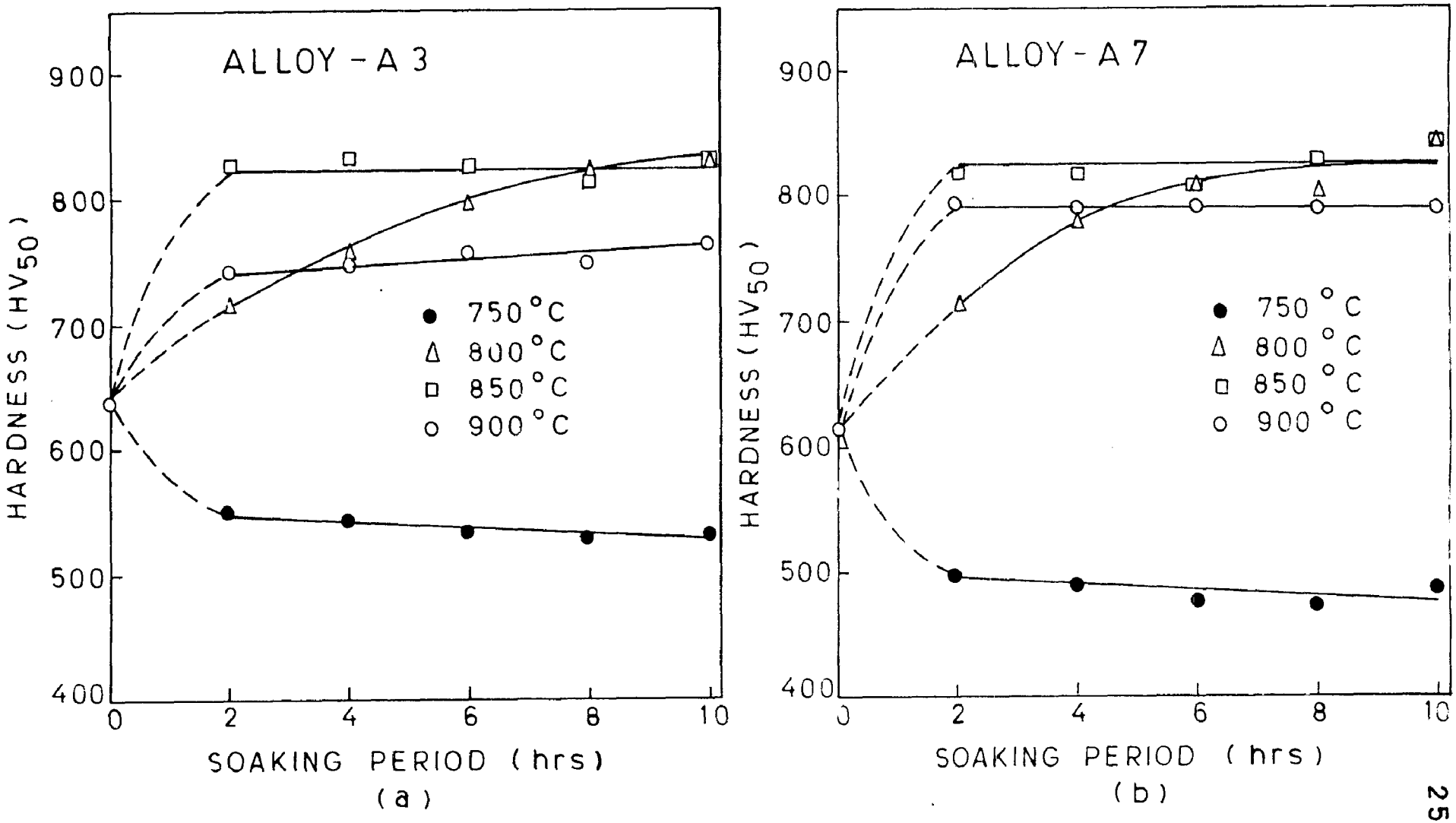

FIG. 5.4 EFFECT OF SOAKING PERIOD ON HARDNESS AT DIFFERENT TEMPERATURES.

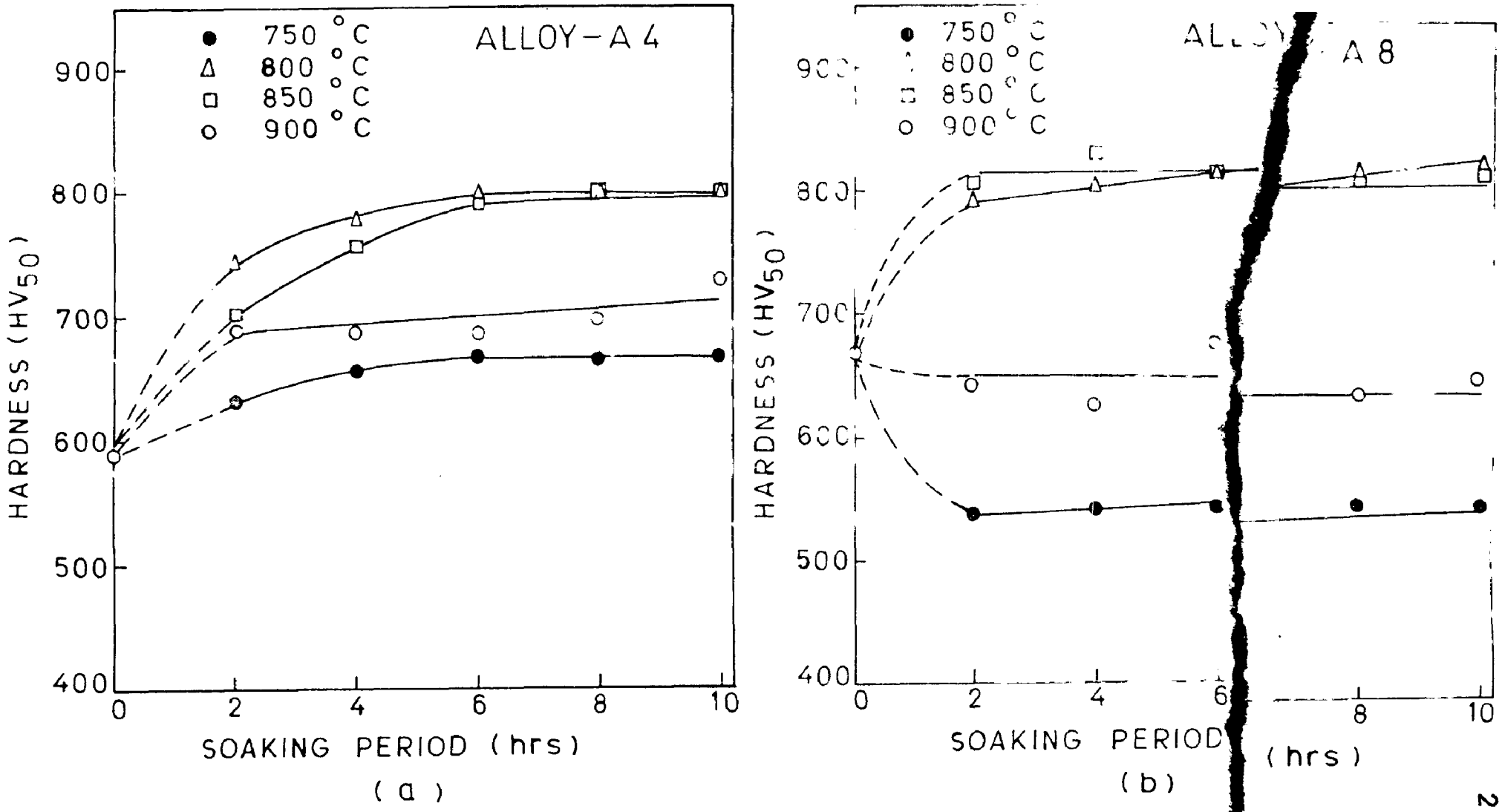

FIG. 5.5 EFFECT OF SOAKING PERIOD ON HARDNESS AT DIFFERENT TEMPERATURES.

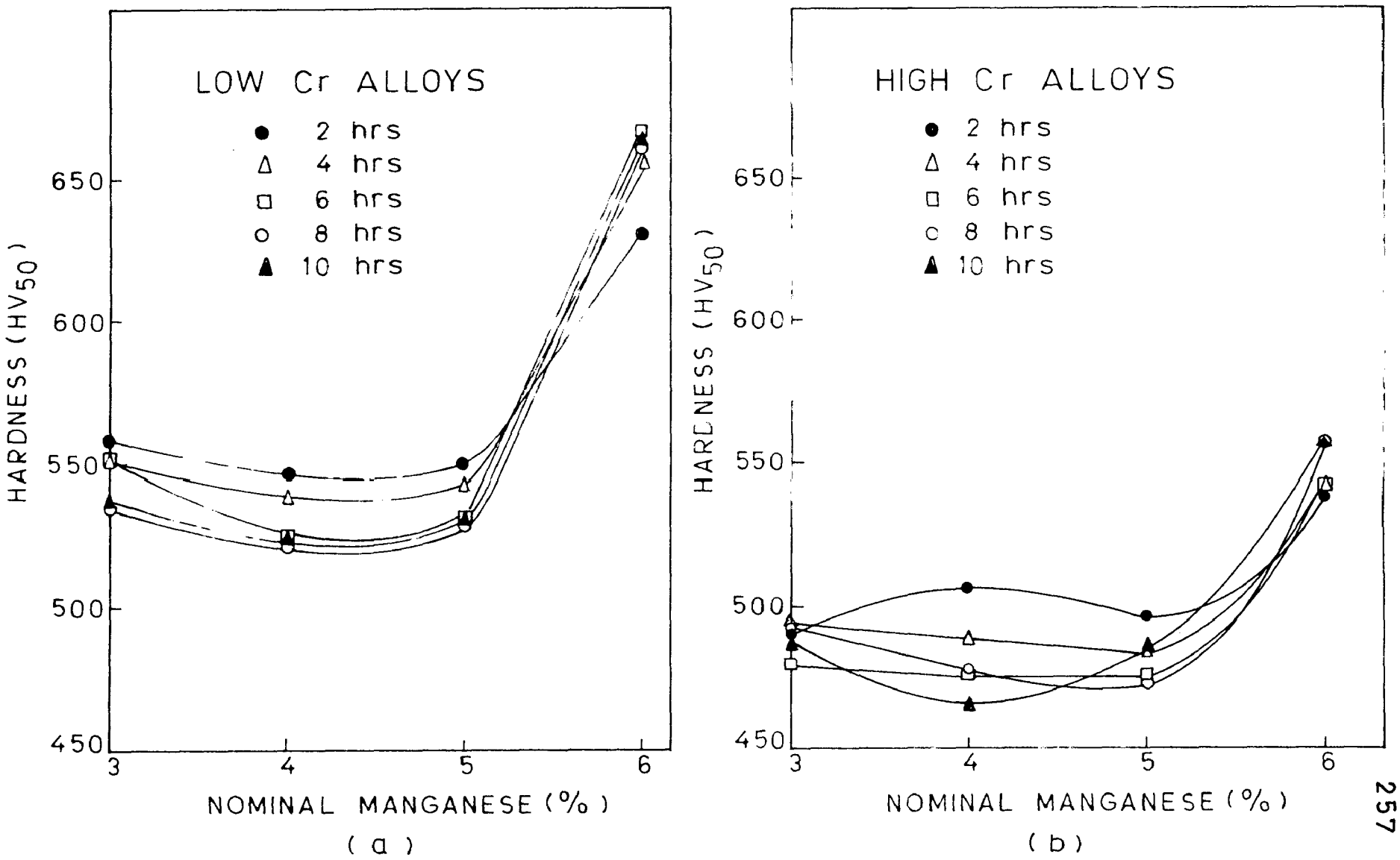

FIG. 5.6 EFFECT OF Mn CONTENT AND SOAKING PERIOD ON HARDNESS AT 750 °C.

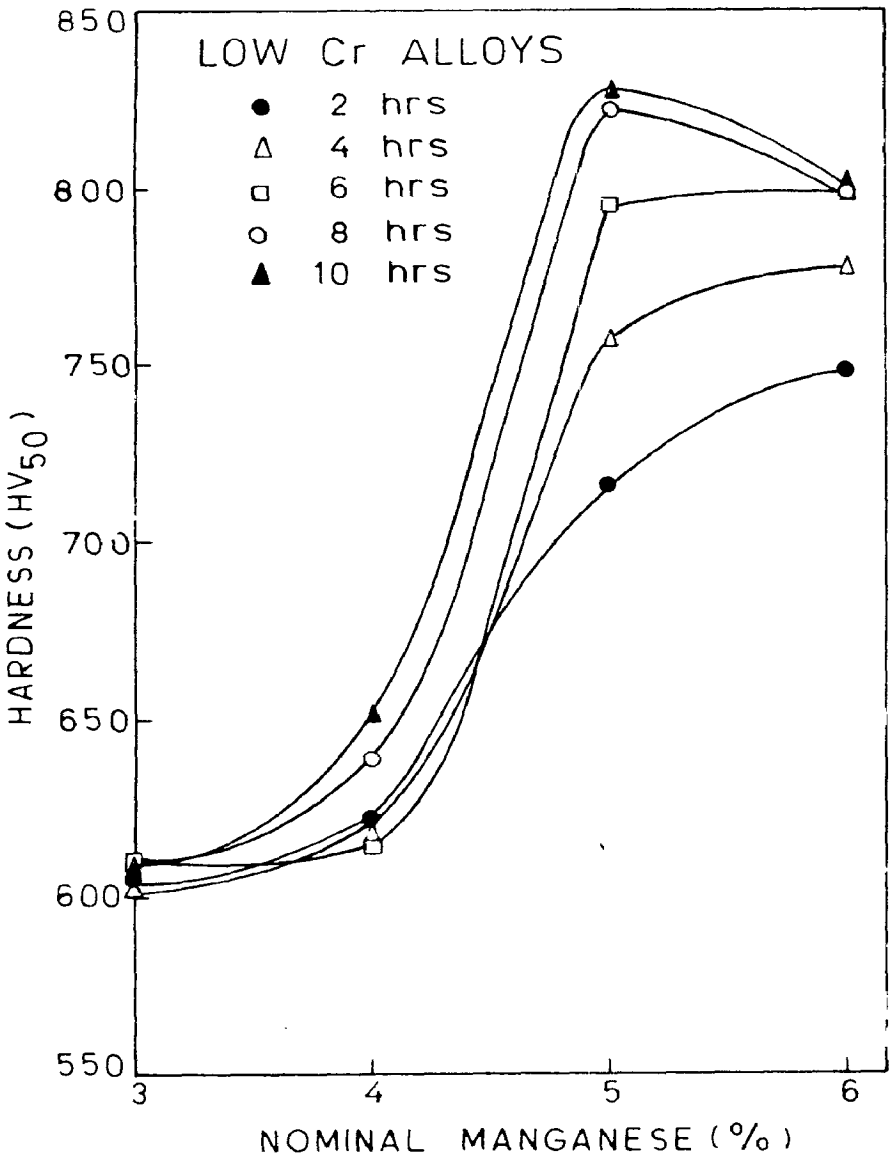

(a)

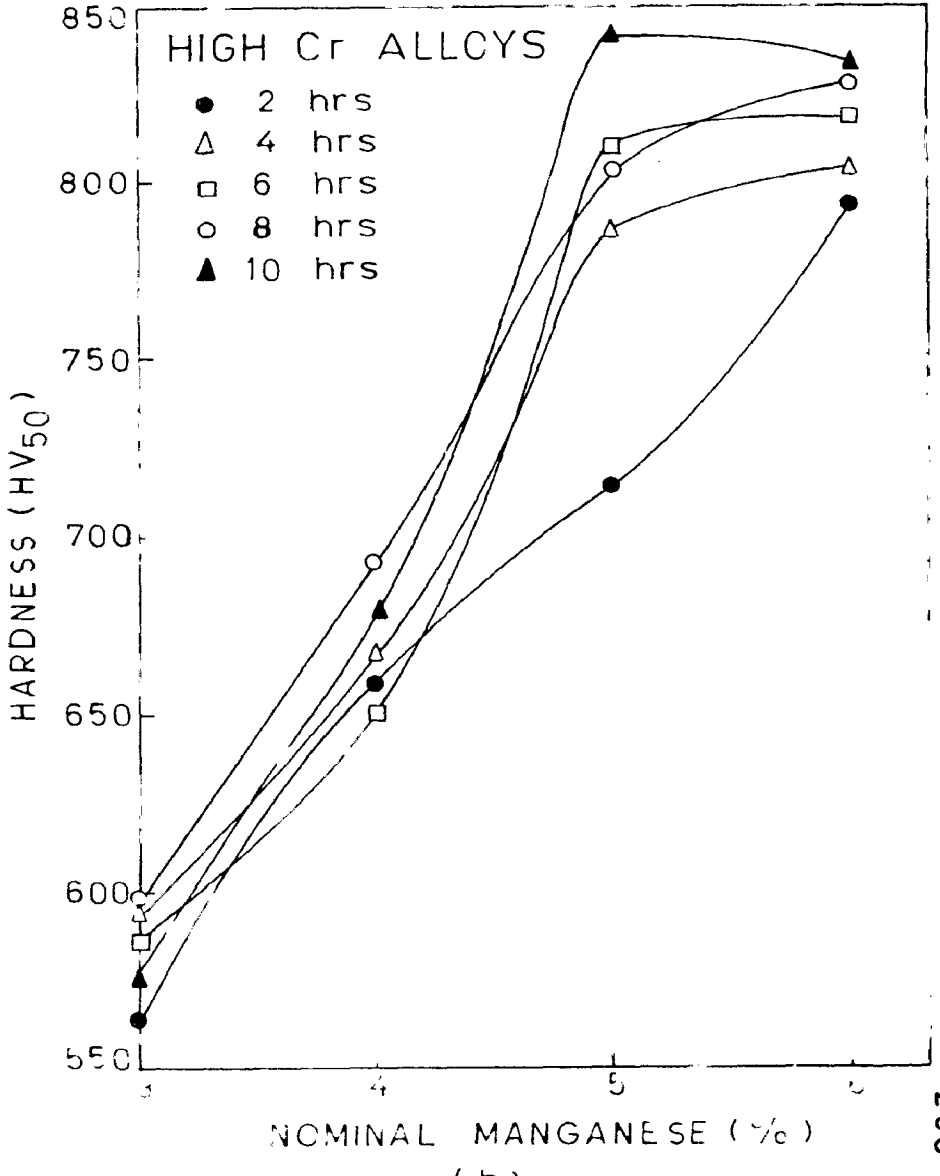

(b)

FIG. 5.7 EFFECT OF Mn CONTENT AND SOAKING PERIOD ON HARDNESS AT 800 °C.

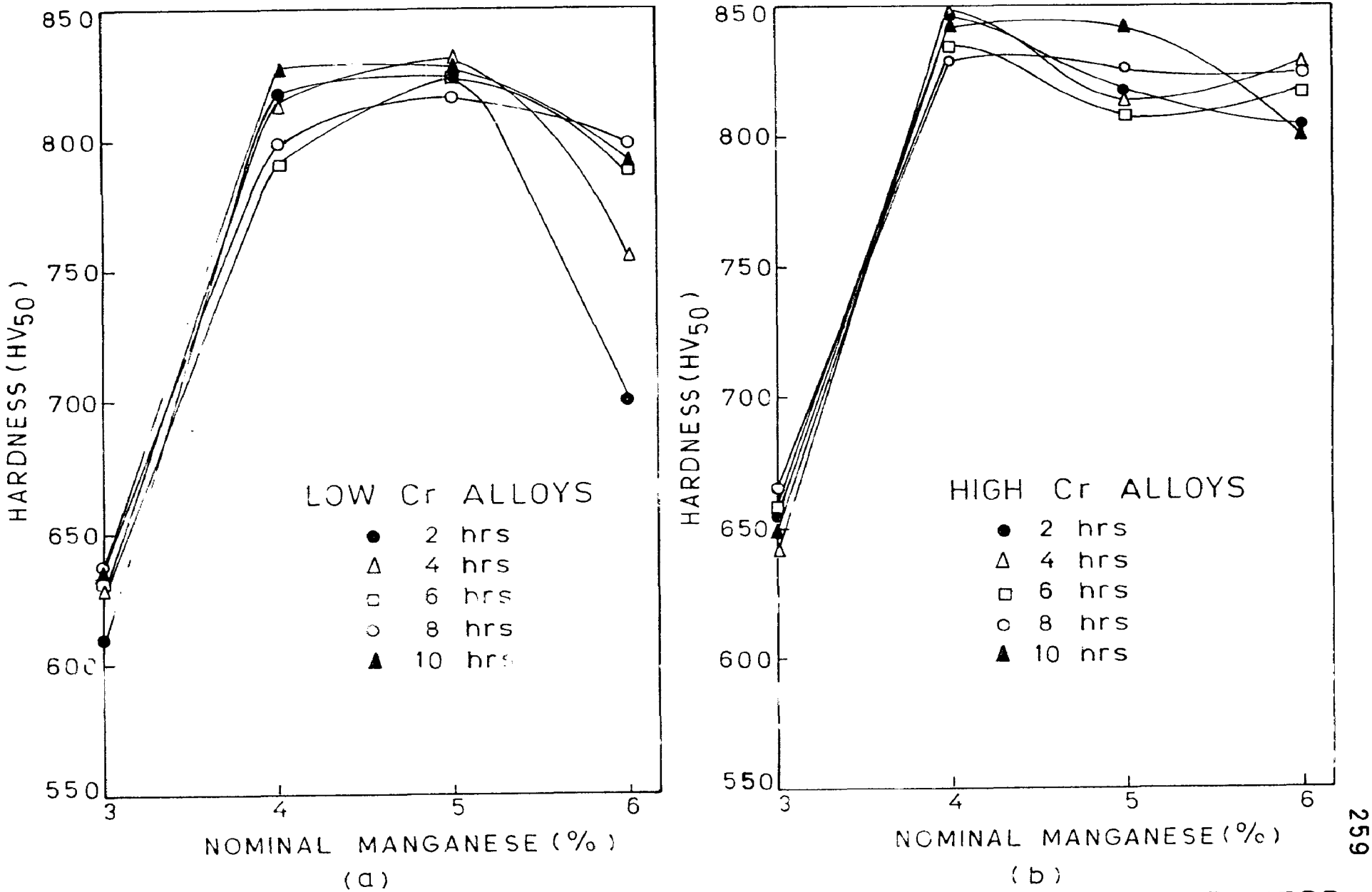

FIG 5.8 EFFECT OF Mn CONTENT AND SOAKING PERIOD ON HARDNESS AT 850 °C.

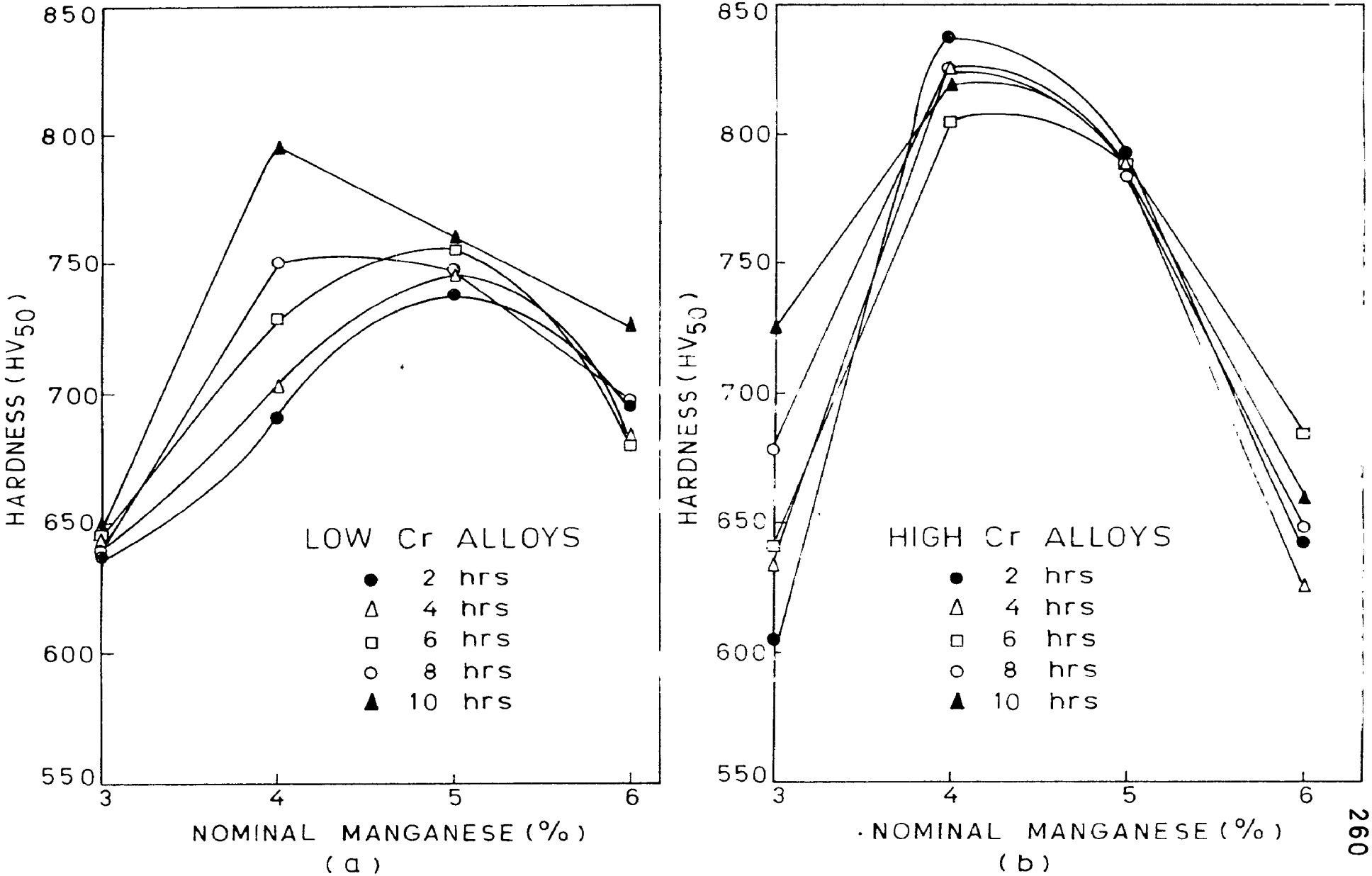

FIG.5.9 EFFECT OF Mn CONTENT AND SOAKING PERIOD ON HARDNESS AT 900 °C.

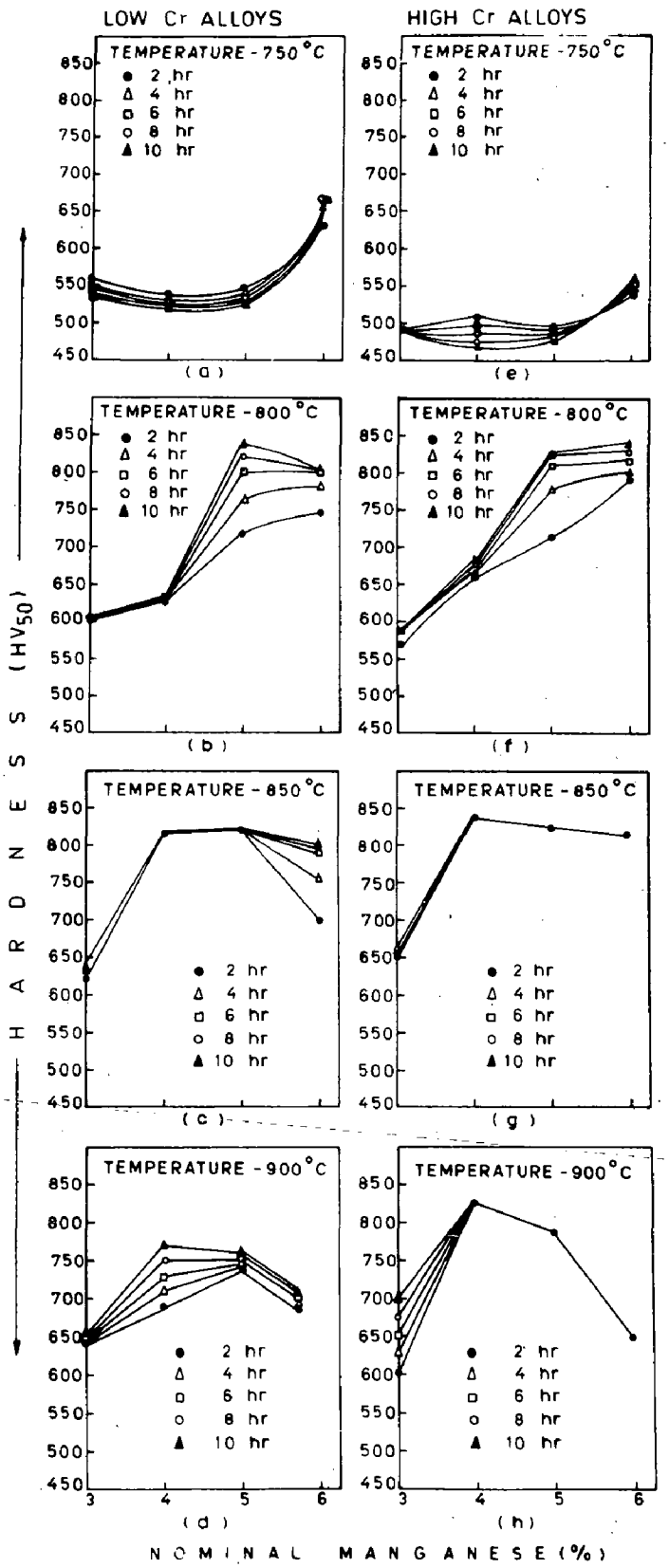

FIG. 5.10 EFFECT OF Mn CONTENT AND SOAKING PERIOD ON HARDNESS AT DIFFERENT TEMPERATURES.

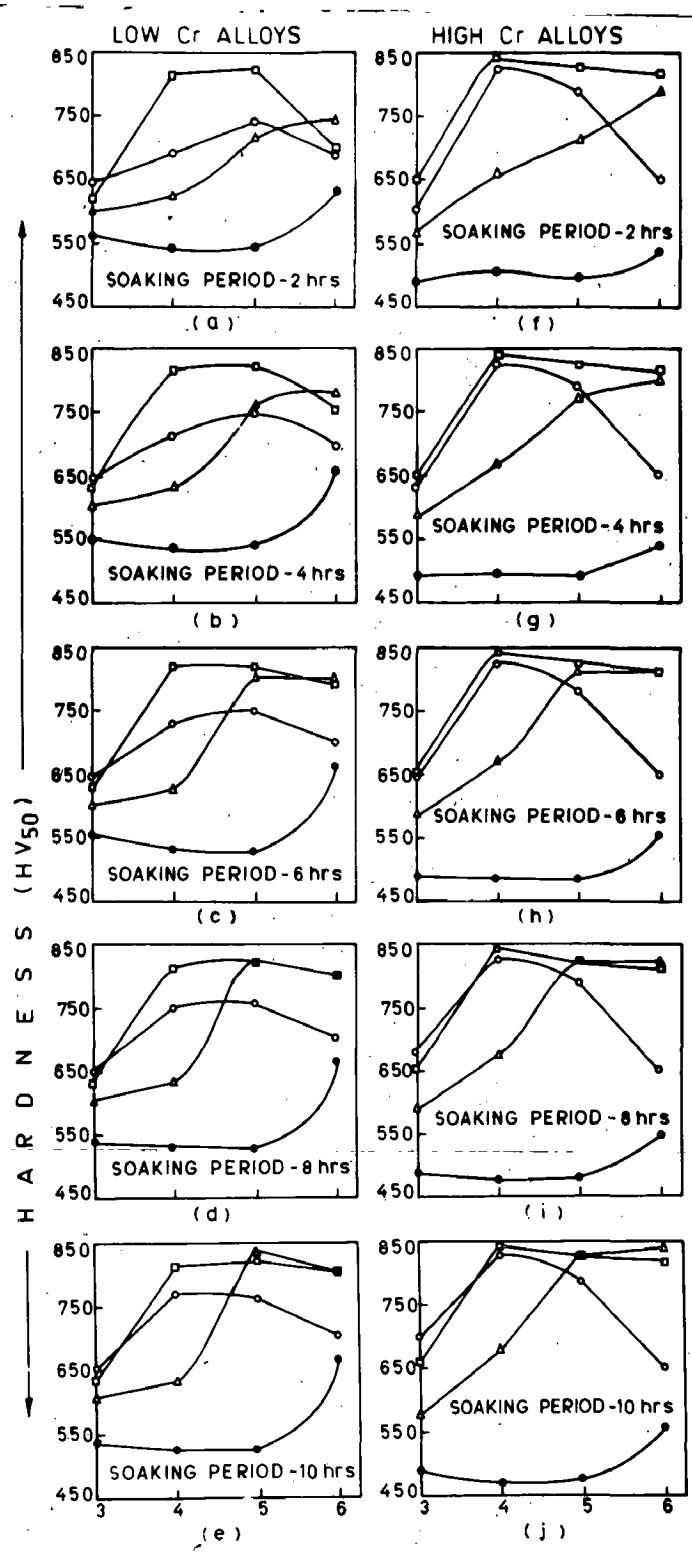

FIG. 5.11 EFFECT OF Mn CONTENT AND TEMPERATURE AT DIFFERENT SOAKING PERIODS.

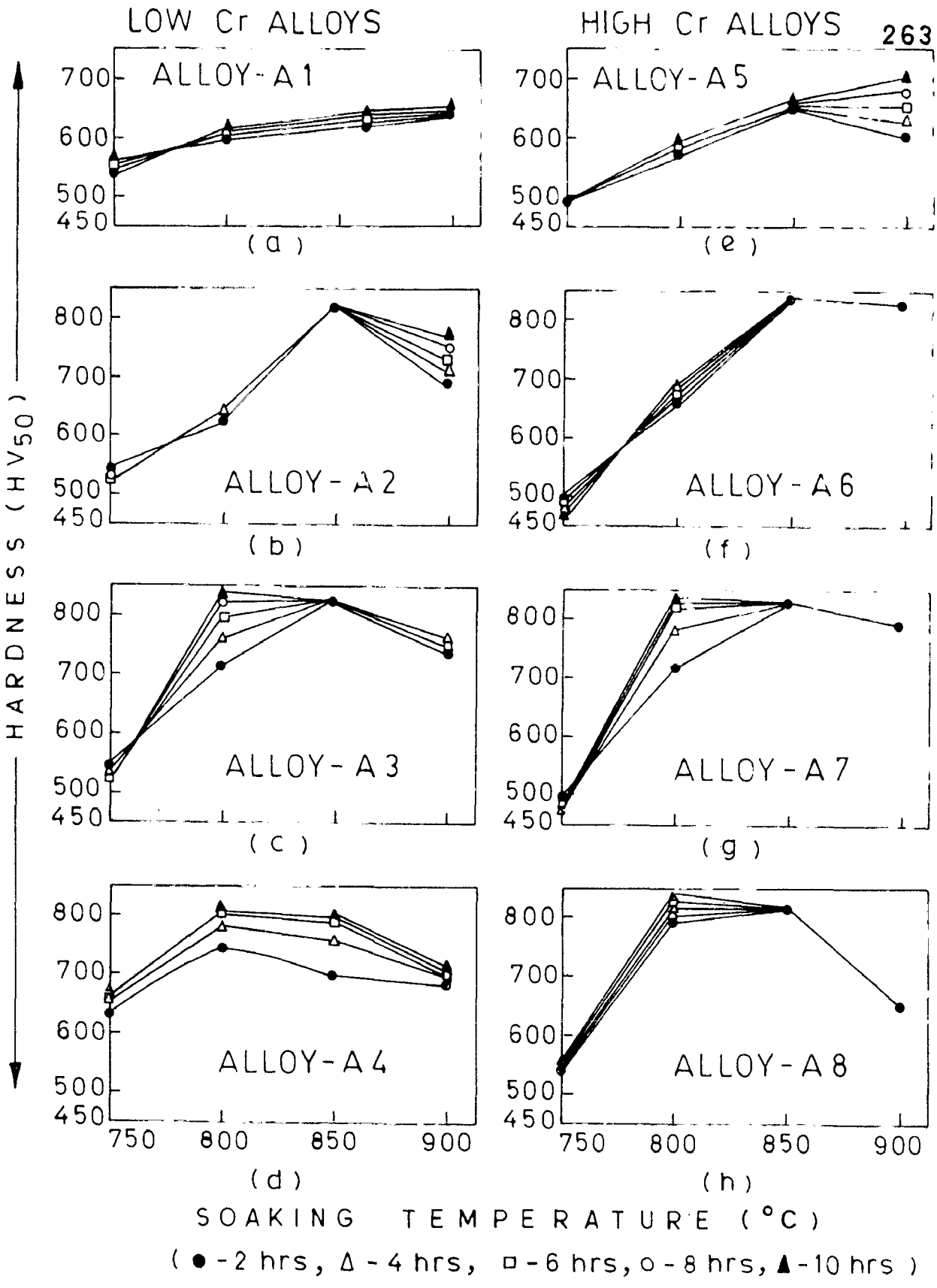

FIG 5.12 EFFECT OF TEMPERATURE AND SOAKING PERIOD ON HARDNESS.

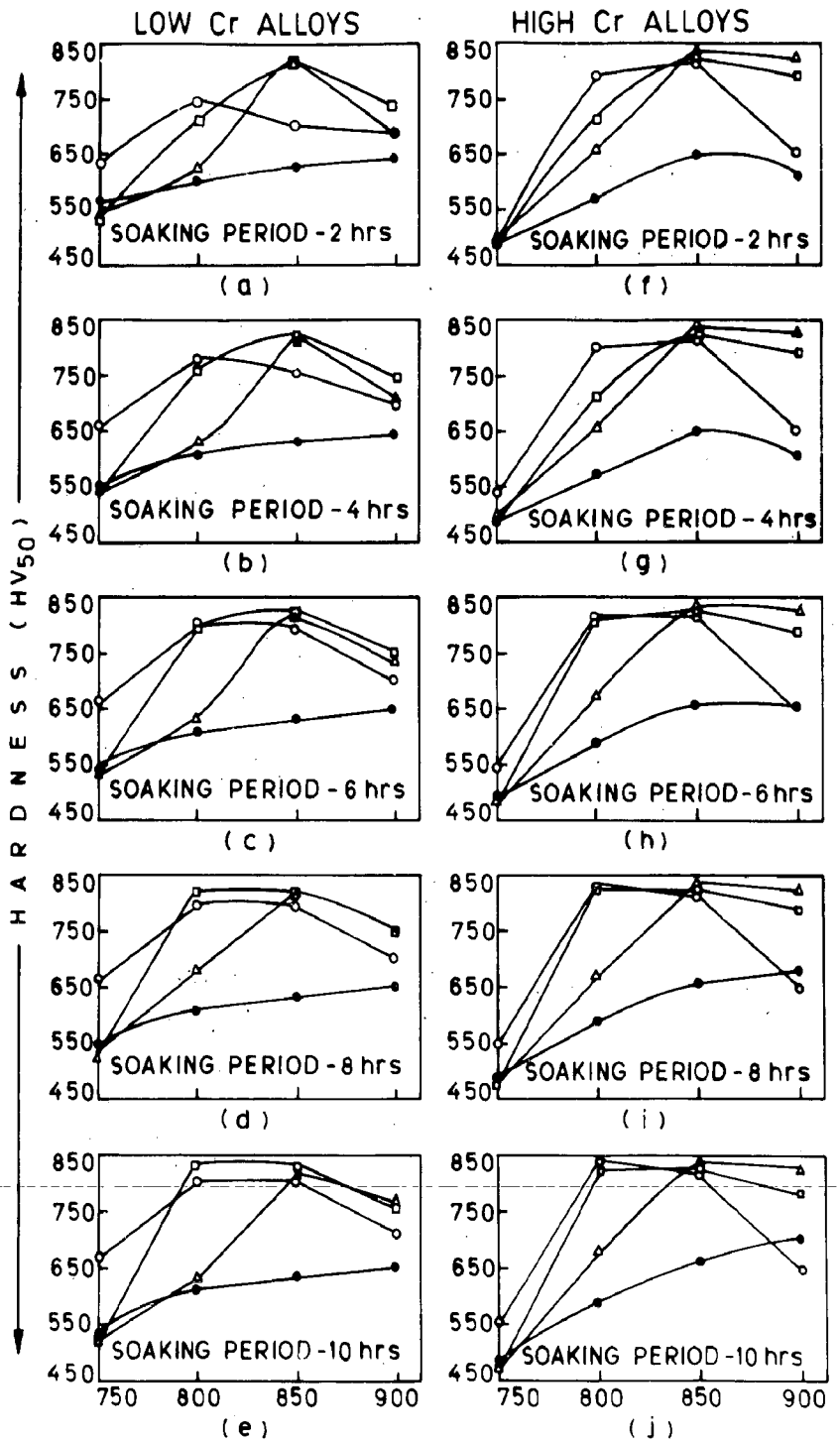

(●-A1alloy, Δ-A2alloy, □-A3alloy, ○-A4 alloy in fig. a,b,c, d & e)

(●-A5alloy, Δ-A6alloy, □-A7alloy, ○-A8alloy in fig. f,g,h,i & j)

FIG. 5.13 EFFECT OF TEMPERATURE ON HARDNESS AT DIFFERENT SOAKING PERIOD.

Figure 5.14

(a) Al, as-cast
Matrix+platy carbide.
(X200)

(b) Al, as-cast
Fine pearlite+carbide.
(X1000)

(c) Al,4h 750°C AC
Dispersed carbide (spherical+needle shaped) in matrix+ discontinuous massive carbide.(X1000)

(d) Al,10h 750°C AC
Same as (c).(X1000)

(e) Al,4h 850°C AC
Same as (c) and (d); nature of free carbide different.(X1000)

(f) Al,10h 900°C AC
Matrix(dark) with dispersed carbide+light etching constituent mostly in intercellular carbide spaces (martensite)+massive carbide.
(X1000)

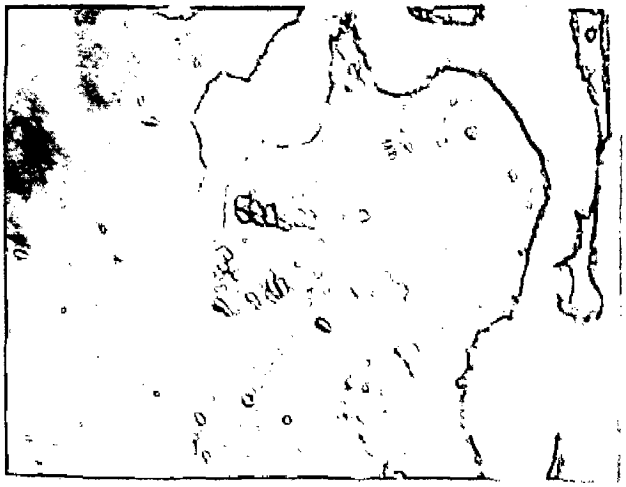

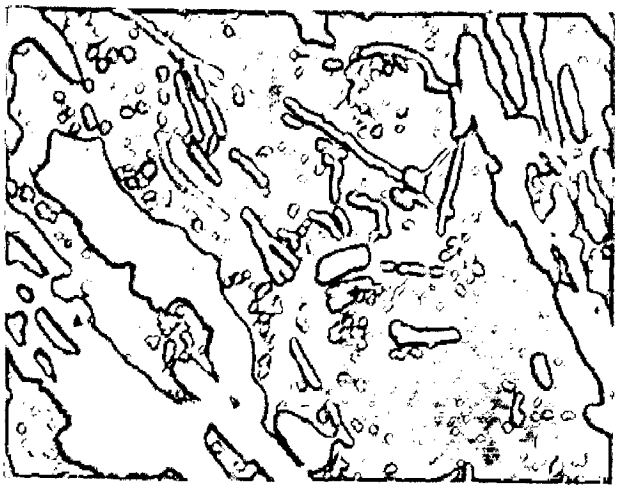

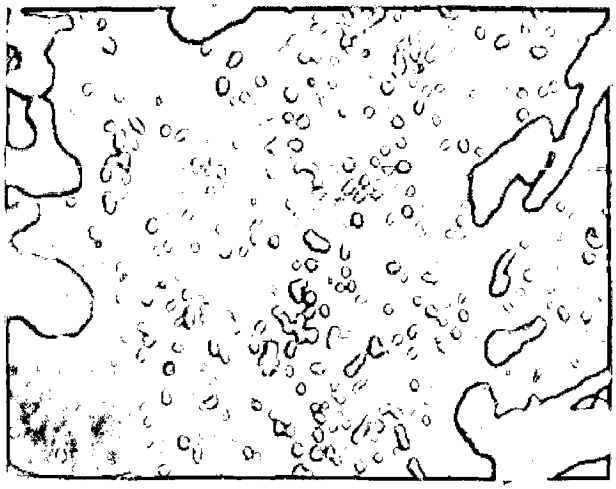

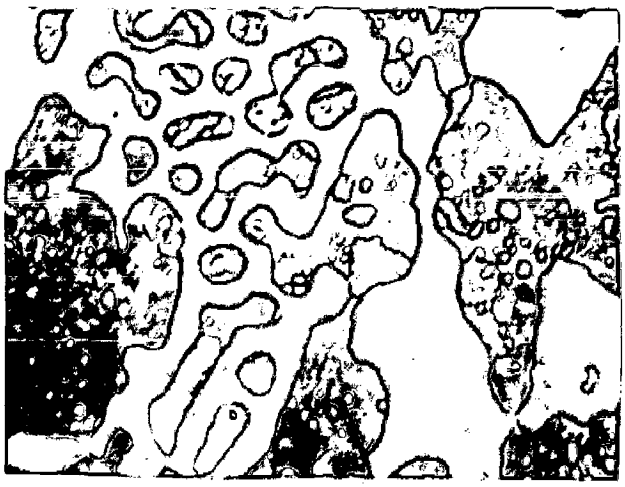

Figure 5.15

(a) A2,as-cast
Matrix+massive and platy carbide.(X200)

(b) A2, as-cast
Matrix perhaps pearlitic +light etching areas (perhaps bainitic) +massive carbide.(X1000)

(c) A2,2h 850°C AC
Matrix containing dispersed carbide+free carbide (partly discontinuous).(X1000)

(d) A2,10h 850°C AC
Matrix containing dispersed carbide with dark and light (perhaps martensitic) areas+free carbide. (X1000)

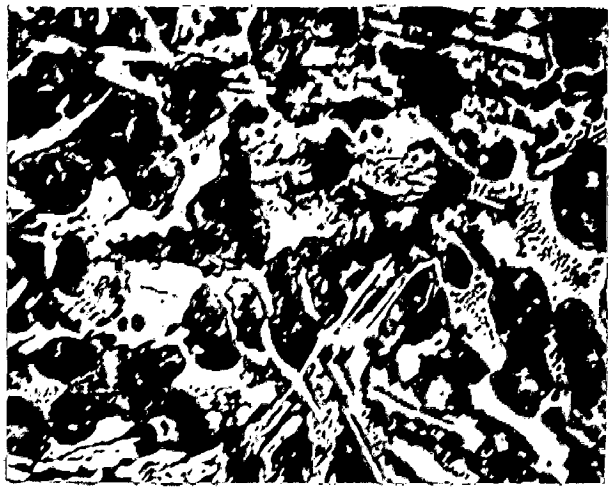

Figure 5.15

(e) A2,2h 900°C AC
Mostly dark matrix with dispersed carbide+light etching areas around plate like free carbide +free carbide+carbide. (X500)

(f) A2,6h 900°C AC
Same as (e); light etching constituent martensitic.(X1000)

(g) A2,10h 900°C AC
Same as (e); Proportion of martensitic areas larger.(X1000)

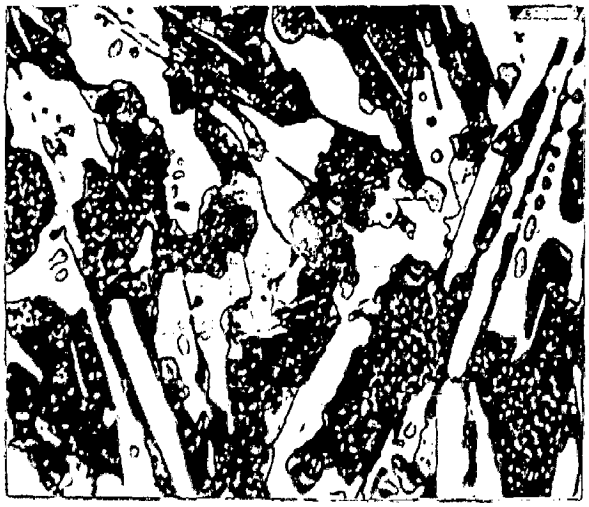


c

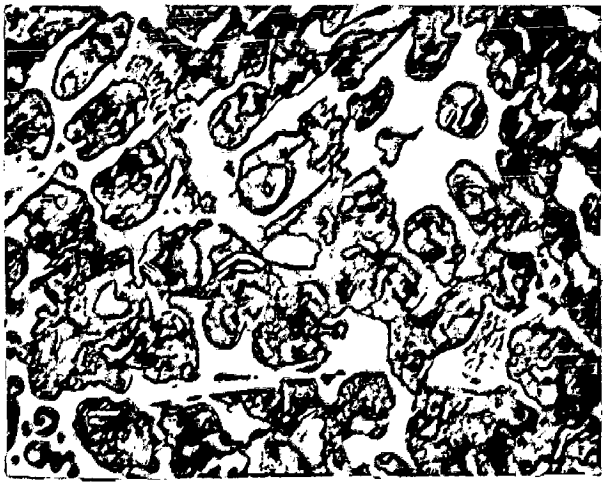

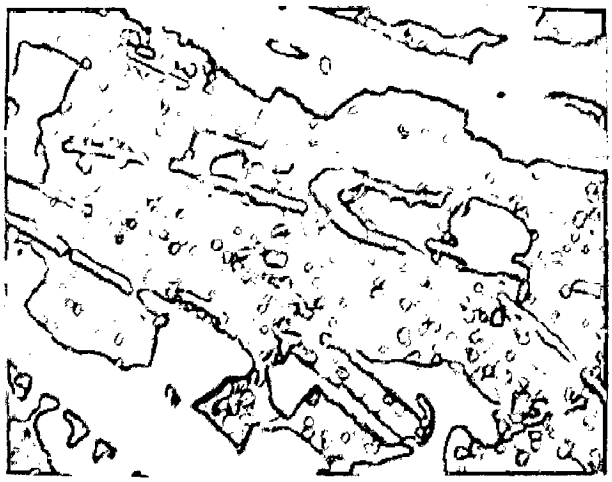

Figure 5.16

(e) A3,10h 800°C AC
Matrix with dispersed carbide+martensite +discontinuous carbide(X1000)

(f) A3,10h 850°AC
Martensitic matrix with dispersed carbide +free carbide.(X1000)

(g) A3,10h 900°C AC
Same as (f).(X1000)

(h) A3,10h 900°C AC
Same as (f)+light grey etching areas around carbide (perhaps austenite). (X500)

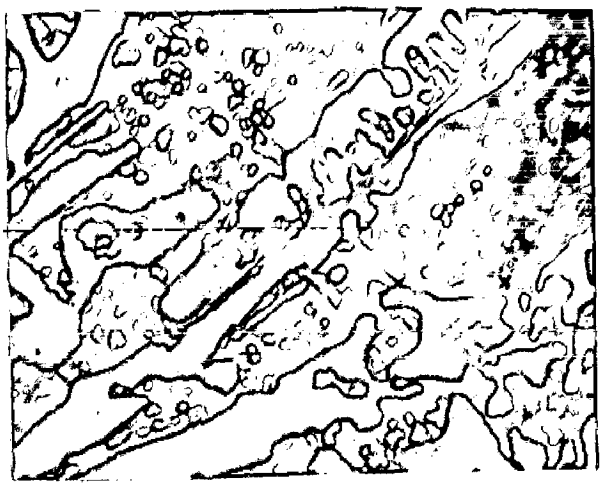

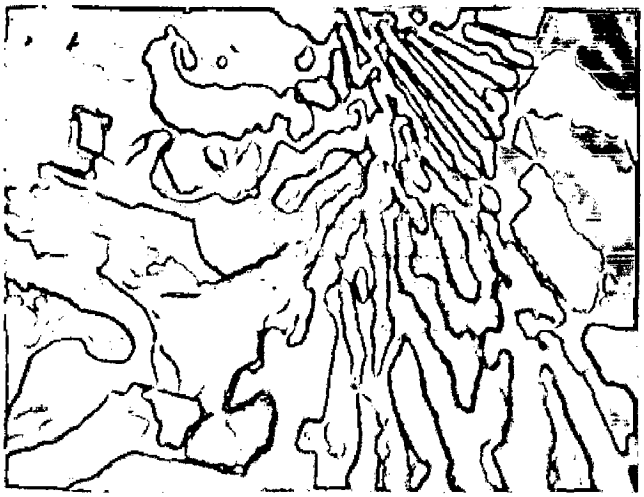

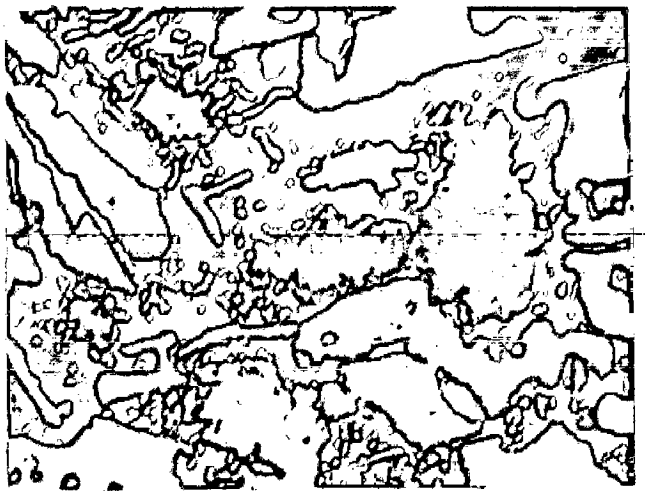

Figure 5.18

(a) A5,as-cast
Matrix+free carbide.
(X200.)

(b) A5, as-cast
Pearlitic matrix+
discontinuous (less
massive)carbide.
(X500)

(c) A5,2h 750°C AC
Same as (b) showing
peculiar free carbide
distribution.(X500)

(d) A5,10h 750°C AC
Same as (b); matrix
microstructure
coarsened hence
resolved.(X500)

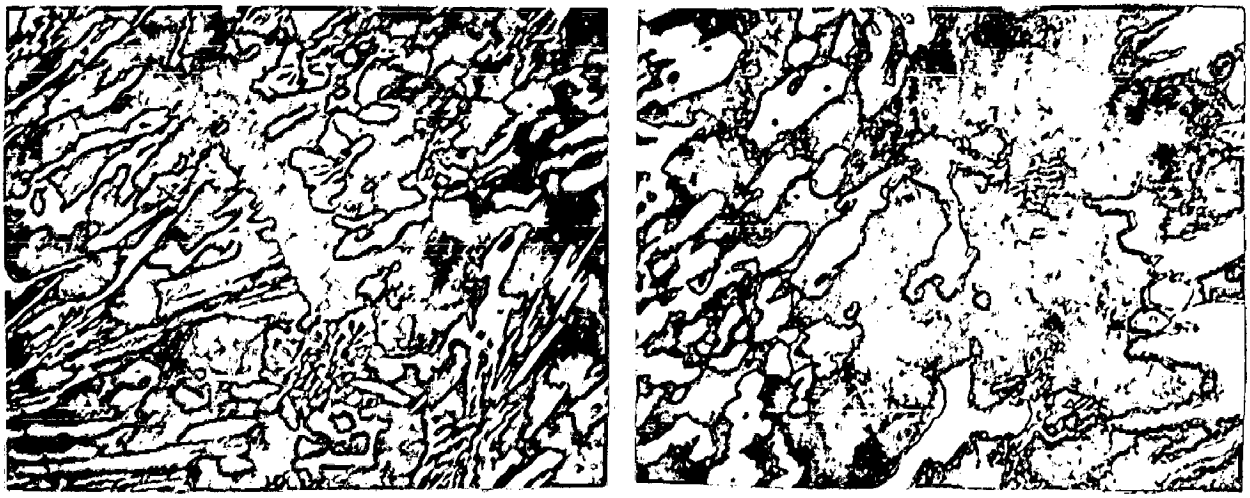

Figure 5.18

(e) A5,2h 900°C AC
Dark matrix+light etching shear transformation product +free carbide. (X1000)

(f) A5,2h 900°C AC
Dark matrix containing dispersed carbide+ revealing presence of hexagonal and polyhedral discontinuous carbide in dispersed form. (X1000)

(g) A5,6h 900°C AC
Same as (e); matrix contains relatively larger proportion of dispersed carbide. (X1000)

(h) A5,10h 900°C AC
Same as (e), light etching areas martensitic. (X1000)

(i) A5,10h 900°C AC
Same as((g) but containing larger volume fraction of martensitic areas. (X500)

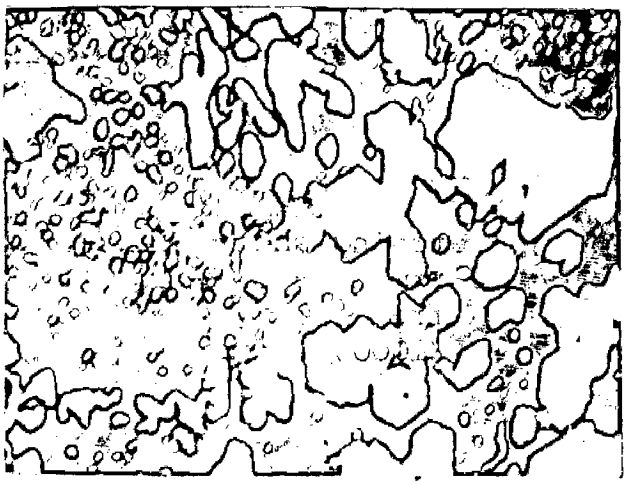

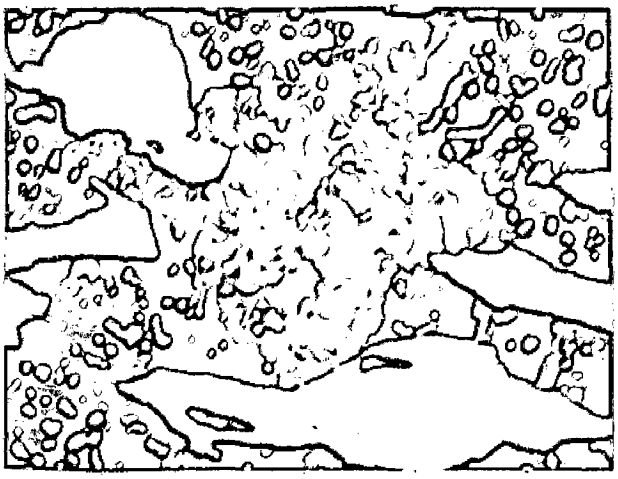

Figure 5.19

(a) A6, as-cast
Matrix with dark and light etching areas +free carbide.(X200)

(b) A6, as-cast
Same as (a); free carbide discontinuous. (X1000)

(c) A6,2h 800°C AC
Tempered martensite +discontinuous carbide. (X1000)

(d) A6,10h 850°C AC
Martensite discontinous carbide.(X1000)

(e) A6,10h 900°C AC
Coarse martensite +discontinuous carbide.(X500)

(f) A6,10h 900°C AC
Same as (e); martensite plate-like in nature. (X1000)

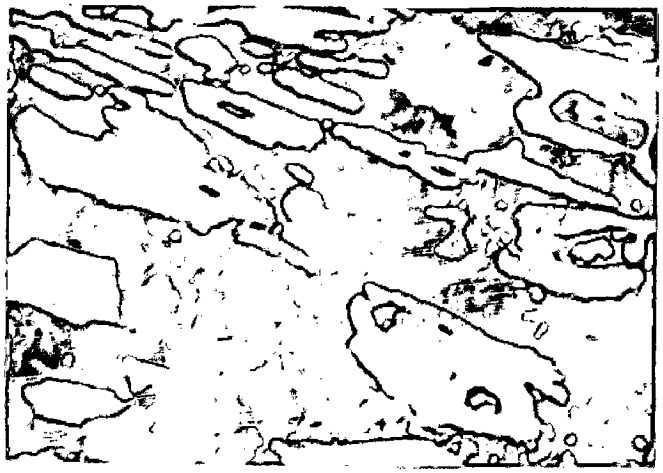

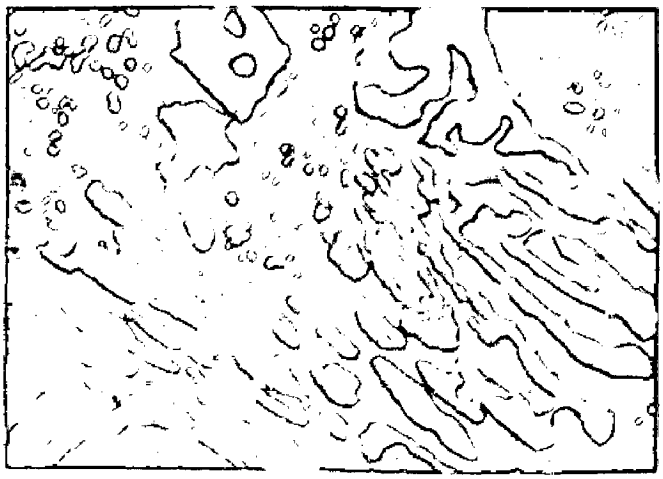

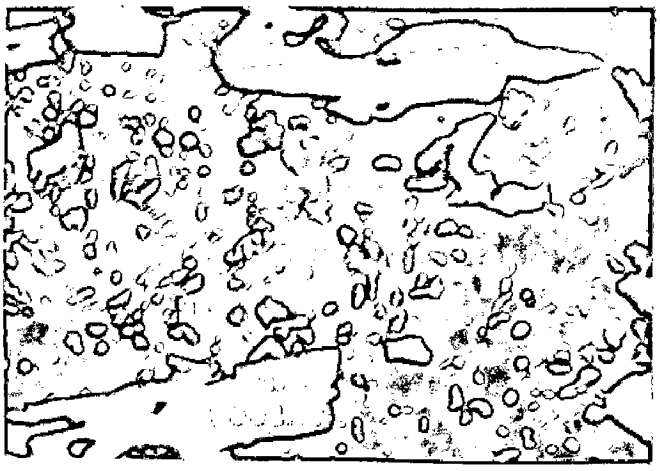

Figure 5.20

(a) A7, as-cast
Matrix with dark and light etching areas+free carbide (X200)

(b) A7, as-cast
Same as (a); light etching areas showing shear transformation product (B/M?) +plate like carbide.(X500)

(c) A7, as-cast
Same as (a) showing different free carbide morphology.(X1000)

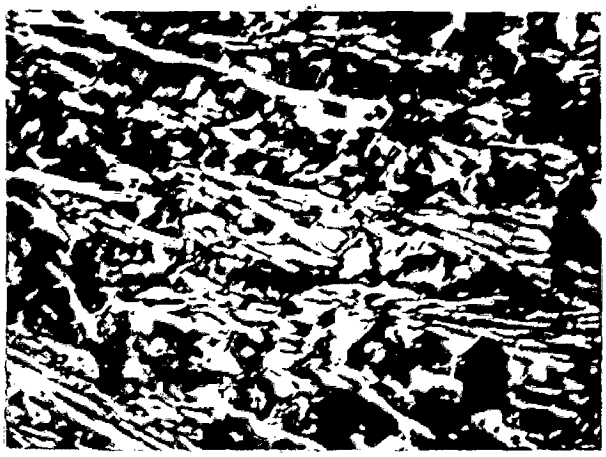

Figure 5.20

(d) A7,2h 800°C AC
Matrix with dispersed carbide+light etching areas (perhaps martensite)+discontinuous carbide.(X1000)

(e) A7,4h 800°C AC
Matrix with shear transformation product +plate-like discontinuous carbide.(X1000)

(f) A7,10h 800°C AC
Same as (e); free carbide occasionally as equiaxed particle. (X1000)

(g) A7,10h 800°C AC
Fine dispersion of carbide in matrix +free carbide tending to be polyhedral.(X1000)

(h) A7,10h 900°C AC
Martensitic matrix containing dispersed carbide+free carbide. (X1000)

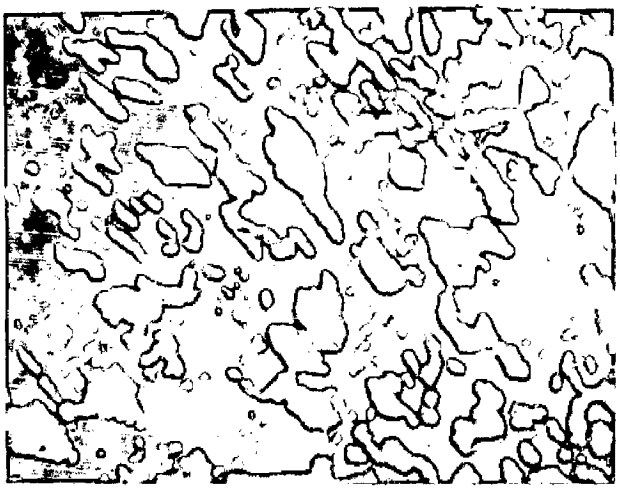

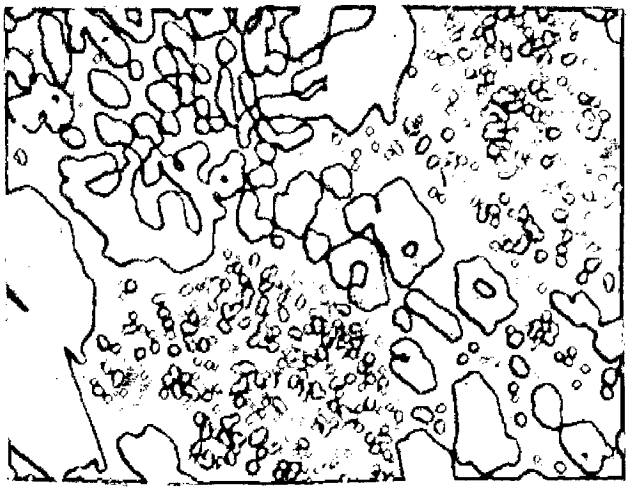

Figure 5.21

(a) A8, as-cast
Matrix with dark and light etching areas+free carbide. (X500)

(b) A8, as-cast
Free carbide in some places tending to be polyhedral/hexagonal +light grey areas perhaps of retained austenite around them. (X500)

(c) A8, as-cast
Dark areas within the matrix showing pearlite structure. (X1000)

(d) A8, as-cast
Showing austenite around free carbide. (X1000)

(e) A8, as-cast
Showing carbide dispersion in light (perhaps austenite) and dark etching areas. (X500)

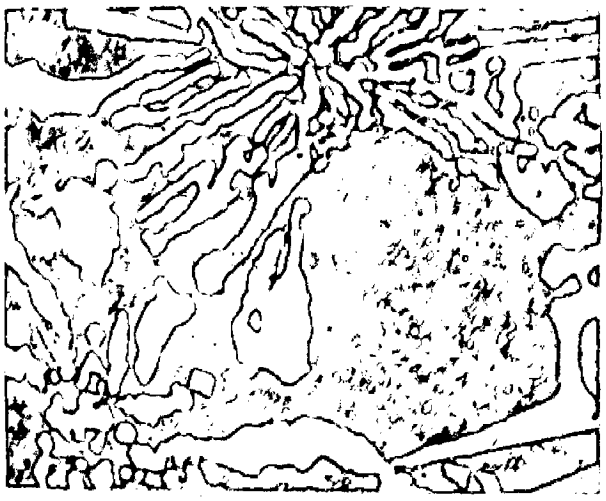

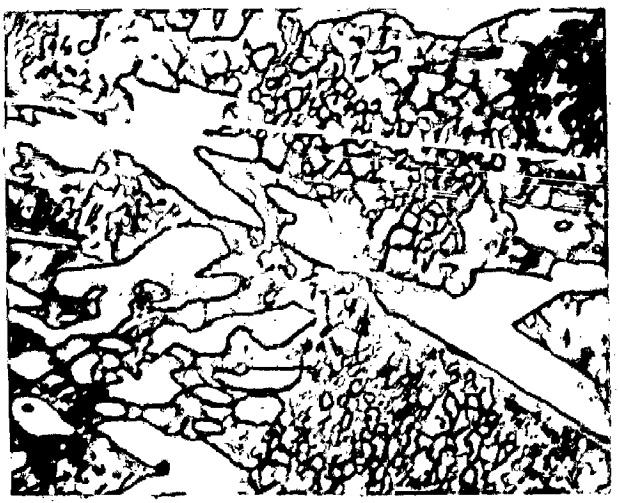

Fig.5.22(a) A2,as-cast Unresolved matrix+free carbide. (X1000)

Fig.5.22(b) A2,10h 850°C AC Matrix containing dispersed carbide +free carbide. (X500)

Fig.5.23(a) A3,10h 850°C AC Matrix containing dispersed carbide, shear nature of matrix structure.(X500)

Fig.5.23(b), A3,10h 850°C AC Martensitic matrix containing dispersed carbide (some are dug out). (X2000)

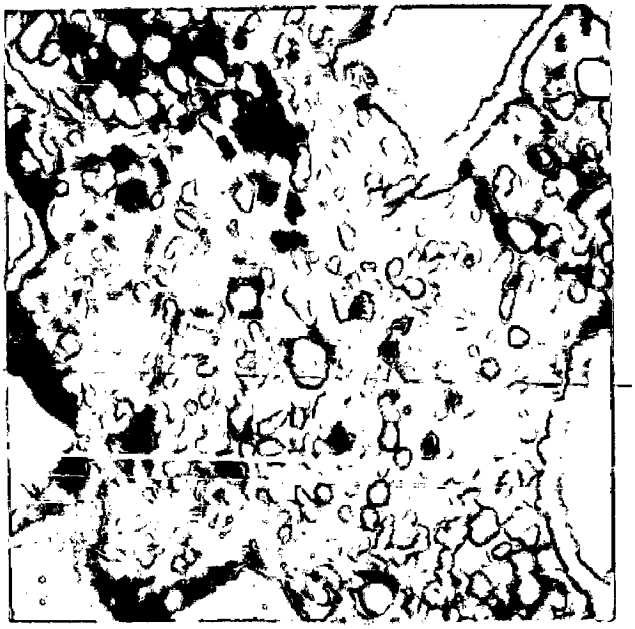

Fig.5.24(a) A4,10h 850°C AC Showing needles of martensite and fine carbide particles (dispersed) in matrix. Needles are mostly in austenitic area. (X500)

Fig.5.24(b) A4,10h 850°C AC Same as Fig.5.24(a). (X1000)

Fig.5.24(c) A4,10h 850°C AC Same as Fig.5.24(b) showing obtuse plates of martensite and dispersed carbide in matrix.(X2000)

Fig.5.25 A8,8h 850°C AC Showing plate like carbide and matrix containing fine dispersion of carbide particles.(X500)

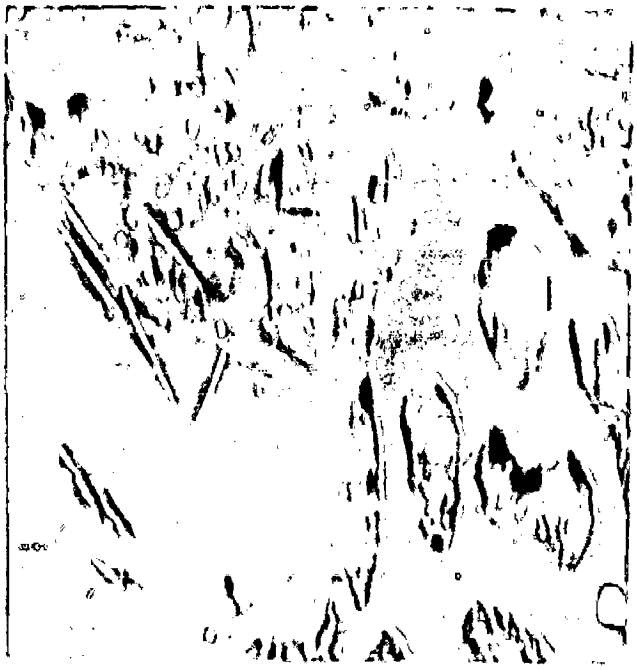

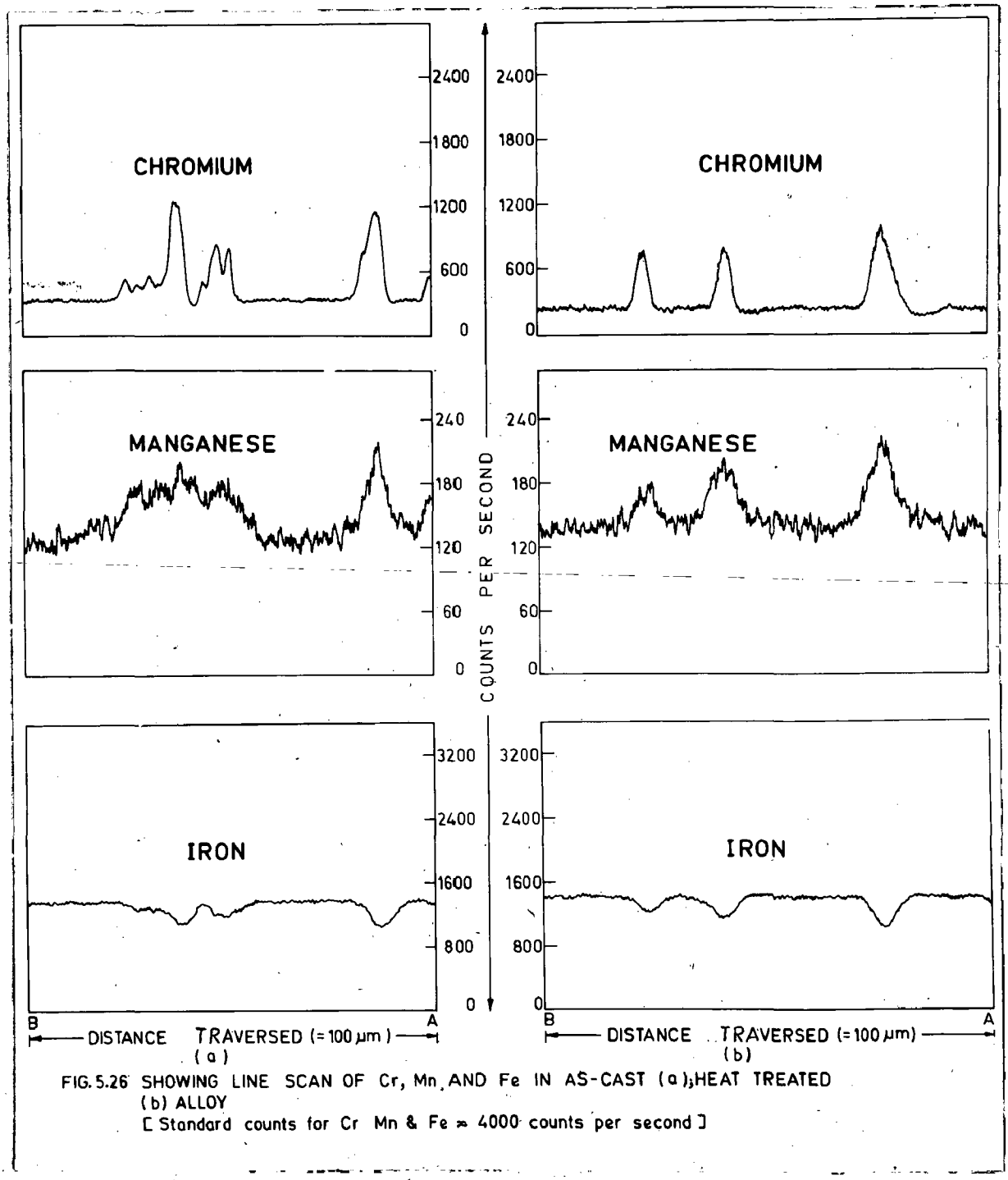

FIG. 5.26 SHOWING LINE SCAN OF Cr, Mn AND Fe IN AS-CAST (a); HEAT TREATED (b) ALLOY
[Standard counts for Cr Mn & Fe ≈ 4000 counts per second]

As-cast structure

Cr

Mn

Si

Fe

Fig. 5.27- Representative X-ray images showing element distribution in as-cast condition

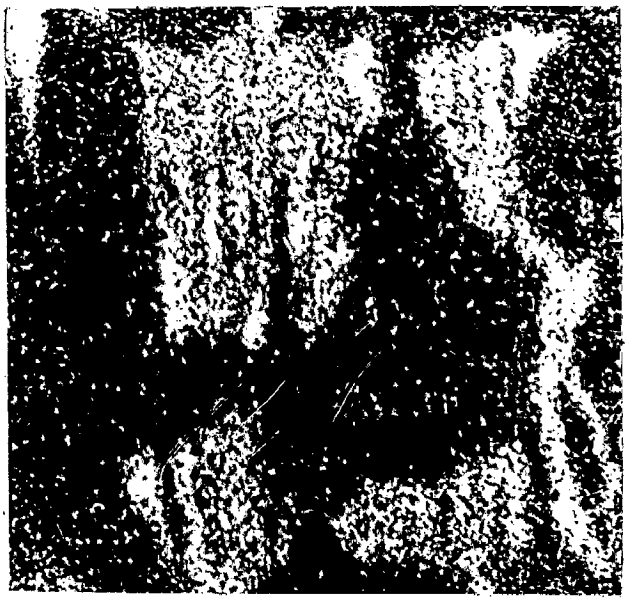

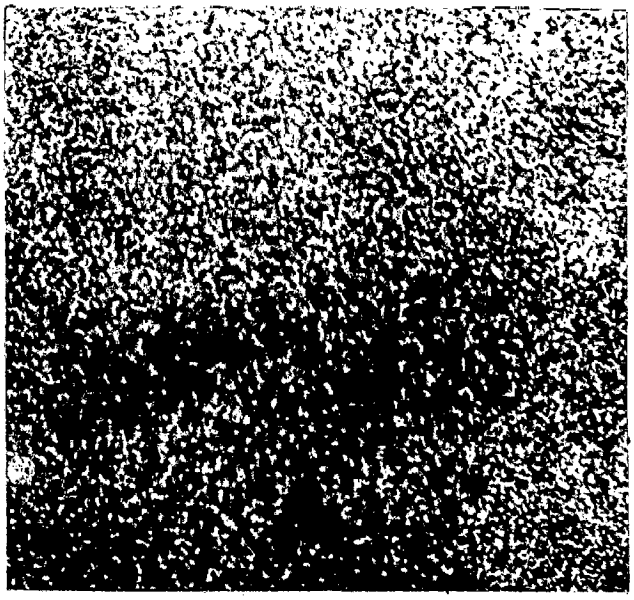

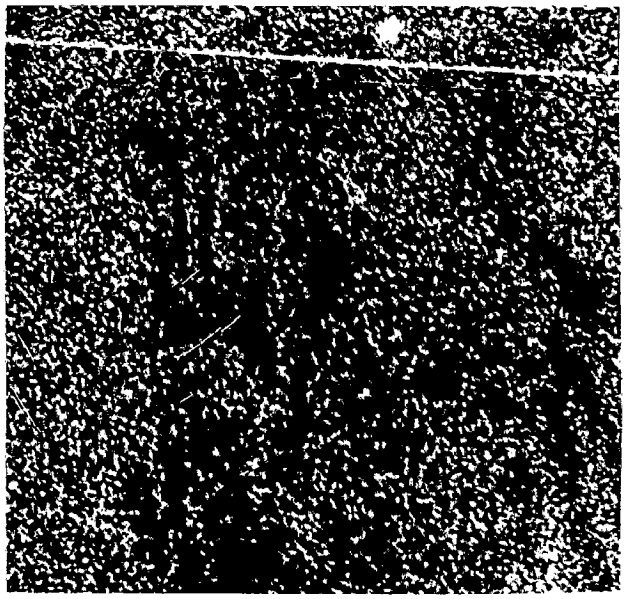

Heat-treated structure .

Cr

Mn

Si

Fe

Fig. 5.28 Representative X-ray images showing element distribution in heat-treated condition

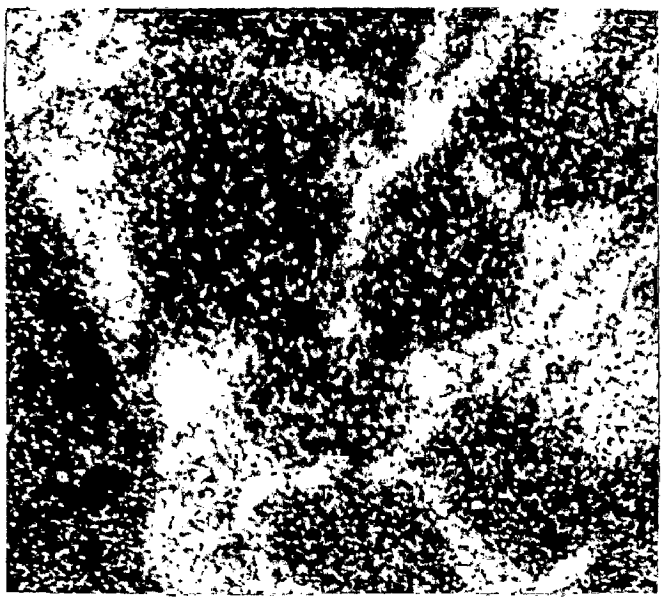

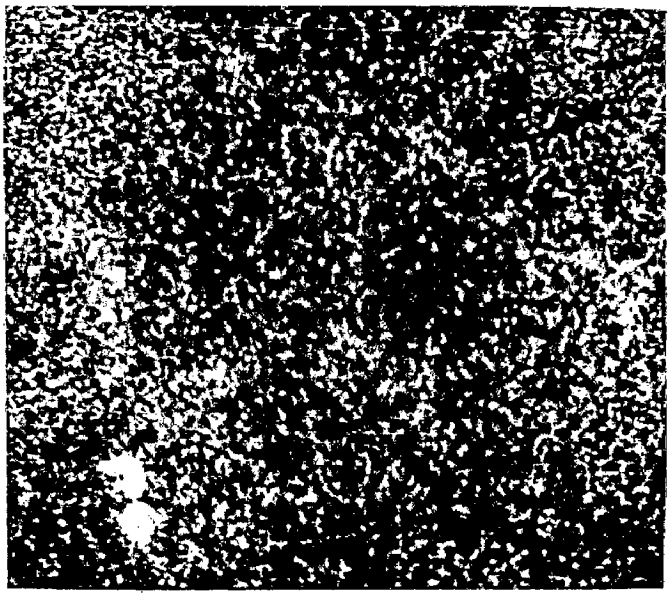

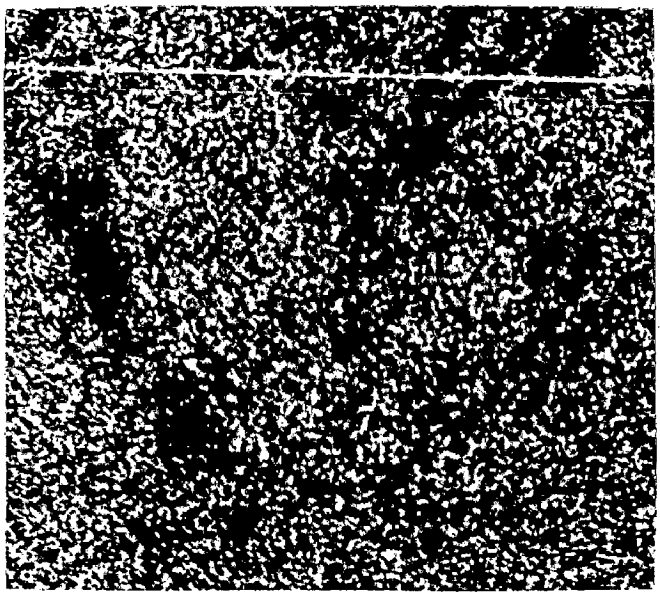

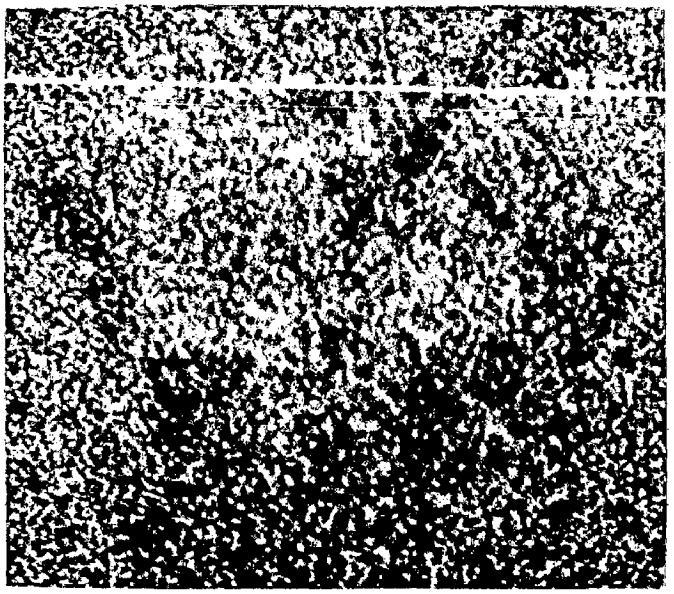

(a)

(b)

Figure 5.29 Composite photograph showing crack path(X500)

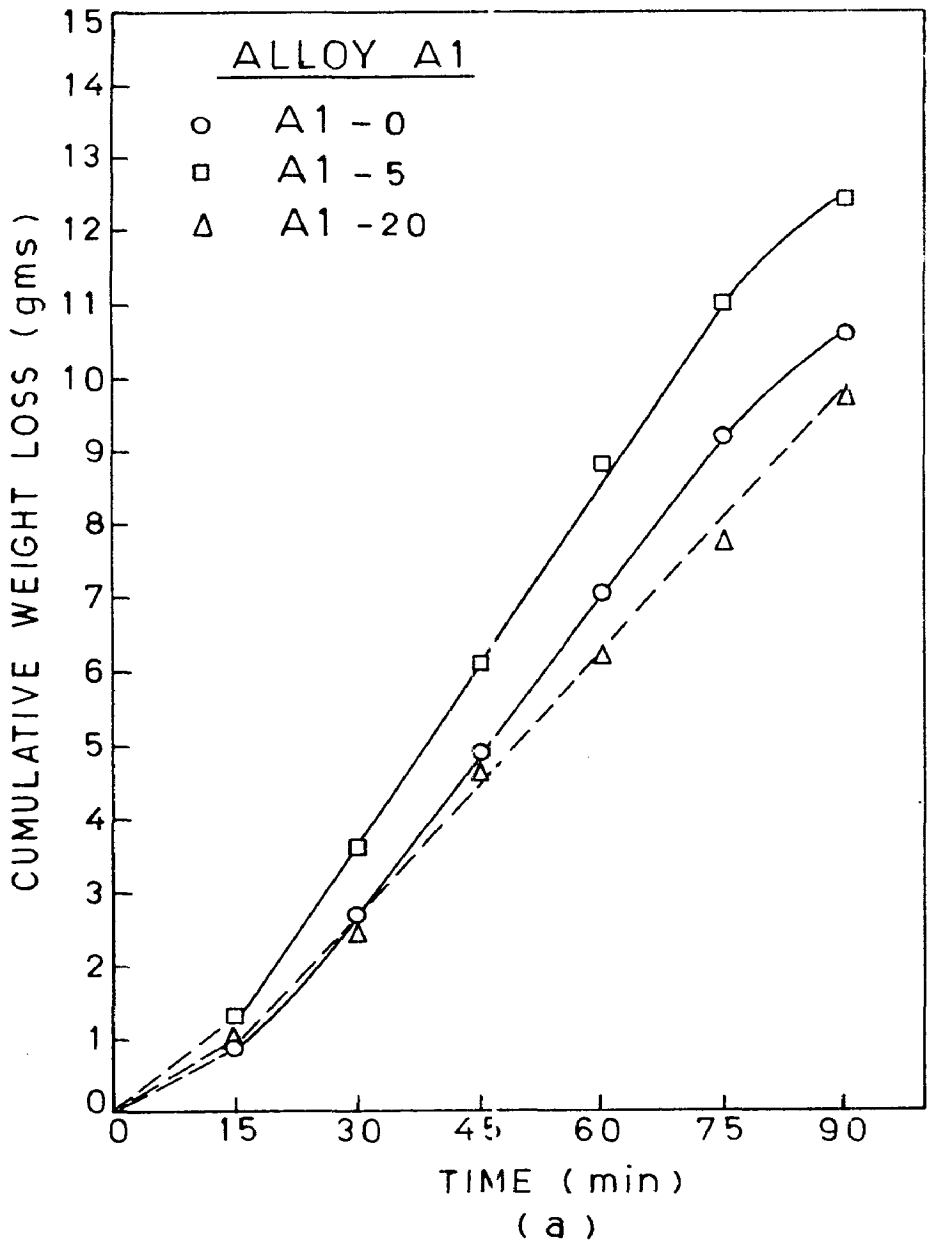

(a)

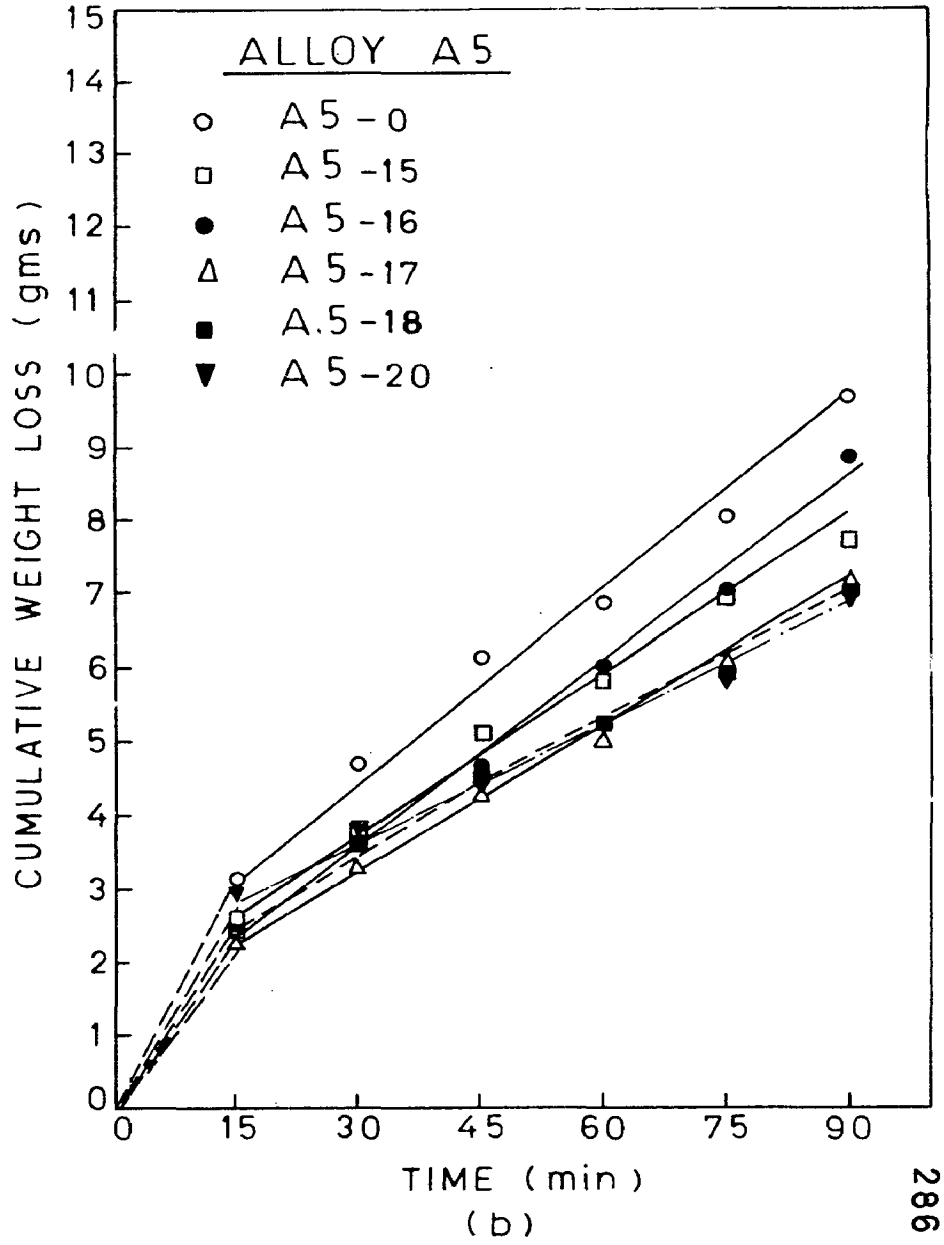

(b)

FIG. 5.31 EFFECT OF HEAT TREATMENT ON GOUGING WEAR.

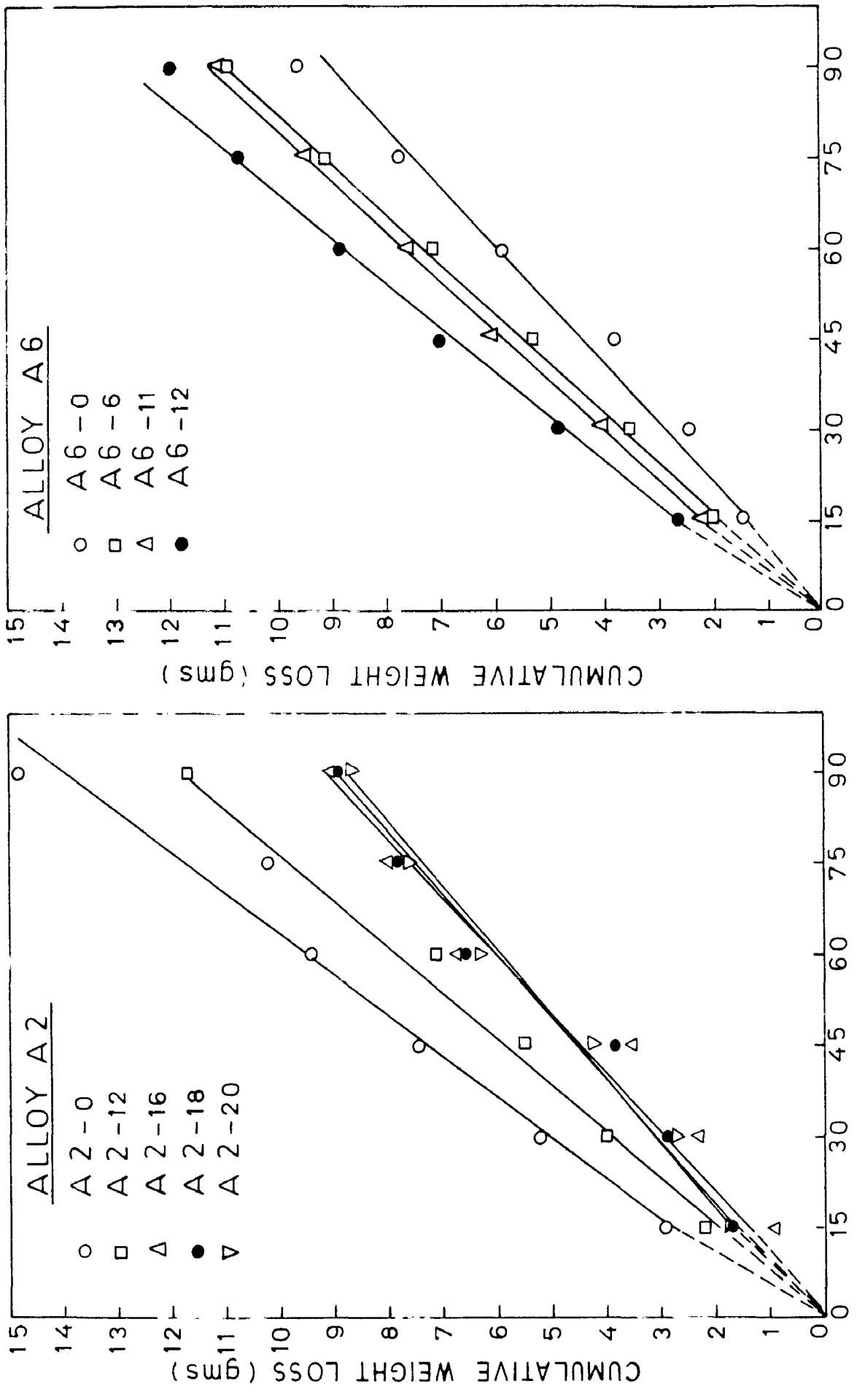

FIG. 5.32 EFFECT OF HEAT-TREATMENT ON GOUGING WEAR.

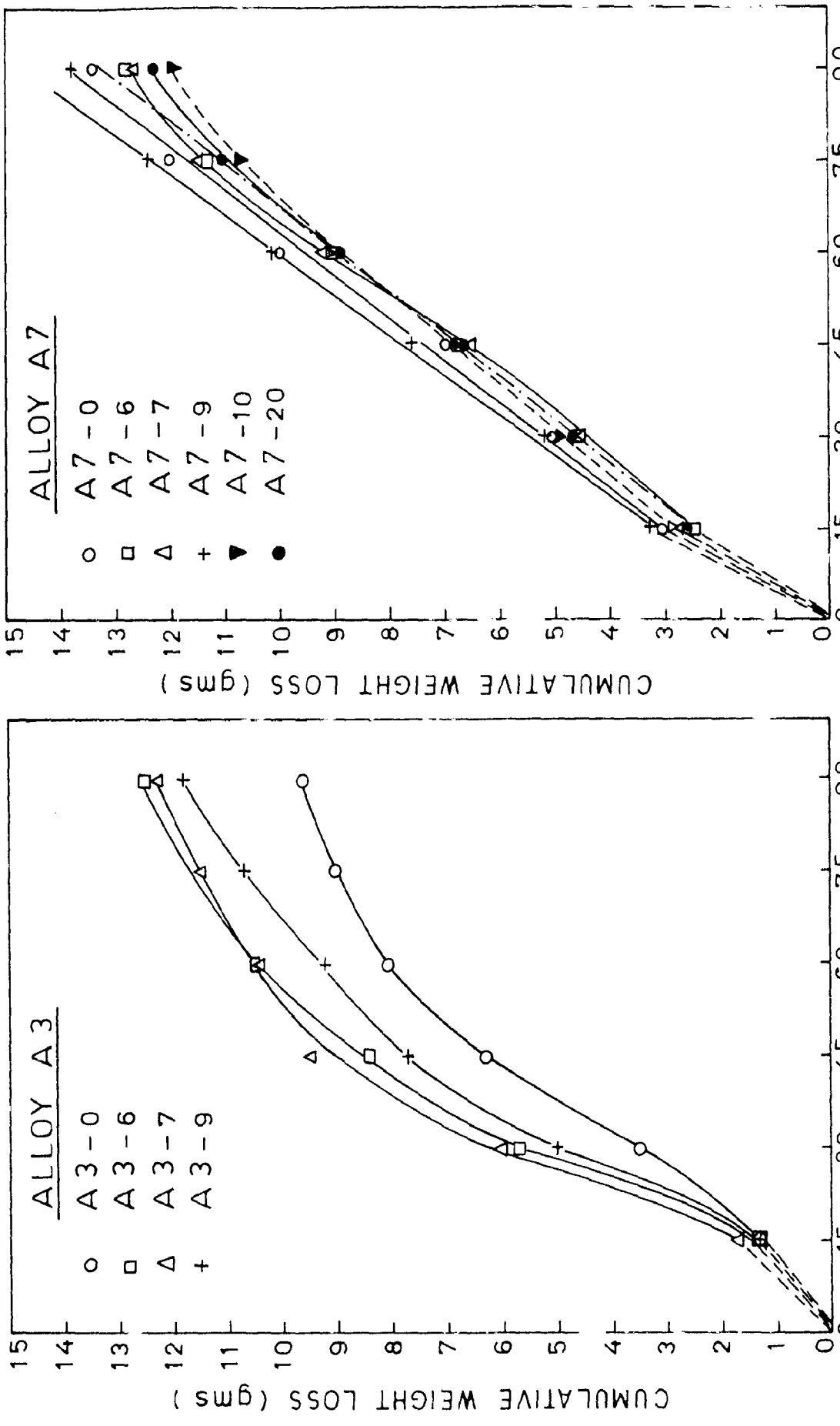

FIG. 5.33 EFFECT OF HEAT TREATMENT ON GOUGING WEAR.

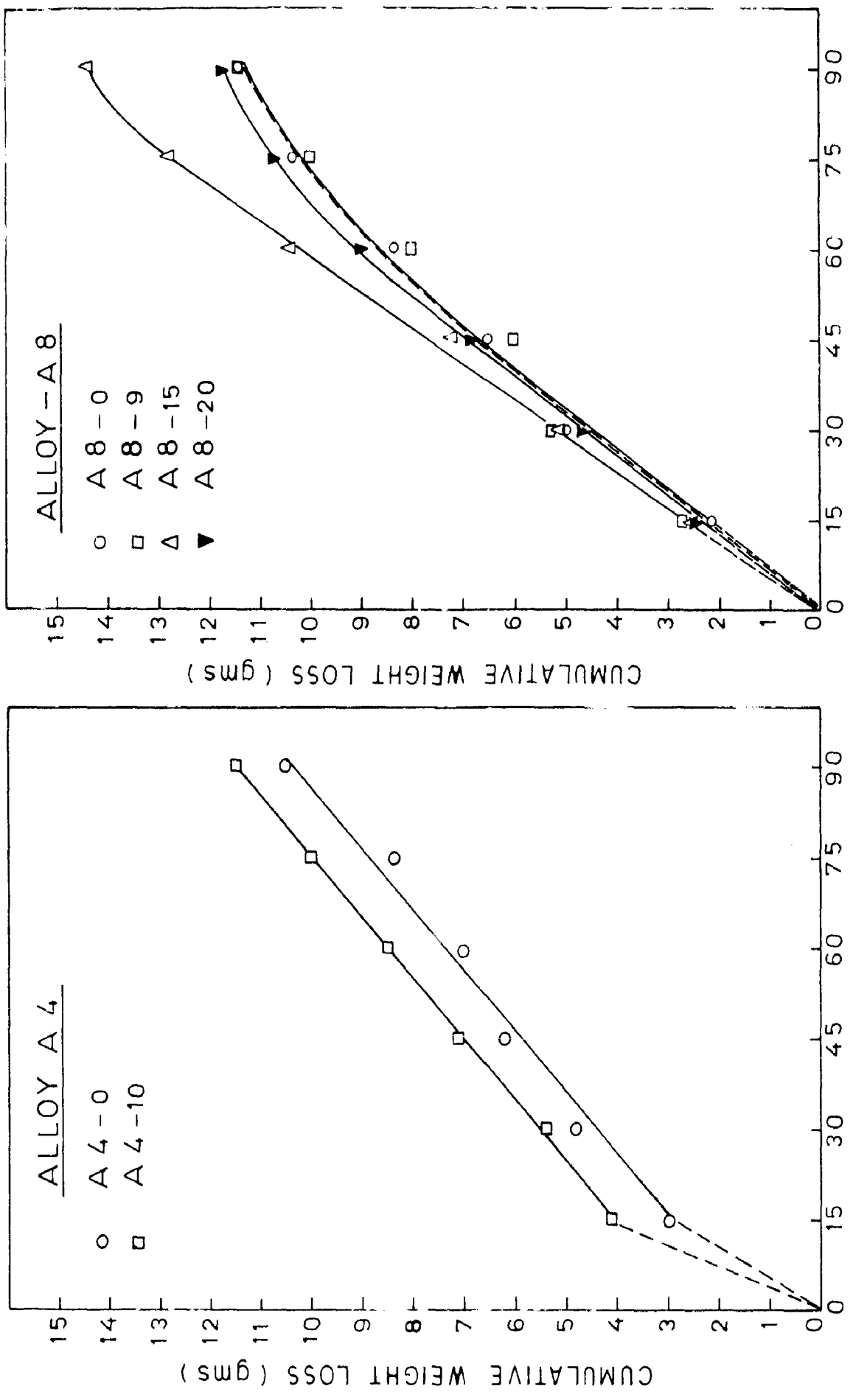

FIG. 5.34 EFFECT OF HEAT TREATMENT ON GOUGING WEAR.

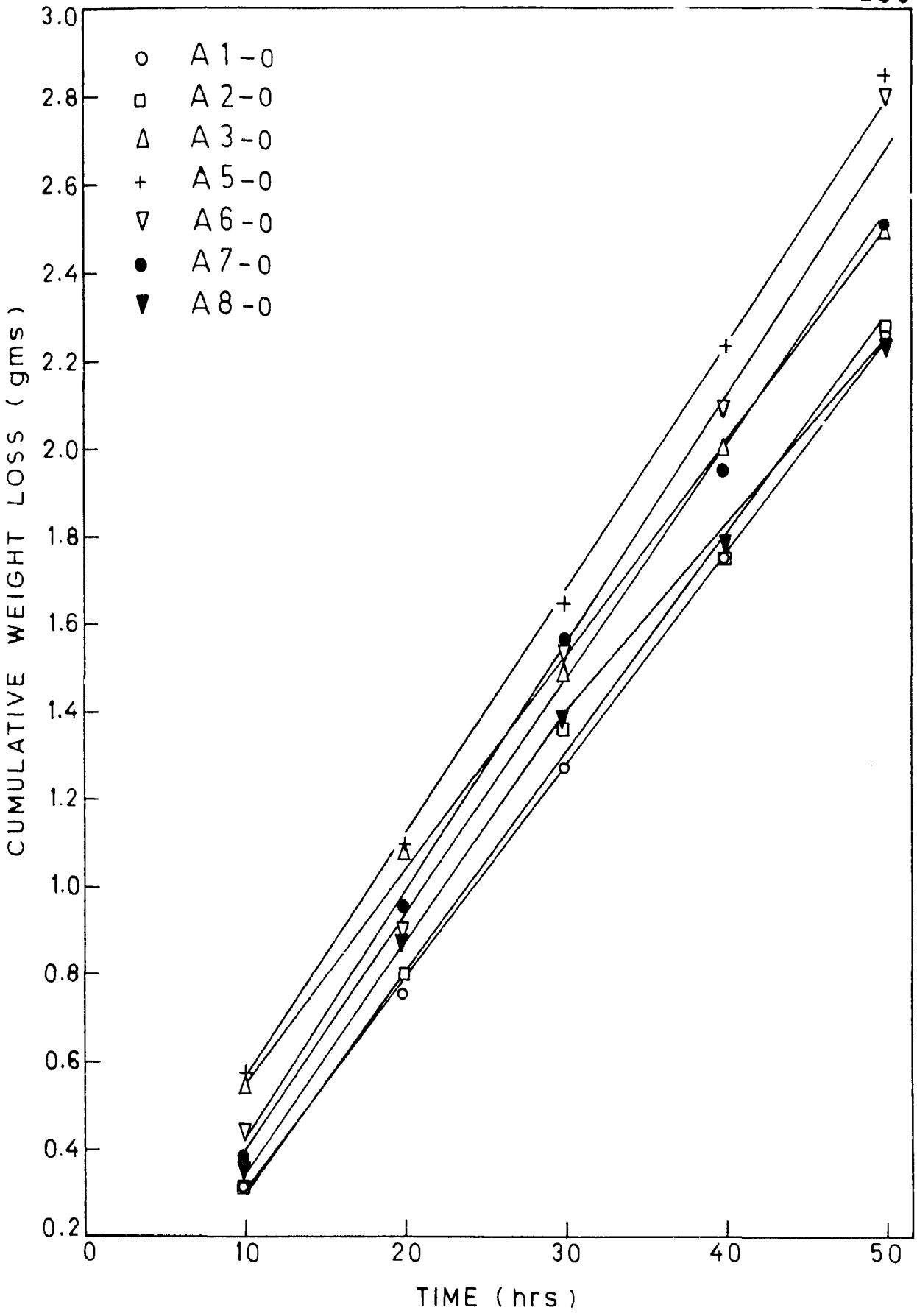

FIG. 5.35 EROSION BEHAVIOUR OF AS-CAST ALLOYS.

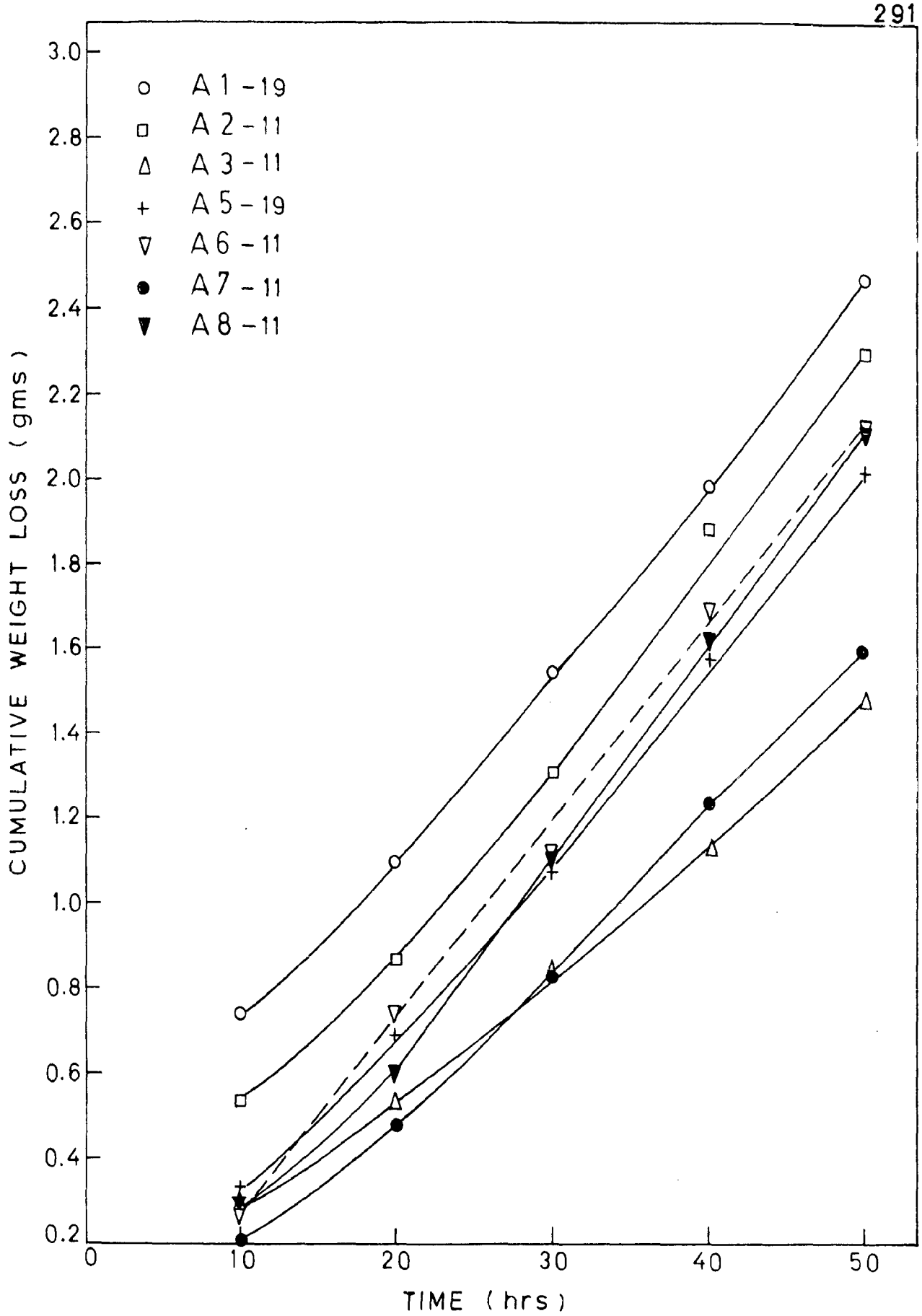

FIG. 5.36 EROSION BEHAVIOUR OF HEAT TREATED ALLOYS (HARDEST ~ 800 - 850 HV_{50})

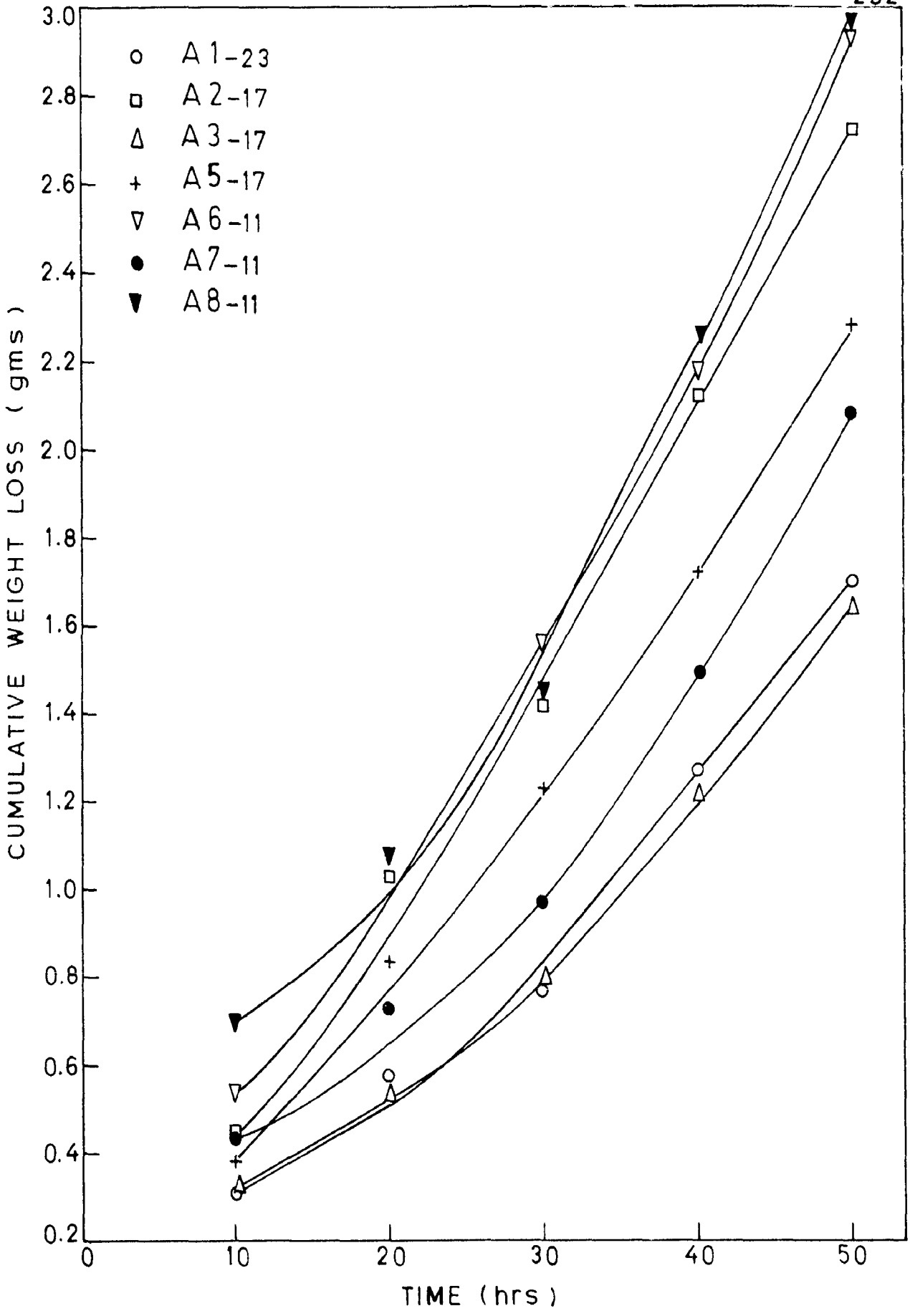

FIG.5.37 EROSION BEHAVIOUR OF HEAT TREATED ALLOYS (MEDIUM HARDNESS ~700-750 HV_{50})

Appendix - Computer Programme

```
00100  C      FILE NAME: :WEAR.FOR
00200  C      PROGRAM FOR QUANTITATIVE ANALYSIS OF METALLOGRAPHIC
00300  C      CONSTITUENTS.
00400  C-----------------------------------------------------------------
00500         DIMENSION ALFA(15),AKA(3),CA(3)
00600         OPEN (UNIT=1,DEVICE='DSK',FILE='AB.DAT')
00700  C-----------------------------------------------------------------
00800  C      FIRST FIVE VALUES OF ALFA(I) ARE FOR CR, NEXT FIVE ARE FOR
00900  C      MN, AND LAST FIVE ARE FOR FE IN THE ORDER (AB,ABB,AC,ACC,ABC
01000  C-----------------------------------------------------------------
01100         READ (1,*) NSET
01200         PRINT 80, NSET
01300         TYPE  80, NSET
01400         READ (1,*) (ALFA(I), I=1,15)
01500         PRINT 140, (ALFA(I), I=1,15)
01600         TYPE  140, (ALFA(I), I=1,15)
01700  C-----------------------------------------------------------------
01800  C      VALUES OF AKA(I) ARE IN THE ORDER CR,MN,FE.
01900  C-----------------------------------------------------------------
02000         DO 300 IJ=1,NSET
02100         READ (1,*) N,(AKA(I), I=1,3)
02200         PRINT 130, N,(AKA(I), I=1,3)
02300         TYPE  130, N,(AKA(I), I=1,3)
02400         PRINT 180
02500         PRINT 90    ;   PRINT 110, N
02600         PRINT 90
02700  80     FORMAT (8X,'NSET=',I3)
02800  90     FORMAT ('  ----------------------------------------
02900  110    FORMAT (2X,'N=',I3)
03000  120    FORMAT (14X,'CA(I)',12X,'CB',13X,'CC')
03100  130    FORMAT (13X,I2,5X,3F15.9)
03200  140    FORMAT (5X, 5F15.9)
03300  150    FORMAT (5X,'CR',3F15.9)
03400  151    FORMAT (5X,'MN',3F15.9)
03500  152    FORMAT (5X,'FE',3F15.9)
03600  160    FORMAT (5X,'JCOUNT=',I3)
03700  170    FORMAT (/)
03800  180    FORMAT (1HO)
03900         CB=AKA(2)     ;     CC=AKA(3)
04000         JCOUNT = 1
04100         DO 200 J=1,5
04200         PRINT 160, JCOUNT
04300         PRINT 120
04400         PRINT 170
04500         DO 100 I=1,3
04600         IF (I.GE.2) GO TO 11
04700         K=I
```

Continued

```
04800    11     CA(I) = 1.0+ALFA(K)*CB+ALFA(K+1)*CB*CB+ALFA(K+2)*CC+
04900           1 ALFA(K+3)*CC*CC+ALFA(K+4)*CB*CC
05000           CA(I) =CA(I)*AKA(I)
05100           GO TO (12,13,14)  I
05200    12     PRINT 150, CA(I),CB,CC
05300           GO TO 15
05400    13     PRINT 151, CA(I),CB,CC
05500           GO TO 15
05600    14     PRINT 152, CA(I),CB,CC
05700    15     GO TO (22,33,100), I
05800    22     CB = CA(I)
05900           GO TO 55
06000    33     CB = CA(I)    ;    CC = CA(I-1)
06100    55     K = K+5
06200    100    CONTINUE
06300           CB = CA(2)    ;    CC = CA(3)
06400           JCOUNT = JCOUNT+1
06500           PRINT 170
06600    200    CONTINUE
06700           PRINT 180
06800    300    CONTINUE
06900           STOP
07000           END
```

generated is also helpful in evaluating the wear rate, W_r, which is given by the expression,

$$W_r = \frac{(W_1 - W_2)}{t}$$

where,

W_1 = weight of specimen before wear,

W_2 = weight of specimen after wear,

t = time of wear in hrs or minutes.

Other parameters of interest are termed as specific wear ratio and grinding ratio.

The specific abrasive wear ratio, w, is defined as,[28]

$$w = \frac{\text{weight of material removed due to wear}}{\text{wheel wear}}$$

$$= \frac{\Delta W}{\frac{\pi}{4}(d_1^2 - d_2^2)t.\rho}$$

where,

ΔW = weight of specimen material removed due to wear = $W_1 - W_2$,

W_1 = weight of the specimen before wear,

W_2 = weight of the specimen after wear,

d_1 = diameter of grinding wheel before wear,

d_2 = diameter of grinding wheel after wear,

t = thickness of the grinding wheel,

ρ = density of wheel material.

The reciprocal value, w^{-1} is a measure of the wear resistance.

The grinding ratio (GR) [29,30] is defined as,

$$GR = \frac{\text{volume of material removed}}{\text{volume of grinding wheel worn in operation}}$$

$$= \frac{\Delta W_1/\rho_1}{\Delta W_2/\rho_2}.$$

where,

ΔW_1 = wt. of specimen material removed in wear test,
ρ_1 = density of the specimen material,
ΔW_2 = weight of wheel material removed in wear test,
ρ_2 = density of the grinding wheel material.

Alternately, wear can also be found by the following method:

Volume change as a consequence of sliding wear is given by the expression[7],

$$\Delta V = k \frac{LS}{3H}$$

where,

L = load,
S = sliding distance,
H = Vicker's hardness and
k = wear coefficient.

Therefore, wear rate is commonly reported as $\Delta V/L$.

For mild wear, k would be $\sim 10^{-8}$ to 10^{-7}, for severe wear it would be $\sim 10^{-4}$ to 10^{-3}. Sometimes a wear factor defined as $\frac{\Delta V}{SL}$ or $\frac{K}{3H}$ is used.[7]

this certain minimum value is yet to be ascertained.[34]

Since both bainite and martensite are harder than pearlite, the resistance to wear of a microstructure consisting of bainite-carbide or martensite-carbide would be in general higher than pearlite-carbide in the order 'martensite-carbide' > 'bainite-carbide' > 'pearlite-carbide'.[13] This is quantitatively substantiated by the data summarized in the paper. Besides reaffirming the superiority of the M+C_b microstructure, the data also reveals that except for the 15 Cr-3 Mo alloy, the wear resistance of the high-Cr white irons initially decreased with an increase in the load (upto ~16 kg) and was independent of it thereafter. Contrary to this, the wear resistance of the Ni-Cr alloys initially decreased with an increase in load (upto 16 kg) and improved thereafter. This tendency was marked in the Ni-Cr alloy (hardness 845 HV) and also in one of the Cr based alloys- 15 Cr-3 Mo (hardness 895 HV).[13] Reasons for this behaviour as also whether it would be observed only above a certain level of hardness are not yet clearly established.

The data reported also revealed that the presence of austenite apparently proved 'counter-productive'. However, whether the superiority of 27 Cr white-iron (hardness 661 HV) and Ni-hard 4 (hardness 719 HV) at lower loads, was due to retained austenite in the two former grades and its absence in Ni-hard 1, is not clear.[13]

Another factor which needs critical examination is the uniformity of the matrix microstructure. In Ni-hard 1, it comprises of bainite/tempered martensite, that in Ni-hard 4 only martensite (+ some γ i.e. austenite), whereas in 27 Cr alloy it is M+P+precipitated carbides. Excluding retained austenite from the discussion for the present, the relatively inferior wear characteristics of Ni-hard 1 may be attributed to the presence of mixed (varied) microstructures. If this were to be so then it is likely that 27 Cr white iron might have exhibited better resistance to wear if the 'non-uniformity' in the matrix microstructure (martensite, pearlite and dispersed carbides) were to be reduced to a minimum i.e. ideally to a single microconstituent. This argument appears to be consistent with the contention that besides the most preferred single microconstituent martensitic matrix, 'austenitic' irons would exhibit better resistance to abrasion than might be expected from their bulk hardness[13,35-39].

The discussion so far has been confined to generalities wherein it has emerged that wear resistance improves with an increase in hardness. Accordingly the conclusion that wear resistance decreases in the order martensite, bainite, pearlite is justifiable. However, since shock resistance and resistance to crack propagation have also emerged as important parameters (section 1.2.3 and 2.2.2.1), a more meaningful assessment of the wear resistance of the different

measure of abrasive wear (resistance). A combination of high hardness coupled with toughness is a better indication of the resistance to wear. Thus morphology and amount of the second phase are of importance.[33] Therefore, the parameter 'log t' rather than the interparticle spacing λ appeared to be a more appropriate basis for representing wear resistance. The authors have gone on to further suggest that a kinetic parameter such as T(C+log t) containing both the tempering temperature and time which will govern the type of phases present, their morphology and distribution (and therefore the physical state of the material) may turn out to be a more suitable parameter than hardness alone which does not necessarily depict the type of phases that are present.[33]

2.2.4.2 Wear Strength

Fracture toughness measurements are gaining in prominence for characterizing wear resistant brittle materials. Important data obtained on the crack propagation behaviour as influenced by microstructure has already been discussed in the appropriate preceding sections. An important parameter needing introduction is termed 'wear strength'. High wear resistance in a structural member is not always sufficient for many practical problems. The product of $\sigma_{0.2}$(0.2%proof) and fracture toughness (K_{IC}) represents useful combination of properties if both high resistance to deformation and

crack propagation are needed.[74]. Similarly the product of wear resistance W^{-1} and K_{IC} can be used to describe the 'Wear Strength' of a structural part under wear loading. Since 'Wear Strength' will depend upon the condition of the wear test, it is not a material property.[31]

Wear strength can be helpful for comparing different structures. Caution needs to be exercised in using this parameter as a structure with a high fracture toughness and a low wear resistance can have the same wear strength as another structure with a low fracture toughness and a high wear resistance[31]. Preliminary experimentation has revealed that for a minimum yield stress of 1000 MPa and a maximum wear strength, isothermally transformed bainitic matrix is the most favourable microstructure.[31]

2.2.5 Concluding Remarks

An attempt has been made to qualitatively establish an inter-relation between the microstructure and resistance to wear in white irons. The microstructure(s) most useful in imparting a high resistance to wear is martensite + carbide, perhaps with controlled quantities of retained austenite. Martensite can be obtained by enhancing hardenability through alloying. The hardness of the carbide phase can be further enhanced through suitable alloying which would also prove useful in retaining austenite in the final microstructure. Presence of austenite may prove additionally beneficial in improving

Unlike other austenite stabilizers, Cu has a variable solubility in γ and α irons. Further, its solubility in α-ferrite also decreases sharply with temperature.[80,84] Therefore the effectiveness of copper would be determined by the extent to which it is retained in solution. Cooling rate shall be an important parameter in this regard. If retained in solution, copper enhances hardenability. On tempering Cu bearing steels and cast irons[85] beyond 500°C Cu if retained in solution, precipitates in an elemental form. This observation has been utilized in developing special high strength structural steels[85] and high strength malleable cast irons.[86]

Its direct influence on wear resistance of cast irons is not of much significance but indirectly it helps in improving it by suppressing the formation of free ferrite.[2,80,84]

Addition of 0.5 to 1% Cu to cast irons considerably improves their resistance to corrosion by dilute H_2SO_4, HCl, sea water etc.[1,2,80]

In general most of the copper partitions to austenite.[9,87] Copper in excess of the amount which can be retained in solution is precipitated during cooling in ferrite and contributes little to the overall hardness and hardenability.[88,89] Sandoz[9] has however reported

that small but measurable quantity of Cu is also dissolved in the cementite phase, its amount being directly proportional to the amount of Cu added.

2.3.2.10 Manganese

Manganese is a powerful deoxidiser and austenite stabilizer.[1] It also renders sulphur inactive by the formation of manganese sulphide.[1] Any Mn in excess of these requirements partially dissolves in the iron and partly forms Mn_3C which occurs in combination with Fe_3C as $(FeMn)_3C$.[1] It enhances hardenability by lowering transformation temperatures (Ar_3 and Ar_1) and by rendering the γ to α transformation sluggish.[1] It increases the depth of chill and hardness if present in excess of the amount needed to neutralize sulphur, because it promotes the formation of finer and harder pearlite. Mn is often employed to decrease or prevent mottling in heavy sections. Normally it is kept below 0.7% in martensitic white irons because it forms stable austenite. In some pearlitic or ferritic alloy cast irons, Mn $\sim$ 1.5% may be used to maintain the specified strength levels. Strength and toughness of martensitic white irons, however, begin to drop if Mn is present in excess of 1.5%.[84] It is reported that abrasion resistance also drops mainly because of austenite retention.

If manganese is increased beyond 1.8% the steel tends

2.3.2.13 Boron

It is a powerful carbide stabilizer. Normally it is not added to gray irons, but enters accidentally from vitreous enamel scrap or from borax bonded refractories and may interfere with chill control methods.[2,92] Boron additions above 0.1% promote chilling and carbide stabilization.

2.3.2.14 Antimony

In certain pig irons it is present in small amounts (upto about 0.2%) as impurity. Sometimes it enters castings in large amounts (upto 0.3-0.5%) through vitreous enamelled scrap.[2] It tends to stabilize pearlite, raises hardness and lowerstensile strength, transverse strength, impact strength and deflection. Even small amounts of antimony (0.1%) lower the impact strength by about 30-50% and increase the tendency of light castings to cracking.[2,92]

2.3.2.15 Bismuth

Bismuth is a carbide former and acts as a carbide-inducing inoculant in cast irons. It promotes the formation of Widmanstatten graphite, causing a marked reduction in tensile strength.[2]

Bismuth acts as a subversive element (like lead, titanium and antimony) to magnesium in the production of nodular iron.[2,93] In amounts 0.002% it is useful in controlling chill and annealability of malleable irons.[2] Bismuth,

in very small quantities (50-100 gms per tonne) effectively suppresses graphite formation in unalloyed or low alloy white irons. It produces a fine grain microstructure free from 'spiking', a condition that sometimes is preferred in abrasion resistant white irons.

2.3.2.16 Lead

Lead may be present in pig irons only in traces and occasionally in amounts 0.003%. . It finds its way into cast irons through scrap or through scrap copper additions.[2,90,94] Lead is very harmful element and should be avoided in all cast irons, as even in traces (0.0007%.), it may produce Widmanstatten graphite which in turn leads to a drastic loss of strength.[2] Mesh graphite may form from lead associated with aluminium[94] and with tellurium[90] and its formation also drastically reduces strength.

2.3.2.17 Tin

Tin is a powerful pearlite stabiliser.[2] Even small additions (0.15%.) are sufficient to produce fully pearlitic structure in irons with a high carbon equivalent (4.7%.).[2] Therefore, tin additions in small amounts are usually employed wherever pearlite stability at high temperatures is desired without promoting grain growth. In gray irons, in amounts upto about 0.15%., it eliminates free ferrite, may raise tensile strength by

(iii) Retained austenite whose presence was more easily detected in alloys with higher Mn(in the lower Cr series) and/or Cr contents.

The repetitiveness was minimized by confining the microstructural examination to (i) the as-cast specimens of all the alloys and (ii) those heat treatments at which distinct changes in the properties (hardness) were observed. Representative microstructures for the different alloys, currently investigated, are summarized in Figures 5.14 to 5.21. As discussed in the earlier paragraph, the three distinct features were discernable.

It was possible to identify pearlitic matrix which was predominantly confined to as-cast microstructures(Figs.5.14b, 5.16b, 5.18b and 5.21c). Similarly martensite could be clearly identified in one of the instances in the as-cast condition(Fig.5.17b) and in a number of instances in the heat treated condition (Figs.5.14f, 5.15f-g, 5.16g-h, 5.17g-h, 5.18e, g-i, 5.19e-f, 5.20h, 5.21i and k). However, the difficulty in identifying the nature of the matrix phase persisted in the remaining instances. Retained austenite could be detected in the alloys A4 and A8 in the as-cast conditions (Figs 5.17a-b and 5.21a-b and d) and in the alloys A3,A4 and A8 in the heat treated condition (Figs.5.16h, 5.17c and 5.21d,e and j).The matrix contained dispersed carbides in most instances (Figs.5.14c-f, 5.15c-g, 5.16e-h, 5.17c-f, 5.18e-i, 5.19c-e, 5.20d-h, 5.21e-k).

Concerning the morphology and dispersion of free carbides,

the higher Cr alloys were better disposed compared with the lower Cr alloys. In the former, carbides were equiaxed even in the as-cast condition (Figs. 5.18b,5.19b,5.21b) and rendered distinctly discontinuous on heat treatment (Figs.5.18f, g and h, 5.19c-f, 5.20d-h, 5.21f,g,i and k). Another important feature of the higher Cr alloys was that the free carbide was rendered equiaxed or even polyhedral in some instances through heat treatment (Figs.5.18f,5.20d and g, 5.21g). In comparison to this, the carbide morphology and dispersion in the lower Cr-alloys tended to be platy and or massive in both the as-cast and heat treated condition (Figs.5.14b,d and f; 5.15b,c,e-g; 5.16b,d; 5.17b,c,f-h). It appeared as though the morphology of the free carbides was somewhat improved with an increase in the Mn content and heat treating temperature. Free carbides in the lower Cr alloys were also rendered discontinuous by heat treatment (Figs.5.14c, 5.15c,d and f, 5.16e, g and h, 5.17c,d,f-h) as in the higher chromium alloys.

For maximum hardening, matrix mcirostructure in most alloys was martensite with dispersed carbides (Figs.5.16e and f; 5.17e-h, 5.19d,e,f; 5.20f-h; 5.21f-g), although in the alloy A2 it was mostly bainitic containing dispersed carbides (Fig.5.15d).

Microstructural examination proved most useful in assessing how 'free' carbide morphology and dispersion was influenced by heat-treatment and alloy content. Taking an overall view, the higher Cr alloys appeared to be better placed compared

with their lower Cr counterparts both with regard to the matrix microstructure and carbide morphology/dispersion. This is equally valid for the location of retained austenite whose distribution was most favourable in the alloy A8 and resembling that observed in Ni-hard 4.[17] The lower Cr alloy A4 was also favourably disposed in this regard(i.e. location of retained austenite).

Scanning electron microscopy was carried out on certain selected specimens to ascertain the nature of the (i) dispersed carbides contained within the matrix and,(ii) the matrix phase. Representative micrographs are shown in Figures 5.22-5.24.

Presence of dispersed carbides in alloy A2(Fig.5.22b), A3(Figs.5.23a and b), A4(Fig.5.24a) and A8 (Fig.5.25) in the heat treated condition and its absence in the as-cast microstructure (Fig.5.22a) has been confirmed. Its adherency with the matrix phase appeared inadequate (Fig.5.23b)

On comparing the microstructures of alloys A3 and A4 (Figs.5.23 and 5.24) it emerged that although the presence of martensite in the latter could be easily detected in the form of platelets even at a magnification of X500, this magnification was inadequate to resolve its presence in the former alloy. Only at a high magnification it was possible to deduce that the matrix in the alloy A3 was martensitic (Fig.5.23b). The obtuse nature of the martensitic plates is further clearly revealed in Figs.5.24(b) and (c).

5.2.3 Microhardness

These measurements were considered essential as they were likely to provide clues to the unanswered questions arising from the microstructural examination namely,

(i) nature of the matrix phase,

(ii) nature of the carbide formed and,

(iii) easy detection of hitherto undetected austenite during microstructural observations. Even partly satisfactory answers to these querries were likely to prove useful in arriving at 'some' understanding of the hardening mechanism(s) in the alloys under investigation.

Measurements were carried out on as-cast and selected heat-treated specimens and the data thus obtained is summarized in Tables 5.10-5.17. The data includes both the average value and all the hardness readings from which the average value was arrived at. The maximum and the minimum values have been shown with the help of asterisks.

Hardness of the carbide phase varied from ~950 to ~2140 VPN and that of the matrix phase from ~ 380 to ~1000 VPN. It was decided that for microhardness values within the range ~550 to ~750 VPN, the matrix constituent would be identified as bainite/tempered martensite and higher than ~750 VPN as martensite. Microhardness of retained austenite varied from ~500 to ~700 VPN (Tables 5.13 and 5.17).

5.2.4 EPMA Studies

They were confined to the alloys A2,A3,A6 and A7 to ascertain (i) the distribution of Mn,Cr,Si and Cu into the different microconstituents (namely matrix and carbide) in the as-cast condition and, (ii) how it (the distribution) was affected by heat-treatment and/or alloy content. The EPMA data is reported in the Tables 5.18 to 5.36. Additionally concentration profiles for Mn,Cr and Fe (Fig.5.26) along with the corresponding X-ray images for Mn,Cr,Fe and Si (Figs.5.27-5.28) have also been provided. As discussed in Chapter IV, concentrations of Mn and Cr were computed by using α-coefficient correction method (Section 4.6.2) while Si and Cu concentrations correspond to first approximations.

A perusal of the Tables 5.18 to 5.36 and Figs.5.26 to 5.28 revealed that :

(1) (a) Concentration level of Cr and Mn distributing into the matrix and carbide phases was influenced by an increase in the alloy content. This is effectively demonstrated with the help of the data (derived from Tables 5.18 to 5.36) summarized below:-

Table A

Alloy	Concentration*			
	Matrix		Carbide	
	Mn	Cr	Mn	Cr
(1) A2 (~4% Mn and ~6% Cr)	3.00	3.61	4.44	14.16
(2) A3 (~5% Mn and ~6% Cr)	4.31	3.96	6.71	14.21
(3) A6 (~4% Mn and ~9% Cr)	3.28	5.58	4.81	28.87
(4) A7 (~5% Mn and ~9% Cr)	4.20	5.99	6.24	27.35

* Average value considering as-cast and heat-treated specimens.

From Table A it is additionally inferred that :

(i) In general Cr concentration is higher than Mn in the matrix in all the alloys except alloy A3. Also, Cr concentration was appreciably higher than Mn in the carbide phase.

(ii) As Cr was increased from ~6 to ~9%. (i.e. ~50%.), Cr concentration in the matrix was increased by about 50% and that in the carbide by about 100%. .

(iii) Similarly as Mn was increased from ~4 to ~5%. (i.e. ~25%.) the concentration of Mn was increased by about 30% in the matrix and by about 50% in the carbide phase.

(b) When Mn content was raised from ~4- 5%. at a constant Cr content, concentration ratios of Mn and Cr in the matrix and carbide phases were as given below:-

Table B

Alloy	Concentration ratio of element	Matrix	Carbide
Low Cr alloys (A2,A3)	$C_{CrA3}/C_{Cr\ A2}$	1.10	1.0
	$C_{Mn\ A3}/C_{Mn\ A2}$	1.44	1.5
High Cr alloys (A6,A7)	$C_{Cr\ A7}/C_{Cr\ A6}$	1.00	0.9
	$C_{Mn\ A7}/C_{Mn\ A6}$	1.28	1.3

This table revealed that whereas the concentration of Cr in the matrix as well as in the carbide remained almost unaltered both in the lower and in the higher Cr alloys, increase in the concentration level of Mn was a little higher in the

in the experimental alloys.

A change that may occur on soaking and is likely to influence the alloy content of austenite involves a reduction in the volume fraction of the carbide phase because of the presence of graphitizing elements Si and Cu. This will lead to (i) a larger availability of both the interstitial and substitutional elements and (ii) the attainment of discontinuous carbide.[98-100] However, a larger availability of the alloying elements is accompanied by a corresponding increase in the volume fraction of the matrix phase. Thus the overall element balance in austenite remains unaltered, however, with the matrix now retaining a higher proportion of the alloy content. Another change that may occur in the high temperature microstructure during soaking involves precipitation of carbides (cf-precipitation in austenitic stainless steels).[117] This carbide is likely to be different from M_3C, would be one needing a larger activation for its formation and one involving a participation of relatively larger amounts of substitutional elements in its formation.[118] Carbide precipitation will also occur during cooling from the heat-treating temperature, mainly because of a decrease in solid solubility of carbon in austenite with a decrease in temperature. The carbide formed will be of the type $(FeMnCr)_xC_y$ (e.g. $(FeCrMn)_7C_3$ or simply M_7C_3 type) as both Mn and Cr are carbide formers.[1,10,77] The other likely changes namely rendering of free carbides

discontinuous and a possible reduction in their volume fraction have already been discussed.

On cooling from the heat-treating temperature, the changes that are likely to occur would depend upon (i) how much higher the heat-treating temperature is with respect to the operative A_1 temperature and (ii) the total alloy content (Mn content since Cr content is fixed) in solution in austenite. The former along with the soaking period will govern the extent of partitioning of alloying elements. The nature of the final microstructure (whether matrix or carbide) will depend upon the alloy content of the parent austenite, the extent of equilibrium attained between γ and carbide at the end of the heat treatment and the extent of precipitation (during soaking/cooling). The last mentioned parameter would decide the 'true' alloy content of the parent γ before it transforms. If at this stage the alloy content is large enough to suppress the formation of equilibrium microstructure(s), the parent phase will most likely transform to non-equilibrium microstructure(s). In the event of the alloy content being marginal i.e. just at the threshold limit at which non-equilibrium microstructure(s) may be preferred over the equilibrium ones, the nature of the matrix microstructure would be governed by the heat-treating temperature and cooling rate (air cooling in the present investigation); the higher the temperature the higher the hardenability (hence larger the

out of which reaction (i) predominates:

(i) $\gamma \xrightarrow{\text{on soaking}}$ carbides + γ (with less alloy content)
γ (with less alloy content) $\xrightarrow{\text{on cooling}}$ P/B/M)] leading hardness increase

(ii) Martensite $\xrightarrow{\text{on heating}}$ α + carbides] Leading to Hardness decrease

The absence of hardening in alloy A8 (Fig.5.5b) on heat treating from 750°C clearly reveals that the basis of explaining an increase in hardness in the alloy A4, when identically heat-treated, is valid. This is because the as-cast matrix micro-structure in alloy A8, unlike in alloy A4, is mostly P/B + some martensite(?) + some austenite (Fig.5.21a-e) and on being heat treated from 750°C such a microstructure will lead to a decrease in hardness because the reaction of the type (ii) as mentioned above, predominates.

This argument also leads to the conclusion that the remaining higher Cr alloys A5 to A7, on being heat-treated from 750°C, will respond in a manner similar to alloy A8. That is what has been observed (Figs.5.2b to 5.5b).

The hardness of the alloy A1 in the heat treated condition increases as the temperature is raised from 800 to 900°C, albeit marginally (it being maximum at 900°C), consistent with the (i) laws governing diffusion controlled processes and (ii) the effect of temperature and cooling rate on the possible formation of shear transformation product (Fig.5.2a). The increase in hardness on heat-treating from 900°C

is accompanied by the formation of martensite in the intercellular carbide spaces (Fig.5.14f) which is beginning to replace spheroidized-matrix structure (Fig.5.14e). A slight increase in hardness over the as-cast hardness on heat treating from 800 and 850°C is perhaps due to an increase in the carbide dispersion. A similar situation exists in alloy A5(Fig.5.2b) except that the slope of the hardness vs time curve at 900°C is steeper than that observed in the alloy A1 (Fig. 5.2a). This can be attributed to the formation of martensite (as in alloy A1), its amount increasing as the soaking period is increased at 900°C (Figs.5.18e-i) and its volume fraction being higher than that observed in alloy A1 (Figs.5.14f and 5.18i). On heat-treating from 800 and 850°C, the basic trend of the curves (observed in A5) is similar to that observed in alloy A1-namely an initial increase in the hardness with soaking period (more on heat treating from 850°C) followed by a levelling off (Fig.5.2a and b). This is an indication that the nature of the microstructure on heat-treating from 800 and 850°C is identical in both A1 and A5 and consisting of a combination of bainite and spheroidized structure their proportions and dispersion being optimum on heat-treating from 850°C. On raising the heat-treating temperature to 900°C, the hardness values upto soaking periods of 4 hours are lower than the corresponding values at 850°C perhaps due to a coarsening of the spheroidized microstructure.

some instances) carbides has also been detected (Table 5.65). Study of the relevant ternary sections of the Fe-Cr-C and Fe-Mn-C phase diagrams reveals that the predominant carbide to form in the alloys under investigation should be M_3C. Further, there is a definite possibility of the M_7C_3 type of carbide forming in addition to M_3C in the experimental alloys in the heat-treated condition.[11] Thus a major part of the findings on the formation of carbides (Table 5.65) is consistent with the information obtained from isothermal sections of the relevant phase diagrams.

The formation of M_5C_2 type of carbide now needs explaining. This carbide has been detected both in the lower as well as in the higher chromium alloys mostly in traces. An examination of the Fe-Mn-C ternary reveals that the M_5C_2 carbide is stable at high temperatures and generally formed at relatively high Mn and carbon concentrations.[11] Recalling the suggestion given earlier that the type of carbide formed during soaking may involve participation of a larger proportion of substitutional elements, the possible formation of M_5C_2 carbide in the heat-treated condition does not appear improbable.

The formation of $M_{23}C_6$ carbide in one of the instances in the lower Cr alloys can be similarly explained and also on the basis of the experimental observation that '$M_{23}C_6$ type of carbide may appear in alloys containing less than 10% Cr.[11]

The microhardness of the carbide phase in the present investigation has been found to be in the range of 1000 to 2160 VPN (Tables 5.10-5.17). Not much data is available on the microhardness of the Fe-Cr-Mn carbides. However, on the basis of microhardness data available on iron-chromium carbides[123,124] and Mn carbides[125,126] it is inferred that the microhardness of the mixed Fe-Cr-Mn carbides, found in the present investigation, is reasonable.

The formation of M_7C_3 and M_5C_2 carbides in addition to M_3C, has been accompanied by an increase in the microhardness of the carbide phase. This is because the two former carbides have crystal structure with lower symmetry elements, namely hexagonal (M_7C_3) [applicable only if the c/a ratio deviates appreciably from the ideal value] and especially monoclinic (M_5C_2).

Another important observation pertaining to free carbides is that heat-treatment in general has rendered them discontinuous in almost all instances (Fig.5.14-5.21). From this it can be inferred that copper, in combination with silicon, has successfully performed the function for which it was added (Sections 2.3.2 and 2.4). The free-carbide morphology in the heat-treated condition has tended to be massive or platy in the lower Cr alloys [atleast at lower Mn contents] (Figs.5.14 to 5.17) and both platy and dispersed

In Iron

	A	Q	Temp.°C
C	6.2×10^{-3}	19.2	350-850(α)
	0.1	32.4	900-1060(γ)
Cr	$8.52^{+3.2}_{-2.33}$	59.9±1.6	800-880(α)
	$10.80^{+3.35}_{-2.56}$	69.7±1.7	950-1400(γ)
Mn	$1.49^{+1.0}_{-0.60}$	55.8±2.5	700-760 (Ferrom.α)
	$0.35^{+0.31}_{-0.17}$	52.5±2.3	800-900 (Param.α)
	$0.16^{+0.06}_{-0.05}$	62.5±1.0	920-1280(γ)
	0.78	60.1	809-901

By substituting the relevant values for the diffusion of Cr and Mn atoms in austenite at a temperature of 900°C,

$$D_{Cr} = 1.3504\times10^{-12} \text{ cm}^2/\text{sec.}$$

and $$D_{Mn} = 4.3056\times10^{-13} \text{ cm}^2/\text{sec.}$$

This leads to the inference that at 900°C Cr atoms diffuse about three times as fast as the Mn atoms. Its direct effect will be that at a given temperature the overall rate of diffusion will be faster in the higher Cr alloys and accordingly microstructural changes involving a modification in the (i) matrix microstructure and (ii) carbide morphology will be more rapid in the higher Cr alloys than in the lower Cr alloys. This is a more convincing argument to explain how higher Cr alloys would respond more favourably to a change

in the free-carbide morphology in general and especially with regard to the alloy system presently under investigation.

Another parameter which needs to be commented upon is the location of retained austenite. From the point of view of arresting crack-propagation, it is most favourable in the alloys A4 and A8 (Figs. 5.17a and b and 5.21b). Factors promoting the retention of austenite around free-carbides are not clearly established. However, since both the alloys A4 and A8 contain ~6% Mn, it is possible that one of the factors perhaps is a high Mn content. This thinking can be further expounded by stating that the overall availability of alloying elements around free carbides will be more than in the other regions of matrix. Accordingly, whenever the overall alloy content is large enough to favour retention of austenite, its location would preferentially be around free carbides. It would also be of interest to experimentally establish which other parameters (e.g. founding parameters) may bring forth retention of γ around free carbides.

6.3.3 Matrix

Matrix microstructure in the experimental alloys has comprised of one or more of the following: (i) pearlite, (ii) bainite/tempered martensite, (iii) martensite, (iv) dispersed carbides and (v) austenite.

The formation of dispersed carbides, which have been an integral part of the matrix microstructure in most

and its usefulness lies in that the heat treating temperature and especially the time can be decided upon solely on the basis that (i) the high temperature microstructure (HTM) of the required configuration is just attained and (ii) it (the HTM) on cooling transforms by a mechanism such that the final microstructure formed conforms to the properties desired.

It is significant to note that the heterogeneity in the Mn distribution is observed to be less in the higher Cr alloys as compared with the lower Cr alloys (Tables 5.18-5.36). This experimental finding can be explained on the basis of the beneficial effect of a higher diffusivity associated with Cr atoms in comparison to Mn atoms (Section 6.3.2). It is noteworthy that the utilization of a higher Cr content has proved useful in overcoming the natural tendency of the Mn atoms towards segregation[130] and is of special relevance to the present investigation which aims at exploring the possibility of utilizing a higher Mn content for developing alloy white irons. The above experimental finding should be regarded as yet another advantage in utilizing Cr contents higher than normally required [over and above what has already been concluded on this theme in the Section 6.3.2].

With the help of the EPMA data, it has been possible to ascertain the alloy content of the different micro-constituents corresponding to heat-treatments inducing

maximum hardening. This data, which is consistent with the fundamental considerations outlined in Section 6.1, is of both fundamental and design interest e.g., observations 7 and 8 (Section 5.2.4) reveal that in the alloy A2, corresponding to heat-treatments 2h 850°C AC and 10h 850°C AC, the Mn content in the matrix is ~3% and accordingly the alloy had to be air cooled from a higher heat-treating temperature (~850°C) to form martensite in comparison to alloy A3 in which the Mn content of the matrix is ~3.7% and accordingly a lower temperature (~800°C) suffices to attain the same result.

Barring a solitary instance[131], the EPMA has perhaps for the first time provided useful information on the partitioning of Mn into the austenite and carbide phases when it is present in amounts much larger than hitherto employed. The overall partition ratio of Mn between the carbide and matrix phase has been found to be ~1.5:1 revealing an appreciably larger concentration of Mn in the carbide phase in comparison to the matrix phase. This is quite contrary to the normal behaviour expected of an austenite stabilizing element (its concentration is expected to be larger in austenite than in the carbide). This would become further evident when the partition ratio of $\frac{\text{Ni in carbide}}{\text{Ni in matrix}}$ is computed from the data reported by Sandoz[43].

The difference in behaviour is because Mn, unlike Ni, has a carbide forming tendency thereby enabling a relatively

TABLE 5.16

EFFECT OF HEAT TREATMENT ON MICROHARDNESS OF ALLOY A7

Heat Treatment	Constituent	Microhardness VPN (25 gm) Variation	Average
As-cast	Carbide	1530, 1320**, 1800*, 1530, 1650, 1800, 1800, 1650, 1650, 1530	1626
	Matrix	715, 585, 715, 680, 755*, 680, 612, 532**, 557, 680	651
2h 800°C AC	Carbide	1950*, 1230**, 1530, 1320, 1320, 1230, 1230, 1650, 1800, 1320	1458
	Matrix	715, 612**, 645, 715, 715, 715, 755*, 715	698
10h 800°C AC	Carbide	2140*, 1650, 1650, 1530, 1650, 1950, 1950, 1800, 1075**, 1800	1720
	Matrix	950*, 950, 890, 890, 840, 715**, 755, 755	843
2h 850°C AC	Carbide	1230**, 1650, 1530, 1650, 1800* 1420, 1650, 1800, 1650, 1650	1603
	Matrix	840, 715**, 715, 755, 840, 890*, 890, 795	805
10h 850°C AC	Carbide	1320**, 1950*, 1950, 1950, 1800 1950, 1800, 1650, 1530, 1320	1722
	Matrix	950, 1010*, 890, 890, 1010, 840**	932

* Maximum value,
** Minimum value .

TABLE 5.17

EFFECT OF HEAT TREATMENT ON MICROHARDNESS OF ALLOY A8

Heat Treatment	Constituent	Microhardness VPN (25 gm) Variation	Average
As-cast	Carbide	1320,1650,1530,1420,1320,1075**, 1530,1650*,1420,1530	1445
	Matrix	612,645,645,612,680,645,557**, 715,715*,645	647
2h 800 °C AC	Carbide	1140,1800,1950*,1530,1650, 1650,1530,1530,1140**,1530	1545
	Matrix	645**,755,795*,755,715, 645,715,680,755,795	726
10h 800 °C AC	Carbide	1420**,1950*,1800,1800,1950, 1800,1650,1950,1800,1800	1792
	Matrix	795,950*,755**,890,890,840,890 950,950,890	880
2h 850°C AC	Carbide	1800,1650,1420,1800,1950*,1650, 1530,1230**,1950,1800	1678
	Matrix	840,795,840,840,795,890*,755**, 755	814
6 h 950°C AC	Carbide	1530,1420,1530,1650*,1530, 1420,1320,1075**,1420,1320	1422
	Austenite	585,612*,557,532**,585,585, 585,612,557,585	580

* Maximum value,
** Minimum value

TABLE 5.19

EFFECT OF HEAT-TREATMENT ON ELEMENT DISTRIBUTION IN ALLOY A2

HEAT TREATMENT - 2h 800°C AC

Constituent	Weight Percent			
	Cr*	Mn*	Si**	Cu**
Matrix	5.371	3.587	1.708	0.694
	1.353	2.799	1.913	0.900
	3.936	2.798	1.810	0.977
	3.920	2.743	1.571	0.926
	3.134	2.886	1.742	0.772
	2.631	2.999	1.810	0.746
	3.896	2.800	1.639	0.720
Average	3.463	2.944	1.742	0.819
Carbide	14.004	4.268	1.434	0.104
	14.706	4.468	1.469	0.180
	13.158	4.325	1.571	0.206
	15.305	4.068	1.503	0.154
	13.276	4.526	1.571	0.129
	14.886	3.895	1.434	0.180
	12.135	4.179	1.537	0.154
	14.818	3.867	1.434	0.231
Average	14.036	4.200	1.494	0.167

* corrected concentration

** approximate concentration

TABLE 5.18

EFFECT OF HEAT-TREATMENT ON ELEMENT DISTRIBUTION IN ALLOY A2

HEAT TREATMENT - As-cast

Constituent	Weight Percent			
	Cr*	Mn*	Si**	Cu**
Matrix	3.549	3.001	1.571	1.106
	2.023	1.085	1.844	0.952
	2.584	2.514	1.639	0.823
	2.847	3.029	1.878	1.080
	3.526	3.059	1.605	1.080
	3.926	2.856	1.810	0.874
	3.028	3.113	1.639	0.926
	3.084	2.513	1.810	0.797
	3.966	3.259	1.434	0.926
Average	3.170	2.714	1.692	0.952
Carbide	13.239	3.523	1.400	0.257
	14.247	4.382	1.400	0.154
	14.605	4.639	1.332	0.206
	12.834	4.868	1.263	0.231
	11.323	3.922	1.469	0.129
	13.039	4.581	1.400	0.206
	14.363	4.240	1.332	0.231
	15.235	4.297	1.263	0.180
	14.239	4.755	1.092	0.154
Average	13.680	4.356	1.331	0.169

* corrected concentration

** approximate concentration

TABLE 5.19

EFFECT OF HEAT-TREATMENT ON ELEMENT DISTRIBUTION IN ALLOY A2

HEAT TREATMENT - 2h 800°C AC

Constituent	Weight Percent			
	Cr*	Mn*	Si**	Cu**
Matrix	5.371	3.587	1.708	0.694
	1.353	2.799	1.913	0.900
	3.936	2.798	1.810	0.977
	3.920	2.743	1.571	0.926
	3.134	2.886	1.742	0.772
	2.631	2.999	1.810	0.746
	3.896	2.800	1.639	0.720
Average	3.463	2.944	1.742	0.819
Carbide	14.004	4.268	1.434	0.104
	14.706	4.468	1.469	0.180
	13.158	4.325	1.571	0.206
	15.305	4.068	1.503	0.154
	13.276	4.526	1.571	0.129
	14.886	3.895	1.434	0.180
	12.135	4.179	1.537	0.154
	14.818	3.867	1.434	0.231
Average	14.036	4.200	1.494	0.167

* corrected concentration

** approximate concentration

TABLE 5.32

EFFECT OF HEAT-TREATMENT ON ELEMENT DISTRIBUTION IN ALLOY A7

HEAT-TREATMENT- As-cast

Constituent	Weight Percent			
	Cr*	Mn*	Si**	Cu**
	6.571	4.259	1.810	0.823
	6.332	4.231	1.708	0.849
	6.199	4.402	1.673	0.720
Matrix	7.063	4.089	1.776	1.055
	6.806	3.916	1.742	1.131
	6.406	3.916	1.673	0.952
	5.720	3.888	1.776	0.926
Average	6.442	4.100	1.737	0.922
	27.958	5.629	1.126	0.105
	20.603	5.164	1.366	0.129
	23.149	6.228	1.297	0.154
Carbide	31.215	6.953	1.092	0.180
	31.241	6.349	1.024	0.154
	33.922	6.006	0.887	0.105
	18.103	7.515	1.332	0.129
	23.671	8.434	1.092	0.154
Average	26.232	6.534	1.152	0.139

* corrected concentration
** approximate concentration

TABLE 5.33

EFFECT OF HEAT TREATMENT ON ELEMENT DISTRIBUTION IN ALLOY A7

HEAT TREATMENT - 2h 800°C AC

Constituent	Weight Percent			
	Cr*	Mn*	Si**	Cu**
Matrix	4.092	3.716	1.605	0.720
	2.348	4.751	1.742	0.746
	7.188	4.316	1.537	0.823
	1.587	3.909	1.571	0.772
	2.137	4.454	1.708	0.874
	7.825	4.889	1.503	0.926
	5.643	3.712	1.469	1.003
	4.847	4.285	1.537	0.797
Average	4.458	4.254	1.584	0.833
Carbide	27.787	6.261	0.990	0.129
	15.775	7.113	1.195	0.105
	29.124	5.283	0.956	0.129
	18.971	6.771	1.126	0.129
	27.680	6.404	0.853	0.154
	31.257	5.746	0.820	0.180
	23.958	6.060	1.058	0.105
	30.748	6.004	0.990	0.105
Average	25.662	6.205	0.999	0.130

* corrected concentration
** approximate concentration

TABLE 5.38

X-RAY DIFFRACTOGRAM OF ALLOY- A2

HEAT TREATMENT- 2h 850°C AC

Sl No.	2 θ	d(Å)	$\frac{I}{I_o}$	(hkl)				
				Matrix		Carbide(s)		
1	48.10	2.377	10			$(112,021)M_3$	$(321)M_7$	
2	51.25	2.240	8			$(200)M_3$	$(102)M_7$	$(020)M_5$
3	54.90	2.101	19			$(121)M_3$	$(202,501)M_7$	
4	55.80	2.070	26					$(510,021)M_5$
5	56.10	2.060	28		$(011)_{\alpha'}$	$(210)M_3$		
6	57.10	2.027	100	$(110)_\alpha$	$(110)_{\alpha'}$	$(022)M_3$ $(103)M_3$	$(421)M_7$	$(31\bar{2},40\bar{2})M_5$
7	58.85	1.972	12			$(211)M_3$	$(511)M_7$	$(51\bar{1},22\bar{1})M_5$
8	62.40	1.869	10			$(113)M_3$	$(222)M_7$	
9	63.20	1.849	7			$(122)M_3$	$(601)M_7$	
10	65.10	1.800	6				$(431)M_7$	$(312,511)M_5$
11	66.90	1.757	4			$(212)M_3$	$(412)M_7$	$(402)M_5$
12	111.75	1.173	17	$(211)_\alpha$	$(211)_{\alpha'}$			$(62\bar{3},91\bar{2})M_5$
13	114.80	1.150	8					$(423,80\bar{2})M_5$
14	119.35	1.122	7					$(13\bar{3},60\bar{4})M_5$

Structure: Martensite

+ some bainite

+ M_3C [isomorphous with Fe_3C(23-1113)]

+ trace M_7C_3 [isomorphous with Cr_7C_3(11-550)]

+ trace M_5C_2 [isomorphous with Fe_5C_2(20-508)]

TABLE 5.39

X-RAY DIFFRACTOGRAM OF ALLOY- A2

HEAT TREATMENT- 10h 850°C AC

Sl. No.	2θ	d(Å)	$\frac{I}{I_o}$	(hkl)		
				Matrix	Carbide(s)	
1	48.00	2.381	18		$(112,021)M_3$	$(321)M_7$ $(311,20\bar{2})M_5$
2	50.60	2.266	11		$(200)M_3$	$(411)M_7$ $(020)M_5$
3	51.80	2.217	11		$(120)M_3$	$(102)M_7$
4	54.65	2.110	23		$(121)M_3$	$(202,501)M_7$
5	55.60	2.077	27	$(011)_{\alpha'}$	$(210)M_3$	$(510,021)M_5$
6	57.00	2.030	100	$(110)_{\alpha}$		$(421)M_7$ $(31\bar{2},40\bar{2})M_5$
7	57.30	2.020	41	$(110)_{\alpha'}$	$(022)M_3$	
8	57.4	2.016	27		$(103)M_3$	
9	58.65	1.977	15		$(211)M_3$	$(511)M_7$ $(51\bar{1},22\bar{1})M_5$
10	62.10	1.878	14		$(113)M_3$	$(222)M_7$
11	63.10	1.851	12		$(122)M_3$	$(601)M_7$
12	64.80	1.807	10			$(431)M_7$ $(312,511)M_5$
13	65.50	1.790	10			$(521)M_7$
14	66.90	1.757	8		$(212)M_3$	$(412)M_7$ $(402)M_5$
15	70.15	1.685	10		$(004,023)M_3$	$(51\bar{2})M_5$
16	75.15	1.588	10		$(130)M_3$	$(11\bar{3})M_5$
17	85.00	1.434	10	$(200)_{\alpha}$		$(801)M_7$
18	107.20	1.203	10	$(112)_{\alpha'}$		$(11\bar{4},821)M_5$
19	111.70	1.170	15	$(211)_{\alpha}$ $(211)_{\alpha'}$		$(62\bar{3},912)M_5$
20	118.90	1.125	12			$(13\bar{3},60\bar{4})M_5$
21	121.40	1.111	10			$(041)M_5$
22	121.90	1.108	10			$(404)M_5$
23	122.20	1.106	10			
24	145.80	1.013	15	$(220)_{\alpha}$		

Structure: Bainite
+ some martensite
+ M_3C [isomorphous with Fe_3C(23-1113)]
+ some M_7C_3 [isomorphous with Cr_7C_3(11-550)]
+ trace M_5C_2 [isomorphous with Fe_5C_2(20-508)]

TABLE 5.40

X-RAY DIFFRACTOGRAM OF ALLOY- A2

HEAT TREATMENT- 8h 900°C AC

Sl. No.	2θ	d(Å)	$\frac{I}{I_o}$	(hkl) Matrix	(hkl) Carbide(s)	
1	48.10	2.377	8		$(112,021)M_3$	$(311,20\bar{2})M_5$
2	51.80	2.218	6		$(120)M_3$	
3	54.90	2.101	17		$(121)M_3$	
4	56.00	2.063	14	$(011)_{\alpha'}$	$(210)M_3$	$(510,021)M_5$
5	57.20	2.024	100	$(110)_{\alpha}(110)_{\alpha'}$	$(022)M_3$ $(103)M_3$	$(31\bar{2},40\bar{2})M_5$
6	58.70	1.976	9		$(211)M_3$	$(51\bar{1},22\bar{1})M_5$
7	62.20	1.875	6		$(113)M_3$	
8	75.40	1.584	5		$(130)M_3$	$(11\bar{3})M_5$
9	85.00	1.434	8	$(200)_{\alpha}(200)_{\alpha'}$		
10	111.90	1.169	18	$(211)_{\alpha}(211)_{\alpha'}$		$(62\bar{3},912)M_5$
11	118.65	1.126	4			$(13\bar{3},60\bar{4})M_5$
12	123.00	1.102	4			$(041)M_5$
13	145.95	1.013	9	$(220)_{\alpha}$		

Structure: Bainite
+ some martensite
+ M_3C [isomorphous with Fe_3C(23-1113)]
+ trace M_5C_2(??) [isomorphous with Fe_3-C_2(20-508)]

TABLE 5.41

X-RAY DIFFRACTOGRAM OF ALLOY- A3

HEAT TREATMENT - As-cast

Sl. No.	2θ	d(Å)	$\frac{I}{I_o}$	(hkl) Matrix	(hkl) Carbides
1	48.00	2.382	5		$(112,021)M_3$
2	49.80	2.301	6		$(411)M_7$
3	50.60	2.267	7		$(200)M_3$
4	54.00	2.133	5		$(202,501)M_7$
5	55.00	2.098	8		$(121)M_3$
6	57.20	2.023	100	$(110)_\alpha$	$(022)M_3$, $(103)M_3$, $(421)M_7$
7	58.78	1.974	12		$(211)M_3$, $(511)M_7$
8	62.42	1.869	7		$(113)M_3$, $(601)M_7$
9	63.12	1.851	5		$(122)M_3$
10	64.50	1.815	3		$(431)M_7$
11	65.50	1.790	3		$(521)M_7$
12	66.85	1.759	4		$(412)M_7$
13	85.00	1.434	9	$(200)_\alpha$	$(801)M_7$
14	94.00	1.324	3		$(641,811)M_7$
15	111.90	1.169	16	$(211)_\alpha$	
16	145.90	1.013	9	$(220)_\alpha$	

Structure: Pearlite/bainite
+ M_3C [isomorphous with Fe_3C(23-1113)]
+ some M_7C_3 [isomorphous with Cr_7C_3(11-550)]

TABLE 5.47

X-RAY DIFFRACTOGRAM OF ALLOY: A4
HEAT TREATMENT- As-cast

Sl. No.	2θ	d(Å)	$\frac{I}{I_o}$	(hkl) Matrix	(hkl) Carbide (s)
1	48.10	2.377	3		$(112,021)M_3$
2	50.10	2.288	4		unidentified
3	50.80	2.258	4		$(200)M_3$
4	54.50	2.116	3		$(121)M_3$
5	55.62	2.076	100	$(011)_\alpha, (111)_\gamma$	$(210)M_3$
6	57.30	2.02	29	$(110)_\alpha (110)_\alpha$,	$(022)M_3$ $(103)M_3$
7	58.82	1.973	5		$(211)M_3$
8	62.30	1.873	3		$(113)M_3$
9	63.30	1.846	3		$(122)M_3$
10	65.00	1.803	15	$(200)_\gamma$	
11	99.00	1.274	3	$(220)_\gamma$	
12	99.60	1.268	3		
13	111.50	1.172	3	$(211)_\alpha$,	
14	112.00	1.168	3	$(211)_\alpha$	
15	126.00	1.087	5	$(311)_\gamma$	
16	137.30	1.040	6	$(220)_\alpha, (222)_\gamma$	

Structure: Austenite
+ martensite
+ M_3C [isomorphous with Fe_3C(23-1113)]

TABLE 5.48

X-RAY DIFFRACTOGRAM OF ALLOY- A4

HEAT TREATMENT- 2h 800°C AC

Sl No	2θ	d(Å)	$\frac{I}{I_o}$	(hkl) Matrix		Carbides		
1	48.35	2.365	8			$(112,021)M_3$		
2	50.95	2.252	10			$(200)M_3$	$(020)M_5$	$(120)M_7$
3	55.08	2.095	13		$(111)_\gamma$	$(121)M_3$		$(012)M_7$
4	55.90	2.067	34	$(011)_{\alpha'}$		$(210)M_3$	$(510,021)M_5$	
5	57.30	2.020	100	$(110)_\alpha(110)_{\alpha'}$		$(022)M_3$ $(103)M_3$	$(31\bar{2},40\bar{2})M_5$	$(121)M_7$
6	58.90	1.970	13			$(211)M_3$	$(51\bar{1},22\bar{1})M_5$	$(300)M_7$
7	61.50	1.895	3				$(221)M_5$	$(112)M_7$
8	62.48	1.868	7			$(113)M_3$		
9	63.35	1.845	8			$(122)M_3$		
10	65.20	1.798	12		$(200)_\gamma$		$(312,511)M_5$	$(022)M_7$
11	67.10	1.753	6			$(212)M_3$	$(402)M_5$	
12	70.40	1.680	7			$(004,023)M_3$	$(51\bar{2})M_5$	
13	75.90	1.575	5			$(130)M_3$	$(11\bar{3})M_5$	
14	79.70	1.512	6	$(002)_{\alpha'}$			$(42\bar{2})M_5$	
15	85.10	1.432	8	$(200)_\alpha(200)_{\alpha'}$				
16	105.00	1.221	6	$(112)_{\alpha'}$			$(11\bar{4},821)M_5$	$(303,500)M_7$
17	112.05	1.168	13	$(211)_\alpha(211)_{\alpha'}$			$(62\bar{3},912)M_5$	$(322)M_7$

Structure: Martensite
+ austenite
+ M_3C [isomorphous with Fe_3C(23-1113)]
+ some M_5C_2 [isomorphous with Fe_5C_2(20-508)]
+ trace M_7C_3 [isomorphous with Fe_7C_3(17-333)]

TABLE 5.49

X-RAY DIFFRACTOGRAM OF ALLOY- A4

HEAT TREATMENT- 10h 800°C AC

Sl No.	2θ*	d(Å)	$\frac{I}{I_o}$	(hkl)		
				Matrix	Carbide(s)	
1	57.40	2.385	8		$(112,021)M_3$	$(311,20\bar{2})M_5$
2	60.80	2.264	7		$(200)M_3$ $(411)M_7$	$(020)M_5$
3	66.00	2.103	14		$(121)M_3$ $(202,501)M_7$	
4	67.02	2.075	80	$(011)_\alpha, (111)_\gamma$	$(210)M_3$	$(510,021)M_5$
5	68.80	2.028	100	$(110)_\alpha (110)_{\alpha'}$	$(022)M_3$ $(421)M_7$	$(31\bar{2},40\bar{2})M_5$
6	69.40	2.012	34		$(103)M_3$	
7	70.90	1.975	6		$(211)M_3$ $(511)M_7$	$(221)M_5$
8	75.58	1.869	5		$(113)M_3$	
9	76.50	1.850	6		$(122)M_3$ $(601)M_7$	
10	79.00	1.801	19	$(200)_\gamma$	$(431)M_7$	$(312,511)M_5$
11	81.20	1.759	4		$(212)M_3$ $(412)M_7$	
12	85.80	1.682	3		$(004,023)M_3$	
13	92.50	1.585	3		$(130)M_3$	$(11\bar{3})M_5$
14	105.80	1.436	15	$(200)_\alpha (200)_{\alpha'}$		
15	119.40	1.327	7		$(641,811)M_7$	$(80\bar{2})M_5$
16	128.70	1.271	10	$(220)_\gamma$		$(53\bar{1})M_5$

Structure: Martensite
+ austenite
+ M_3C [isomorphous with Fe_3C(23-1113)]
+ some M_7C_3 [isomorphous with Cr_7C_3(11-550)]
+ trace M_5C_2 [isomorphous with Fe_5C_2(20-508)]

* Target- Cr

TABLE 5.50

X-RAY DIFFRACTOGRAM OF ALLOY- A4

HEAT TREATMENT- 10h 850°C AC

Sl. No.	2θ	d(Å)	$\frac{I}{I_o}$	(hkl) Matrix			(hkl) Carbide(s)	
1	47.85	2.388	24				$(112,021)M_3$	$(411)M_7$
2	55.00	2.097	24				$(121)M_3$	$(202)M_7$
3	55.70	2.073	100			$(111)_\gamma$		
4	55.90	2.066	100		$(011)_{\alpha'}$		$(210)M_3$	$(421)M_7$
5	57.35	2.018	100	$(110)_\alpha$	$(110)_{\alpha'}$		$(022)M_3$	
6	57.60	2.010	67				$(103)M_3$	
7	58.70	1.976	27				$(211)M_3$	
8	62.50	1.887	27				$(113)M_3$	$(222)M_7$
9	63.25	1.847	24				$(122)M_3$	$(402)M_7$
10	64.95	1.804	21			$(200)_\gamma$		
11	81.60	1.482	27		$(002)_{\alpha'}$			
12	83.55	1.454	18	$(200)_\alpha$				$(801)M_7$
13	85.50	1.427	24		$(200)_\alpha$			
14	91.15	1.356	33					$(641)M_7$
15	91.50	1.352	36					$(622)M_7$
16	97.20	1.291	15			$(220)_\gamma$		
17	111.80	1.170	39		$(211)_{\alpha'}$			$(642)M_7$
18	112.05	1.168	45	$(211)_\alpha$	$(211)_{\alpha'}$			$(1011)M_7$
19	126.30	1.086	42			$(311)_\gamma$		
20	137.50	1.039	27			$(222)_\gamma$		
21	138.40	1.036	30					
22	139.10	1.034	27		$(022)_{\alpha'}$			
23	148.15	1.007	30		$(220)_{\alpha'}$			

Structure: Martensite
+ austenite
+ M_3C [isomorphous with Fe_3C(23-1113)]
+ trace M_7C_3 [isomorphous with Cr_7C_3(3-0975)]